CITY UNIVERSITY

DEPARTMENT OF MECHANICAL ENGINEERING & AERONAUTICS

ORGANIC FLUID MIXTURES AS WORKING FLUIDS FOR THE TRILATERAL FLASH CYCLE SYSTEM

by

RUI PITANGA MARQUES DA SILVA

A Thesis submitted for the
Degree of
Doctor of Philosophy
in Mechanical Engineering

MAY 1989

À memória da minha tia Alcina

ABSTRACT

The requirements for power generation systems have been reviewed together with the various energy sources available for them. Geothermal energy has been examined in more detail and the principal methods of recovering power from it which are currently employed are discussed. A novel method for improved power recovery from geothermal sources called the Trilateral Flash Cycle (TFC) system is described which has the special requirement of an efficient two-phase expander. Optimum results are obtained from this cycle if a working fluid is used which leaves the expander as dry saturated vapour.

A binary mixture of hydrocarbons was therefore sought which, by variation of the constituent proportions, would satisfy this requirement for a range of inlet temperatures when the condensing temperature is constant.

Methods of estimating mixture properties are reviewed and the chosen thermodynamic model, as well as a computational procedure for evaluation of vapour-liquid equilibria of organic binary mixtures at high pressures, are described. This is based on the Redlich-Kwong-Soave cubic equation of state. By this means a mixture of n-pentane and 2,2-dimethylpropane (neopentane) was found to be the most suitable for the TFC system for expander inlet temperatures between 150-180°C.

Temperature-entropy (T-S) diagrams of this organic binary mixture were obtained for several compositions.

Bubble and dew pressures of (n-pentane + 2,2-dimethylpropane) have been determined experimentally for five different compositions at six different temperatures, (333.15 K, 353.15 K, 373.15 K, 393.15 K, 413.15 K, and 433.15 K).

Vapour pressures of pure n-pentane and pure neo-pentane were also determined at these temperatures. The critical point of neo-pentane was measured to assess the accuracy of the isothermal compression apparatus used.

Theoretical predictions were found to be in good agreement with experimental measurements.

CONTENTS

LIST OF FIGURES

LIST OF TABLES

NOMENCLATURE

a,b	equation of state parameters
a_{ij}, b_{ij}	equation of state parameters for mixtures
B	second virial coefficient
A_i,B_i,C_i	constants in Antoine vapour pressure equation
A,B,C,D,	constants of four-term polynomial equation for heat capacity
c_p	ideal gas heat capacity
f	fugacity in kPas
g	molar excess Gibbs function
h	height of column of fluid in mm
H_i	Henry's constant
H	enthalpy in kJ/kg
ΔH	residual enthalpy in kJ/kg
k_{ij}	interaction parameter
M	masses of the dead-weights in kg
m	slope of $\sqrt{\alpha}$ versus $\sqrt{T_r}$
P_{sat} or P_{si}	vapour pressure of component i in kPas
p_a	atmospheric pressure
P	pressure in kPas
POY	Poynting correction factor
q_i	pure component surface area parameter in UNIQUAC model
R	universal gas constant = 8.3143 kJ/kg mol·K
S	entropy in kJ/kg·K
ΔS	residual entropy in kJ/kg·K
T	temperature in ·K

U	energy interaction parameter in UNIQUAC model
V	volume in m^3
x_i	mole fraction of component i in the liquid phase
W	downward force exerted by weights in N
y_i	mole fraction of component i in the vapour phase
Z	compressibility factor - dimensionless

Greek symbols

α	correction factor in RKS equation of state
ϕ	fugacity coefficient, dimensionless
θ_i	area fraction in UNIQUAC model, dimensionless
τ	parameter in UNIQUAC model
ρ	density
ω	Pitzer's acentric factor, dimensionless
γ	activity coefficient, dimensionless
μ	chemical potential
Ω_a, Ω_b	dimensionless coefficient in RKS equation of state

Subscripts

a	air
c	critical point
ℓ	liquid
m	mercury
o	reference state
i,j	components of mixture
f	saturated liquid

g	saturated vapour
mix	mixture
r	reduced coordinate
w	dead-weight

Superscripts

V	vapour phase
L	liquid phase
id	ideal
E	excess
o	reference state
sat	saturated
res	residual

ACKNOWLEDGEMENTS

It is a pleasure to express my gratitude to many who have helped somehow in this research project.

I am very grateful to my sponsor CNPq (Conselho Nacional de Pesquisas) who granted me a scholarship and whose financial support has made this research project possible.

I owe an inestimable debt to my supervisor, Dr.Ian K. Smith, for encouragement throughout the course of my studies at The City University.

Generous assistance towards the improvement of the computing programs and discussion of numerical techniques was given by Professor V. Price who deserves very special thanks.

I acknowledge with thanks the fruitful discussions and assistance by Dr.P. Rathbone of I.C.I.'s Physical Chemistry Department at Runcorn, and Dr.P. Topalis of Imperial College Chemical Engineering Department on the methods and difficulties of Vapour-Liquid Equilibrium determination. I am also indebted to Mr.G.Leather of I.C.I. Mond Division who provided me with a useful computing program for the evaluation of Antoine's vapour pressure equation constants.

I am greatly indebted to Dr.C. Aldis for helping and commenting on plotting routines. I am grateful too to Professor M.L. McGlashan of the Chemistry Department of University College, London, whose knowledge and wisdom have stimulated me towards the finding of successful fluid mixtures.

To Dr.B. Ghiassee of Chemistry Department of University College, London and Mr. T. Rose of the same department at the City University who respectively have helped me in conducting the experiments and preparing the samples of fluid mixtures my sincere thanks.

I am indebted to Mr.C. Whitehead for his expertise on the vacuum line and preparation of fluid mixtures. I acknowledge with thanks, Mr.R. Jacobs for his glassblowing craft.

My sincere appreciation goes also to Mrs. S. Johnson for her expert typing of the manuscript.

As a final note, I would like to thank my colleagues in my office and in the office next door at The City University with whom I have shared in a healthy environment witticism, jolliness, dullness, aggravation, sadness and contentment throughout the course of this project.

CHAPTER 1

INTRODUCTION

Alternative sources of energy for power generation have been the focus of worldwide attention in the past twenty years to satisfy the increasing need for clean, inexpensive energy supplies. Particular emphasis has been given to the use of non-fossil fuels such as geothermal heat. Much research effort has been devoted to design thermodynamic systems to maximise the conversion of heat into mechanical or electrical power from hot fluids found naturally or created artificially at depths of 1-3 km in the earth's crust [1].

Based on sound thermodynamic considerations specifically applied to power recovery from low-grade heat such as geothermally heated water or hot liquids from chemical plants, Smith [2], has conceived and developed what he describes as the Trilateral Flash Cycle (TFC) system. A T-s diagram of a TFC is shown in Figure 1.1. Both the Rankine and the Trilateral Flash Cycle undergo pressurization, heating, expansion, and condensation of the working fluid. However, in the Rankine cycle, a T-s diagram of which is shown in Figure 1.2, the working fluid, whether steam or organic is evaporated in the boiler and passes through a turbine as essentially dry vapour in order to produce work. In the Trilateral cycle the working fluid is heated in the liquid phase only and changes from a saturated liquid to a liquid-vapour two-phase mixture during expansion.

In so doing, work is extracted by means of a positive-displacement machine such as a rotary vane, or Lysholm screw expander. As will be shown, theoretically the Trilateral Flash Cycle offers a far better conversion efficiency than the conventional steam or organic Rankine cycle.

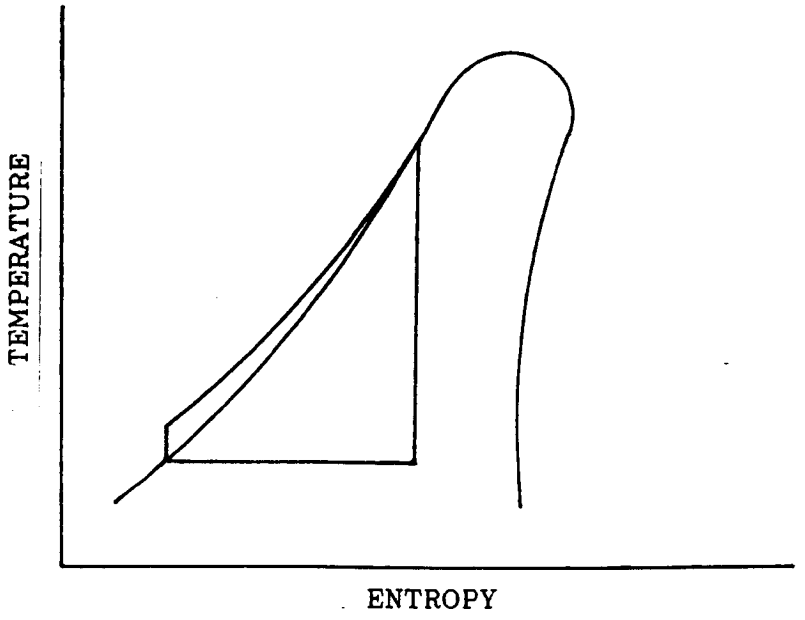

Figure 1.1. Trilateral Flash Cycle Temperature-entropy diagram.

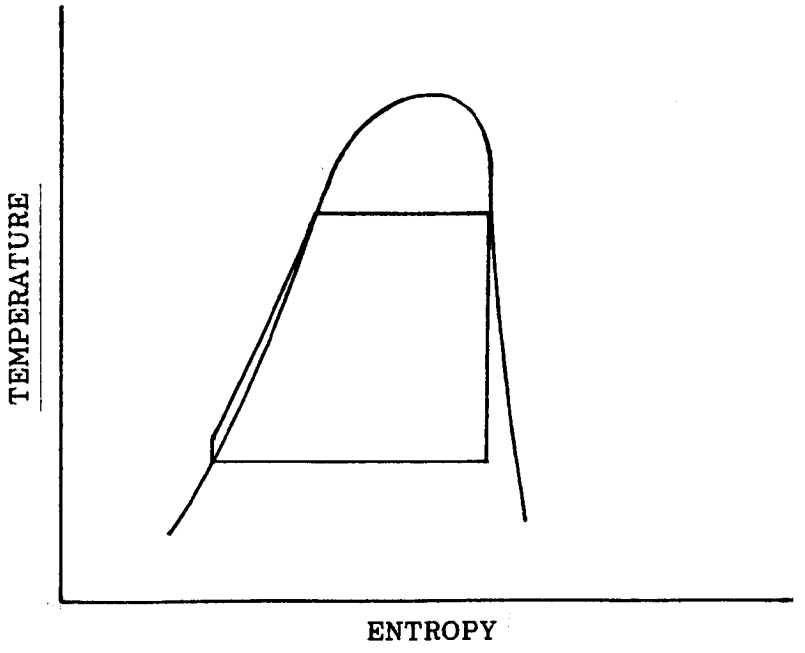

Figure 1.2. Simple Steam Rankine Cycle Temperature-entropy diagram.

However, screw expanders must be physically much larger than turbines to produce the equivalent of power output because fluid velocities through them are low. If a single TFC expander is to generate more than about 3 MW, it needs to be in the form of a single or two-stage screw, followed by a turbine, if the screw size is not to be excessively large. For this to be efficient the working fluid must attain the nearly dry state at the end of expansion as shown in Figure 1.3. This scheme is favoured because the bulk of the power will then be generated in the turbine with a high overall adiabatic efficiency and at a relatively low expander cost.

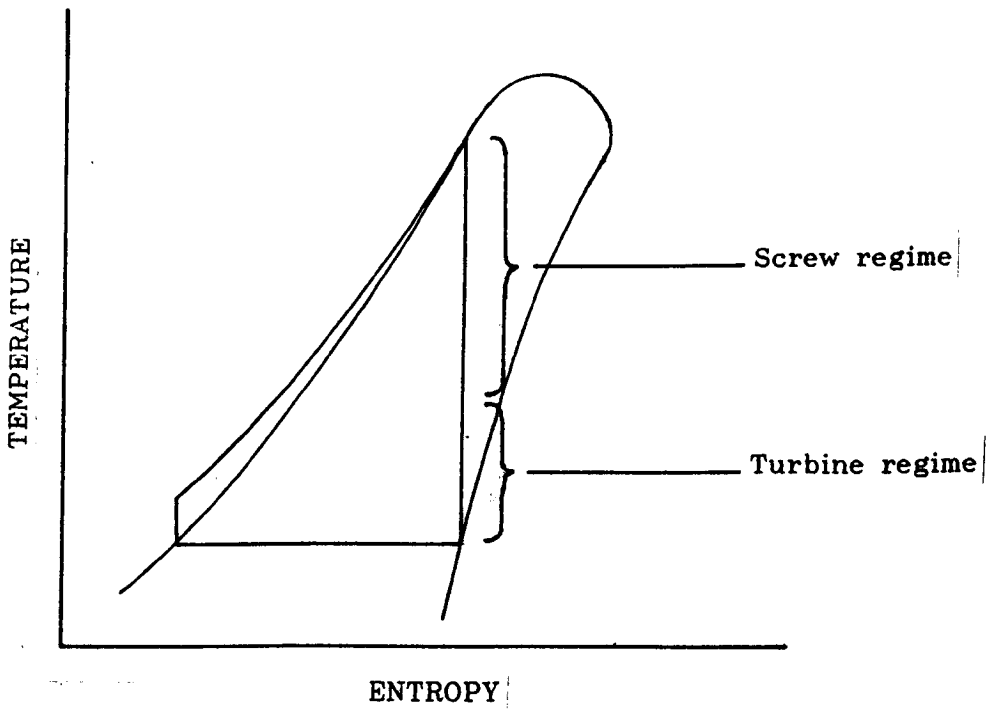

Figure 1.3. Trilateral Flash Multi-Stage System
Temperature-Entropy diagram.

The aim of this research project is to attempt to make such an expander arrangement possible by developing a suitable binary mixture of organic compounds as the working fluid.

Graphical representation of thermodynamic parameters in the form of temperature-entropy diagram is a useful means for preliminary evaluation of working fluid suitability. For this purpose, a thermodynamic model is then needed to estimate the properties of mixtures over an entire range of composition without the need for experimental physical data for each composition.

Most correlations for mixture thermodynamic properties for a wide range of pressures make use of equations of state [4]. These are a suitable means of correlating a variety of thermodynamic properties (enthalpy, entropy, fugacity) from a very limited set of experimental pure component and mixture data. The accuracy of results predicted relies on the choice of the equation of state as well as on the mixing rules adopted.

1.1. POWER PLANT DESIGN AND CRITERIA

Power plant system design is an important function for engineers. The quality of the system design affects both the capital and operating costs as well as the system reliability.

The methodology of arriving at an optimal power plant design is complex, not only because of the arithmetic involved, but also because of many qualitative judgements that have to be introduced[5]. Figure 1.4. shows a general system design flowchart.

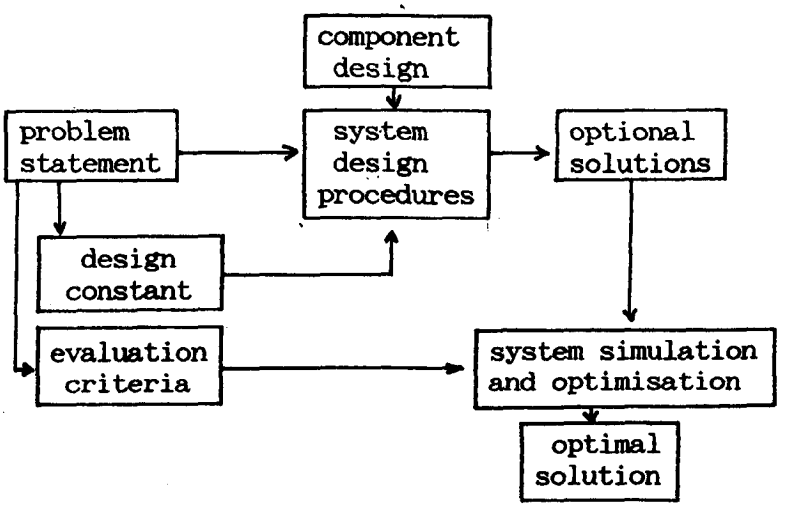

Figure 1.4. A general system design flowchart.

The inputs to the system design include, along with the problem statement or specification, the component design information and constraints. The problem statement may specify a general goal of the system under consideration. Since the system consists of many

components, the component information must be known and available in input form. The design constraints may be in the form of available space or in the form of environmental impacts [6].

The system design procedures will generate optional solutions (system designs). Apparently, not all these solutions are equally acceptable. Some will be better than others. In the next step, therefore, schemes must be developed to search for the best solution (the best system design). This is a function of the optimization and simulation procedures.

System simulation assumes knowledge of the performance characteristics of all components. Simulation is used when it is not possible or not economical to observe the real system while optimization is the process of finding the conditions that give the maximum or minimum value of a function. In the power plant system design, optimization generally means a search process for a system design that will have an optimal performance. More specifically, the optimal system is the system that will result directly, or indirectly, in the lowest production cost and at the same time will have an acceptable impact on the plant environment.

The principal aim of power plant design is to ensure [7]:

i) reliability of electricity supply

ii) safe and simple plant operation

iii) protection of the environment

iv) minimum electricity cost taking into account construction costs and expenses for operation and maintenance.

The process of selection of the type of power plant to be installed in the system requires evaluation of the power market. The value of electrical energy to this market is influenced by many complex conditions such as market demand, load factors and generation sources. Competing sources of electrical energy include geothermal, fossil fuel, hydroelectric and nuclear power generating plants.

The cost of geothermal power varies with each resource and must be determined for the particular case being considered.

1.1.1. Thermal Power Plant Performance, Costs, Safety and Environmental Considerations

1.1.1.1. Performance

The performance of generating plant can be expressed in terms of plant net heat rate as follows [7]:

$$\text{Plant net heat rate} = \frac{\text{heat input}}{\text{net kW output}}$$

By definition, the plant net thermal efficiency is:

$$\text{Plant net efficiency } (\eta) = \frac{\text{net output}}{\text{heat input}}$$

Table 1.1 indicates typical performance of various generating systems. It is seen that plant efficiency varies in a wide range with the fossil fuel steam plant on the top and the simple gas turbine system at the bottom. The efficiencies in Table 1.1 are achieved only when the generating plants operate at a full load. In part-load operation the plants generally experience deteriorating performance.

Table 1.1.Typical Thermal Efficiency of Various Generating Systems

Generation Type	Unit Size (MW)	Thermal Efficiency (%)
Steam (oil)	200-800	32-40
Steam (coal)	200-800	30-38
Steam (BWR and PWR)	500-1100	31-34
Gas Turbine (open cycle)	50-100	22-28
Combined gas/steam turbine	300-400	36-40
Diesel engine	10-30	27-30

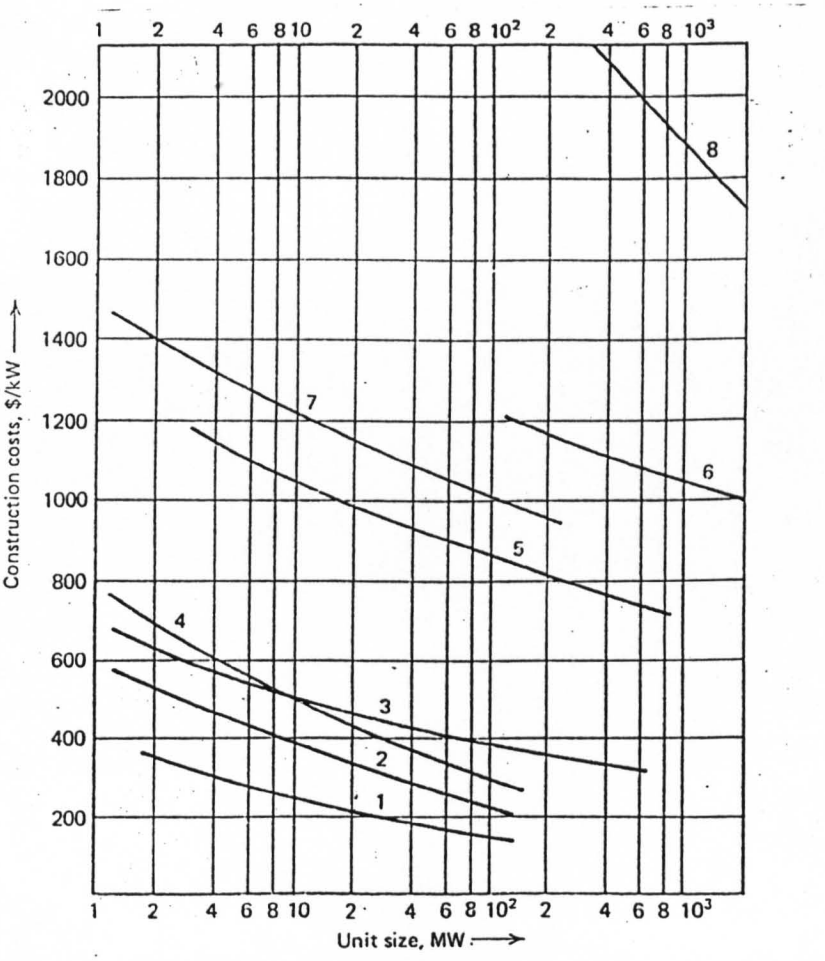

1—Jet type gas-turbine plants without recuperator.
2—Jet type gas-turbine plants with recuperator.
3—Industrial type gas turbine plants with recuperator.
4—Diesel plants for continuous service.
5—Conventional steam power plants, oil-fired.
6—Conventional steam power plants, bituminous coal-fired —2400 psia 1000 F/1000 F.
7—Low-pressure low-temperature nonreheat.
8. Nuclear power

Figure 1.5. Average construction costs for 1985 startup [9].

1.1.1.2. Costs

The costs of a generating system consist mainly of the following expenses [5]:

a) Planning and design

b) Land and site preparation

c) Building and machinery foundation

d) Plant equipment, including all transportation fees

e) Erection and start-up

f) Interest during the construction period

g) Administrative work

h) Operation and Maintenance costs.

Figure 1.5 shows average approximate construction costs for 1985 start-up in U.S. dollars per kilowatt installed. The actual construction costs are likely to vary considerably with plant location, equipment origin, and system design. In recent years, construction costs have risen considerably and will tend to rise further because of inflation and increasing demands for improved plant safety and protection of the environment.

In all types of power plant there is an economy of scale, that is, the construction costs per kilowatt decrease with unit size. Figure 1.5 indicates that the economy of scale is largest for nuclear power plants. This is mainly because several structural and equipment components such as containment, shielding, control and instrumentation cost nearly the same amount in large and small nuclear plants.

With geothermal plant the scale effect is much less pronounced for the following reasons [10]:

i) Drilling costs are more or less directly proportional to the installed plant capacity

ii) Turbo-generator costs are less subject to scale effect, partly because there is more limited choice of the maximum plant unit size and partly because admission pressures and temperatures are usually modest.

Figure 1.6 shows estimated capital costs as a function of resource temperature for the TFC power plant [11] based on 1987 prices. Capital costs are seen to vary significantly with resource temperature. The same influence of resource temperature on plant performance can also be noted in the strong sensitivity of capital cost to flow rate at lower temperatures. Although these costs are significantly higher than those for fossil fuel fixed plant and the efficiencies are much lower, the TFC can still compete with fossil fuel fixed plant, especially at outputs of less than 100 MW, due to the geothermal brine costs being much less than those of fossil fuels.

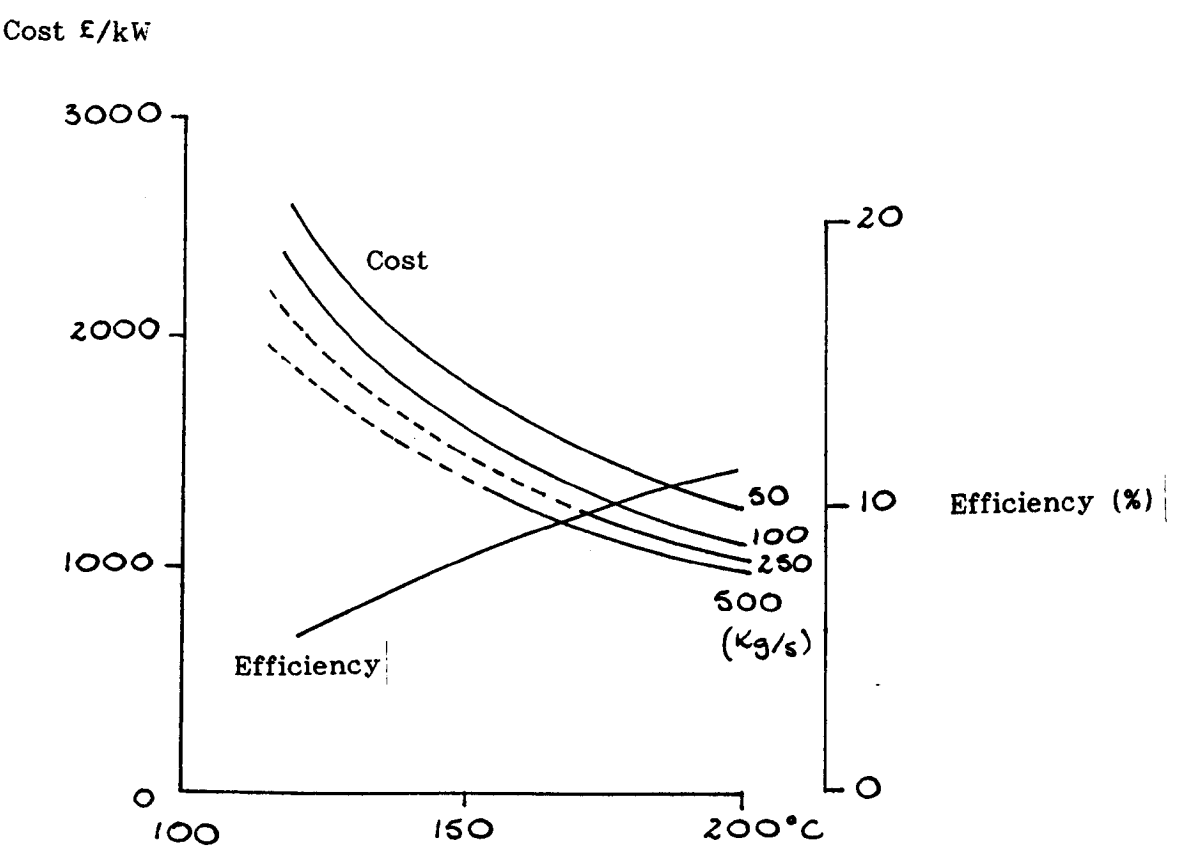

Figure 1.6. Cost estimation for TFC system.

1.1.1.3. Safety

An important aspect of power plant design, particularly in nuclear plants, is safety. Some engineering safety principles representing a set of ideals which should be met as far as reasonably practicable are [12]:

i) The plant design should be conservative and should satisfy the requirements of appropriate and accepted codes or standards. Where departures from forms of construction covered in such codes are proposed, it should be demonstrated by sound analytical methods, experimental evidence, or relevant past experience, that the proposed departures do not reduce the design safety standards.

ii) The design, manufacture and construction should employ proven techniques and it should be possible to conduct such analyses of the design as may be necessary for the purpose of demonstrating adequate integrity at any specified time throughout plant life.

iii) Every effort should be made in the design, manufacture, construction and operation to avoid the occurrence of defects in the structure. Analyses should be provided to demonstrate that at any specified time in the life of the plant:

a) an adequate margin exists between the capability of defect detecting equipment and dangerous defects,

and b) where defects are detected they can be accepted or an adequate repair made.

1.1.1.4. Environmental Considerations

1.1.1.4.1. Effects of Power Plants on the Environment

Generation of electricity from power plants gives rise to solid, liquid, gaseous and radioactive waste products which require control to prevent unacceptable pollution of air and water and interference with the use of land or enjoyment of the natural landscape. Air and water pollution can cause damage to health and agriculture and to the availability of natural water supplies. Also uncontrolled operation of many types of plant gives rise to objectionable levels of noise. The environmental control problems associated with the production of electricity are concerned with [13]:

i) Gaseous and particulate combustion products.

Carbon dioxide and monoxide, sulphur oxides, nitrogen oxides, smoke, dust and fumes from coal, oil-fired and geothermal power plants.

ii) Liquid effluents.

Oil spills and seepages from oil-fired power plants.

iii) Solid wastes.

Ash and clinker from coal-fired power plants.

iv) Waste heat

All power plants, particularly geothermal power when low thermodynamic efficiency of only 8% to 16% leads to a much greater proportion of waste heat.

v) Radioactive.

Disposal of nuclear spent fuel from nuclear reactors.

vi) Noise.

Operation of all types of plant.

vii) Damage to visual amenity and encroachment on landscape.

Chimneys, cooling towers, storage and handling installations, electric power transmission lines and equipment.

Table 1.2 displays pollutant emissions associated with generation of electricity.

Table 1.2. Pollutant emissions (means) for generation of electricity

Fuel	kg Pollutant/tce fuel				
	SO_2	NO_2	C_mH_n	CO	Dust
Heating oil	23	7	0.2	0.1	1.0
Gas	-	5	-	-	-
Hard Coal	26	7	0.1	0.5	3.5
Brown Coal	23	8.5	0.1	0.1	4.5

Source: Zur Friedlichen Nutzung der Kernenergie, Federal Ministry of Research and Technology (Ed.)

tce = tons of coal equivalent

1.1.1.4.2. Environmental Cost-Benefit Aspect

Practical solutions, however, require economic and political realities and priorities. The concept of "zero pollution" is economically impracticable and the ideal solution in socio-economic terms is one which minimizes the sum of the total cost (to the community) of environment damage and the cost (primarily to industry but ultimately to the user of the energy) of environmental protection [14].

1.1.1.4.3. Environmental impact of geothermal power

The environmental effects of utilization of geothermal energy are usually considerable. The overwhelming preponderance of pollutants from geothermal energy conversion operations will derive from the geothermal fluid itself. Other potential pollutants associated with exploration, development and facility construction phases are expected to be minor or transient in nature [15].

Geothermal vapours contain non-condensable gases, which cause serious difficulties in operating plants. The gas composition of "The Geysers" in the U.S.A. is 63.4% CO_2, 15.3% CH_4, 14.7% H_2, 3.5% Ar, 1.7% H_2S, 1.3% NH_3, 0.1% H_2BO_3 [16].

A geothermal power plant also requires a large area of land. At the Geysers a well yields about 7 MW and is effectively for a land area of approximately 1.5 km^2. So for a 1000 MW plant (about 150 wells), a surface of about 30 km^2 is needed [16].

Removal of large quantities of water can also cause shifts in the rock layers, which are the cause of "seismic effects", i.e. local earthquakes.

1.2. ENERGY SOURCES: A BRIEF OVERVIEW

A secure supply of energy is unquestionably a matter of fundamental importance, not only for an individual country, but also for all of humanity. The nature of the problem to which mankind has to address itself is surely unique in human history. It is the global task of assuring a cheap and continuous flow of energy in the massive and increasing quantities which all modern societies need both in the industrialised and developing world [17]. Therefore, it is understandable that for years, the question of future energy supply has been a central issue of public debate in all parts of the world. Despite many efforts, it is very difficult as experience shows[18] for a country to develop an appropriate plan for a future-oriented energy supply system. Although efforts are being made all over the world, it appears only partly possible for civilization as we know it, to switch from petroleum as the primary energy source to other forms of energy [19].

No widely accepted methodology exists for projecting energy supply and energy demand for periods of ten to twenty-five years into the future [20]. Most predictions of the future energy demands, both for single countries and for the entire world, have been revised downward several times in the last few years. However, it is perhaps instructive to illustrate a scenario (a term used to represent a plausible future) of probable world energy demand and fuel for the near future. This is shown in Figure 1.7, from [21].

The various curves are based on three assumptions:

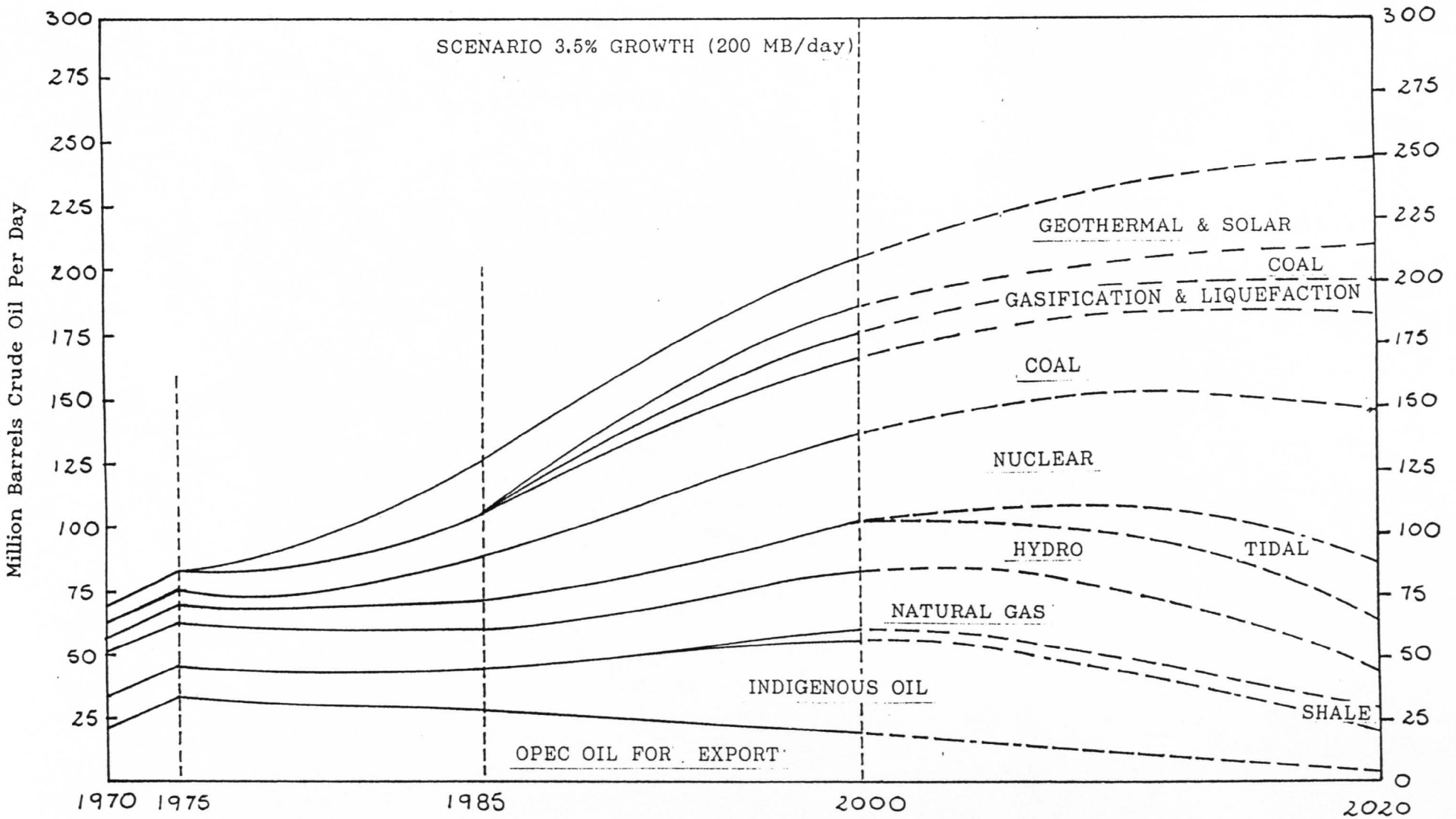

Figure 1.7. Probable World Energy Demand and Fuel Mix 1977-2000

i) that world development growth does not exceed 3.5%.

ii) that all countries put forth maximum effort in the development of alternative energies.

iii) that the actual energy savings - by means of absolute economy and more efficient utilization - reach the level of 27 million barrels per day oil equivalent (MBOE) by the year 2000 and 35 MBOE by the year 2020.

The alternatives of wind, wave, solar, and geothermal are expected to provide about 18% of the total energy by the year 2000 [21].

1.2.1. Prospective Methods of Energy Production & Some Related Technological, Economical and Environmental Problems.

There are basically two types of energy sources available to meet the energy demands of humanity: those which are found in the earth's crust (fossil and nuclear fuels) and are not renewable and those which are continuously available (solar, wind, tidal, and geothermal energy). The long-term options for energy supply derive from the division of energy sources into renewable and non-renewable types. Although there is no immediate danger of current methods of energy production being unable to cover energy demand [22], the stock of fossil fuels will be exhausted within the foreseeable future and in the opinion of the author significant attention should be paid to the development of alternative sources of energy.

For large-scale utilization, nuclear energy appears to be the best immediate possibility from a technological and economical point of view [23].

The feasibility of industrial utilization of energy, realised in the fission of heavy nuclei, has brought about a radical change in the situation that existed in the past. As a result, the fission of heavy nuclei has become quite competitive with conventional fuel in those parts of the world where the cost of the latter has increased due to transportation costs or in those countries lacking traditional energy resources.

The role of nuclear power in meeting the world's energy needs is likely to remain important [24]. Nuclear power stations serve best as generators of 'base load' electricity - that is, that proportion of a country's needs which is more or less constant. Peaks in demand are catered for principally by the use of oil, gas or coal-fired plant. A single nuclear power station, generating perhaps 1250 MW of electricity could supply a very large proportion of a small country's electricity needs [25].

The importance of using nuclear power is not limited to eliminating world fuel shortages. Nuclear power may be of social importance as well. Atomic energy may lead to the situation where all countries in the world have an equal chance, because of the high specific energy content of atomic fuels [25]. However, some of the

problems of disposal, i.e. development of storage facilities for spent fuel elements prior to their reprocessing to retrieve plutonium, the reprocessing itself, preparation of the wastes for permanent storage, and their final disposal, have not been completely satisfactorily solved, although it is said by the competent authorities that these problems are solvable.

It appears that more and more people consider the final disposal of radioactive wastes to involve a new dimension. If the fuel elements are not reprocessed the storage site must guarantee safety for many thousand years since the half-life of plutonium 239 is 24000 years [24]. In other words, the present generation is enjoying the energy released, but it is passing on to later generations the atomic waste in its permanent storage depots. Such a depot will probably always require a certain amount of watching. In this connection, people sometimes speak not only of "environmental damage" but of "damage to posterity" [26].

The incalculable "human factor" can never be completely excluded as a possible source of danger. It must be emphasized that with respect to technology, there is no such thing, as absolute security, but only a greater or lesser degree of reliability. Recent events at Chernobyl power plant have shown that there will never be an absolutely safe nuclear power plant. A reactor safety study can therefore make no prediction whether the risk associated with nuclear energy will be accepted [27].

1.2.1.2. Fusion

While a great deal of energy can be obtained by the fission of a gram of very large nuclei, such as those of uranium and plutonium, even more can be obtained by the fusion of a gram of hydrogen nuclei into heavier ones. This is the process that has kept the thermo-nuclear reactions in the sun and can supply energy to fulfil the requirements of many generations. Of course, the possibility of large-scale utilization of fusion energy still requires intensive efforts and very costly research. Although extremely difficult physical and technical problems remain to be solved, confidence is growing that by the end of the century, a pilot fusion power plant will have been built [29]. Since it is relatively uncertain when controlled nuclear fusion will be achieved, it is difficult to answer questions about the value of a fusion reactor and therefore its related costs and contribution to world's energy needs.

1.2.1.3. Hydroelectric Power

Wherever possible, hydroelectric power should be used on a large-scale. Hydroelectric power represents a generally non-polluting, reasonably low cost, and storable energy source. There is great potential for new hydroelectric plants of varying size throughout the world, since the utilization of artificially pumped storage serves to even out the load factor on power plants and to store excess output from intermittent natural energy systems.

1.2.1.4. Thermal Energy of Seas and Oceans

Humanity has not yet used the potential possibility of producing energy from the difference in temperature of the warm surface and the cool deeper ocean water. The difference can be of the order of 15°C [30]. This is an enormous reservoir of energy, but huge quantities of fluid must be pumped and massive heat-exchangers operated. Here again, before one can use the source of energy in an economically useful way, one has to solve many technological problems while the projected plant costs of around $6,000/kW make it economically unattractive at present.

1.2.1.5. Solar Energy

The potential for harnessing solar energy is immense. The amount of energy is huge but the problem lies in how best to collect it, concentrate it economically and then integrate it with existing energy systems [31]. Solar radiation is an almost ideal source of power in terms of "purity" and preservation of the thermal balance of the earth as shown in Figure 1.8.

The yearly amount of solar radiation reaching the surface of our planet is about 16000 times as much as the world's consumption of energy [31]. Thus solar radiation can, in principle, offer a new option for the power industry.

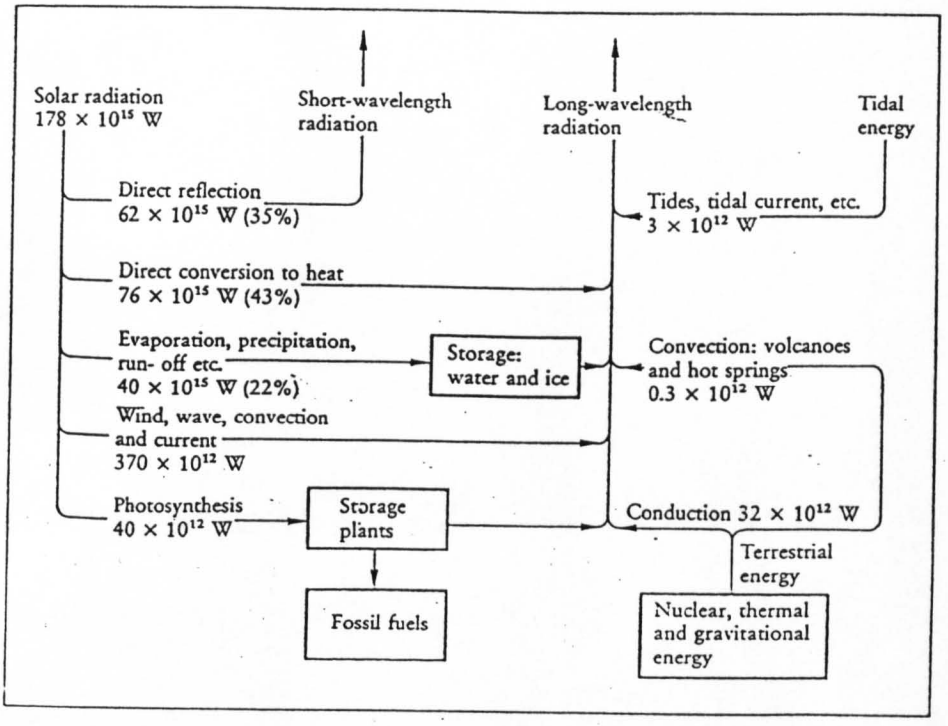

Source: World Energy: looking ahead to 2020. Report by the Conservation Commission of the World Energy Conference, Guildford (UK) and New York: IPC Science and Technology Press 1978.

Figure 1.8. The energy balance of the Earth.

In spite of promising possibilities for utilization of solar energy, its being "pure" and "free", its abundance and its almost unrestricted level of application, this source of power is not free from some major disadvantages inhibiting its utilization. Three basic features causing difficulty in its earth-board use should be noted.

(a) A low density of flux of solar radiation near the earth's surface [32].

(b) Uncontrollable and rather occasional conditions under which the solar radiation reaches the earth's surface. The density of flux of direct solar radiation on the earth's surface is less than 1 kW/m^2 [32] of incident rays. This density means

that any solar plant for generation of electrical or thermal energy must have considerable area of absorbing or reflecting surfaces since the power of this plant is in proportion to its area. A low density of employed energy to solar radiation results in high capital expenditure when constructing solar facilities and frequently calls for application of mirror-oriented concentrating systems to increase the density of the flux of the radiant energy at the radiation collector.

(c) The land required for such conversion schemes is very extensive, and the most suitable location for such systems would clearly be the desert areas of the world, where land is virtually valueless for agriculture. However, the machinery will require water supplies for the cooling side of the turbine system, which may raise important difficulties in many desert areas.

The other major difficulty stems from changeable conditions of the arrival of solar energy. A variable arrival of solar energy at a particular terrestrial spot is due to both regular causes (the rotation of the earth about its axis and about the sun, governing the daily and annual radiation) and to random causes brought by weather (clouded or cloudless sky, variation in the transparency of the atmosphere, etc.). Thus, to provide for power supplies to meet actual loads, suitable storage systems for solar energy are needed [33].

1.2.1.6. Biomass

Another possible way in which solar energy can be captured is through the phenomenon of photosynthesis in plants, trees, etc., now coming to be known as biomass. Due to collection, storage and transportation problems, biomass energy could hardly figure in the gigawatt range and its development, though useful, would essentially be confined to small units on a very localised basis [34].

1.2.1.7. Tidal Energy

Among various types of mechanical energy of the sea high tides under certain conditions may be regarded as promising for large-scale energy generation. Such conditions, however, exist at only a few points of the world ocean and construction of high-capacity tidal electric stations will scarcely take place in the next 10 - 15 years [35]. In perspective, the proportion of possible generation of tidal stations will not be of any significance in the world energy balance, even if all suitable sites on the ocean shore were used. Figure 1.9 displays a comparison of potential for energy from renewable sources.

Solar energy		geothermal energy		Tidal energy	
Energy falling on the entire earth	$192 \cdot 10^{12}$ tce/y[4]	Total heat content		Total power potential of the tides	$3.2 \cdot 10^{9}$ tce/y
Energy from utilization of solar radiation on 0.2% of the land surface at 20% efficiency	$15 \cdot 10^{9}$ tce/y	Heat content below the continents (about $150 \cdot 10^{6}$ km²)		Technically utilizable tidal power potential	$60 \cdot 10^{6}$ tce/y
		– to 5000 m depth	$\approx 8 \cdot 10^{14}$ tce		
		– to 10000 m depth	$\approx 90 \cdot 10^{14}$ tce		
Technically usable hydroelectric potential	$2200 \cdot 10^{3}$ MW	Contribution of geothermal energy of the electric capacity of the world		Contribution of tidal energy to the electric capacity of the world	
– in 1978 (installed)	$372 \cdot 10^{3}$ MW	– in 1978 (installed)	1325 MW	– in 1978 (installed)	240 MW
– in 2000 (estimated)	$840 \cdot 10^{3}$ MW	– in 2000 (estimated)	$100 \cdot 10^{3}$ MW	– in 2000 (estimated)	$60 \cdot 10^{3}$ MW to $100 \cdot 10^{3}$ MW

[4] 1 tce/year ≙ 0.928 kW 1 tce ≙ $8.140 \cdot 10^{3}$ kWh

Sources: World Energy Conference 1980: Survey of Energy Resources 1980, Munich, September 1980
World Energy: looking ahead to 2020. Report by the Conservation Commission of the World Energy Conference, Guildford (UK) and New York, IPC Science and Technology Press 1978
Federal Institute for Geosciences and Natural Resources, Hannover, Federal Republic of Germany, 1976
Essam El-Hinnawi, Energy, Environment and Development, 10th World Energy Conference, Istanbul, September 1977

Figure 1.9. Survey of Solar, Geothermal and Tidal Energy

1.2.1.8. Wind Energy

Important factors bearing upon the economic viability of wind energy in large-scale power systems are:

i) the random nature of wind, particularly its speed.

ii) its low density so that a large device is needed to extract any considerable amount of power.

iii) power output from a turbine is dependent upon the cubic of wind speed[36].

A positive feature of wind energy utilization is the annual repeatability of mean wind speeds. Other favourable aspects include:

i) reasonably small land occupancy.

ii) reasonably low environmental impact, especially with careful attention to design.

iii) continually improving cost comparison.

iv) wind power can be used in places where there are no other ways of producing energy, e.g. isolated regions such as small islands.

Classical estimates of energy expectable worldwide by land-based wind plant have been set at 3.6×10^{18} J per annum. This is roughly the order of world production of electricity in 1950[37]. A more realistic estimate needs to be made perhaps to take account of environmental constraints and the occupation of the market by other replenishable sources.

1.3. GEOTHERMAL ENERGY

Geothermal energy is one of several low-grade heat sources that recent research has rendered more attractive for recovery of power. It can be expected to make a considerable contribution as an alternative source of power generation, where heat can be harnessed at shallow depths.

Despite a long history (the first geothermal electric generation station started up at Larderello in Tuscany in 1904[38]), it was not until the relatively recent development of Wairakei geothermal field in New Zealand in the mid-1950s and Geysers in California in the 1960s that great interest began to be displayed in geothermal energy as an alternative heat source for power. Several geothermal power plants have already been built in countries which are located in the

so-called Pacific fire-belt and it is likely that additional economic geothermal areas will be developed elsewhere for electrical power generation in the near future. Armstead [39] studied the past and present growth trends (shown in Figure 1.10) and also the expected growth during the next few years.

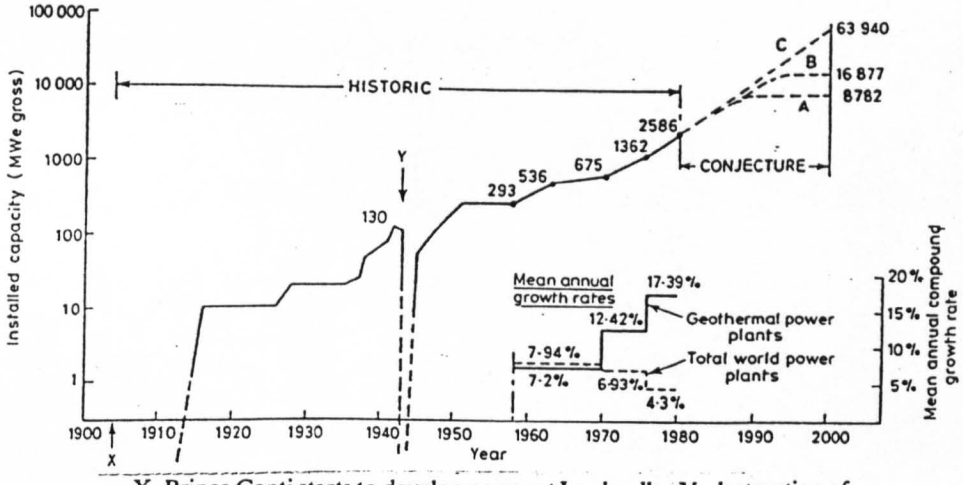

X, Prince Conti starts to develop power at Larderello; Y, destruction of Italian plant by war damage; A, definitely planned in 1980; B, tentatively planned in 1980; C, continued growth at 1976/80 rate.

Figure 1.10. World total of gross installed geothermal power capacity and growth trends.

It is interesting to notice that it took more than a half century (from 1904 to 1958) for the total geothermal electric power generation to reach 293 MW. By contrast, during the 1970s the growth of installed geothermal capacity increased sharply as the cost of conventional fuels began to rise. The total geothermal electric power installed was 4,812 MW by 1987. Curves A and B represent the growth expected based on definitely and planned construction of geothermal power plants. Curve C shows continued growth at 1976/80 rate (17.4% p.a.) extrapolated until the end of the century.

Extrapolation of geothermal growth into the future is bound to be speculative but it is not inconceivable that one day it will be possible to extract natural heat for power generation in large quantities at any convenient point on the earth's surface.

1.3.1. Geothermal Fields

Geothermal heat or natural heat can be found beneath the continents where the Earth's crust varies from 25 to 40 km of thickness [40]. It bears to the rest of the planet a similar relationship to that of an eggshell to an egg except that it is far from uniform. An interesting characteristic of the Earth's surface is that it works as a very effective insulating blanket which moves slowly over the underlying mantle. In reality it is not a continuous shell but consists of plates. In the regions where these plates are thinned, weakened, or fractured, molten rock has been able to intrude to shallower depths. According to theory of Plate Tectonics, thermal effects of plate interaction often extend several hundred kilometres from the boundary[40] and these zones are sometimes associated, though not always, with volcanic activity. It is within these active zones (e.g. Pacific fire-belt) that most geothermal fields are located [41]. Looking into the future when it may perhaps become possible to win natural heat at any place on the earth's crust we shall of course extract geothermal energy as closely as possible to the markets. At present, however, we are constrained to exploit this form of energy only where it can be tapped.

If the geothermal field is of good quality and capacity, the generation of electricity could perhaps economically justify the transmission of power over one or two hundred kilometres or even more. Differences of geology, underground permeability, fluid temperature, fluid corrosiveness, capacity of installation, site assessibility, local wage levels and other local factors can result in very wide differences in costs between two or more developments constructed at the same time in different parts of the world [40,41]. Figure 1.11. displays a schematic diagram of a characteristic geothermal reservoir in a permeable rock showing possible heat transfer and fluid circulation after White [42].

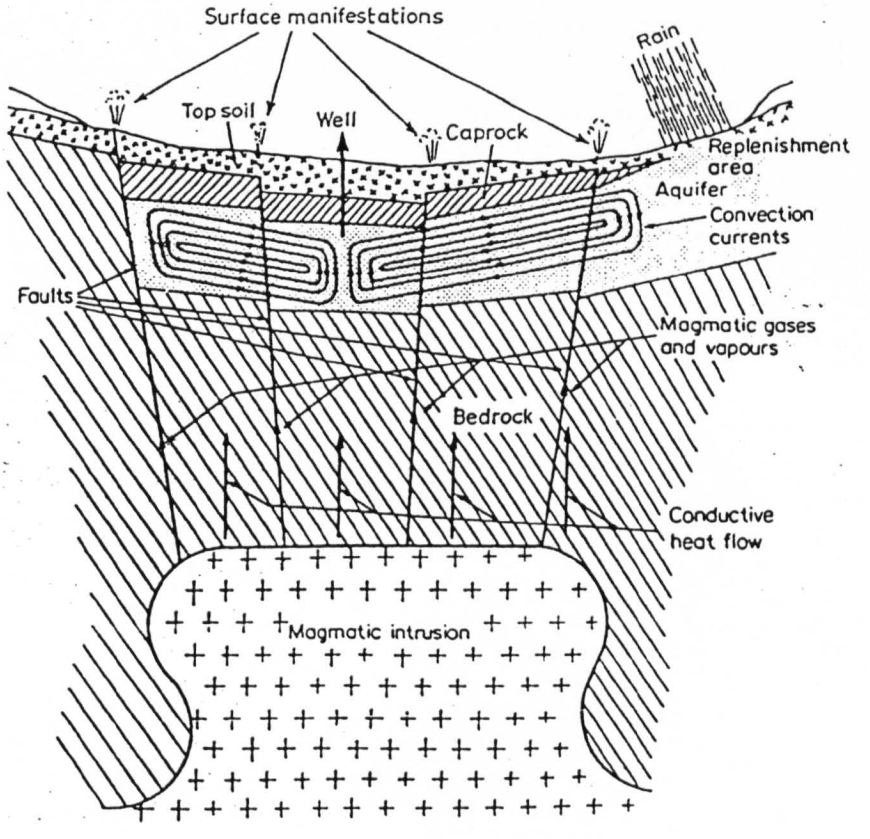

Figure 1.11. Schematic diagram of geothermal reservoir.

Disregarding the complex geological details, a geothermal field may be defined [43] as a thermal area where the presence of permeable rock formation underground allows the containment of a working fluid without which the area could not be exploited. The working fluid-water and/or dry steam serves as a medium for conveyance of underground heat.

Depending on geological circumstances, exploitable geothermal fields may be broadly classified into three groups: [43]

(i) vapour-dominated or high-enthalpy fields

(ii) liquid-dominated or low-enthalpy fields

(iii) hot dry rock or petrothermal fields.

1.3.1.1. Vapour-dominated fields

In this category the underground fluid is stored as superheated steam. In these reservoirs the pressure is not high enough to prevent underground boiling and a drill hole into the reservoir produces superheated steam, which under suitable pressure after filtering can be fed directly into a turbine generator. This type of geothermal field is the most favourable economically [44] for power generation. However, it is estimated [45] that only about one-twentieth of geothermal resources fall into this category.

1.3.1.2. Liquid-dominated fields

In the liquid-dominated or low-enthalpy fields the underground fluid persists as liquid water occasionally containing a small percentage of steam. Extensive amounts of geothermal energy occur in the form of hot water (normally a dilute aqueous solution, although some brines are far from dilute containing up to 30% of dissolved solids) [46].

1.3.1.3. Hot dry rock fields

In a petrothermal or hot dry rock field no, or very little, water is available and energy can be extracted by hydraulic fracturing to create a large crack connecting two drilled holes and then operating the system as a closed pressurized-water heat-extraction loop [47].

Figure 1.12 shows histograms of depth and penetration rates for geothermal wells in the Imperial Valley and The Geysers [48].

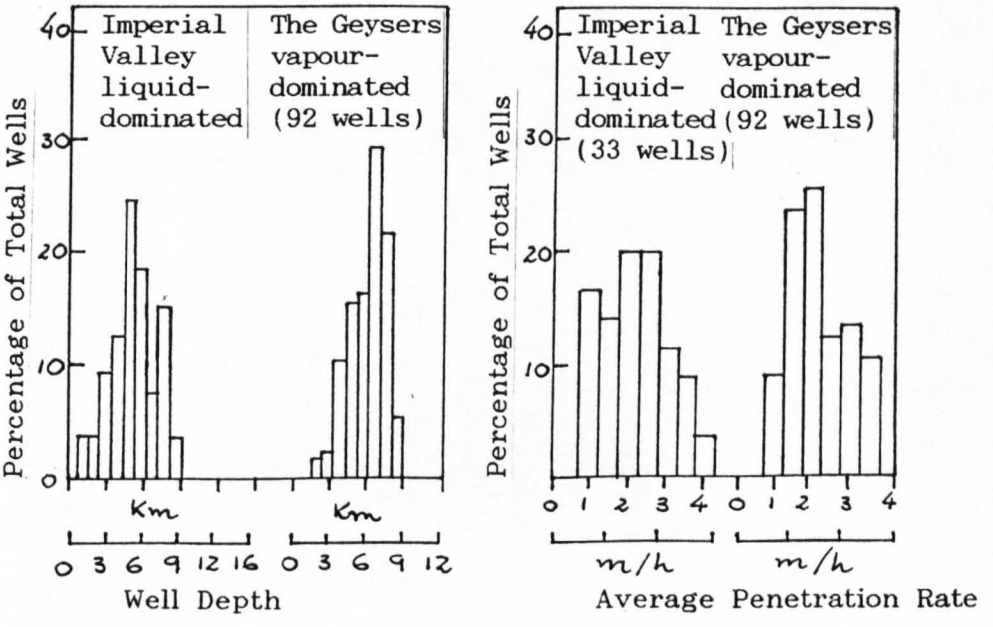

Figure 1.12.

1.4. GEOTHERMAL POWER CONVERSION CYCLES: A BRIEF PRESENTATION

A variety of systems for the recovery of power from geothermal sources has been proposed and tested over the past twenty years. The choice of the most suitable is still a subject of controversy [49]. Most investigations of geothermal power have agreed that if wells producing dry steam (vapour-dominated fields) are found, the use of steam directly in turbines is the preferred means of developing mechanical or electrical power [50]. However, if a geothermal field is liquid-dominated the same degree of unanimity is not found [51].

1.4.1. Flash Steam system

The most commonly used conversion process for power generation from hot brine is the flash steam process. The two-phase well head mixture is piped to a flash vaporizer or vessel where the pressure is reduced, causing part of the brine to vaporize. Steam and brine enter the separator drum in which steam and brine are separated. The brine flows to a reinjection well or other disposal area. Steam exits the separator entering the turbine for power generation and is then condensed at a pressure below atmospheric pressure for disposal or for use in the cooling tower.

When the brine contains a high proportion of dissolved solids a scrubber is normally used to remove entrained salts. Figure 1.13 shows a schematic diagram of a flash steam process with one flashing stage. Its corresponding T-s diagram is shown in Figure 1.14.

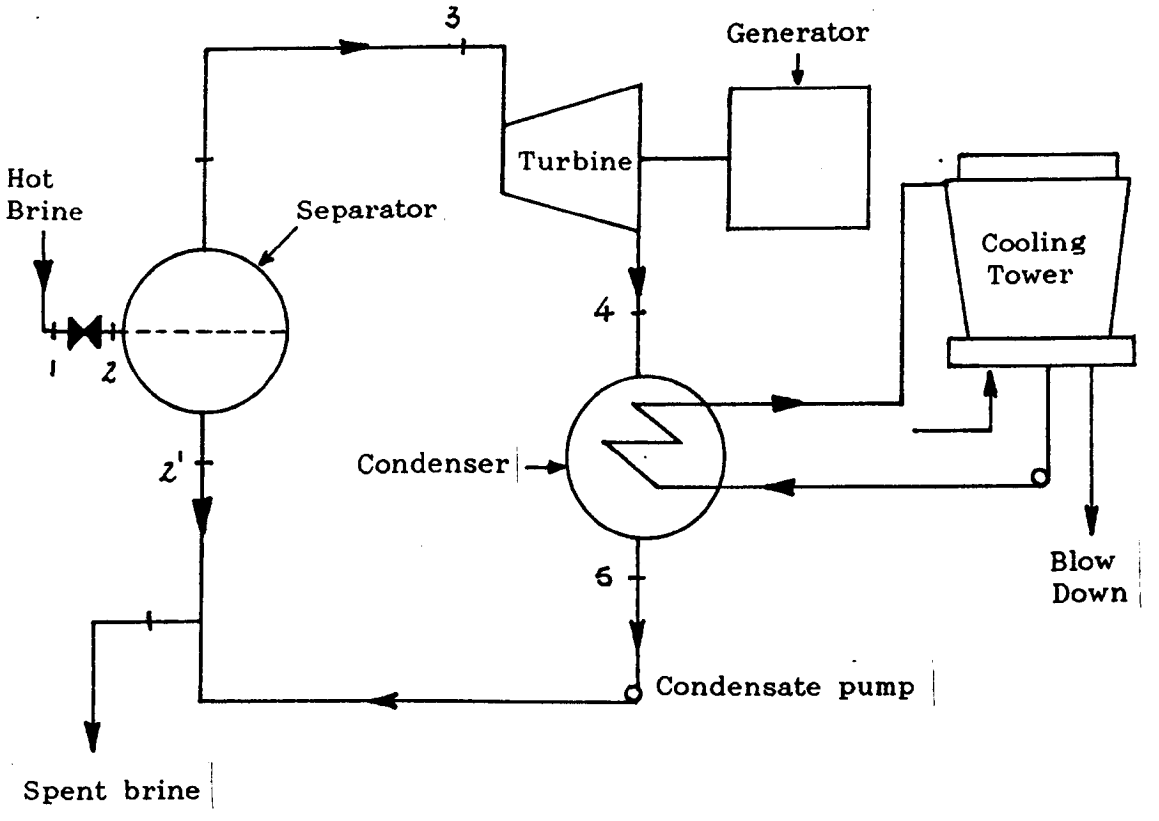

Figure 1.13. Flow diagram of a Single-Flash system

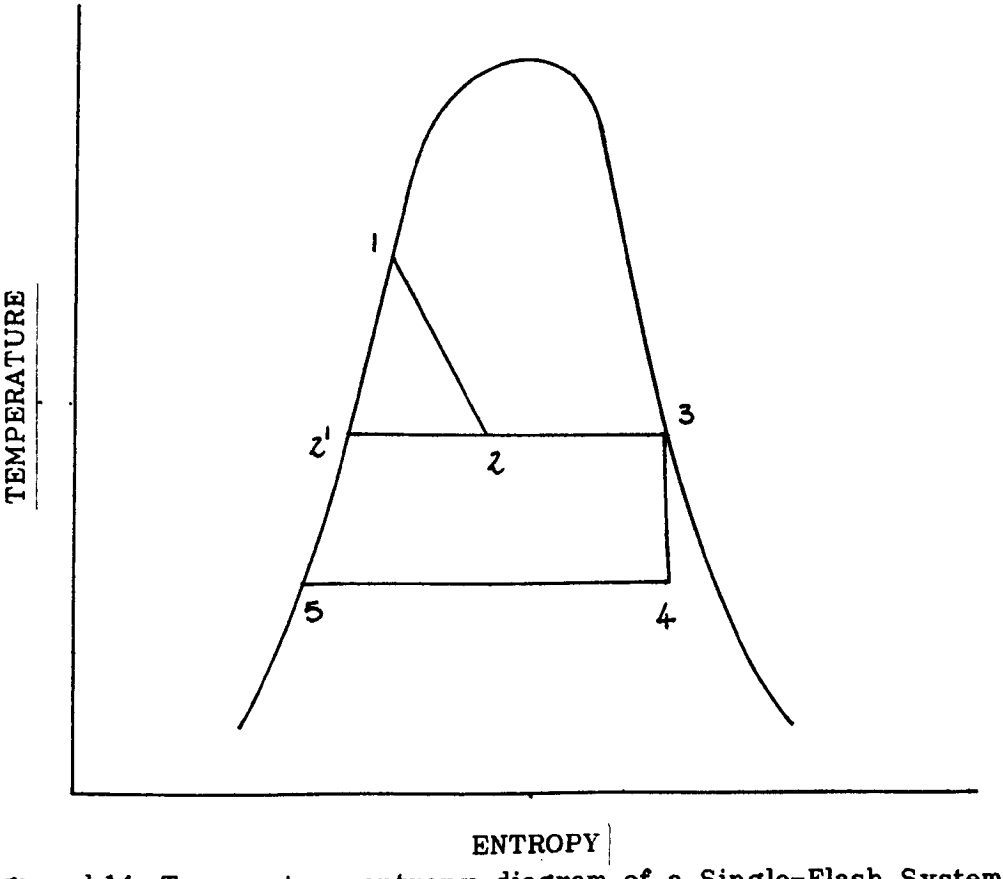

Figure 1.14. Temperature-entropy diagram of a Single-Flash System

Ideally, the maximum power would be extracted from a well head mixture in a liquid-dominated field by using an infinite number of flash-vessels each connected one to each individual turbine stage. In practical systems where economic considerations generally outweigh thermodynamic reasoning, the number of flash stages will be limited to two. A double flash steam flow diagram is shown in Figure 1.15.

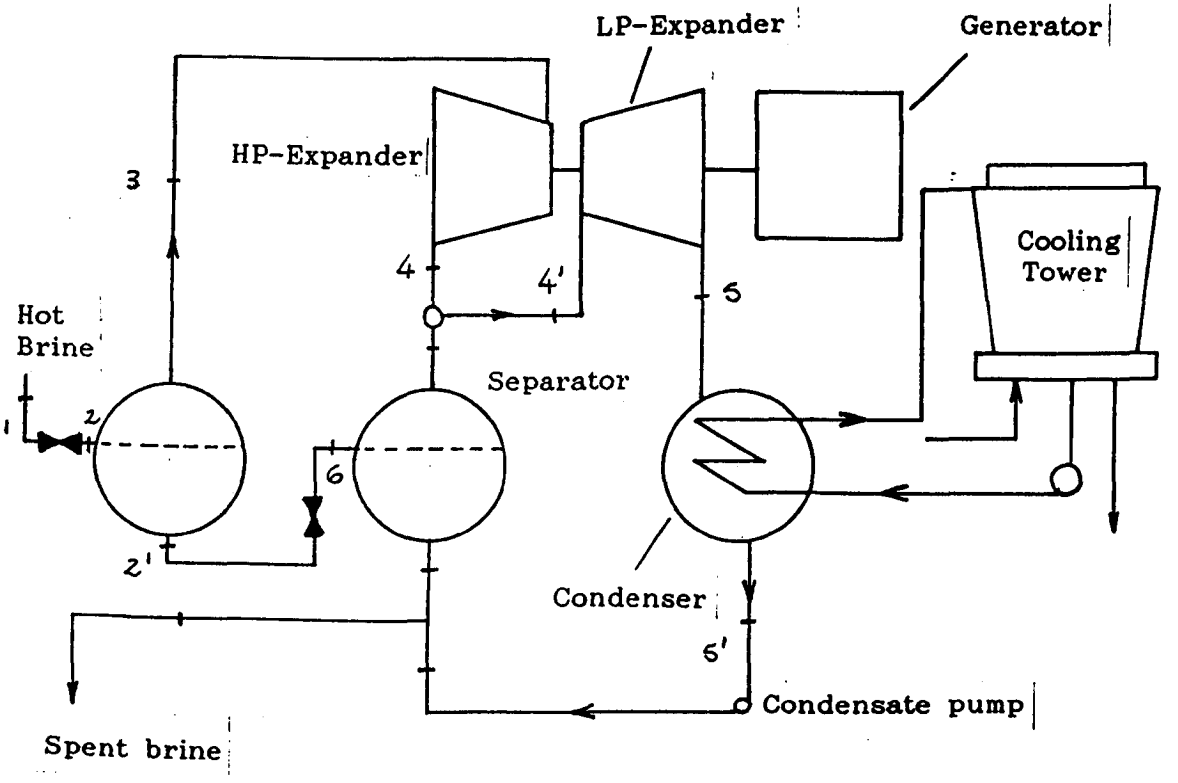

Figure 1.15. Flow diagram of a Double-Flash system

The hot brine from the first stage separator flows to the second stage flash vessel, where the pressure of the brine is reduced to that of the steam leaving the first stage steam turbine. The resulting steam and brine mixture is separated in the second stage separator. The steam from the second stage separator joins the steam leaving the first turbine and enters the second stage turbine.

If the pressure in the second stage separator is below atmospheric a pump is required for removal of the separated brine.

A T-s diagram of the Double-flash process is displayed in Figure 1.16.

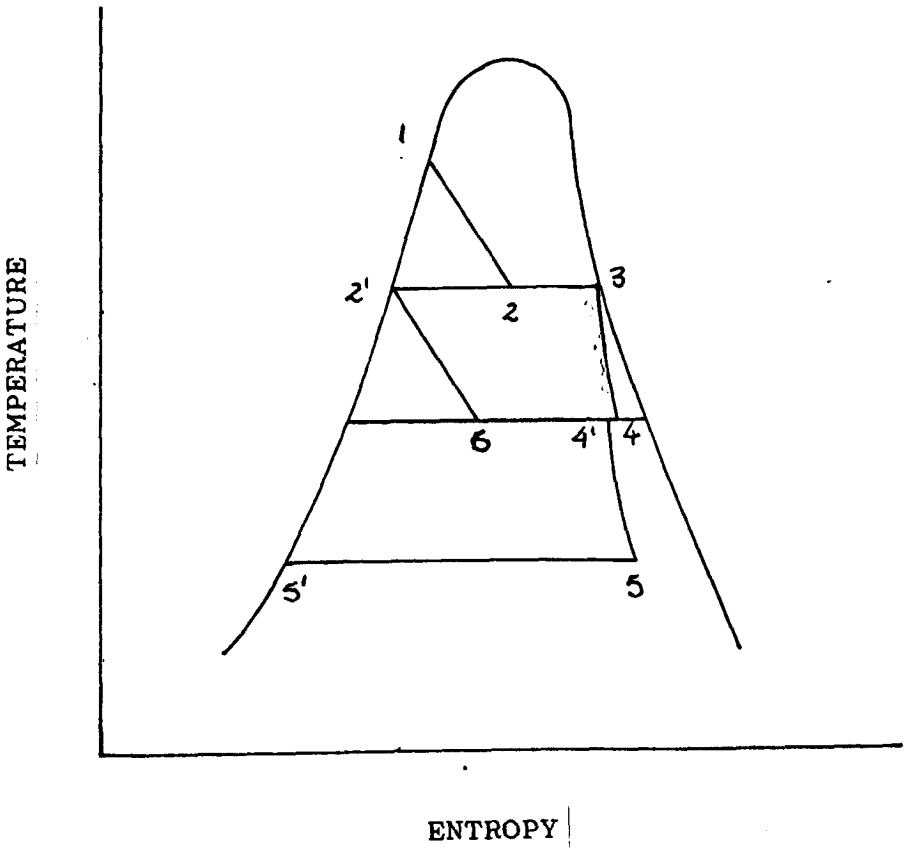

Figure 1.16. Temperature-entropy diagram of Double-Flash system.

The main advantages of the Flash Steam cycle are as follows:

i) It is a well-established system and depending on the temperature of the geothermal brine the dual flash cycle will produce between 20% to 30% more power than a single flash system with the same brine rate [52]. The gain achieved results from more of the brine heat being converted to turbine output power.

1.4.2. Total Flow System

Another method is the Total Flow process which expands the entire mixture well head flow to condensing temperature while at the same time extracting the available work. In this process shown schematically in Figure 1.17, the total brine-steam mixture flows directly through a mixed-phase expander to drive a turbine generator. Figure 1.18 displays a temperature entropy diagram for the Total Flow concept.

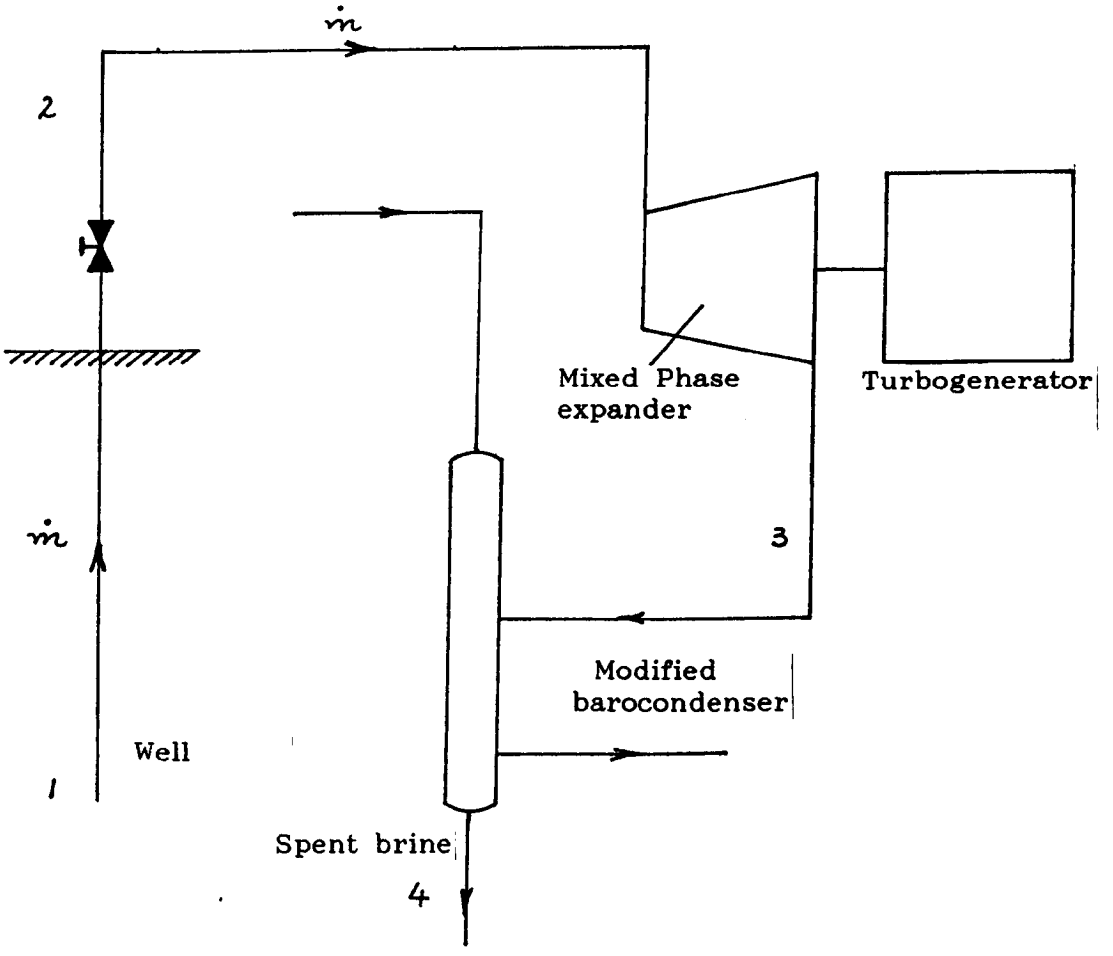

Figure 1.17. The Total Flow Concept.

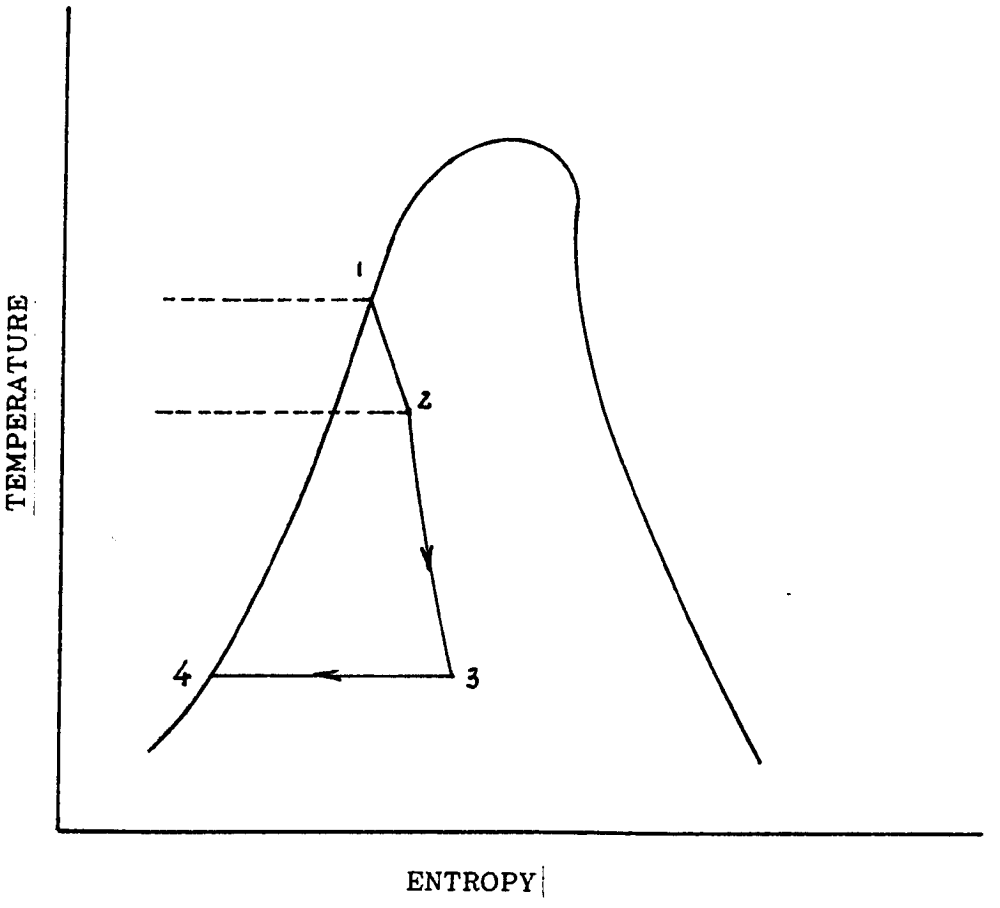

Figure 1.18. Temperature-entropy diagram of Total Flow.

Although the Total Flow concept is simple and would provide the most direct means of geothermal energy conversion, efficiently and at low cost, two deficiencies were found which to date have not been overcome. These are:

i) The poor adiabatic efficiencies of two-phase expanders.

Experiments on Lysholm twin screw, biphase and rotary separator turbines have shown that, with water as the working medium, maximum adiabatic expansion efficiencies of only 65% appear to be attainable [55].

ii) Water as the working fluid involves enormous volume ratios and machine sizes if expansion below 200°C is desired. Thus, rotor diameters of the order of 4 m or more[56] would be necessary to recover 10 MW output from a single unit.

1.4.3. Organic Rankine Cycle or Binary Cycle

Unlike the flashed steam cycle, this system does not use the geothermal brine as the working fluid in the power plant. Instead the geothermally heated water is used as the heating medium only to supply heat to a separate more volatile fluid which operates in a closed-loop Rankine cycle. Figure 1.19 displays a schematic diagram of a binary cycle.

Figures 1.20 and 1.21 display T-s diagrams of subcritical and supercritical binary cycles.

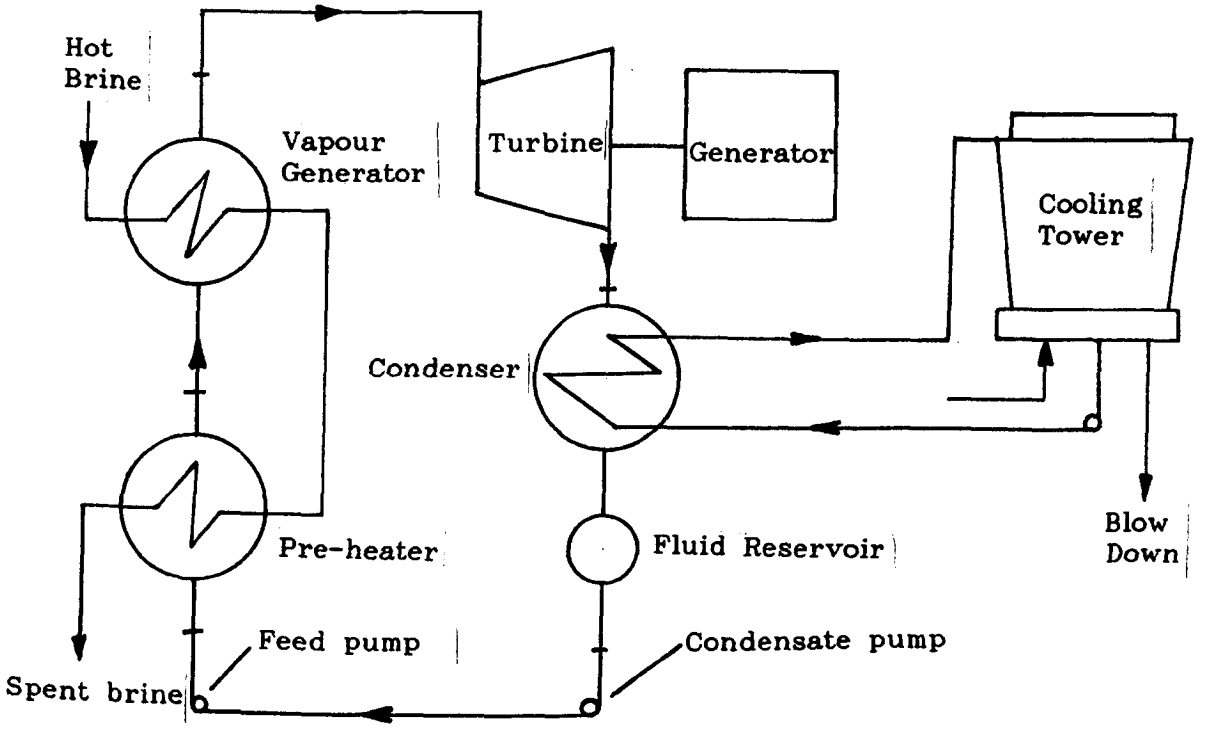

Figure 1.19. Flow diagram of a Binary System

The well head flow, if two-phase, enters a separator and the steam leaving the separator flows through the steam exchanger where the steam is condensed by heat transfer to the organic working fluid. The organic working fluid undergoes a sequence of pressurization in the liquid-phase, heating, evaporation and expansion in a turbine from which work is extracted. It is liquefied in a condenser by heat transfer to the coolant fluid or to atmosphere and finally returned to the heat exchanger inlet by a feed pump. The condensate of the geothermal steam joins the brine and flows through the liquid heat exchanger where the liquid is cooled further by heat exchange to the organic working fluid. The liquid is then rejected to waste or to a disposal area.

The main advantages of this sytem are as follows:

i) Organic fluid cycles have higher cycle efficiencies than steam cycles for the same heat input conditions because higher fluid temperature can be achieved.

ii) It can make use of geothermal fluids that occur at much lower temperatures than would be economic for flash utilization.

iii) It enables use to be made of geothermal fluids that contain high proportions of non-condensable gases. These fluids result in a serious penalty for Flash Steam systems.

iv) It confines chemical problems to the heat exchanger alone.

v) The high molecular weight of organic fluids and the higher condenser pressures associated with greater volatility require the use of turbines which have much smaller diameters and fewer stages than their steam equivalent. Therefore the turbine costs are much reduced.

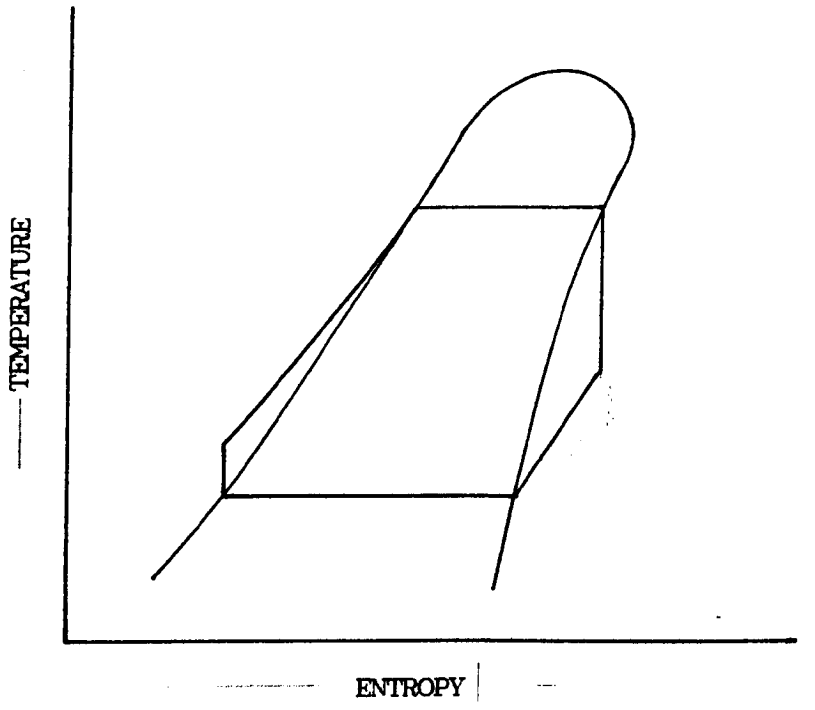

Figure 1.20. Temperature-entropy diagram of subcritical organic Rankine cycle (Binary cycle).

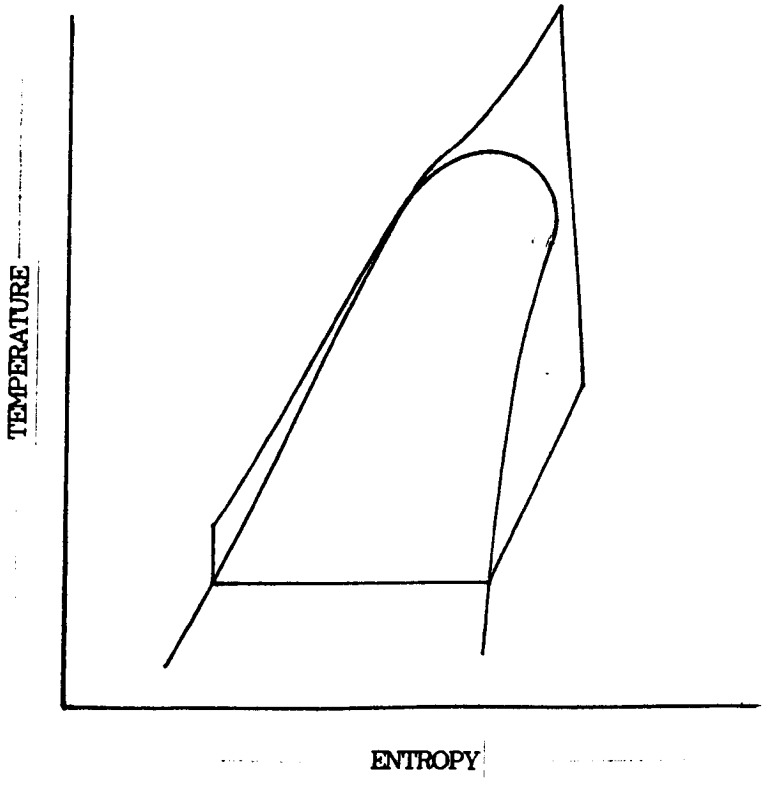

Figure 1.21. Temperature-entropy diagram of supercritical organic Rankine cycle (Binary cycle).

ii) Low cost, although in the dual flash cycle system additional secondary steam lines are required on a single unit to accommodate the large specific volume flow of low-pressure secondary steam. Therefore the increase in performance must be weighed against additional costs.

iii) In some cases the temperature of the condenser cooling tower can be raised to a high enough temperature to supply heat to a district heating system (i.e. in excess of 60°C [53].

Some disadvantages associated with the Flash Steam cycle are as follows:

i) Any noncondensables in the steam must be pumped from the condenser to atmosphere by mechanical pumps or by steam ejectors using steam that would otherwise drive the turbine. Carbon dioxide is of particular concern not only because it is frequently present in very large concentrations but it is also essential that it should be released during the initial reduction in pressure at the primary steam flash. Normally the concentration of CO_2 in the hot brine declines with use, but if it remains high, extra pump work required to effect its removal from the condenser can in some cases be prohibitively high [54].

ii) If the geothermal fluid is not of sufficiently high grade for steam turbines to be applied efficiently and economically an alternative cycle should be considered.

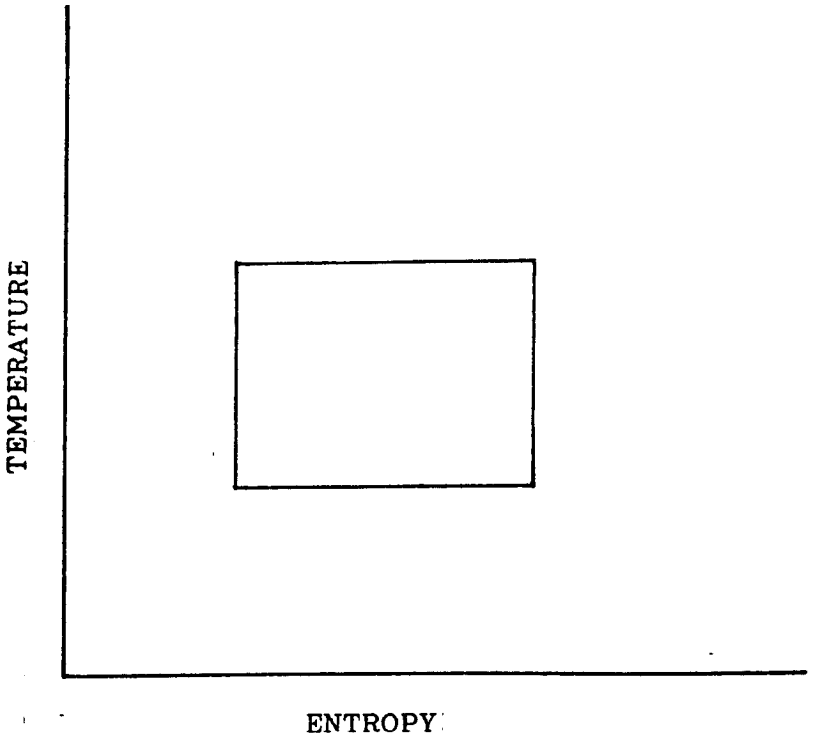

Figure 1.23. Carnot cycle temperature-entropy diagram.

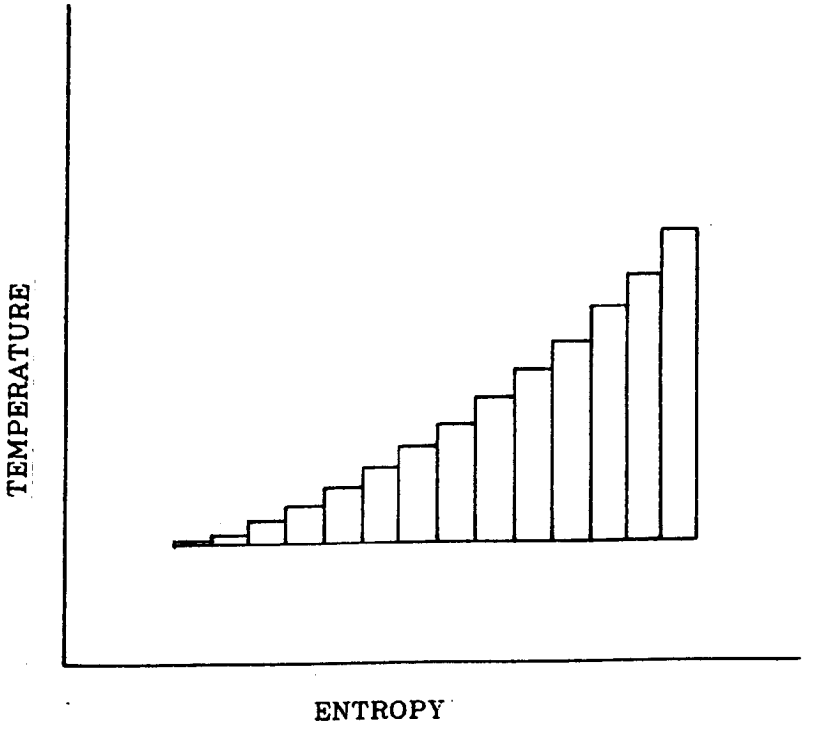

Figure 1.24. Infinitesimal Carnot cycle temperature-entropy diagram.

A thermodynamic appraisal of this cycle demonstrating its usefulness was also indicated by Wilson and Radwan [58]. Figure 1.25 displays a temperature-entropy diagram of a more accurate approximation of what Wilson called an ideal Trilateral cycle. It can be shown that its efficiency is given by:

$$\eta = \frac{(T_1 - T_2) - T_2 \ln \frac{T_1}{T_2}}{T_1 - T_2}$$

where T_1 is the temperature of the heat source.

T_2 is the temperature of the heat sink.

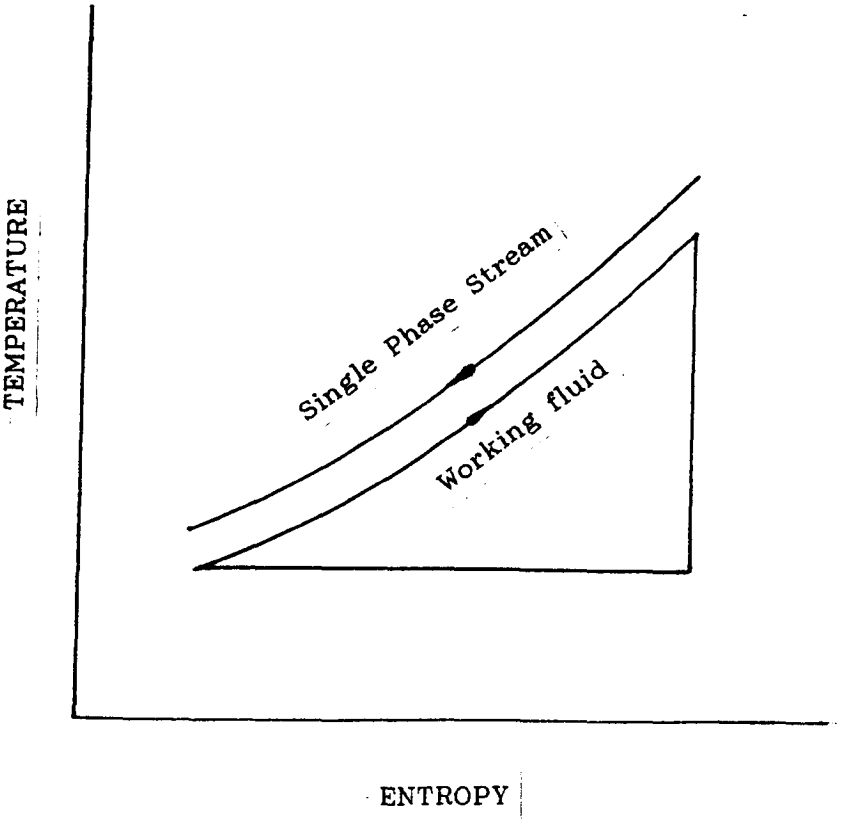

Figure 1.25. Temperature-entropy diagram of Ideal Trilateral Cycle.

vi) Most organic fluids have a positive slope saturated vapour line as shown in Figure 1.20 and the expansion in the turbine is of dry vapour only. This leads to higher expansion efficiencies than are possible from wet steam turbines especially at the relatively small outputs of geothermal power plants.

There are, however, the following disadvantages:

i) It necessitates the use of heat exchangers which are expensive, wasteful in temperature drop and can be the focus of scaling.

ii) Because of imperfect matching between the hot water and the organic fluid it is not possible to achieve simultaneously a good recovery of heat and an optimum cycle efficiency as shown in Figure 1.22 for a subcritical cycle.

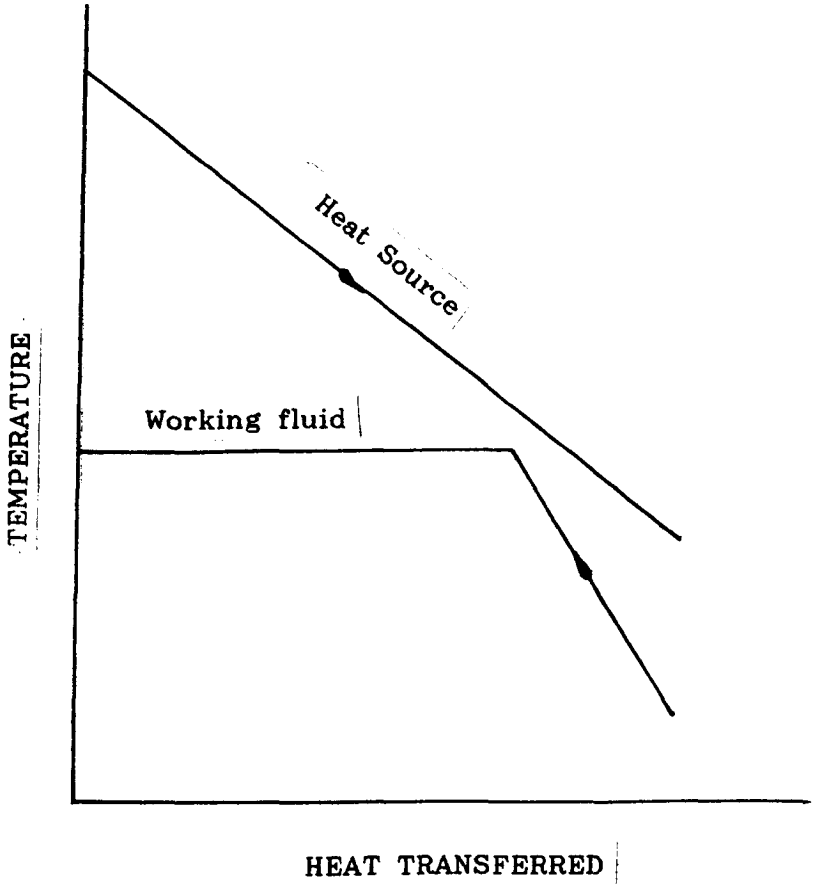

Figure 1.22. Organic Fluid-Heat source match

iii) The positive slope of the saturation vapour line generally leads to some lost work in the turbine due to the working fluid leaving it in the superheated state. The desuperheating thus needed prior to condensation can, in some cases, be used to preheat the working fluid before entry to the boiler in a regenerator. However, this would lead to a further reduction in the amount of heat recoverable in the heat exchanger from the geothermal hot water. This drawback may be overcome if an isentropic saturation vapour-line working fluid is used such as iso-Pentane.

iv) Organic fluid condensers are more expensive than steam condensers due to the poor heat transfer properties of organic working fluids.

v) The toxic and flammable properties of organic fluids imply that much higher safety standards are needed for their containment than for water in Steam Rankine plants and hence Organic systems are more expensive.

vi) Large quantities of cooling water are needed.

vii) Most organic fluids are thermally unstable restricting the number of possible working fluid choices.

1.5. THE IDEAL TRILATERAL CYCLE

When power is to be recovered from a heat source in which the transfer of heat is dependent upon a fall in resource temperature, such as geothermally heated water, then the ideal cycle is not the Carnot cycle (see Figure 1.22). Smith [57] has shown that this ideal thermodynamic cycle should be instead a succession of infinitesimal Carnot cycles. This is represented in a temperature-entropy diagram in Figure 1.24.

1.5.1. The Trilateral Flash Cycle

The Trilateral Flash cycle can be said to fall into the same category as the Organic Rankine cycle. However, unlike the latter, the working fluid is heated in the liquid phase only and its phase changes during the expansion process whose condition may be either wet, saturated or even superheated depending on the characteristics of the working fluid as shown in Figures 1.1 and 1.3. This leads to a much better matching between the heat source and working fluid than is possible with an Organic Rankine Cycle as shown in Figure 1.20. Instead of a turbine, the Trilateral cycle uses a Lysholm twin-screw machine as the expander [59].

Hence the overall conversion efficiency of the TFC system is considerably higher as can be seen in Figure 1.26, where the conversion efficiency or utilization efficiency defined by Smith (see Ref.57) and Elliott [60] is as follows:

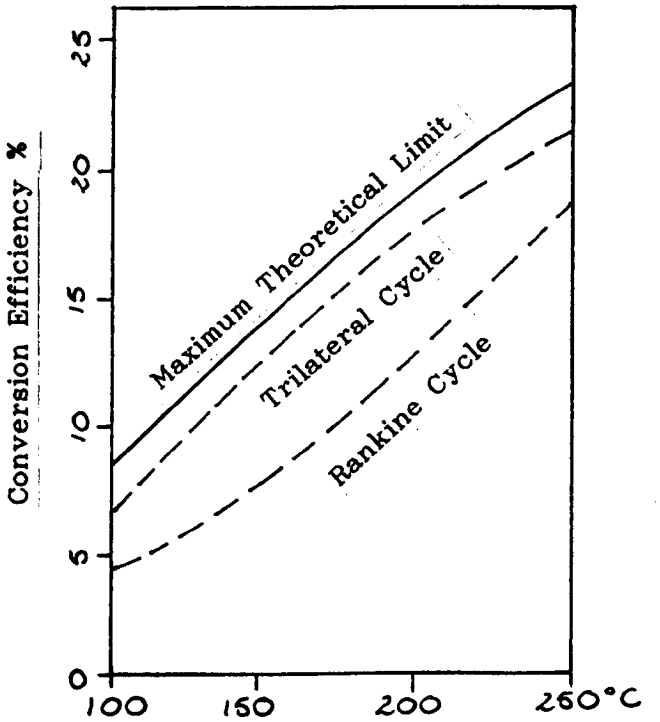

Figure 1.26. Conversion efficiency versus Source Inlet Temperature °C [57]

Conversion efficiency = Cycle efficiency x Recovery efficiency.

The recovery efficiency being defined as the ratio of actual to available source-fluid temperature drop as follows:

$$\eta_{rec} = \frac{T_A - T_B}{T_A - T_C}$$

where η_{rec} = the recovery efficiency

T_A = the initial temperature of source fluid

T_B = the final temperature of source fluid

T_C = the condensing or rejection temperature

These temperatures are illustrated in Figure 1.27.

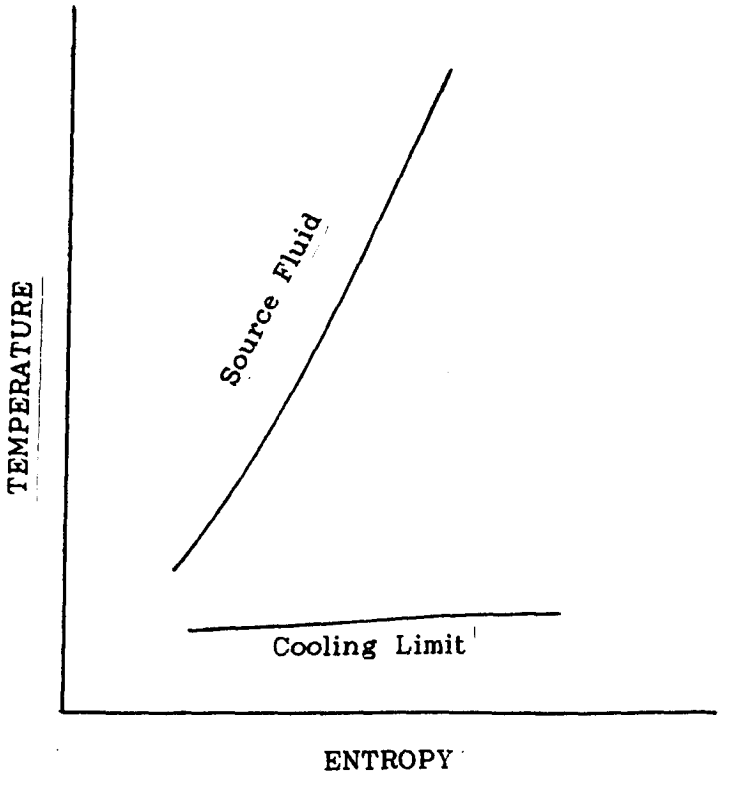

Figure 1.27. Heat source and cooling curve.

The main advantages of this sytem are as follows:

i) Its ability to absorb nearly all the available heat from a single phase fluid stream.

ii) Its feature of supplying heat to the working fluid at high temperature.

iii) Higher overall conversion efficiencies than organic Rankine cycle systems.

iv) All other advantages associated with organic Rankine systems mentioned previously except (vi).

However, there are also some disadvantages associated with the Trilateral Flash system.

i) A rather large volume change in the expansion process.

ii) The working fluid feed pump work is relatively large because of low enthalpy drop of the volatile fluid during the expansion process.

iii) The primary heat exchanger, with its very small log mean temperature difference and the twin-screw expander are both more expensive than the heater and turbine of organic Rankine cycle systems.

iv) As with organic Rankine cycle systems, the toxic and flammable nature of organic fluids imply a power plant built to a higher standard of safety. Hence, it is more expensive than a steam-turbine plant.

v) Thermal stability criteria should be taken into account when choosing suitable organic working fluids.

vi) Large quantities of cooling water are needed.

1.6. THE TRILATERAL FLASH MULTI-STAGE EXPANDER SYSTEM AND BINARY MIXTURES

As was pointed out by Wilson and Radwan[61] the design of a thermal power plant can be seen as an optimization procedure of its different parts. Essentially, it consists of matching heat source and heat sink with thermodynamic cycle, cycle with working fluid, working fluid with expander and expander with load characteristics. The working fluid/expander match is fundamentally a matter of choosing an expander to extract the maximum possible work from the working fluid. However, the expander efficiency is not the only criterion and often the size and weight of the expander is of great importance.

Extensive studies carried out by House [62] at the Lawrence Livermore Laboratory on possible applications for the helical rotor as an expander for the Total Flow conversion scheme have shown exceedingly large diameters. His results are summarized in Table 1.3.

Power Output (MW)	Rotor Diameter (m)	Length (m)
40	9 - 12.7	13.5 - 19
10	4.5 - 6	6.5 - 9.5
5	3	3 - 4.5

Table 1.3. Rotor Diameter and Length for Total Flow System

As a class, positive-displacement machines, such as the helical rotor are limited in volume flowrate capacity, relative to turbomachines. This is related to the fact that positive displacement machines have much lower velocities and smaller flow cross-sectional area than turbomachines. Therefore these expanders must be physically large to produce significant power output. Figure 1.28 shows a helical rotor which operates by direct expansion of two-phase fluid meshing rotors.

However, Smith [see Ref.57], noted that if an organic working fluid were used in place of water the volume ratio in the expansion process could be reduced from 3900 : 1 to approximately 100 : 1 while the volume flowrate at exit and therefore machine sizes could be reduced by a factor of approximately 10. His investigations were related to the practicability of the Trilateral Flash power plant on a comparative basis to the well established organic Rankine cycle. Examples of these comparisons are given in Tables 1.4 and 1.5. Turbine efficiencies of 80% and screw expander efficiencies of 78% were assumed. Supplies of 75 kg/s of geothermally heated water as the heat source and cooling water at 20°C were considered.

Fluid	Source Inlet Temp.	Nett Power Output	Turbine Power	Feed Pump Power	Volume Ratio of Turbine Expansion	Turbine Exit Volume Flow Rate
	°C	kW_e	kW	kW_e		m^3/s
Water	150	2058	2330	0.5	6.7	200.6
R.12	150	2063	3330	479.0	4.1	4.1
R.113	150	2241	2464	38.2	6.0	24.6
	100	590	682	7.3	2.5	12.8
R.114	150	2509	2910	188.0	6.5	8.0
	100	581	702	33.8	2.3	3.6
n-Pentane	150	2348	2598	56.0	5.7	18.0
	100	578	674	10.9	2.5	8.9

Table 1.4. Rankine Cycle System Characteristics

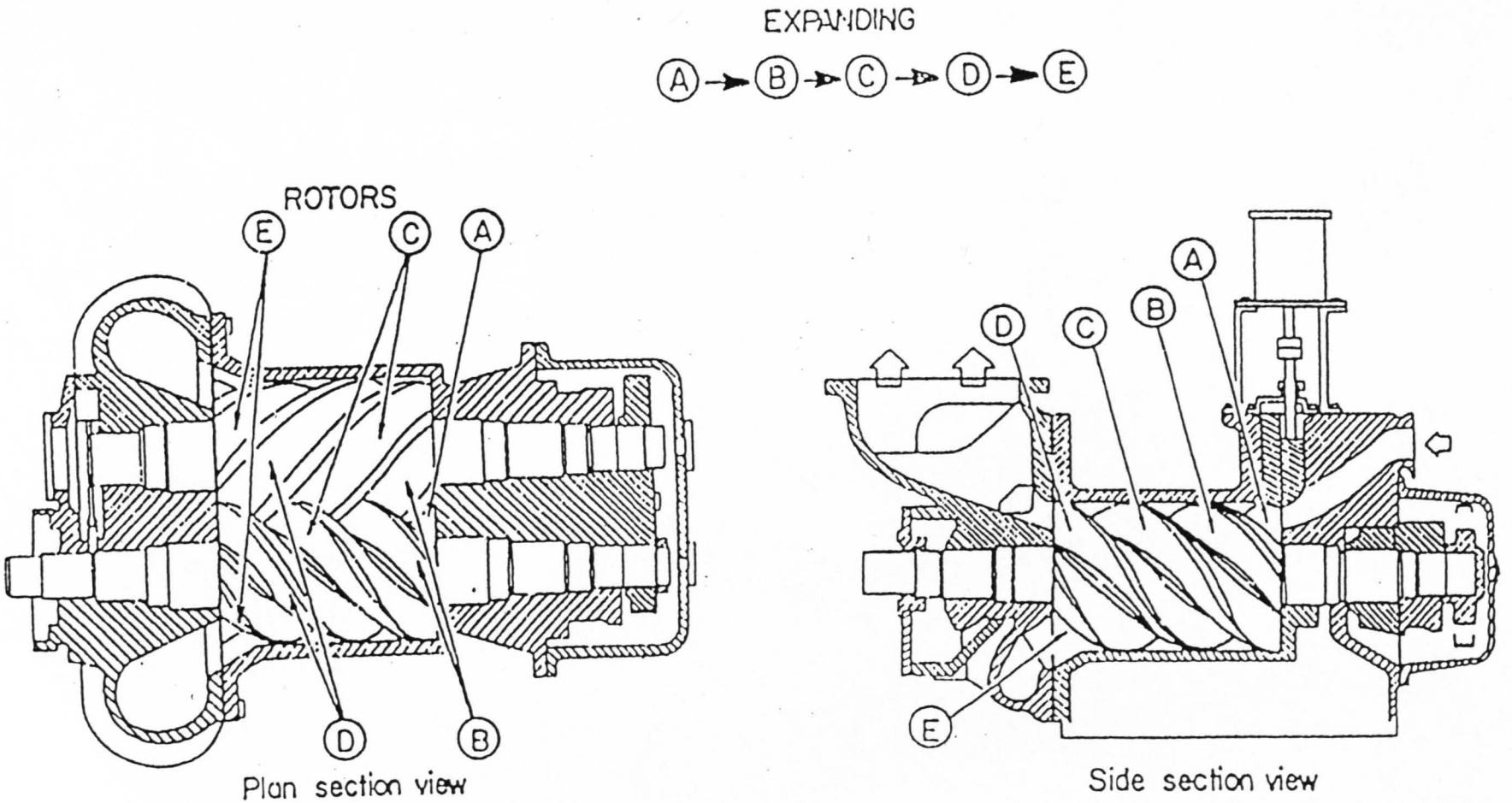

Figure 1.28. The helical rotor.

Fluid	Source Inlet Temp.	Nett Power Output	Turbine Power	Feed Pump Power	Volume Ratio of Turbine Expansion	Turbine Exit Volume Flow Rate
	°C	kW_e	kW	kW_e		m^3/s
Water	150	3685	4027	43	3989.0	329.8
R.11	150	3333	4196	556	71.0	22.0
R.113	150	3474	4077	301	165.9	44.9
	100	1156	1428	102	109.4	26.4
R.114	100	1020	1486	291	29.2	7.1
n-Pentane	150	3520	4181	355	118.8	30.3
	100	1075	1369	128	76.2	17.6

Table 1.5. Trilateral Flash Cycle System Characteristics

The principal uncertainty in estimating the potential performance of a Trilateral Flash cycle system is the evaluation of the expander efficiency since all other components are identical to those of an organic Rankine cycle system. However, it should be noted that the close matching of the working fluid and heating medium temperatures as well as more rejected heat in the Trilateral system give rise to a larger and more expensive heater and condenser than in their Rankine system counterparts. Further detailed studies involving cost estimation of key components revealed that a viable trilateral system would have to have a two-phase expander whose efficiencies would fall in the 70 - 75% range. This study was based on an assumption that organic Rankine turbine efficiencies vary between 75 - 80% according to manufacturer's brochures [63]. A test rig was then set up at The City University Thermo-Fluids Research Laboratory to assess experimentally the potential of this novel heat engine. Successive runnings revealed that adiabatic expansion efficiencies of over 70% were possible at power outputs of as little as 30 kW from Lysholm twin-screw expanders using common refrigerants as working fluids [see Ref.57].

Other types of two-phase expanders were thought by Smith[57] as suitable for very high liquid content. These are:

i) a two-phase turbine

ii) a rotary vane positive displacement machine

iii) a single screw positive displacement machine.

Early studies by Burkett [64] demonstrated that the building of two-phase turbines had not been successful. Screws and vanes due to their limited volume flowrate capacities are only suitable for relatively small power outputs if expanders are to be kept at reasonable sizes. Rotary vanes were the focus of a major development programme carried out by General Electric in the U.S.A. as an alternative to turbines in Rankine systems [65]. General Electric obtained over 84% efficiency for a unit of only 1 kW power output reported in the same reference which is very impressive since Ormat Turbines [see Ref.62] only achieve 75% in their organic turbines. Cranfield Institute of Technology was also involved in the development of a multi-vane expander as a prime mover for extracting power from low-grade heat sources using organic Rankine cycle systems. Several papers were published [66,67,68]. However, their multi-vane expander design achieved lower efficiences, due to leakage past the vane edges. Figure 1.29 shows a schematic representation of a multi-vane expander. The annular space bounded by two adjacent vanes, the rotor, the stator and the end plates form separate compartments. As the rotor continues to rotate the control volume increases as the vapour expands doing work.

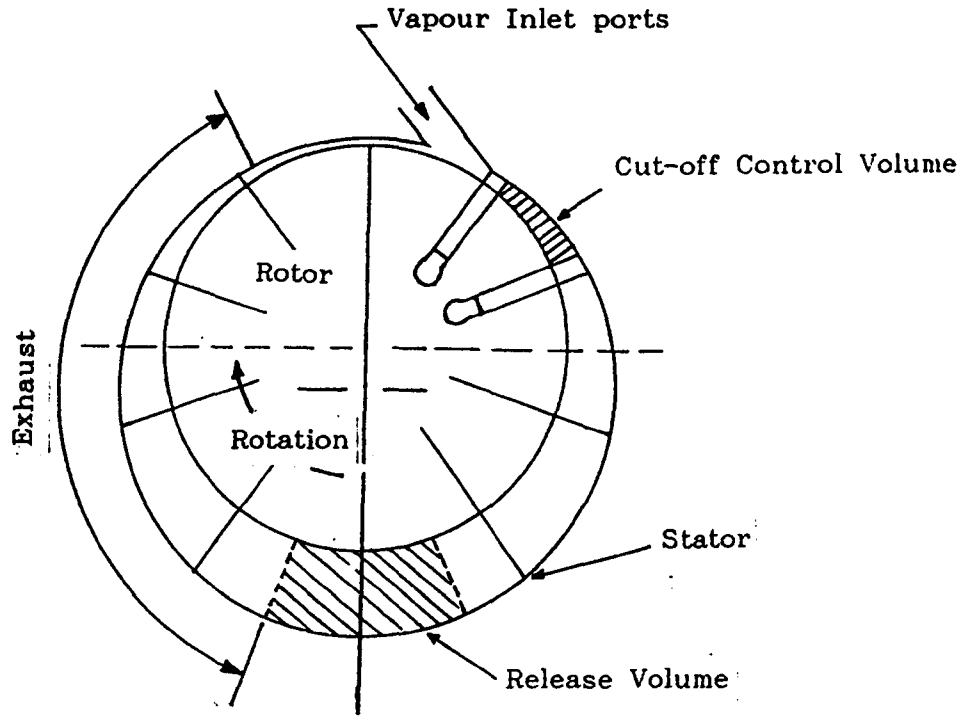

Figure 1.29. Rotary Sliding Vane.

Smith [see Ref.57] proposed to concentrate on a study of rotary vanes and Lysholm screws for power outputs of up to 30 - 50 kW to assess the potentials of both two-phase expanders. For sliding vanes efficiencies were poor. The maximum efficiency obtained was approximately 50% while for the Lysholm twin-screw as prime mover efficiencies of up to 72% were achieved. Despite this outstanding achievement with the screw, a crucial question remained to be answered. How to design a Trilateral Flash power plant to generate electricity in the megawatt range keeping expanders at a reasonable size? After all, the maximum size of screw machines so far made is much less than that of turbines and outputs of about 5 MW are thought to be a present maximum. One possible solution, Smith [see Ref.57] suggested was by staging or by carrying out the high

pressure expansion in one or two screw stages and the low pressure expansion in a single stage turbine in which the fluid leaves the screw expander nearly dry and completely vaporises in its passage through the turbine as shown schematically in Figure 1.31. A temperature-entropy diagram of this screw-turbine arrangement is already shown in Figure 1.30.

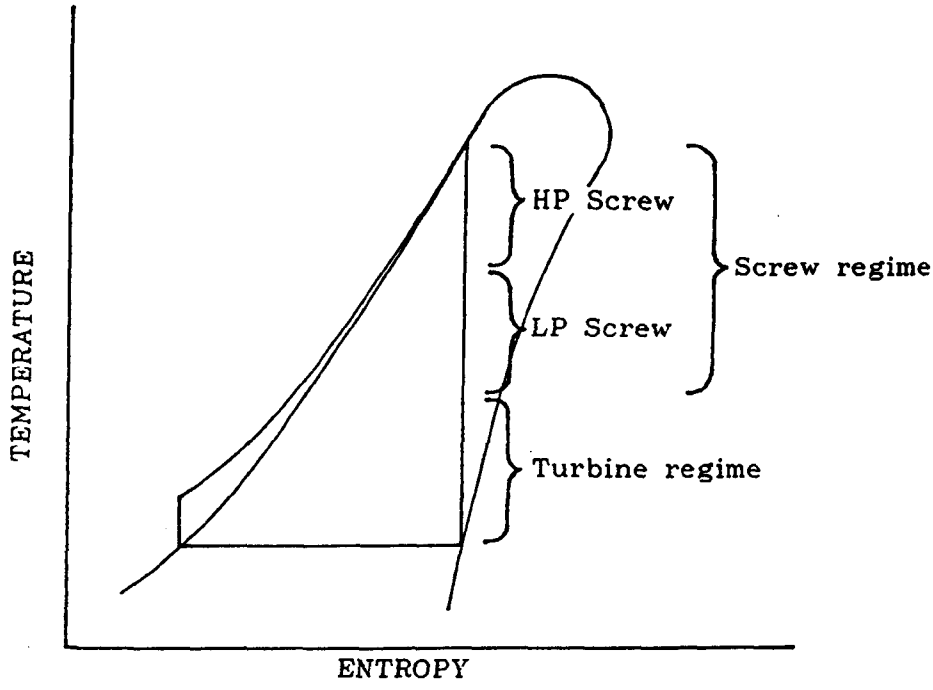

Figure 1.30. Temperature-entropy diagram of screw-turbine arrangement.

To achieve this, the next natural step was to investigate a suitable working fluid whose saturation line should be similar to that one depicted in Figure 1.30. For the range of temperature (120°C - 200°C) where the Trilateral Flash cycle conversion efficiency is superior to the organic Rankine cycle, Smith found n-Pentane to be a quite reasonable fluid. At an initial temperature of just over 180°C this organic compound reaches nearly dry vapour conditions while at 166°C, 3 methyl-1-butene appears to be quite good. This latter

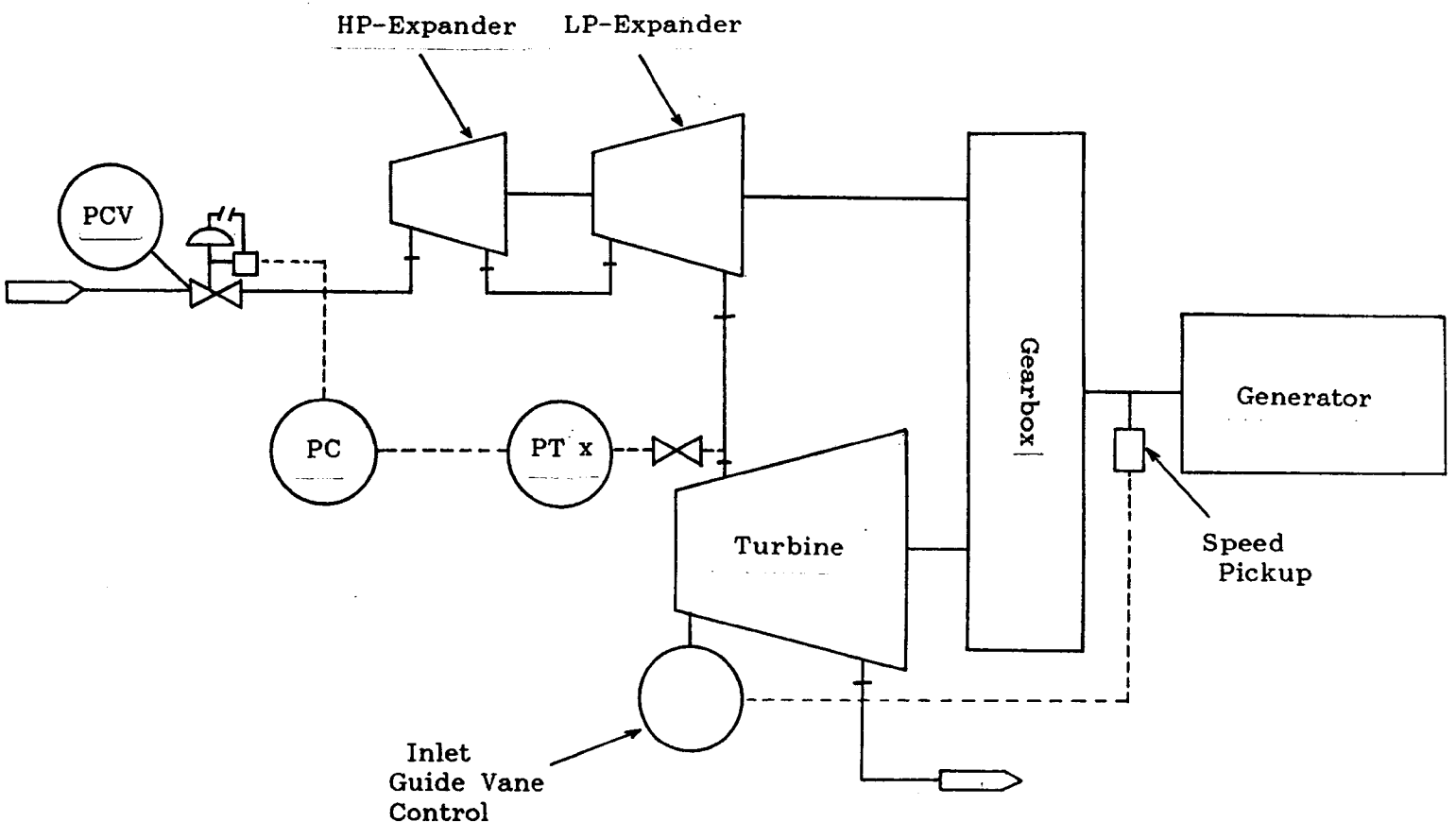

Figure 1.31. Schematic diagram of the screw-turbine arrangement.

volatile fluid due to its double bond is thermally unstable [69] and therefore unsuitable for this purpose. At temperatures in the range 150°C - 180°C he had been unable to find a pure fluid suitable, hence the idea of investigating binary mixtures of organic fluids whose saturation vapour line has a strong positive gradient.

1.7. BINARY ORGANIC MIXTURES AS WORKING FLUIDS

1.7.1. Binary Organic mixtures as working fluids in refrigeration cycles.

In recent years, non-azeotropic organic mixtures of freons (halocarbons) and alkanes have been identified as potential working fluids to increase the performance of vapour compression cycle heat pumps [70,71,72,73,74].

Traditionally heat pumps (shown schematically in Figure 1.32) use a single substance as working fluid. If a non-azeotropic mixture is substituted for a single pure substance, the evaporating temperature will rise and the condensing temperature fall as phase change occurs.

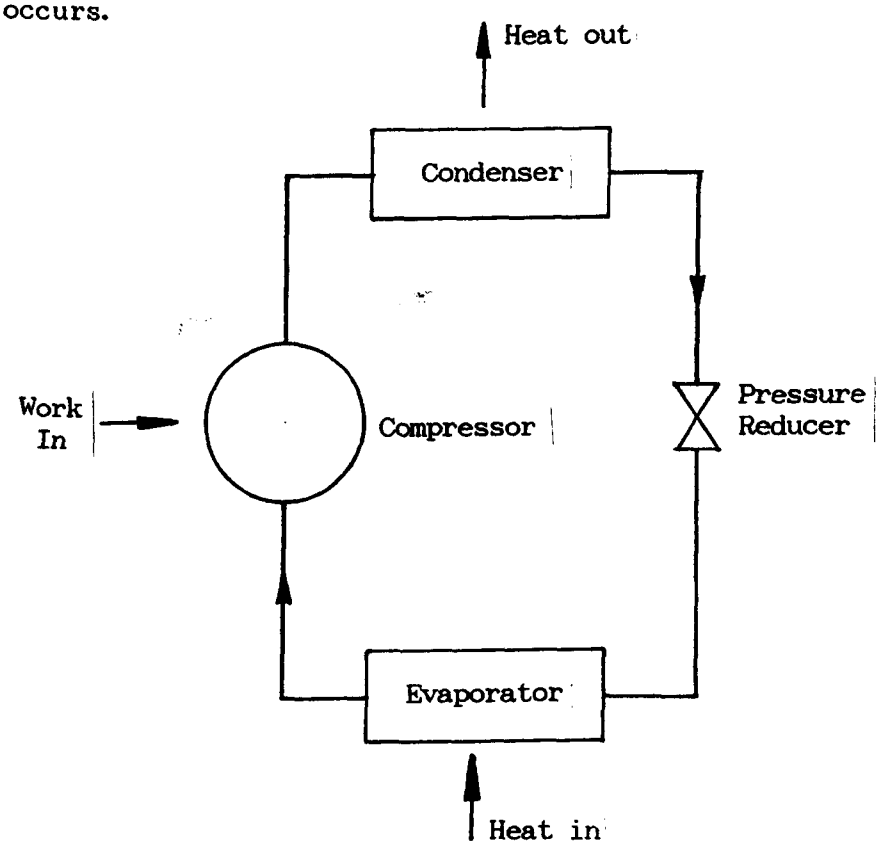

Figure 1.32. Schematic diagram of a Heat Pump

Boiling and condensation do not take place at constant temperature as in the case of a single substance (neglecting pressure drops) but span a range from bubble point (onset of boiling) to the dew point (end of boiling). The major change in the operating cycle (see Figure 1.33) will be the slope of the lines representing the condenser and the evaporator [75]. Since in most applications of a heat pump, sensible heat is to be added to or be subtracted from external fluids (therefore the evaporating temperature must be below the lowest temperature of the heat source and the condensing temperature must be above the highest temperature of the heat sink. It is possible to increase the coefficient of performance (COP) through a better matching between evaporating temperature and heat source as well as condensing temperature and heat sink. This can be demonstrated by making use of a simple thermodynamic analysis.

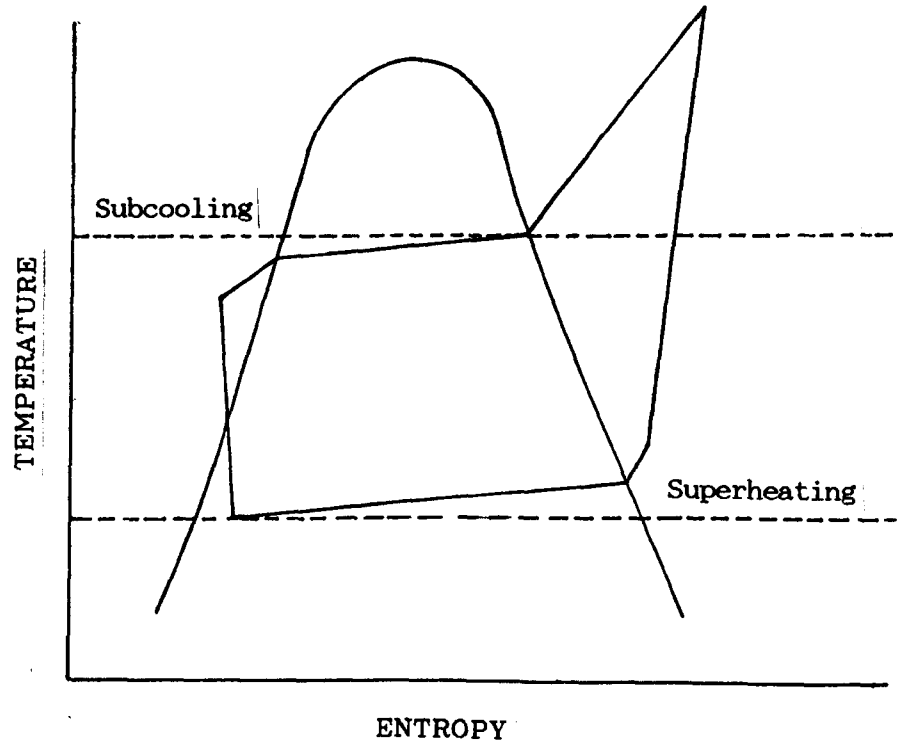

Figure 1.33. Operating Cycle for Non-Azeotropic Mixture

Figure 1.34 shows T-s diagrams of idealised heat pump cycles. (Carnot cycles correspond to a pure working fluid and the cycle known as Lorenz cycle to a non-azeotropic mixture working fluid). If we assume:

i) no pressure drops in the heat exchangers

ii) isentropic compression of a liquid and vapour mixture leaving the evaporator

iii) isentropic expansion of a liquid leaving the condenser

the COP of the cycles is given by:

$$COP = \frac{\text{heat out}}{\text{work in}} = \frac{\text{area 1} + \text{area 2}}{\text{area 1}}$$

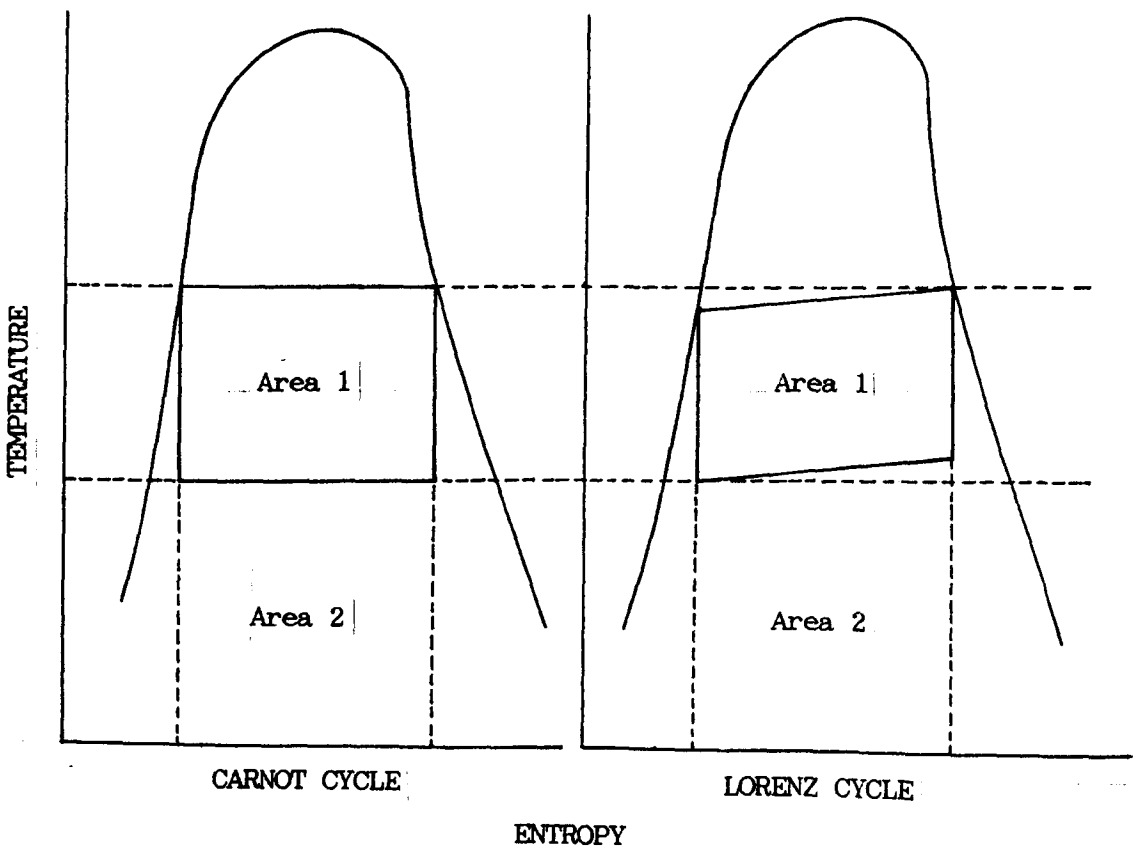

Figure 1.34. Comparison of Carnot and Lorenz cycles.

Since area 1 is smaller in the Lorenz cycle than in the Carnot cycle for the same overall temperature difference the COP for the Lorenz cycle will be higher. Because of the unrealistic assumptions in this analysis the resulting COP is significantly higher than can be achieved in practice. However, use of non-azeotropic mixtures as working fluids does improve the COP of a vapour compression cycle heat pump.

Extensive studies of the use of non-azeotropic mixtures in heat pumps were carried out by the Institut Francais du Petrole [76,77,78]. In their investigations, mixtures of R.11, R.22, R.11/R.13 and butane/hexane were considered. Berntsson [79] reported experimental results for mixtures of R.12 and R.114. A similar mixture was chosen by Stoicher and Walunas [80] when considering the design of a domestic refrigerator. In this application energy reductions of 10% are suggested. The authors point out that there are a number of uncertainties in the behaviour of non-azeotropic mixtures such as miscibility with oil which must be investigated before commercial exploitation. Dupont Chemicals patented a new design of heat pump using a mixture of R.13B1 and R.152A [81] as a working fluid.

1.7.2. Binary Organic Mixtures as Working Fluids in Power Cycles

Geothermal power conversion cycles are a field of research whereby binary organic mixtures have also found scope of application [82]. Most investigations are currently being carried out on binary conversion systems that use a geothermal brine to heat a secondary organic working fluid in a Rankine cycle.

Demuth [83] analysed several binary organic mixtures for moderate temperature geothermal resources. He concluded that for a 280°F (~138°C) resource temperature a mixture of 90% propane and 10% iso-Pentane in a supercritical Rankine cycle showed the highest value of net geofluid effectiveness (net energy produced per unit mass geofluid flow). This working fluid showed improvements of about 42% relative to the highest performing single-boiling iso-Butane cycle and 20% relative to the reference dual-boiling iso-Butane cycle.

For a 360°F (~182°C) resource temperature, he reported mixtures of 96% iso-Butane and 4% heptane, 65% iso-Butane and 35% iso-Pentane and 95% propane 5% hexane, which resulted in improvements in geofluid effectiveness of about 6% relative to a 90% iso-Butane/10% iso-Pentane mixture at 580 psia heater pressure (conditions test comparable to those encountered at 50 MW plant at Heber, California). Figures 1.35 and 1.36 display some of his results. Later Demuth and co-workers [84] produced condensing curves for an extensive variety of alkane mixtures (23 in total with systems of propane-hydrocarbon and iso-Butane-hydrocarbon).

In the Heat Cycle Research Program (sponsored by the U.S. Department of Energy) aimed at developing technology to a more effective utilization of moderate temperature geothermal resources, Bliem [85] carried out an investigation on mixtures of halocarbons. He reported that a mixture of R.114 and R.22 with varying compositions is at least as good as the hydrocarbon mixtures previously analysed for 360°F resource temperature. The magnitude of the net geofluid effectiveness for R.114/R.22 mixtures is the same

as for the best hydrocarbon mixtures investigated by Demuth et al.[84]. Perhaps the first practical utilization of a binary mixture in a geothermal power plant is to be found in Heber, California [86] where a binary pair of iso-Butane and iso-Pentane was used as the power-cycle working fluid to closely match resource temperature. This particular mixture has been extensively studied by Levelt-Sengers et al. [87] and Tleimat et al. [88].

A Japanese patent [89] relating to the use of an organic binary mixture as working fluid was found in this review. The invention describes a mixture of acetone and toluene (80% toluene) as an operating fluid for Rankine cycle engines used to recover the thermal energy of low grade heat. A somewhat unusual application of a non-azeotropic halocarbon binary mixture was also detected: Kajikawa, Takazawa, Murata, and Nishiyama [90] selected a mixture of R.22 and R.12 to be used as working fluid in a closed cycle ocean thermal energy conversion scheme.

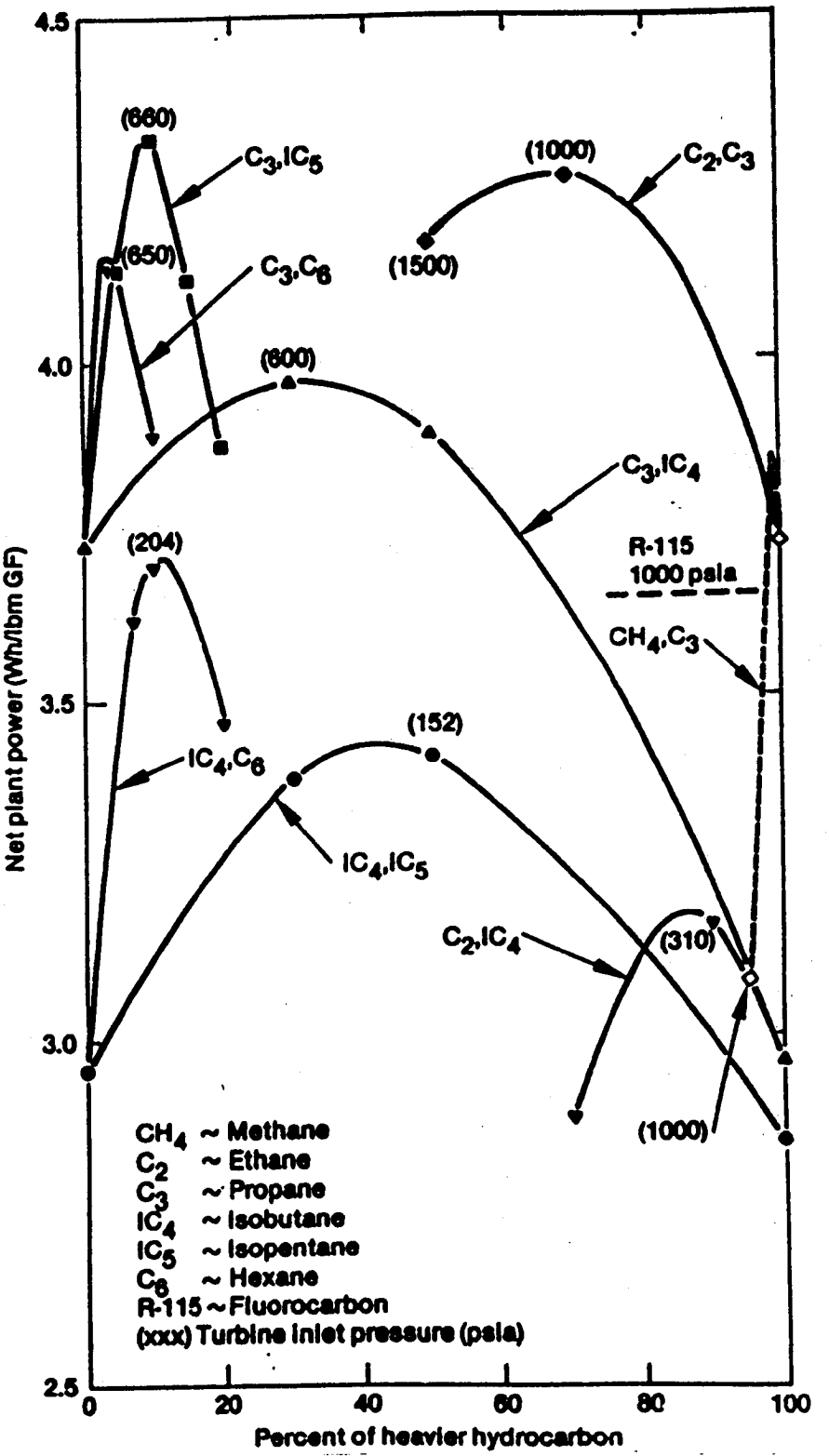

Figure 1.35. Net Plant Power versus Maximum Effectiveness for Single-Heating Cycles, T_{GF} = 280°F.

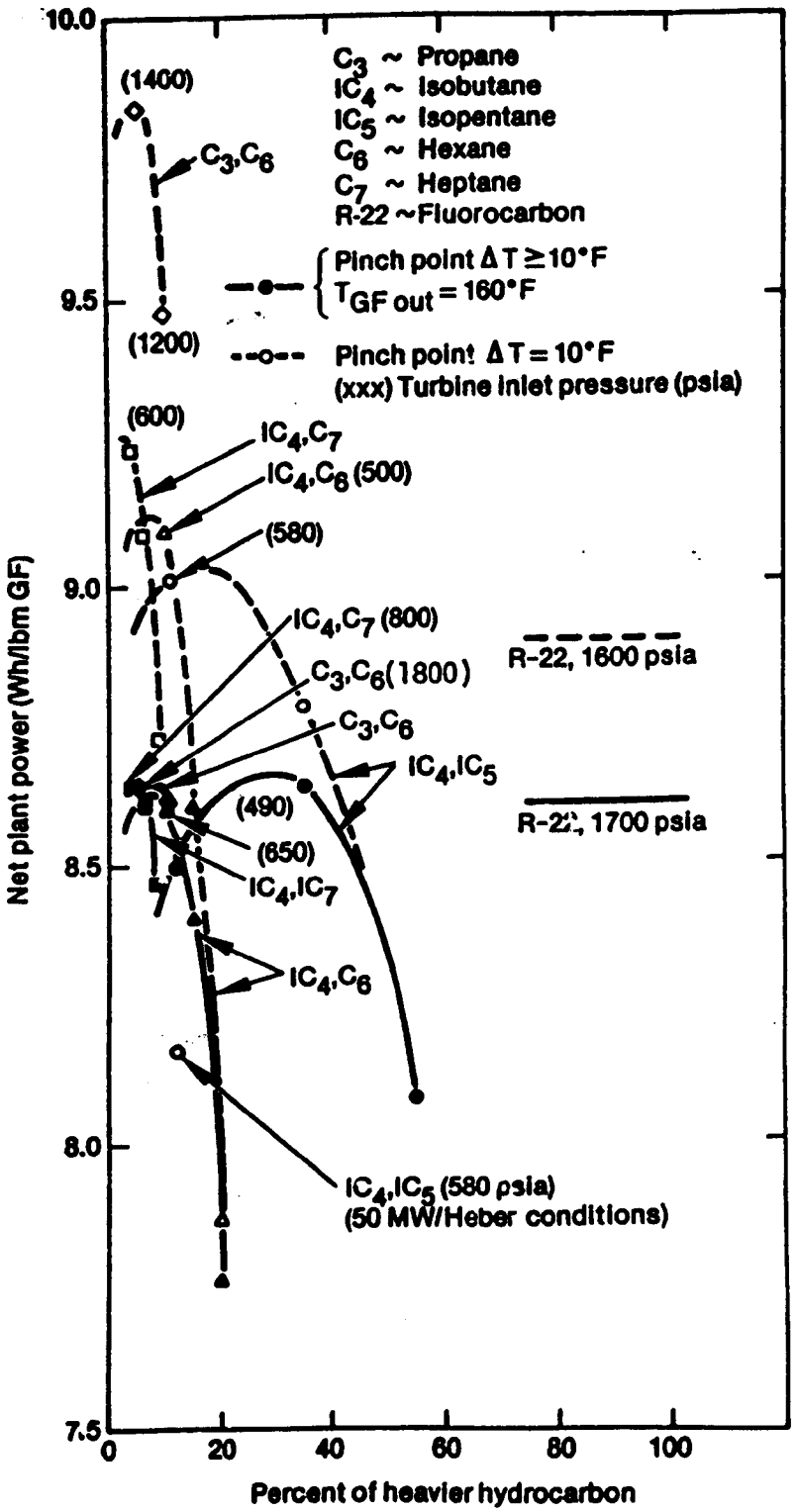

Figure 1.36. New Plant Power versus Maximum Effectiveness for Single-Heating Cycles, T_{GF} = 360°F.

REFERENCES

1. Moore, G. "Geothermal Energy: A Natural Resource". Electronics and Power. 1986.

2. Smith, I.K. and Martin, P.R. "Power from low-grade heat resources: Project SPHERE - An evaluation of the Trilateral Wet Vapour Cycle". C.M.E. January 1985.

3. Eskesen, J.H. "Flashed steam/steam turbine cycles" in Chap.4 Source book on the Production of Electricity from Geothermal Energy. U.S. Dept. of Energy, 1980.

4. Starling, K.E., Speipcevich, C.M., Fish, L.W., Gin, K.M., Aboul-Foutoh, K.H., Kumar, K.H., Lee, T.J., Milani, J.S. and Zemp, K.L. "Development of Working Fluid Thermodynamic Properties Information for Geothermal cycles: Phase 1", Report No. ORO-52499-2, University of Oklahoma, Norman, U.S.A.

5. Stoecker, W.F. "Design of Thermal Systems". McGraw-Hill, New York, 1971.

6. Sesonske, A. "Nuclear Power Plant Design Analysis" U.S. Atomic Energy Commission, TID-26241, Oak Ridge, Tenn. 1973.

7. El Wakil, M.M. "Power Plant Technology". McGraw-Hill, New York, 1980.

8. Morse, F.T. "Power Plant Engineering". 3rd Edition, Revised, New York, D.Van Nostrand Co. Inc. 1973.

9. Gill, A.B. "Power Plant Performance". Butterworths London. 1984.

10. Bloomster, C.H. and Maeder, P.F. in Chap.7. Economic Considerations in Source book on the Production of Electricity from Geothermal Energy. U.S. Dept. of Energy, 1980.

11. Abubaker, M., Smith, I.K, and Heppenstall, T. "A Comparison of Three Surface Plant Options for the Conversion of Geothermal Energy from Hot Dry Rocks". IRD Report. 86/17.

12. "Power plant Evaluation and Design Reference Guide" (Ed.by Tyler G. Hicks), McGraw-Hill, 1986.

13 Berkowitz, D.A. et al. "Power Generation and Environmental Change" M.I.T. Press, Cambridge, Mass. and London, U.K. 1971.

14. Schurr, S.H. "Energy Economic Growth and the Environment: Resources for the Future". John Hopkins, 1972.

15. Axtmann,R.C. "Environmental Impact of a Geothermal Power Plant", Science, Vol.187, No.4179, 1975.

16. Stanford Research Institute; Environmental Analysis for Geothermal Energy Development in the Geysers Region. Report for the California Energy Resources Conservation and Development Comission, Vol.I, Summary, 1977.

17. Meadows, D.H. et al. "The Limits to Growth, a report for the Club of Rome's Project on the Predicament of Mankind". New York, Universe Books, 1972.

18. Bohn, Th. "Energy requirements and problems of its covering in: K.J. Euler, A. Scharmann (Eds.) Energy Supply of the Future, Munich, Thiemig, 1977.

19. Curran, S.C. and Curran, J.S. "Energy and Human Needs" Scottish Academy Press, 1979.

20. "Energy from surplus to scarcity?" Ed. K.A.D. Inglis, Barking; Applied Science Publishers, 1980.

21. "Must the World run out of Energy" A Crown Agents Publication on Alternative Energy, 1978.

22. Grenon, M. "On Fossil Fuel Reserves and Resources". International Institute for Applied Systems Analysis, Laxenburg, Austria, RM-78=35, 1978.

23. "Nuclear Power: Issues and Choices". Ed. McGeorge Bundy. Ballinger, Cambridge, Mass., 1977.

24. Fisher, J.C. "Energy Crisis in Perspective". Wiley International, New York, 1974.

25. Cohen, B.L. "Nuclear Science and Society". Anchor/Doubleday, Garden City, N.Jersey, 1974.

26. "Nuclear Power and the Environment: Questions and Answers" American Nuclear Society, Chicago, 1976.

27. Domberg, N. "Can we afford to make the fast reactor safe?" Nature, Vol.280, pp.270-272, 1979.

28. Oldenburg, O. and Rasmussen, N.C. "Modern Physics for Engineers" McGraw-Hill, New York, 1966.

29. Phillips, J.A. "Recent Developments in Nuclear Fusion" (Division 4, 4.1-1), 10th World Energy Conference, Istanbul, pp.1-14, Sept.1977.

30. Hagen, A.W. "Thermal Energy from the Sea" Noyer data Corporation, London, 1975.

31. Reisfeld, R. "Possibilities of Solar Energy Utilization". Die Naturwissenschaften, Vol.66, no.1, pp.1-8, 1977.

32. Duffie, J.A. and Beckmann, W.A. "Solar Energy-Thermal Process" John Wiley & Sons, New York, 1974.

33. Meinel, A.B. and Meinel, M.P. "Applied Solar Energy". Addison-Wesly Co. London, 1977.

34. Lipinsky, E.S. "Fuels from Biomass: Integration with Food and Materials Systems". Science, Vol.199, 644-651, 1979.

35. Tidal Power: Citations from the International Aerospace Abstracts Data Base. John H. Freys, New England Research Applications Centre, 1980.

36. Hunt, V.D. "Wind Power: A Handbook on Wind Energy Conversion Systems" New York Van Nostrand Reinhold, 1981.

37. Deudney, D. and Flavin, C. "Renewable Energy". W.W.Nortan Co., New York, 1983.

38. Muffler, L.J.P. "Geothermal Energy", The Science Teacher, Vol.39, No.3, 1972.

39. Christopher, H. and Armstead, H. "Geothermal Energy" E & F N. Spon, Ltd., England, 1983.

40. Garnish, J. "Heat from the Earth in Must the World Run out of Energy?" A Crown Agent's publication on alternative energies.

41. Bowen, R. "Geothermal Resources", Applied Science Publishers Ltd., London, 1979.

42. White, D.E. "Characteristics of geothermal resources" in Geothermal Energy, Ed. by P.Kruger and C.Otte, Stanford University Press.

43. Facca, G. "The Structure and Behaviour of Geothermal Fields" in Geothermal Energy, a review of research and development. Earth Sciences, Vol.12, UNESCO, Paris, 1973.

44. Anderson, J.H. "The Vapour-Turbine cycle for Geothermal Power Generation" in Geothermal Energy Resources, Production and Stimulation (Ed. P. Kruger and C. Otte) Stanford University Press,1973.

45. Austin, A.L. "Status of the Development of the Total Flow System for Electric Power Production from Geothermal Energy" in Source book on the production of Electricity from Geothermal Energy (Ed. in Chief,J. Kestin), U.S. Dept. of Energy.

46. White, D.E. "Preliminary Evaluation of Geothermal Areas", Paper G2, U.N. Conference on New Sources of Energy, Rome, 1961.

47. Batchelor, A.S. "An Overview of Hot Dry Rock Technology", I.E.E. Conf.Publ. 233, 1986.

48. Altseimer, J.H. "The subterrene rock-melting concept applied to the production of deep geothermal wells" Proc. 11th Intersociety Energy Conversion Eng. Conference, State Line, Nev., Sept.12-17, pp.717-723.

49. Elliott, D. "Comparison of Brine Production Methods and Conversion Processes of Geothermal Electric Power Production" EQL No.10, 1975.

50. Holt, B. and Ghormley, E.L. "Energy Conversion and Economics of Geothermal Power Generation at Heber, California, Valles Caldera, New Mexico, and Raft River Idaho, Case Studies" EPRE ER-301, Nov.1976.

51 Polansky, G.F.and Lamb, J.P. "Thermodynamic Analysis of Energy Conversion Plants using Geopressured Geothermal Fluids" Report ME EFS 8001 (June 1980) Centre for Energy Studies, University of Texas, Austin.

52. Ibid. 49.

53. Einarsson, S.S. "Geothermal Space Heating and Cooling" Procs 2nd U.N. Symp. on Development and use of Geothermal Resources, Vol.3, p.2117, 1975.

54. Hajela, G.P. and Katz, B. "Effects of Non-condensable Gases on Geothermal Power Generation" SAE Paper 789315, 1978.

55. Weiss, H. et al. "Performance Test of a Lysholm Engine" Lawrence Livermore Lab. Report No.UCRL-51861, 1975.

56. House, P.A. "Helical Power Expander Applications for Geothermal Conversion", Lawrence Livermore Lab. Report UCRL-52043, 1975.

57. Smith, I.K. "PROJECT SPHERE: An assessment of the Practicability of the Trilateral Wet Vapour Cycle for Recovery of Power from Low Grade Heat Sources" Thermo-Fluids Engineering Research Centre Report, The City University, 1985.

58. Wilson, S.S. and Radwan, M.S. "Appropriate Thermodynamics for Heat Engine Analysis and Design" Int.J. of Mech. Eng. Educ., Vol.5, No.1, 1977.

59. Lysholm, A.J.R. "A New Rotary Compressor". Proc. of I.Mech.E., Vol.150, 1942.

60. Elliott, D.G. "Theory and Tests of Two-Phase Turbines". Jet Propulsion Laboratory Publication, 81-105, 1982.

61. Ibid. 58.

62. Ibid. 56.

63. Ormat Turbines.

64. Burkett, D.J. "Performance of Model Turbine Blading Operating on an Air Water Mixture" Admiralty Research Report, ARL/M5/6/HY/11/1, 1971.

65. Robertson Jr., C.S. and Eckard, S.E. "Multi-phase Expanders by Adding Power can Improve the fuel economy of long haul Diesel Trucks" SAE Paper 780639, 1978.

66. Badr, O., O'Callaghan, P.W., Hussein and Probert, S.D. "Applied Energy", Vol.16, No.2, 1984.

67. Badr, O, O'Callaghan, P.W., Hussein and Probert, S.D. "Applied Energy, Vol.20, No.4, 1985.

68. Badr, O, Probert,S.D. and O'Callaghan P.W. Proc. Int.Mech. Eng., Vol.200, No.A2, 1986.

69. Blake, E.L., Hamman, W.E., Edwards, J.W. Reichard, L.E. and Art, M.R. "Thermal Stability as a Function of Chemical Structure". J. Chem and Eng. Data, Vol.6, No.1, 1961.

70. Cooper, W.D. and Burchardt, H.J. "The use of refrigerant mixtures in air-to-air heat pumps". Procs. of XVth Int. Congress of Refrigeration, 1979.

71. Launay, P.F. "Improving the efficiency of refrigerators and heat pumps by using a non-azeotropic mixture of refrigerants" Oak Ridge National Lab, ORNL/Sub 81/7762/1, 1981.

72. Schnitzer, H. and Berntsson, Th. "Improvement of COP of compression heat pumps through the use of non-azeotropic mixtures". BHRA Conference, York, Sept.1984.

73. Kruse, H. "The advantages of non-azeotropic refrigerant mixtures for heat pump applications" Int. J. of Refrigeration. Vol.4, No.3, May, 1981.

74. Cohen, G., Asselineau, L., Jacques, J., and Rojey, A. "Heat pump operating with a non-azeotropic fluid mixture" Meeting on heat pump research, development and application, Brussels, 1978.

75. Sauer, H.J. and Howell, R.H. "Heat Pump Systems" John Wiley & Sons, New York, 1983.

76. Rojey, A, Meyer, C, Choffe, B, Jacques, J. and Asselineau, L. "Heat pump operating with a mixture of fluids" Institut Francais du Petrole, Reuil-Mailmaison, France, 1980.

77. Ramet, C, Rojey, A, Baglione, H, Reinge, L. and Durandet, J. "Compression heat pumps operating with non-azeotropic fluid mixtures". Procs of Four Contractors Meetings, Brussels, 1982.

78. Choffe, B, Jacques, J., Meyer, C., and Rojey, A. "Heat pump operating with a non-azeotropic fluid mixture". Procs. of 7th Energy Technology Conference, Washington, D.C., 1980.

79. Berntsson, A.T. "Measurements on a water-to-water heat pump using mixtures of R.22 and R.114 as working fluid". Earth Heat Pump Group, Gotenborg, Report No.8, 1982.

80. Stoecher, W.F. and Waluhas, D.J. "Conserving energy in domestic refrigerators through the use of refrigerant mixtures". ASHRAE Trans., Vol.87, No.1, 1981.

81. Dupont Chemicals "A New Dupont developmental heat pump refrigerant mixture of freon 13B1 and 152A. Press release RT-72.

82. Source book on the production of electricity from geothermal energy by Jospeh Kestin (Ed.in Chief) Brown University, Rhode Island under sponsorship of U.S. Dept. of Energy Contract, No.EY-76-S-4051-A002.

83. Demuth, O.J. "Analysis of Mixed Hydrocarbon Binary Thermodynamic Cycles for Moderate Temperature Geothermal Resources". E6 and G, Idaho, Inc., Feb, 1981, EG6-P6-6-80-04).

84. Demuth, O.J. "Condensing Curves for a Number of Mixed Hydrocarbon Working Fluids" E6 and G, Idaho Falls, Report No. EG6-GTH-5456, July, 1981.

85. Bliem, C.J. "Preliminary Performance Estimates of Binary Geothermal Cycles Using Mixed Halocarbon working fluids", E6 and G Idaho Falls, Report EG6-EP-7312, July, 1986.

86. "Heber Binary Cycle Geothermal Demonstration Power Plant: Summary of Technical Characteristics" Electrical Power Research Institute, (Adv. Power Syst. Div. Rep. EPRI AP4612) June 1986.

87. Gallager, J.S., Levelt-Sengers, J.M.H., Morrison, G. and Sengers, J.V. "Thermodynamic Properties of Iso-Butane-Iso-Pentane Mixtures from 40 to 600°F and up to 1000 psia". National Bureau of Standards Report No.DOE/SF/11653-T11, July 1984.

88. Tleimat, B.W, Dizon, G.V., Zhao, S, Rie, H, and Laird, A.D. "Condensation Film Coefficients for Mixtures of Iso-Butane and Iso-Pentane", University of Berkeley, Water Thermal and Chemical Technology Centre, U.S.A. J.of Energy, Vol.7, No.6, Nov-Dec.1983.

89. Operating Fluid for Waste Heat Recovery. Japanese Patent No.57-164193 (1982) Journal Announcement: GTRA 18613; NSA 1100.

90. Kajkawa, T, Takazawa, H. Murata, A. and Nishiyama, K. "Non-azeotropic binary mixture working fluid OTEC cycle by using mixture of R.22 and R.12. Denshi: Gijutsu Sogo Kenkyusho Bulletin of the Electrotechnical Lab., Japan, 1986.

CHAPTER 2

WORKING FLUID SELECTION

2.1. INTRODUCTION

For the purpose of power plant design, the working fluid can be considered as an additional variable[1]. The selection of an optimum working fluid for a given application is an inter-related subject [2] consisting of quantifiable considerations such as performance, equipment and cost but also unquantifiable or difficult to quantify factors such as toxicity, thermal and chemical stability, safety and flammability.

The choice of an organic working fluid for refrigeration or power cycles is governed primarily by the physical and thermodynamic properties of the fluid. Although much of the information developed in the chemical and refrigeration industries on the use of organic fluids in thermodynamic cycle equipment is directly applicable to Organic vapour power plant design, additional information specific to the TFC system must also be considered[3].

2.2. WORKING FLUID REQUIREMENTS FOR THE TRILATERAL FLASH CYCLE

An ideal working fluid for the TFC system, if it exists, can be characterised reasonably well by the following requirements:

(i) To maximise the expander efficiency the saturation vapour line should have a large positive slope, when displayed in a T-s diagram, to attain exit conditions as near as possible to a dry vapour. It appears that a strong rightward slope to the saturated vapour line is caused by a very large molecule. The slope is related to the number of atoms in the molecule (as we shall see in Chapter 7).

(ii) The overall pressure drop through the expander should not be too great to avoid large leakage losses in the screw expander.

(iii) The maximum fluid temperature should not be too close to the critical point to avoid excessive pressures and to maintain close temperature matching with the heat source in the heater.

(iv) The fluid specific energy should be high. This is needed because the specific enthalpy drop in two phase adiabatic expansion is much less than in the dry vapour phase. Exit losses from the expander can thereby become relatively very large. For this reason comparatively low molecular weight is required and hence hydrocarbons are preferable to halocarbons.

(v) In the normal power plant condensing temperature range of 20° - 40°C (≈ 35°) the condensing pressure should preferably be higher than 1.0 bar to keep the expander compact and, in addition, to reduce air leakage into the condenser.

(vi) The working fluid should have high sonic velocity. If the mean molecular weight of the fluid is very large, say, greater than 150, the sonic velocity of the fluid then becomes low, especially in the liquid-vapour two phase region where it can attain values as low as 25 m/s. For this reason halocarbons (freons) are not as good as hydrocarbons.

(vii) The liquid density should be low. This is desirable because the volumetric expansion ratio in two phase expansion is very large and the design of a two phase expander is therefore difficult. Due mainly to their lower liquid density, hydrocarbons have an expansion ratio roughly half that of halocarbons with the same vapour density at exit.

(viii) The working fluid should be thermally stable at the critical region, essentially non-fouling, non-toxic and non-flammable and compatible with normal materials of constructions.

(ix) Liquid and vapour viscosities should be low, to minimize frictional pressure drops and maximize convective heat transfer coefficients.

(x) The working fluid should be readily available and cheap.

Should binary organic mixtures be considered as working fluids, the following are additional requirements:

(xi) The difference between bubble and dew points should be small in order to keep condensation nearly isothermal. If this is not the case, the recoverable power from the adiabatic expansion process will be greatly reduced. A small difference between bubble and dew points can be partially achieved if each component present in the mixture has the same number of atoms per molecule.

(xii) The two fluids should mix with one another at all proportions to yield a homogeneous mixture.

(xiii) The mixture critical temperature will probably be in the 160° - 190°C range unless the critical pressure is much greater than that of most pure organic fluids when a higher critical temperature may be permissible. Binary combinations of hydrocarbons (e.g. alkanes) also offer the possibility of achieving higher critical pressures specially if each component has different molecular sizes (e.g. methane and n-nonane). This is due to the non-linear additivity of critical pressures. Therefore high back pressure may be obtained to keep the expander small.

As may be seen from the above requirements, the choice of suitable candidates for a working fluid is not governed by its thermodynamic properties alone. The less easily quantifiable characteristics are reviewed in more detail in the following subsections.

2.3. CHEMICAL ASPECTS OF ORGANIC WORKING FLUID SELECTION

2.3.1. Thermal Stability Limits of Organic Working Fluids

While water as a working fluid is considered to be stable up to 590°C when dissociation begins to occur [4] organic fluids in general start to decompose at a much lower temperature. Therefore, it is essential that the peak cycle temperature should be below the stability temperature of the working fluid. Stability temperature is normally defined as the temperature above which the working fluid breaks down into lower molecular weight compounds at a significant rate.

The thermal stability of organic compounds is closely related to their chemical structure. Blanc and co-worker [5] attempted to correlate decomposition temperature on the basis of concepts of bond strength, resonance, nature of chemical bond, reaction mechanisms and free radicals. Trenwith and Watson [6] studied thermal decomposition of three fluorochloromethanes and found their modes of decomposition fairly complex.

Experimental determination of thermal stability is carried out by two methods:

(i) capsule tests where a small quantity of fluid is heated in a sealed vessel at a fixed temperature

(ii) loop tests where the fluid experiences the cycle conditions it would be subjected to in the proposed application.

Miller, Thompson and Null [7] used capsule tests to identify classes of chemicals suitable as working fluid for organic Rankine cycles. From 110 fluids studied they concluded that only four classes of organic compounds are stable up to 720°F (382°C).

(i) toluene and benzene/toluene mixtures

(ii) fluorinated benzenes

(iii) mixtures of water with pyridine and the monomethypyridines

(iv) perfluoroalkanes and perfluoroethers.

Thermal stability data on organic working fluids are scattered. Furthermore, comparing the thermal stability data given by different sources, a discrepancy of even one hundred deg.C on the stability temperature is often encountered [8]. Table 2.1 presents the thermal stability temperatures of some organic working fluids.

2.3.2. Lubricating Oil Effects

With the exception of a few oil-free engines [9], organic fluids must co-exist with lubricating oil. The selection of a suitable oil requires careful consideration of the desired physical and chemical properties, as well as the working fluid and materials of construction to be used. Several investigations of the behaviour of organic fluids in contact with oils have been conducted [9, 10, 11,12]. In general, these studies have shown that some oils reduce the stability of organic fluids more than others and increased temperature accelerates the refrigerant-oil reaction. The reaction rate is also dependent on the kinds of metal in contact with the oil and organic fluid and the amount of air, moisture and additives present in the oil [13].

Usually when in contact, an organic fluid and a lubricating oil have mutual solubility. Organic fluids may be completely miscible, partially miscible, or immiscible according to their mutual solubility relations with lubricating oils. In the case of partial miscibility, the mutual solubility is a function of the fluid/oil ratio and increases with increasing temperature. Above a certain temperature, the critical solution temperature, the fluid and oil are completed miscible [13].

TABLE 2.1. Thermal stability of some Organic Compounds

Fluid	Chemical Formula	Approximate thermal stability limit °C
Trichlorofluoromethane (R11)	CCl_3F	300
Dichlorodifluoromethane (R12)	CCl_2F_2	500
Monochlorofluoromethane (R22)	$CHClF_2$	250
Trichlorofluoroethane (R113)	$C_2Cl_3F_3$	110
Dichlorotrifluoroethane (R114)	$C_2Cl_2F_4$	380
Monoisopropylbiphenyl (CP9)	$(C_6H_5)(C_6H_4)-CH(CH_3)_2$	370
Toluene (CP25)	C_7H_8	480
Monochlorbenzene (CP27)	C_6H_5Cl	320
Pyridine (CP32)	C_5H_5N	370
Thiophene (CP34)	C_4H_4S	290
Perfluoro-2-butyltetrahydrofuran	$C_8F_{16}O$	320
Perfluropentene (FC88)	C_5F_{12}	200
Fluorinol (Trilfluoroethanol/ water mixture)		290
Dowtherm A (Biphenyl-Biphenyl oxide eutectic 26.5%/73.5 wt.%)		370
Biphenyl	$(C_6H_5)_2$	370

Compiled from References [4], [15], [16].

The dissolving of an oil in an organic working fluid affects the thermodynamic properties of the fluid. The vapour pressure of an organic fluid-oil solution at a given temperature is usually less than the vapour pressure of the pure organic fluid at that temperature. The magnitude of the vapour pressure depression depends on the fluid/oil ratio, being quite small when the fluid/oil ratio is large, and vice-versa. In a TFC system the dissolved oil content in the working fluid must be minimal or the system performance is severely affected by the resultant loss of vapour pressure during the two-phase expansion.

Similarly, the dissolving of an organic working fluid in an oil affects the properties of the oil. In particular, the viscosity of an organic fluid-oil solution at a given temperature is generally less than the viscosity of the pure oil at the same temperature.

2.3.3. Working Fluid Degradation Effects

An important consideration in system operation is the effect of working fluid degradation. Formation of non-condensable gases will reduce the condenser effectiveness resulting in high condenser pressure and therefore system performance. While this effect can be eliminated by incorporation of an automatic purge on the condenser, it adds to the complexity and cost of the system and is not desirable. Fluid degradation gives rise to corrosive degradation products, primarily acidic in nature, with unacceptable corrosion on the fluid side [14]. Corrosion rates must be very low for a long-life commercial system. Another effect is the formation of deposits on

the surfaces of the components which can lead to problems such as reduced heat exchanger and turbine performances and plugging of tubes. Deposits may result from the corrosion products formed by reaction of the working fluid or contaminants (such as O_2/H_2O) with materials of construction.

The system materials in contact with the working fluid almost invariably have an effect on the degradation rate of the fluid. In certain cases, particularly the refrigerants, this effect is extremely pronounced. Metals usually have a catalytic effect on the degradation rate, and the presence of a lubricant in the system can significantly lower the upper temperature limit of the fluid. The halogenated refrigerant fluids well illustrate this characteristic. Based on a 1% per year homogeneous decomposition rate (no surface effects) the maximum use temperature for continuous exposure is reported by du Pont [15] as:

R22	$CHC\ell RF_2$	250°C
R11	$CC\ell_3F$	> 300°C*
R114	$CC\ell F_2CC\ell F_3$	380°C
R115	$CC\ell F_2CF_3$	390°C
R12	$CC\ell_2F_2$	500°C
R13	$CC\ell F_3$	540°C**

* *conditions not found where decomposition proceeds homogeneously*

** *rate behaviour too complex to permit extrapolation to 1% per year.*

In contrast, the recommended maximum temperature by du Pont for continuous exposure in the presence of oil, steel and copper is only 110°C for R11 and R113; 120°C for R12 and R114; 135°C to 150°C for R22 and >150°C for R13.

Thus, although the inherent stability of the refrigerants is very high, in the presence of oil, steel and copper it is drastically reduced with the tendency to react decreasing in the order R11>R12>R114>R115>R22. Conversely, in the absence of oil, steel and copper R22 is the most unstable of the refrigerants[15].

2.3.4. Effect of System Contaminants

Because of the possible sensitivity of the working fluid to the materials to which it is exposed, contaminants in the system can rapidly accelerate the degradation rate and corrosive effects on metals in the system. Of particular importance are trace quantities of O_2 and H_2O from air in-leakage to the system as well as residual amounts remaining in the system after pump-down and fluid charging. Both O_2 and H_2O are very reactive with practically all organic working fluids (particularly when operating near their upper temperature limit) producing organic acids [14]. These organic acids can be extremely corrosive to steel and even to stainless steel; in certain cases, their corrosive action is as strong as that of mineral acids, such as nitric or hydrochloric.

For very long-life power plants, even very small leaks can result in potentially significant amounts of O_2/H_2O in the system. This possibility must be considered in the system design and operation.

Of course, development of large leaks will lead to a high condenser pressure by the non-condensable gases and result in shutdown of the plant and repair of the leak. However, development of very small, pinhole leaks gives rise to additional trace amounts of O_2/H_2O without noticeably affecting system performance but with potentially disastrous effects such as fluid degradation and corrosion.

Other contaminants can be produced by degradation of the fluid over a long period and by the reaction products with the materials of construction. These contaminants can act as catalysts in certain cases, accelerating the rate of decomposition as time progresses, and leading to system destruction.

Contaminants left in new power plants or refrigeration systems can also drastically affect fluid degradation. In the air conditioning industry, for example, great attention is paid to cleaning the internal parts of the system before charging with refrigerant and oil. Traces of impurities in the working fluid can also sometimes degrade thermal stability.

2.4. FLAMMABILITY AND TOXICITY OF ORGANIC WORKING FLUIDS

As mentioned in section 2.1 flammability and toxicity of organic working fluids are rather difficult factors to be quantified when compared to other design considerations. Generally speaking, safety in power plants related to flammability hazards depends on sound design and construction, careful training of operators, and the adherence to shut down procedures. In organic Rankine cycles using

geothermal energy sources where plants are normally located away from urban centres toxicity and flammability hazards can be tolerated. Although the nature of the geothermal fluid (primarily water) by itself reduces the possibility of fire and explosion, organic systems are generally hermetically sealed. Therefore, no serious threat concerning power safety exists during normal operation. In gas or oil-fired plants, explosions may occur caused either by the ignition of accumulations of unburnt fuel or by the ignition of flammable vapours released from the articles heated. In contrast, the worst condition in an organic Rankine or Trilateral plant could give a warning when a certain percentage (usually 30%) of the lower explosive limit [16] is reached. This could also initiate measures such as increasing ventilation, closing valves and shutting down machinery. By the use of foam or inert fire-extinguishers, even very high flammable fluids may be tolerated. Toluene, for example, a compound of very low flash point has been used in a total energy system [17] as the working fluid.

The toxicological problems related to organic working fluids arise mainly from inhalation of vapours or contact with skin. Dosages are governed by threshold limit values (TLV). Threshold limit values of toxic materials in the atmosphere have been set by the American Conference of Governmental Hygienists (ACGIH) and are reviewed annually.

A table of flammability and toxicity of more than 50 organic working fluids prepared by Owen[18] is reproduced in Appendix A.

2.5. FURTHER COMMENTS

The choice of suitable candidates for a working fluid is not governed, as mentioned in section 2.1, by its thermodynamic properties alone. Thermal stability, for example, plays an important role in selecting fluids and may even dictate the choice. The requirement limits the use of unsaturated hydrocarbons, which are unstable due to their double and triple bonds, as well as halocarbons (freons). The latter group, though attractive for its non-flammability, can, however, be used in subcritical Organic Rankine cycles where the volatile fluid is heated to much lower temperatures or in TFC systems which receive heat from low temperature resources. A particular drawback pertinent to this class of compounds is related to the depletion of the stratosphere ozone layer. Although knowledge of troposphere chemistry is still in its infancy the continuing release of halocarbons (mainly through aerosols) is thought to be the principal reason for the destruction of the ozone layer and the increased greenhouse effect. Furthermore, halocarbons possess heavy molecular weight and therefore undesirable low sonic velocity in the two-phase region. This requirement is of primary importance, if the expander is to be kept to a reasonable size. These considerations drastically reduce the range of candidate fluids. Contenders are reduced to alkanes, cyclic hydrocarbons and possibly amines where high flammability cannot be avoided. Organometallic compounds known for their thermal stability if suitable may have to be discarded on grounds of costs.

REFERENCES

1. Bjerklie, J.W. "Working fluid as a Design Variable for a Family of Small Rankine Power Systems", ASME Paper 67-GT-6, 1967.

2. Luchter, S. "A Quantitative Method of Screening Working Fluids for Rankine Cycle Power Plants", ASME Paper 67-GT-12, 1967.

3. Warner, D.K. and Barber, R.E. "Working Fluid Selectionfor a small Rankine cycle Total Energy System for Recreation Vehicles", Proc.of 1973 I.E.C.E.C. No.739049, 1973.

4. Fraas, A.P. "A potassium-steam binary vapour cycle for better fuel economy and reduced thermal pollution", J.Engineering for Power, Vol.95, pp.53-63, 1973.

5. Blake, E.L., Hamman, W.E., Edwards, J.W., Reichard, L.E. and Art, M.R. "Thermal Stability as a function of chemical structure", J. of Chem. Eng. Data, Vol.6, 1, 1961.

6. Trenwith, A.B. and Watson, R.H. "The Thermal Decomposition of Chlorofluoromethanes", J.of Chemical Society, Part II, pp.2368-2372, 1957.

7. Miller, D.R., Thompson, Q.E., Hull, H.R. and Barber, K.F., "Working Fluids for automotive Rankine engines", Proc. of 7th I.E.C.E.C. pp.315-326, 1972.

8. Angelino, G. and MorOni, V. "Perspectives for Waste Heat Recovery by means of Organic Fluid Cycles", J.of Engineering for Power, Vol.95, pp.75-81, 1973.

9. Spauchus, H.P. and Doderer, G.C. "Reaction of Refrigerant 12 with Petroleum oils", ASHRAE Journal, February, 1961.

10. Steinle, H. "Chemical Reactions between Refrigerants and Oils in Refrigerating Machines" ASHRAE Trans., Vol.70, 1964.

11. Elsey, H.M. et al. "A Method of Evaluating Refrigerator Oils", Refrigerating Engineering, March, 1950.

12. Walker, W.O. et al. "Stability of Mixtures of Refrigerant and Refrigerating Oils". ASHRAE Journal, August, 1962.

13. Rizzuti, C.J. et al. "Effects of Additives and Oil Refining on Refrigerant-Refrigerator Oil Stability", ASHRAE Journal, July, 1962.

14. Jain, M.L., Demirgian, J., Krazinski, J.L. Bushby, H. and Mattes, H. "Determination of Thermal-Degradation Rates of Some Candidates Rankine-Cycle Organic Working Fluids for Conversion of Industrial Waste heat into Power". Ann.Ind.Energy Conservation Tech. Conf., Houston, U.S.A., 1984.

15. "(Freon) Fluorocarbons: Properties and Applications". Freon Product Information Bulletin G.I.E.I. du Pont, de Nemours Inc., Wilmington, Delaware, U.S.A.

16. Health and Safety Executive, Technical Data Note 45, "Industrial use of flammable gas detectors", HMSO London.

17. Adam, A.W. and Monahan, J. "100 kW Organic Rankine cycle Total Energy System", Proc.of 8th I.E.C.E.C. pp.126-130, 1973.

18. Owen, J.R. Internal Report. "The Organic Rankine Cycle, a review of applications and factors affecting working fluid selection" under contract no.B/SR/8530, Dept.of Mech.Eng., The City University, 1976.

CHAPTER 3

AIM OF RESEARCH

The necessary T-s diagram for a working fluid which would permit adiabatic expansion from saturated liquid to dry vapour with an isentropic efficiency of approximatley 80% is shown in Figure 3.1. As already stated in Section 1.7. such a fluid is required if a turbine, which is associated with high efficiency and flexibility of operation, can be used as the final main component of a TFC expander arrangement. At the onset of this research, the only identified fluid which could be used for this purpose, without the risk of decomposition, to condense at an average power plant temperature of the order of 35°C was n-pentane. With this fluid, an initial saturated liquid temperature of at least 180°C is necessary.

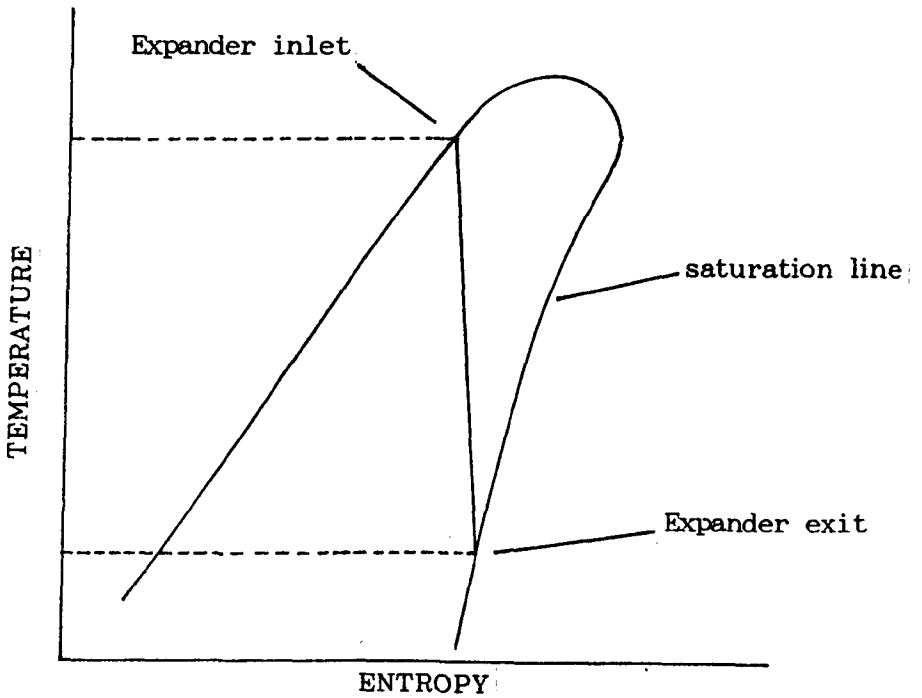

Figure 3.1. T-s diagram of desirable working fluid mixture.

The first objective of the research was therefore to find other working fluids which would enable a turbine to be used in the TFC system at lower peak temperatures.

A further object was to devise a binary mixture of fluids whose proportions could be varied to allow for a turbine version of the TFC to be used over a range of peak temperatures from the lowest possible up to a value where pure alternatives were available. An additional advantage of such a mixture is that over the useful life of a geothermal resource, whose maximum temperature slowly decreases, the component proportions could be gradually changed to maintain an optimum conversion efficiency for the system.

To meet the requirements of the first objective, reliable analytical procedures for the prediction of pure fluid properties were already available at City University. However, to investigate the properties of mixtures an analytical procedure had to be developed to predict enthalpy and particularly entropy which would be accurate at relatively high saturation pressures.

To verify the validity of the predicted properties of a suitable mixture, confirmatory measurements of estimated bubble and dew point pressures would be required.

The essential practical aims of the investigation were therefore:

i) To devise such an analytical procedure for mixtures and apply it to combinations of fluids until a desirable mixture was found to conform with the requirements of section 2.2.

ii) To confirm the predicted properties of the best mixture by experiment.

CHAPTER 4

CLASSICAL THERMODYNAMICS OF FLUID PHASE EQUILIBRIA

4.1. CHEMICAL POTENTIAL AND FUGACITY

Gibbs introduced concepts in his epoch-making article "On the Equilibrium of Heterogeneous Substances" [1] which govern multi-component phase equilibria such as the chemical potential. The chemical potential can be expressed as:

$$\mu_i = \left[\frac{\partial G}{\partial n_i}\right]_{T,P,n_j}$$

and is a function of T,P and all n components. However, the chemical potential is a rather abstract quantity and is devoid of "physical reality". Lewis [2] in 1907 showed that it was possible to derive a concept, equivalent to that of chemical potential, with a more meaningful physical sense. He called this function, fugacity (from the Latin fuga = escape). This concept can be derived by the following simple transformation.

From Maxwell's relations we have:

$$\bar{V}_i = \left\{\frac{\partial \mu_i}{\partial P}\right\}_T$$

where $\bar{V}_i$ is the partial molar volume.

Using the ideal gas equation of state to express $\bar{V}_i$ as a function of P and T and integrating at constant temperature, we obtain:

$$\mu_i - \mu_i^o = RT \ln \frac{P_i}{P_o} \qquad (4.1)$$

However, this equation is only true for a pure ideal gas. Replace P/P_o by f/f_o in the equation to obtain:

$$\mu - \mu_i^o = RT \ln \left\{\frac{f_i}{f_i^o}\right\} \qquad (4.2)$$

where f_i is the fugacity of any component in any phase, ideal or not, and f_i^o is its value at a suitable standard-state. To quote Lewis [2] "Now, at least theoretically, every substance can be brought isothermally into the state of a perfect gas. For, if we admit that every substance at a finite temperature has a finite vapour pressure, then if the pressure upon a substance is decreased without limit the substance will eventually vaporize, and with further diminution in pressure the vapour will approach nearer and nearer to the condition of a perfect gas. Therefore, instead of completing our definition of fugacity by assigning to it some arbitrary value in a chosen state, such as the liquid state at one atmosphere, it is better to complete the definition by making the fugacity of a perfect gas equal to the pressure. Fugacity will be regarded as having the same dimensions as pressure". To complete the definition of fugacity, Lewis stated:

$$\frac{f_i}{y_i P} \to 1 \text{ as } P \to 0$$

where f_i = fugacity

P = pressure

y_i = vapour mole fraction.

Tunnell [3] pointed out, however, that there is no way of proving that the limit of the indeterminate form is unity as follows:

$$\lim_{P \to 0} \frac{f(T,P)}{P} = 1$$

and suggested an alternative definition:

$$RT \ln f(T,P) = RT \ln p - \int_0^P \left\{ \frac{RT}{P} - V \right\} dP \qquad (4.3)$$

The definition given by Eqn.4.2 does not determine the numerical value of the fugacity, but only the ratio of the fugacities of a substance in two isothermal states. The numerical value may be assigned at each temperature in one state. While either μ_1^o or f_1^o is arbitrary, both may not be chosen independently; when one is chosen the other is fixed.

Lewis called the ratio f/f^o, activity. The activity of a substance provides a measure of the difference between the substance's chemical potential at the state of interest and that at its standard state.

The fugacity of a substance can be thought of as a "thermodynamic pressure" [4] since it accounts for non-ideal behaviour. The fugacity of a component in a mixture of ideal gases equals its partial pressure. The equation of thermodynamic equilibrium may be re-written as follows:

$$T^L = T^V \quad \text{(where superscripts L and V stand for liquid and vapour)}$$

$$f_i^L = f_i^V \qquad (4.4)$$

4.2. FUGACITY METHODS FOR ENGINEERING APPLICATIONS

For practical purposes the fugacities are normally re-written in terms of a number of variables which are experimentally accessible such as x,y (mole fractions), T (absolute temperature) and P the total pressure assumed to be the same for both phases.

The vapour-phase fugacity, f_i^V may be expressed with the aid of an auxiliary function called the fugacity coefficient ϕ_i^V as follows:

$$f_i^V = y_i \, \phi_i^V \, P \qquad (4.5)$$

where y_i is the vapour-phase mole fraction.

The liquid-phase fugacity f_i^L is usually re-written in one of three possible ways.

(i) by means of the fugacity coefficient ϕ_i^L and the liquid-phase mole fraction x_i

$$f_i^L = x_i \, \phi_i^L \, P \qquad (4.6)$$

(ii) by means of the activity coefficient γ_i and the standard state or reference fugacity f_i^o

$$f_i^L = x_i \, \gamma_i \, f_i^o \qquad (4.7)$$

or

(iii) by means of the activity coefficient γ_i^* and the Henry's constant

$$f_i^L = x_i \, \gamma_i^* \, H_{i,m} \qquad (4.8)$$

Equations (4.5) and (4.6) form the basis for calculating vapour-liquid equilibrium (VLE) from equations of state (Benedict-Webb-Rubin, Lee-Kesler, Redlich-Kwong-Soave, Peng-Robinson, etc.). Equations (4.5), (4.7) or (4.8) form the basis for calculating VLE from molecular activity coefficient models (Van Laar, Wilson, UNIQAC, etc.) and from group-contribution models (UNIFAC, ASOG, etc.). The reference fugacity f_i^o of pure components i in equation (4.7) may be calculated as follows:

$$f_i^o = P_i^s \, \Phi_i^s \, POY_i \qquad (4.9)$$

where P_i^s is the vapour pressure of pure component i at the temperature of the system, Φ_i^s is the fugacity coefficient at the saturation of pure component i, and POY_i is the Poynting correction factor.

The pure component vapour pressures P_i^s are often calculated by means of the Antoine equation:

$$\ln P_i^s = A_i - B_i/T+C_i$$

where values for A_i, B_i and C_i (Antoine's constants) may be found in the literature [5,6,7].

At low to moderate pressures (up to about 10 bars)[8] the values of Φ_i^v (Eqn.4.5) and Φ_i^s (Eqn.4.9) may be estimated from the virial equation of state truncated after the second term.

$$\frac{PV}{RT} = 1 + \frac{BP}{RT}$$

Experimental values of the second virial coefficients B may be found in Dymond et al. [8]. The coefficient B corresponds to interaction between pairs of molecules. Although particularly valuable in describing exactly other properties of gases such as viscosity, sonic velocity and heat capacity, the virial equation of state fails to represent the liquid state even with a large number of terms [9]. At high densities the infinite series diverges [10].

The Poynting correction is an exponential function of the pressure. It accounts for the compression of the liquid to a pressure P greater than P_i^s. It is calculated by the following expression:

$$POY_i = \exp. \int_{P_i^s}^{P} \frac{V_i^c \, dP}{RT}$$

where V_i^c is the partial molar volume of the condensed phase. The Poynting correction factor is small at low and moderate pressures and is often neglected. It may become large at extreme high pressures (over 1000 bar) or at low temperature [4]. Equations (4.7) and (4.8) are equivalent relations for the evaluation of liquid fugacities. This is so because we distinguish two types of ideality: one leading to Raoult's law and the other leading to Henry's law as we shall see in the next section.

When fugacities are to be calculated by equations (4.5) and (4.6) (equation of state method) the fugacity coefficients are related to volumetric properties by a rigorous analytical relation derived by Beattie [11]. This is as follows:

$$\ln \Phi_i = \frac{1}{RT} \int_V^{\infty} \left[\left[\frac{\partial P}{\partial n_i} \right]_{T,V,n_j} - \frac{RT}{V} \right]^{\alpha} dV - \ln \left[\frac{PV}{n_T RT} \right] \quad (4.10)$$

where α is the total number of phases containing n_T moles, n_i is the number of moles of component i and R is the gas constant. The mole fraction is n_i/n_T.

A solution is said to be ideal in the sense of Raoult's law when (Eqn.4.7) reduced to $f_i^L = f_i^o x_i$ (by making $\gamma_i = 1$) holds for the entire range of composition (from $x_i = 0$ to $x_i = 1$)[13]. For such a solution when $x_i = 1$, the fugacity of pure liquid i at the temperature of the solution equals its standard-state fugacity f_i^o.

4.3. IDEAL SOLUTIONS: RAOULT'S AND HENRY'S LAWS

4.3.1. Raoult's Law

When considering the behaviour of an actual gas we use the behaviour of an ideal gas, a theoretical abstraction, as a standard of reference, since the properties of an ideal gas can be predicted with certainty. Similarly, when dealing with solutions we imagine an ideal solution whose properties are additively composed of those of its components. When two liquids are mixed to give an ideal solution, there is no heat exchange with the surroundings nor will any heat exchange result from the dilution of the solution of either component. The total volume will be equal to the sum of the volumes of the components at constant temperature and pressure. When applying these simplifying assumptions to a liquid solution in equilibrium with its vapour we have:

Letting

$$\mu_i^L = \mu_i^V$$

$$\underset{\text{liquid phase}}{\mu_i^{Lo}(T) + RT \ln x_i} = \underset{\text{vapour phase}}{\mu_i^{Vo}(T) + RT \ln P_i} \qquad (4.11)$$

where $\mu_i^{Vo}(T)$ is the standard chemical potential of component i in the gaseous state. The relationship (4.11) still holds if component i is entirely in the liquid state when in this case $x_i = 1$ and $P_i = P_i^s(T)$, therefore:

$$\mu_i^{Lo}(T) = \mu_i^{Vo}(T) + RT \ln P_i^s \qquad (4.12)$$

Subtracting (4.11) from (4.12) we have:

$$RT \ln x_i = RT \ln \frac{P_i}{P_i^s}$$

where P_i^s is the saturated vapour pressure

and finally

$$x_i = \frac{P_i}{P_i^s} \qquad \text{or} \qquad y_i P = x_i P_i^s$$

This relation is called Raoult's law. It simply states that the partial pressure of component i in the vapour phase is proportional to the mole fraction of the same component in the liquid phase. Figure 4.1. illustrates Raoult's law.

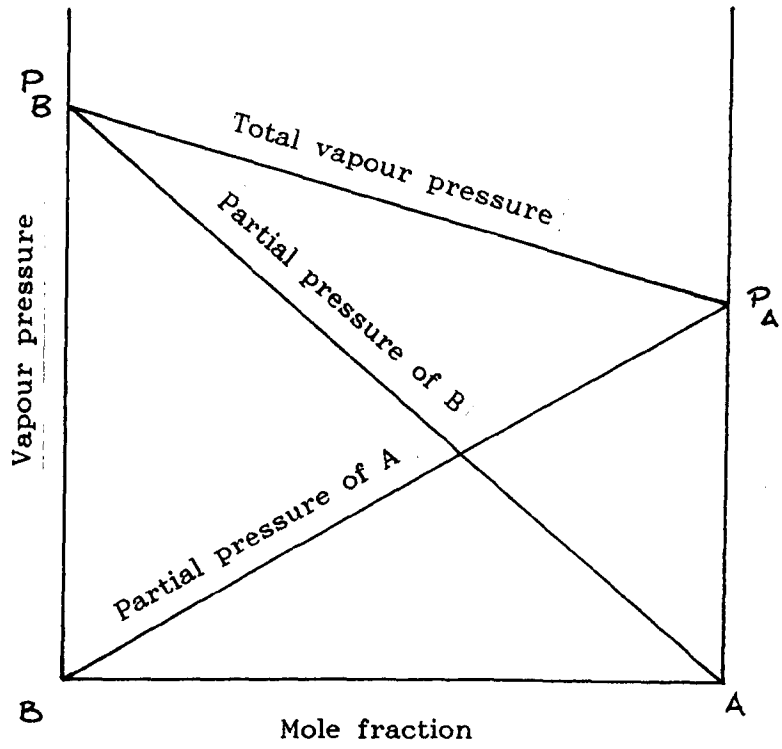

Figure 4.1. Raoult's Law

4.3.2. Henry's Law

Another model of ideal behaviour, appropriate for nonelectrolyte solutions is based on Henry's law. To illustrate the usefulness of an ideal solution based on Henry's law a typical plot of f_i^L versus x_i for one of the components of a binary solution at constant T and P is shown in Figure 4.2.

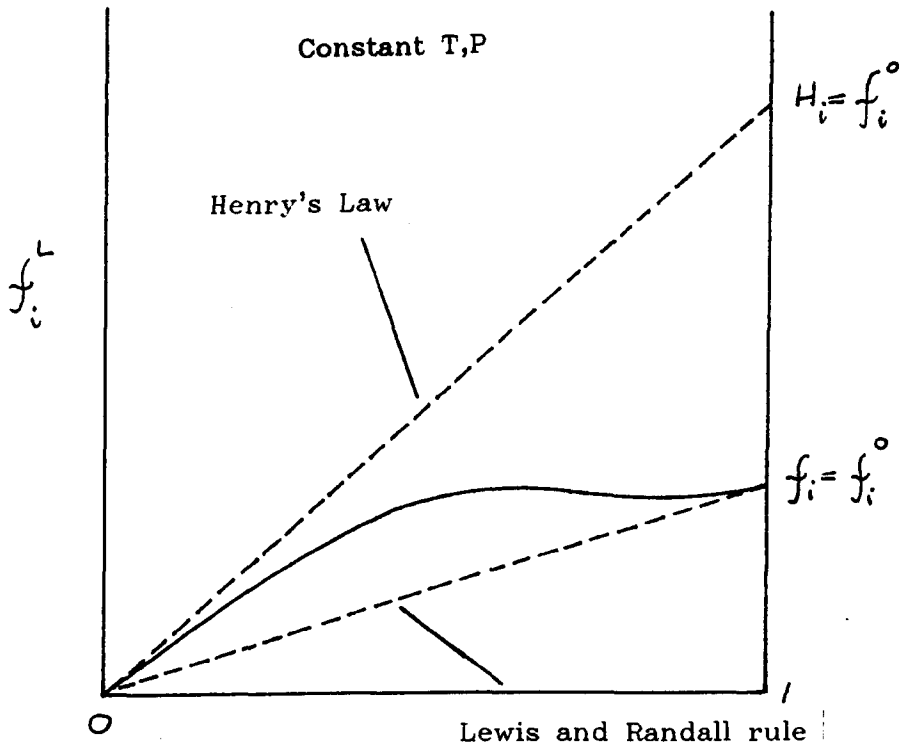

Figure 4.2. Henry's Law

At both ends of the graph one encounters two limiting cases: one when $x_i \to 1$ and the curve representing f_I^L becomes tangent to the straight line given by equation $f_I^L = x_i f_i$ (Lewis and Randall rule) and the other when $x_i \to 0$ (dilute solution) and the curve representing f_I^L becomes tangent to the straight line which is expressed mathematically by

$$\lim_{x_i \to 0} (f_i/x_i) = H_i$$

This is the statement of Henry's constant H_i, the slope of the limiting tangent is called Henry's constant.

Finally, equations (4.7) and (4.8) are now clarified except for the evaluation of Henry's constant.

Let us consider a gas 2 dissolved in a liquid 1. The vapour pressure of pure liquid 1 is P_i^s. The Henry's law constant may then be written as:

$$H_{2,1} = H_{2,1}\,(P_i^s)\,\exp \int_{P_i^s}^{P} \frac{V_2^{-\infty}}{RT}\,dP$$

where $H_{2,1}(P_i^s)$ is the Henry's constant at pressure P_i^s and $V_2^{-\infty}$ is the partial molar volume of gas dissolved at infinite dilution in the liquid. It may be shown that $H_{2,1}(P_i^s)$ is the limit value calculated from experimental solubility data as follows:

$$H_{2,1}(P_i^s) = \lim_{x_i \to 0} (f_2^V/x_2)_T$$

where x_2 is the solubility in the liquid corresponding to a vapour-phase fugacity f_2^V.

4.4. NORMALIZATION

It is convenient to define the activity coefficient in such a way that for an ideal solution it is equal to unity. If activity coefficients are defined with reference to an ideal solution in the sense of Raoult's law then for each component i present

$$\gamma_i \to 1 \qquad \text{as} \qquad x_i \to 1$$

This is called the symmetric convention. Normalization (that is, becomes unity) holds for both solute and solvent. However, if activity coefficients are defined based on Henry's law (ideal dilute solution) then:

$$\gamma_1 \to 1 \quad \text{as} \quad x_1 \to 1 \quad \text{(solvent)}$$

$$\gamma_2 \to 1 \quad \text{as} \quad x_2 \to 0 \quad \text{(solute)}$$

This is called the unsymmetrical convention.

4.5. THE VAPOUR-LIQUID EQUILIBRIUM CALCULATION

The fugacity method using an equation of state (as indicated by Eqn.4.5 and 4.6) to describe the vapour and liquid phases was preferred here to activity coefficient imperfect liquid models as we shall see in detail in Chapter 5. The accuracy of the results predicted relies on the choice of the equation of state as well as on the mixing rules adopted.

The equations of equilibrium to be satisfied are of the form:

$$f_i^V = f_i^L$$

$$y_i \, \Phi_i^V = x_i \, \Phi_i^L$$

where the vapour and liquid fugacity coefficients are functions of the temperature T, the pressure P and the vapour and liquid mole fractions, as follows:

$$\Phi_i^V = f(T,P, y_1, \ldots .y_N)$$

$$\Phi_i^L = f(T,P, x_1, \ldots \ldots x_N)$$

There are basically four types of vapour-liquid equilibrium calculations. Given either pressure P or the temperature T, and the mole fractions of one phase, then the unknowns are either the temperature T or the pressure P and the mole fractions of the other phase. This can be summarized as follows:

GIVEN	FIND
$P, x_1, x_2, \ldots\ldots x_N$	$T, y_1, y_2, \ldots\ldots y_N$ (Bubble Temperature)
$P, y_1, y_2, \ldots\ldots y_N$	$T, x_1, x_1, \ldots\ldots x_N$ (Dew Temperature)
$T, x_1, x_2, \ldots\ldots x_N$	$P, y_1, y_2, \ldots\ldots y_N$ (Bubble Pressure)
$T, y_1, y_2, \ldots\ldots y_N$	$P, x_1, x_2, \ldots\ldots x_N$ (Dew Pressure)

Solutions of these simultaneous equations can only be carried out efficiently using a digital computer.

With a knowledge of the pressure P, the temperature T, and composition of the mixture, thermodynamic properties (enthalpy, entropy, etc.) can be analytically calculated as these are functions of the same variables (P, T and composition).

REFERENCES

1. Gibbs, J.W. "On the Equilibrium of Heterogeneous Substances" The Scientific Papers of J. Willard Gibbs, Dover Publications, 1961.

2. Lewis, G.N. "Outlines of a new system of Thermodynamic Chemistry" Proc. Am.Acad. Vol.43, 260, 1907.

3. Tunnell, G. "The Definitions and Evaluation of the Fugacity of an element or compound in the Gaseous state".

4. Prausnitz, J.M. "Molecular Thermodynamics of Fluid-Phase Equilibria". Prentice-Hall International, 1969.

5. Boublik, T., Fried, V. and Hala, E. "The Vapour Pressures of Pure Substances". Elsevier, 1973.

6. Dykyj, T and Repas, M. "Tlak Nasytenej Pary Organickych Zlucenin". Vydavatelstvo Slovenskej Akademic Vied, Bratislava, 1979.

7. Reid, R.C., Prausnitz, J.M. and Sherwood, T.K. "The Properties of Gases and Liquids". McGraw-Hill, Fourth Edition, 1986.

8. Dymond, J.H. and Smith, E.B. "The Virial Coefficients of Pure Gases and Mixtures: A Critical Compilation". Clarendon Press, Oxford, 1980.

9. Hayden, W.H. and O'Connell, J.P. Ind.Eng.Chem.Proc.Design Dev., Vol.14, 209, 1975.

10. Mason, E.A. and Spurling, T.H. "The Virial Equation of State". International Encyclopedia of Physical Chemistry and Chemical Physics. Topic 10, Vol.2, Pergamon Press, 1969.

11. Beattie, J.A. Chem.Rev., Vol.44, 141, 1949.

12. Denbigh, K.G. "The Principles of Chemical Equilibrium" Cambridge University Press, 1966.

13. Walas, S.W. "Phase-Equilibrium Chemical Engineering". Butterworth Publications, 1985.

CHAPTER 5

A REVIEW OF THERMODYNAMIC ANALYSIS OF BINARY ORGANIC MIXTURES

5.1. INTRODUCTION

The main application of the Thermodynamics of Vapour-Liquid Equilibria is in the design and operation of distillation columns, absorption towers, extraction units and other types of separation equipment where phase-equilibrium data is needed [2]. Quantitative information[3] on phase-equilibria, either theoretical or experimental, constitutes an essential requirement for design engineers whose main task is the separation of liquid and gaseous multi-component mixtures into pure components or into fractions of desired composition. This is one of the most important functions of chemical engineering.

Although multi-component processes are much more common in chemical engineering processes than binaries we shall concentrate on the latter, for the aim of this research project is the choice of a suitable binary organic mixture to be used as a working fluid in the Trilateral power plant. Bearing in mind that the techniques used in vapour-liquid equilibrium are absolutely general (a binary system being a particular case of multi-component mixtures) we shall proceed to examine the two methods which have been used in essentially all applied phase-equilibrium work.

When attempting to review a vast subject such as the Thermodynamics of Fluid-Phase Equilibria one almost necessarily overlooks articles which might have theoretical and/or practical importance not through negligence or prejudice but simply because of limited space and time. Here are briefly presented, in the author's opinion, the most useful methods. Emphasis is given to cubic volume equations of state (EOS) since the Redlich-Kwong-Soave EOS was chosen to be used in this research project, as will be shown later. Even the review of equations of state alone is a formidable task. Robert Reid [1], in the year 1980/81 only, counted 885 papers concerning the use of EOS.

5.2. FUNDAMENTAL CONCEPTS

As was pointed out in Chapter 4, we can calculate fugacities by two methods: (i) use an equation of state applicable to both liquid and vapour phases, or (ii) use an equation of state only for calculating the vapour-phase fugacity and an entirely different method expressed by activity coefficient for calculating liquid fugacities.

In both cases, the starting point is the equality of fugacities:

$$f_i^V = f_i^L \qquad i = 1,2,.....,N \text{ components} \qquad (5.1)$$

where for a N-component mixture f_I^V is the fugacity of component i in the vapour phase and f_I^L is the fugacity of component i in the liquid phase.

In the activity coefficient approach, Eqn.5.1, is re-written as follows:

$$y_i \, \Phi_i^V \, P = x_i \, \gamma_i \, f_i^{OL} \qquad (5.2)$$

where f_i^{OL} is the standard state liquid fugacity and γ_i is the fugacity coefficient of component i and Φ^V the vapour fugacity coefficient. If the vapour phase is an ideal solution $\Phi_i^V = \Phi_i^{sat}$, neglecting the so-called Pointing correction:

$$y_i \, P = x_i \, \gamma_i \, p_i^{sat} \qquad (5.3)$$

where Φ_i^V and Φ_i^L are the fugacity coefficients of component i in the vapour and liquid phases respectively.

For any particular phase equilibrium problem, a very important decision is which of these two methods is the most suitable. Therefore it is most important to analyse the advantages and disadvantages of both methods. The relative merits of each approach are summarized in Table 5.1 extracted from [4]. For what Pitzer [5] called "normal fluids", i.e. those which are either non-polar or else slightly polar and which do not associate strongly (e.g. by hydrogen bonding) and whose intermolecular motion must be classical (quantum effects neglected), vapour-liquid equilibria can often be successfully calculated at high pressures by making use of some empirical equation of state. However, many mixtures which are dealt with in conventional separation, though not in this case, are strongly polar in nature or have hydrogen-bonding components in which case the activity coefficient approach must be used.

Method	Advantages	Disadvantages
(a) Equation of state approach	1. No standard states 2. P-V-T-x data are sufficient in principle no phase equilibrium data needed. 3. Easily utilizes theorem of corresponding states 4. Can be applied to critical region	1. No really good equation of state available for all densities 2. Often very sensitive to mixing rules 3. Difficult to apply to polar compounds, large molecules or electrolytes.
(b) Activity coefficient approach	1. Simple liquid-mixture models are often satisfactory. 2. Effect of temperature is primarily in f^{o} (standard fugacity) not in γ. 3. Applicable to wide variety of mixtures including polymers and electrolytes.	1. Need separate method to find V. 2. Cumbersome for super-critical components 3. Difficult to apply in critical region.

Table 5.1. Brief comparison of methods (a) and (b).

From a strictly thermodynamic point of view, using an equation of state for all fluid phases is more practical [6]. This is because a standard-state liquid fugacity f_i^{OL} does not have to be specified. In the activity coefficient approach where specification of f_i^{OL} is required; the definition of f_i^{OL} is arbitrary and dictated only by convenience [7]. It is necessary that f_i^{OL} be the fugacity of component i at the same temperature as that of the solution at some fixed composition and at the same specified pressure. When in a binary mixture, fugacities are being estimated at a temperature above the critical temperature of one of the components its standard liquid fugacity becomes hypothetical. In that event, the choice of a properly defined activity coefficient and standard-state introduces formal difficulties which are often computationally inconvenient and for practical implementation, require parameters from experimental

data that are only rarely available [6,7]. This situation is avoided when the equation of state approach is used since the expression for phase-equilibrium does not involve standard liquid fugacity.

At low and moderate pressures (up to 10 bar) [7] for systems containing polar compounds (e.g. binary systems of water-ammonia, ketones-acids, water-hydrocarbons, alcohols-aldehydes) or polymers, the activity coefficient method for liquid-phase mixtures is preferred [6].

The liquid phase activity coefficients ϕ_i^L are related to molar excess. Gibbs function g^E as follows [7]

$$g^E = RT \sum_i x_i \ln \gamma_i$$

and

$$RT \ln \gamma_i = g_i^{-E}$$

where g_i^{-E} is the partial molar Gibbs function. The molar excess Gibbs function g^E is defined as:

$$g^E = g - g^{id}$$

where g is the molar Gibbs function of a mixture at a given temperature T, pressure P and composition x_i, while g^{id} is the molar Gibbs function for the mixture at the same conditions assuming ideality.

Many different models for g^E and hence γ_i have been used over the years like Margule [8], Van Laar [9], Redlich-Kister (which is equivalent to Margule's relation). These semi-empirical relations for calculation of activity coefficient were to some extent derived from a classical thermodynamic relation, i.e. the Gibbs-Duhem equation (which relates the activity coefficient of one component in a solution to those of the others). This well-known equation, along with Gibbs-Helmholtz (which relates the effect of temperature on the activity coefficient to the enthalpy of mixing) and an equation relating the partial molar volume to the effect of pressure on the activity coefficient are classical thermodynamic relations whose practical applications are limited [6]. By contrast, if one has a sound equation of state applicable to all phases, one can calculate not only fugacities from volumetric data but also all the other configurational properties such as the enthalpy, entropy and volume change on mixing [6].

In 1964, Wilson [10] introduced the local composition concept, i.e. that interactions between molecules depend primarily on "local concentrations" which he expressed as volume fractions. These concentrations are defined in probabilistic terms, the Boltzmann distribution of energies. This new concept has opened the way for the development of some of the most popular activity coefficient models in use today, like Wilson [10,11], NRTL (Non-Random Two-Liquid) [12], and UNIQUAC (Universal Quasi-Chemical) [13,14]. These models form part of a very large subject and details are beyond the scope of this thesis. It is nevertheless worth

mentioning in very general terms the UNIQUAC method. As will be shown later, this model forms the basis of a group-contribution technique called UNIFAC.

5.3. THE UNIQUAC MODEL

In the UNIQUAC model, the molar excesss Gibbs function is given by two terms:

$$g^E = g^E(\text{combinatorial}) + g^E(\text{residual})$$

The combinatorial term takes into account liquid phase non-idealities due to differences in molecular size and shape and may be written as follows:

$$g^E(\text{combinatorial}) = \sum_i x_i \ln \frac{\Phi_i}{x_i} + \frac{Z}{2} \sum_i q_i x_i \ln \frac{\theta_i}{\Phi_i}$$

where Φ_i and θ_i are volume and area fractions calculated from pure component volume and surface area parameters r_i and q_i and from mole fractions x_i. Z is the co-ordination number and is normally set equal to 10.

The residual term takes into account non-idealities due to intermolecular interactions. It may be written as follows:

$$g^E(\text{residual}) = -\sum_i q_i x_i \ln \left(\sum_j \theta_i \tau_{ji}\right)$$

The summation in both equations should be taken over all components. The values of τ_{ji} are calculated from the following equation:

$$\tau_{ji} = \exp\left[-\frac{a_{ji}}{RT}\right]$$

where

$$a_{ji} = \frac{Z}{2}\frac{U_{ji} - U_{1i}}{RT}$$

The values of U_{ji} characterise the energy of interaction between sites i and j on the lattice.

5.4. GROUP CONTRIBUTION METHODS

In addition to the two methods already described, there are also methods for determining activity coefficients based on what is called the Group-Contribution approach. Group-contribution methods allow for the prediction of liquid phase activity coefficients for binary and multi-component mixtures for which little or no experimental information is available. In any Group-Contribution method, the basic idea is that whereas there are thousands of chemical compounds, the number of functional groups which constitute these compounds is much smaller. The groups are structural units such as CH_3, OH and others, which when added form the parent molecules. Instead of considering a liquid mixture as a solution of molecules, the mixture is considered as a solution of groups. The activity coefficients are then determined by the properties of the groups rather than by those of the molecules. This is a great advantage. The activity

coefficients of a large number of very different mixtures may be calculated from characteristic parameters representing a few groups and the energetic interactions betwen the groups.

The ASOG (Analytical Solution of Groups) and UNIFAC (Universal Functional Group Activity Coefficient) are the most established group-contribution models to date[15] for the prediction of liquid phase activities in non-electrolyte mixtures. In both methods the activity coefficients are calculated from two terms:

$$\ln \gamma_i = \ln \gamma_i^C + \ln \gamma_i^R$$

The combinatorial term $\ln \gamma_i^C$ takes into account differences in size and shape of the molecules and the residual term $\ln \gamma_i^R$ describes the non-idealities due to energetic interactions between the groups.

Kojima and Tochigi [16] presented a comprehensive treatment of the ASOG method for VLE calculations. The UNIFAC method was conceived in Berkeley [17] and has been extensively developed by Fredenslund et al.[18] in Denmark and by Gmehling et al.[19] in Germany. Others group-contribution methods have been developed in recent years notably the TOM project of Kehiaian et al.[20,21,22]. These group-contribution models have a limited pressure range of applicability [23,18] due to the methods used for the vapour phase calculations and its detailed techniques are beyond the scope of this thesis.

Although the activity coefficient models continue to be of great practical interest for calculation of fugacities of compounds whose molecules are either polar or large or hydrogen-bonded, it is normally only suitable for application in the low to moderate pressure range. At high pressures [7] the equation of state approach appears to be more adequate, especially when phase-equilibria are to be calculated for mixtures of hydrocarbons and halocarbons (freons) (i.e. Pitzer's normal fluids) which were primarily targetted as possible good working fluids. That is the reason why the equation of state method is adopted here and we shall proceed to examine, what appear to be, the most useful ones.

5.5. EQUATIONS OF STATE

5.5.1. Introduction

It is well known that if a given mass of gas is compressed isothermally at very high temperatures, the volume decreases

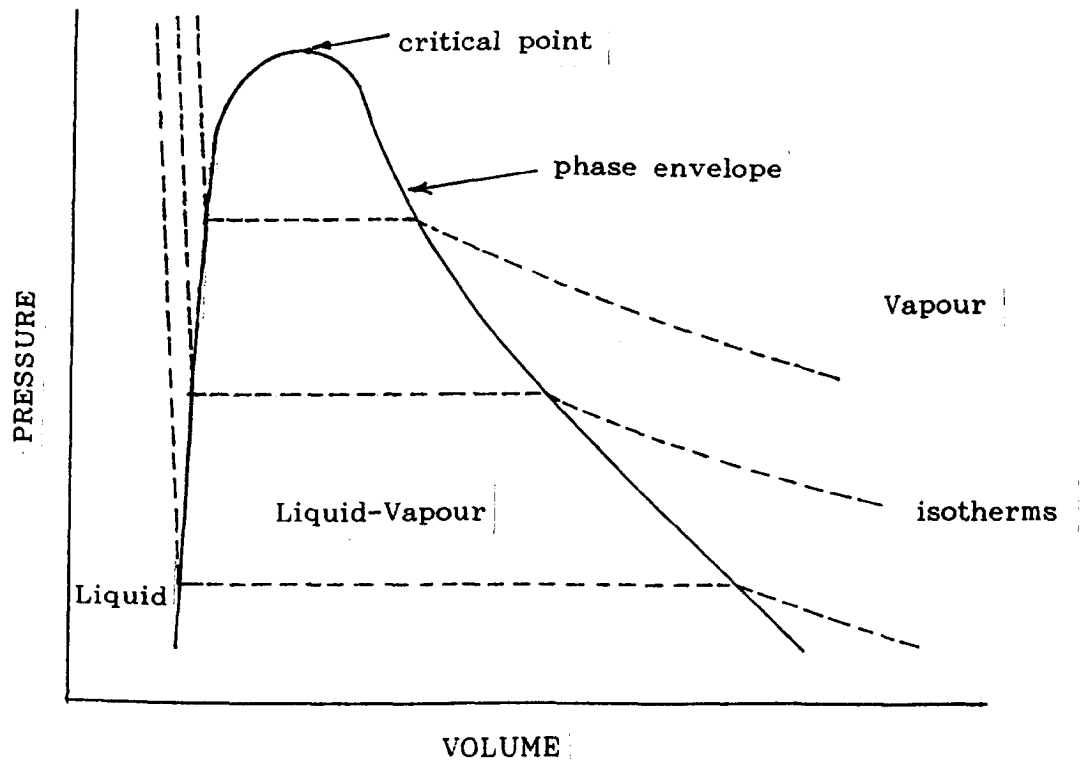

Figure 5.1. Plots of isothermals on a P-V diagram.

continuously and the isothermal P-V curve is continuous, with a continuous first derivative, and has the shape of a hyperbola given by the ideal-gas relation PV = NRT as shown on line 'a' in Figure 5.1.

Below the critical point (P_c,V_c) we find two phases capable of coexistence and two separate curves at the same temperature are experimentally determined, one for the change in volume of the liquid with pressure, and one for the change in volume of the vapour with pressure. However, it is attractive to assume that these two branches are really a single curve and that a single mathematical equation can be found to fit both vapour and liquid regions, as shown by the dotted line in Figure 5.1. The famous Van der Waal's equation of state satisfies these conditions qualitatively, but it describes the actual curves in the liquid region only roughly.

Ever since Van der Waal's time, equations of state have grown to be a very large and prolific field of research with more than a hundred equations published [23]. Some are associated with very eminent names, such as Clausius, Boltzmann, and Planck. Publications in this field are so numerous nowadays that Reid [1] counted 4779 papers in the 1967-82 period concerning the use of EOS. Most of these equations have been claimed to be better in some respects than earlier ones either because of a sound theoretical basis or greater accuracy in some particular range of temperature or pressure or for some particular substance. However, very little use has been found for most of them [23].

Equations of state may be classified arbitrarily into three groups[24]:

i) Virial Type or Complex Equations of State

ii) Perturbed Hard Body EOS

iii) Cubic (Van der Waals type EOS).

Only groups (i) and (iii) will be discussed in more detail in this review due to their practical importance.

5.5.2. Virial Type or Complex Equations of State

5.5.2.1. The BWR EOS

In the period 1940-52 extensive calculations for hydrocarbon mixtures, e.g. those found in processing natural gas and light petroleum fractions were reported by Benedict, Webb and Rubin (BWR) who used an eight-constant equation of state [25]. The celebrated BWR equation was designed as an improvement on the Beattie-Bridgman EOS [26] to rectify its inability to represent behaviour of liquids and gases above the critical density. The BWR equation is empirical and similar in form to the virial equation which represents the compressibility factor Z as a polynomial in density. The original BWR equation given below did not work well at low temperatures and high densities:

$$P = RT\rho + (B_o RT - A_o - \frac{C_o}{T^2})\rho^2 + (bRT - a)\rho^3 + a\alpha\rho^6 + \frac{C_o}{T^2}\rho^3(1 + \gamma\rho^2)\exp(-\gamma\rho^2)$$

Several modifications have been proposed. Figure 5.2 shows isotherms of n-Pentane with the BWR equation at 125, 150, 175, and 200°C displaying characteristic valleys.

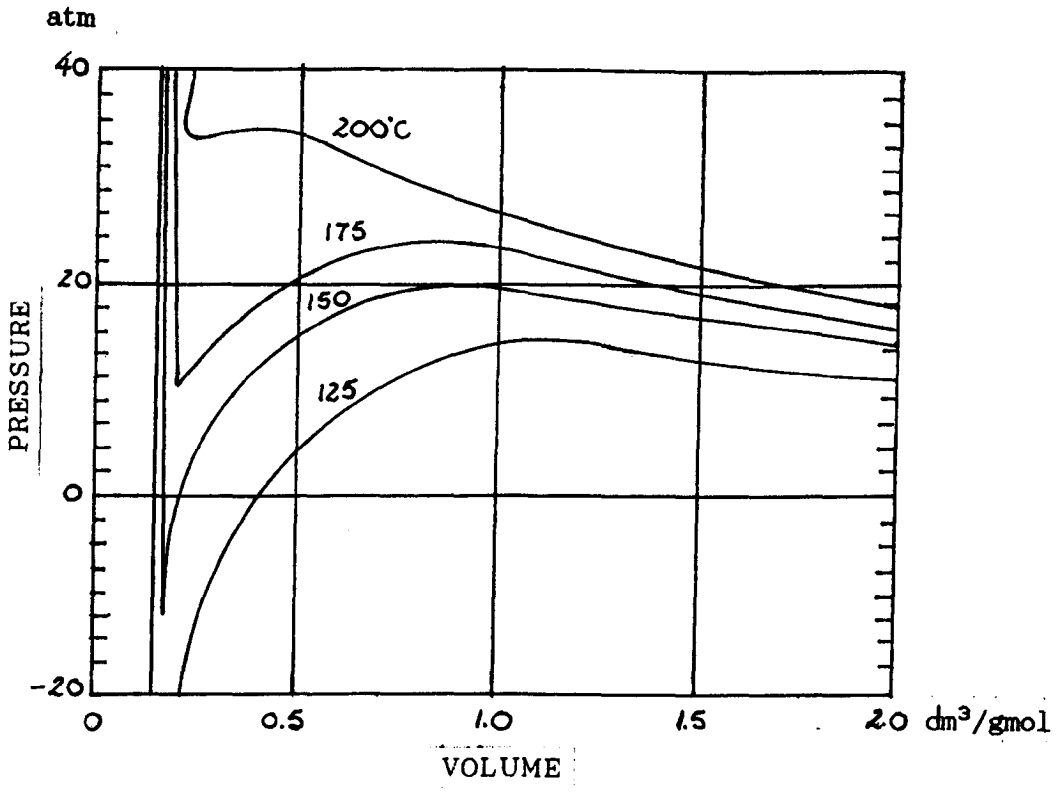

Figure 5.2. Isotherms of n-pentane with BWR equation

Perhaps the most successful modification which extended the application to low temperatures was made by Starling [27]. Later Lim and Hopke [28] performed a multi-property analysis for methane through pentane, nitrogen and carbon dioxide and their binary mixtures. Figures 5.3, 5.4, 5.5, and 5.6 show some of their results. They obtained good results for densities, residual enthalpies, and residual heat capacities, but their predicted equilibrium ratios for multi-component mixtures are often no better than those obtained with the simpler Peng-Robinson or Redlich-Kwong-Soave equations of state. This weakness is due to the purely empirical composition dependence of the BWR equation [23].

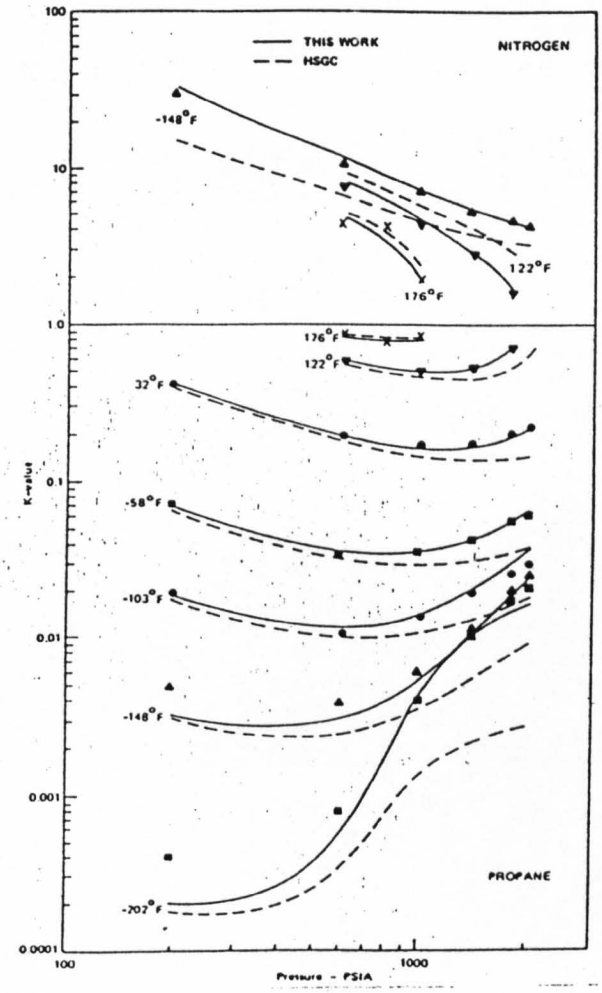

Figure 5.3. Comparison of BWRS calculations with experimental K-values for the propane-nitrogen system.

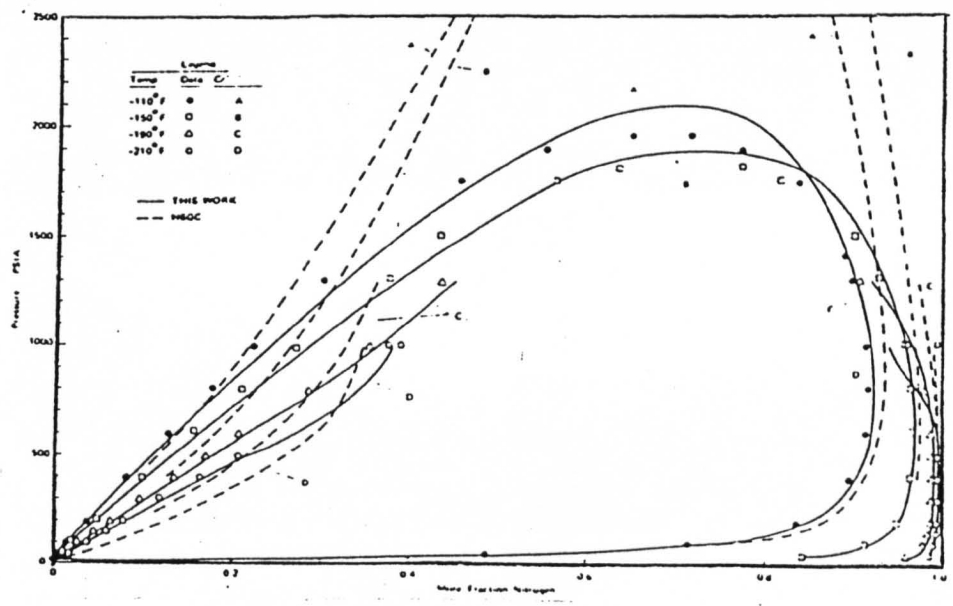

Figure 5.4. Comparison of BWRS calculations with experimental P-x diagram for the ethane-nitrogen system.

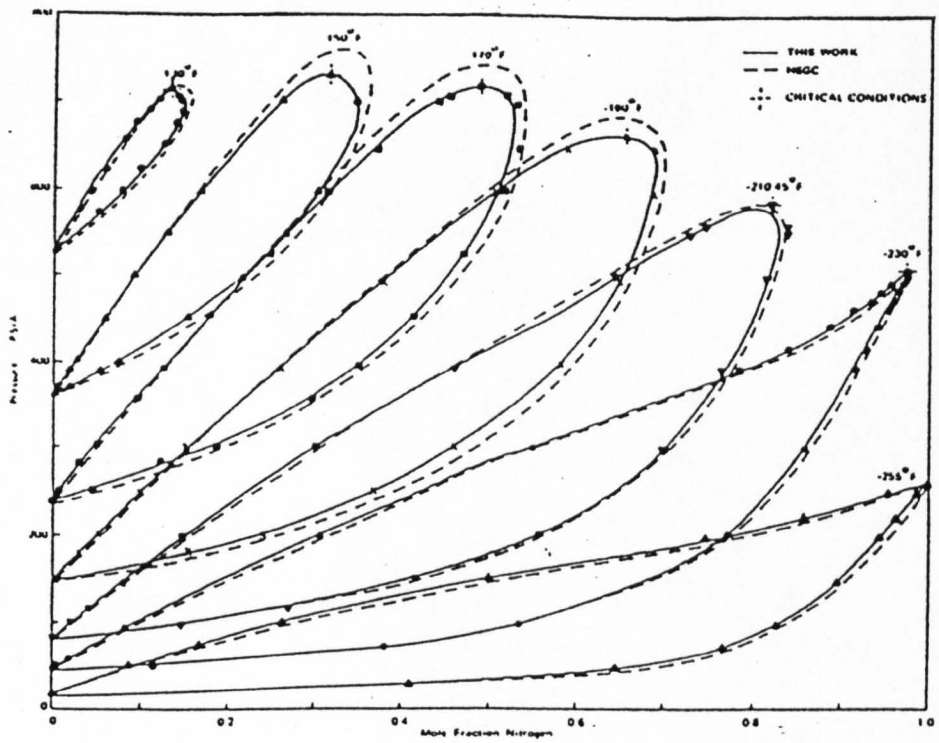

Figure 5.5. Comparison of BWRS calculations with experimental P-x diagram for the methane-nitrogen system.

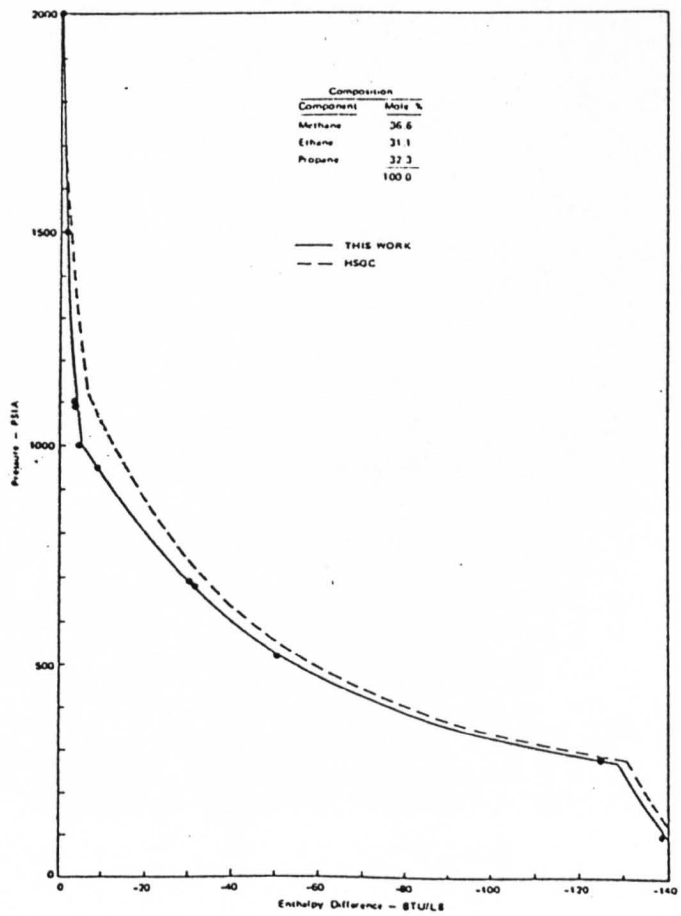

Figure 5.6. Comparison of BWRS predictions with experimental isothermal enthalpy through two-phase region for the methane-ethane-propane system.

The BWR equation may be extended with more terms in the polynomial. It is clear that the more constants in an equation of state, the more flexibility in fitting experimental data, but it is also evident that to obtain more constants, one requires more experimental information. Bender [29,30] has presented an extended BWR equation which is extremely reliable for mixtures of the lighter hydrocarbons, carbon dioxide, oxygen and nitrogen. However, it requires 20 parameters per component plus three parameters per pair of components in the mixture.

Extension to hydrocarbons heavier than n-decane was made possible by a generalization of Bishnoi et al. [31,32] and by Nishiumi [33]. Nishiumi [34] also proposed an extended BWR equation applicable to polar substances.

5.5.2.2. The Lee-Kesler EOS

It has been observed [35] for simple fluids (e.g. argon, krypton, xenon) that at a temperature equal to $^{7}/_{10}$ of the critical, the saturation pressure P^s divided by the critical pressure is given by:

$$\frac{P^s}{P_c} = \frac{1}{10} \left(\frac{T}{T_c} = \frac{7}{10}\right)$$

Bearing in mind that all substances have the same reduced vapour-pressure, Pitzer [36,37] defined, what he called, the acentric factor (ω) as follows:

$$\omega \equiv - \log_{10} \frac{P^s}{P_c} - 1.000 \quad \text{at} \quad \frac{T}{T_c} = T_r = \frac{7}{10}$$

The form is chosen to make $\omega = 0$ for simple fluids and $\omega > 0$ for more complex fluids.

The acentric factor is a macroscopic measure of the extent to which the force field around a molecule deviates from that of simple fluids (spherical molecules). The Pitzer's acentric factor is most useful because it can be calculated from experimental data.

Any property of the fluid, in reduced or dimensionless form, is assumed to be given by a function of the three variables: reduced pressure, reduced temperature, and acentric factor. The compressibility factor Z may be written:

$$Z = Z\ (P_r,\ T_r\ \omega)$$

It is found that a linear equation in ω is usually adequate:

$$Z = Z^{(\omega)}\ (P_r,\ T_r) + \omega\ Z^{(1)}\ (P_r,\ T_r) \qquad (5.4)$$

Lee and Kesler [38] considered a generalised equation of state of the form (5.4) suggested by Pitzer.

$$Z = Z^{(o)} + \frac{\omega}{\omega^{(r)}}(Z^{(r)} - Z^{(o)})$$

where superscript (o) stands for a simple fluid ($\omega = 0$) and (r) for a reference fluid (n-octane) in corresponding states with the fluid in question. For each of the pivot fluids, the compressibility factor is obtained by a Benedict-Webb-Rubin type equation.

$$Z = \frac{P_r V_r}{T_r} = 1 + \frac{B}{V_r} + \frac{C}{V_r^2} + \frac{D}{V_r^5} + \frac{C_4}{T_r^3 V_r^2}(\beta + \frac{\gamma}{V_r^2})\ \exp(-\frac{\gamma}{V_r^2})$$

where

$$V_r = \frac{P_c V}{RT_c}$$

C_4, β, and γ are constants

B, C and D are functions of T_r.

Lee and Kesler showed that their equation is applicable to a large variety of mixtures in the petroleum and related industries. This treatment has also the advantage of requiring very little experimental data on a fluid for its utilisation[39]. Plöcher et al.[40] modified the Lee-Kesler correlation emphasizing "asymmetric mixtures", i.e. those which contain both small molecules (e.g. hydrogen, oxygen, nitrogen, etc.) and large molecules (e.g. high boiling paraffins, aromatics, etc.). They obtained equilibrium ratios which are slightly better than those predicted by cubic equations of state.

5.5.3. Perturbed Hard Body Equations of State

An important theoretical group of EOS which has seen an active development in recent years is based on the Beret and Prauznitz [41] and Donohue and Prausnitz [42] "Perturbed Hard Chain Theory" (PHCT).

It is known that a major disadvantage of the Van der Waals family of EOS is the incorrect repulsion term ($^V/_{v-b}$). Carnahan and Starling [43] in 1969 developed a simple analytical equation which

gives a precise representation of the simulated behaviour for hard spheres replacing the repulsive term by a theoretical "exact" one. This is as follows:

$$Z = \frac{PV}{NKT} = \frac{(1 + y + y^2 - y^3)}{(1 - y)^3}$$

where $y = b/4V$ and b is a measure of the volumes occupied by the molecules. Beret and Prausnitz and Donohue and Prausnitz extended the Carnahan-Starling repulsive term for chain like molecules while their attraction term is based on an expression for intermolecular potential derived by Alder et al. [44]. This equation is written as:

$$Z_{PHCT} = 1 + c\,(Z_{cs} - 1) - ca/RTV$$

The repulsive term includes the new parameter, c, which is to account for the chain like nature of molecules (for spheres c = 1, for chains c > 1). The form of PHCT equation is justified by considering the attractive term as a "perturbation" on the reference model (the hard chain model) [45]. Important developments are being carried out including the "Chain of Rotators" COR concept of Chien et al [45] and the "Cubic Chain of Rotators" (CCOR) [46]. The "Chain of Rotators" equation was extended to polar fluids by Masuoka and Chao[47] although no mixture results were reported. Nevertheless, a simplified cubic form of this equation has been used for mixtures involving polar compounds [48,49]. Although theoretically important these equations have not yet found great practical impact.

5.5.4. Cubic EOS (Van der Waals family)

More than a hundred years ago (1873), Van der Waals[50] proposed a cubic in volume equation of state to account for non-ideal gas behaviour. It has the form:

$$P = \frac{RT}{V - b} - \frac{a}{V^2}$$

where a is a constant which takes account of the molecular force field interactions and b is also a constant which compensates for the volume occupied by the molecules. These physically meaningful parameters yield a qualitatively correct and simple, but quantitatively inaccurate, analytical description of the behaviour of real gases. To improve the accuracy and extend the range of validity, a vast number of equations of state, most of them empirically based on Van der Waals', have been proposed over the years. Despite the fact pointed out by Abbott[51,52] that a cubic equation of state cannot reproduce all thermodynamic functions with desirable accuracy they continue to appear in the literature in an ever increasing number. References [[53-59] contain new proposals for empirical Van der Waals type equations. The attractiveness of cubic equations of state and the desire to design new ones may be explained by their:

i) simplicity

ii) reliability

iii) relative ease of handling by a digital computer

iv) and that some forms are better than others as have been shown by several authors [52,60,61].

The Van der Waals family of EOS may be arbitrarily divided into cubic and "near-cubic" according to their dependence on volume. They express the pressure by two terms for the repulsive and the attractive forces, as follows:

$$P = P_{repulsive} + P_{attractive}$$

Until now perhaps the most successful modification is the one made by O. Redlich and J.N.S. Kwong in 1949[62]. They modified the attractive term in the Van der Waals EOS by a perturbation about the original term and further multiplied the parameter a by the inverse of the square root of the temperature as follows:

$$P = \frac{RT}{V - b} - \frac{a}{V^2\sqrt{T}}\left(1 - \frac{b}{V} + \left(\frac{b}{V}\right)^2 - \left(\frac{b^3}{V}\right) + \ldots\ldots\right)$$

The Redlich-Kwong EOS is usually written in the form:

$$P = \frac{RT}{V - b} - \frac{aT^{-1/2}}{V(V+b)}$$

As can be seen from Table 5.2, extracted from [63], the RK EOS represents an improvement over Van der Waals' for the following properties.

	b/V_c	$Z_c = P_cV_c/RT_c$	$(\partial \ell nP/\partial \ell nT)_V$ at the critical point
experimental	0.24 -0.26	0.23 - 0.31	5 - 7
Van der Waals	0.3333	0.375	4
Redlich-Kwong	0.26	0.333	5.58

Table 5.2. Comparison between Redlich-Kwong and Van der Waals' Equations of State.

i) A more realistic value of b/V_c leads to a better prediction of the critical isotherm, Figure 5.7, but bearing in mind that according to the investigations of Levelt Sengers et al.[64] no cubic equation of state can accurately describe the critical isotherm. They reported that the critical isotherm for real fluids is somewhat flatter than the fourth degree curve but not as flat as a fifth degree one.

ii) An improvement in PVT prediction leading to (a) better vapour enthalpies as demonstrated by Van Ness[65] and (b) better vapour fugacities.

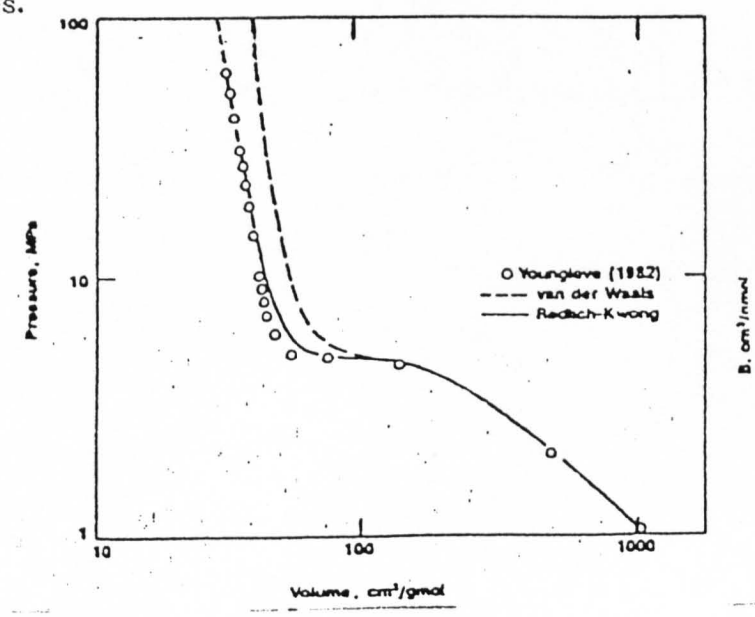

Figure 5.7. Critical isotherm of argon.

Ever since Redlich and Kwong published their equation of state, most investigators have turned their attention to the possibility of making the parameter "a" (and possibly b as suggested by Zudkevitch and Joffe[66]) temperature dependent. This was first correlated by Wilson[67] in 1966 who wrote "a" as a function of T at subcritical temperature as follows:

$$a = a_c\ (1 + m\ (1 - T/T_c))$$

with $m = 0.57 + 1.62\ \omega$.

Wilson assumed that (a/RT) is a linear function of the reciprocal temperature and estimated the constant m from the slope of the vapour pressure curve at the critical point using the correlation by Riedel[68]. Later in 1972 G.Soave[69] developed a similar correlation for the "a" parameter:

$$a = a_c\alpha(T_r,\omega) = a_c(1 + m_o(1 - \sqrt{T/T_c}))^2$$

where $m_o = 0.48 + 1.574\omega - 0.176\omega^2$

with

$$a_c = 0.42748R\ T_c^2/P_c$$

$$b = 0.08664\ RT_c/P_c$$

Soave constrained his correlation to match the saturated vapour pressure at a reduced temperature of 0.7 in accordance with the definition of the acentric factor. In 1976 D.Y.Peng and D.B. Robinson[70] developed a similar correlation to yield:

$$P = \frac{RT}{V - b} - \frac{a}{[V(V+b)+b(V-b)]}$$

with $m_o = 0.37464 - 1.54226\ \omega - 0.26992\ \omega^2$.

Here "a" is a temperature function of the same form as used by Soave. The constant m_o in Soave's correlation is determined so that it is consistent with the accentric factor while in Peng-Robinson's correlation m_o is determined by a least square fit of the equation of state to experimental saturated vapour pressure data.

The essential difference between these correlations lies in their compressibility factor at the critical point, z_c = 0.3333 for Soave's Z_c = 0.307 for Peng and Robinson's. This somewhat explains why Peng and Robinson's correlation predicts better liquid densities than Soave's (see also Table 5.2). Skogestad[71] pointed out that values of liquid densities from PR EOS are still not good enough for engineering applications, and ".... the VLE calculations are hardly affected at all. Therefore the Peng-Robinson equation does not represent any real improvement compared to RKS from a practical point of view. In fact, it mostly creates problems because the engineer is faced with two instead of one equation to use".

An interesting feature of the Van der Waals' family of EOS as shown by Martin[60], Abbott[52] and Vera et al.[72] is related to the fact that they can be expressed in a more general form as follows:

$$P = \frac{RT}{V - b} - \frac{a(V - k_3 b)}{(V-b)(V^2+k_1 bV + k_2 b^3)}$$

By making k_3 = 1 and introducing the accentric factor as a third parameter (with $k_1 = 1 + 3\omega$ and $k_2 = -3\omega$) Schmidt and Wenzel[73] proposed the following equation:

$$P = \frac{RT}{V - b} - \frac{a}{V^2 + (1+3\omega)bV - 3\omega b^2}$$

A similar form by making $k_3 = 1$ and $k_2 = -(c-1)$ and $k_1 = c$ was proposed by Harmans and Knapp in 1980[74] is given by:

$$P = \frac{RT}{V - b} - \frac{a}{V^2 + cbV - (c-1)b^2}$$

where parameters a, b and c are related to T_c, P_c and ω as follows:

$$a = \Omega_a \frac{R^2T^2}{P_c} \; ; \qquad b = \Omega_b \frac{RT_c}{P_c} \qquad \text{and } c = 1 + \frac{1 - 3}{\beta}$$

in which

$$\Omega_a = 1 - 3 + 3^2 + \beta(3 - 6 + \beta)$$

$$\Omega_b = \beta$$

and

$$= 0.3211 - 0.080\ \omega + 0.0384\ \omega^2.$$

This equation reduces to the Redlich-Kwong by making c = 1 and to Peng-Robinson for c = 2.

There is even a rebirth of the Clausius EOS[75] after a comprehensive review by Martin[60] which concluded that this was the best cubic equation of state although he was only interested in vapour-phase properties. Good results were obtained by Kubic[76] when using Clausius' equation by making the translation parameter c temperature dependent.

$$P = \frac{RT}{V - b} - \frac{a}{(V + cLT)^2}$$

for binary systems of halocarbons and hydrocarbons as can be seen in Figures 5.8, 5.9, 5.10 and 5.11 extracted from [7].

He abandoned the parameter "a" with a Soave-type temperature function suggested by Joffe[77]

$$a = (27\ R^2/T_C^2/64P_C)\ (1 + m\ (1 - (T/T_r)^{1/2}\ ))^2$$

introducing a different correlation.

Although these EOS mentioned above may be nicely derived algebraically from one another or be a particular case of one another, the Redlich-Kwong-Soave and Peng-Robinson EOS continue to be the most popular methods among chemical engineers for VLE calculations of hydrocarbon mixtures at high pressures[78]. These VLE methods are still the subject of further studies. Peneloux and Rauzy[79] applied the volume translation concept introduced by Martin[60] to Soave's EOS to improve its capability to predict better liquid densities while retaining its accuracy for prediction of VLE parameters. The range of applicability of RKS and PR equations of state has even been extended in recent years. Soave[80] introduced a second adjustable parameter "n" in his EOS in an attempt to cover polar compounds. Stryjek and Vera[81] have modified PR EOS to improve its use at low reduced temperature. Chang et al.[82] and Robinson et al.[83] have attempted to correlate a number of methanol containing systems with RKS and PR respectively. Lin[84] specifically studied CO_2-hydrocarbon mixtures using PR EOS and concluded that the best k_{ij} for these systems is 0.125. Yesavage[85] developed

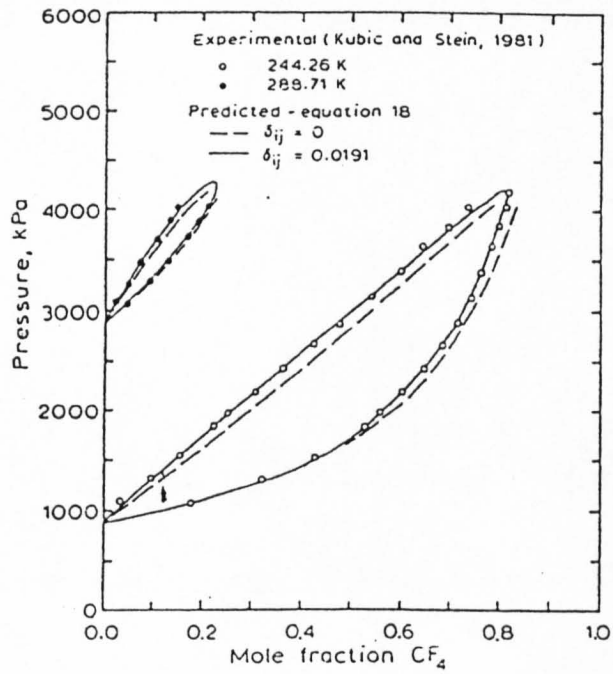

Figure 5.8. Pressure equilibrium phase-composition diagram for tetrafluoromethane-chlorotrifluoromethane.

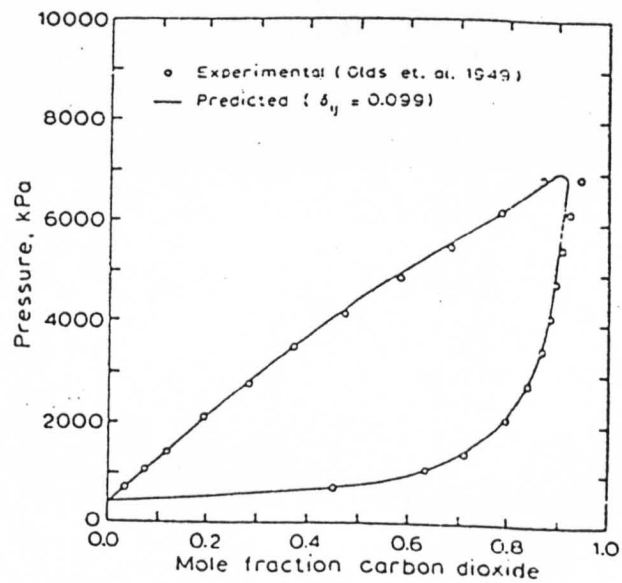

Figure 5.9. Pressure equilibrium phase-composition diagram for carbon dioxide-n-butane at 310.93 K.

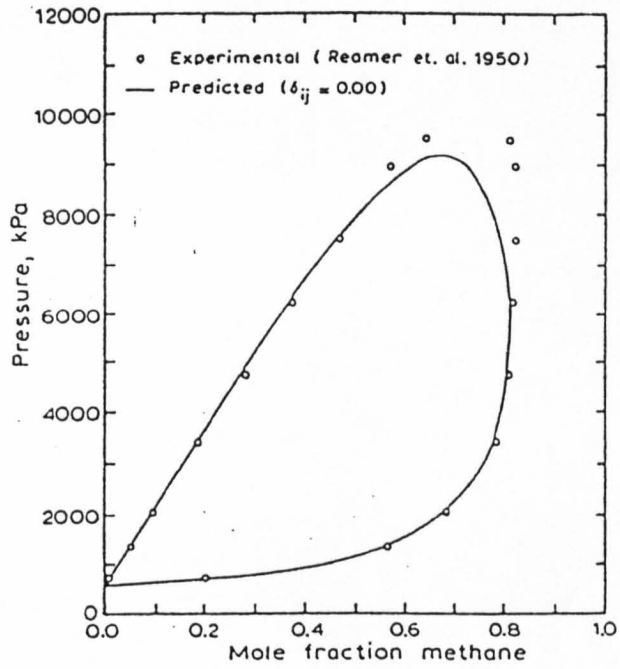

Figure 5.10. Pressure equilibrium phase-composition diagram for methane-propane at 277.59 K.

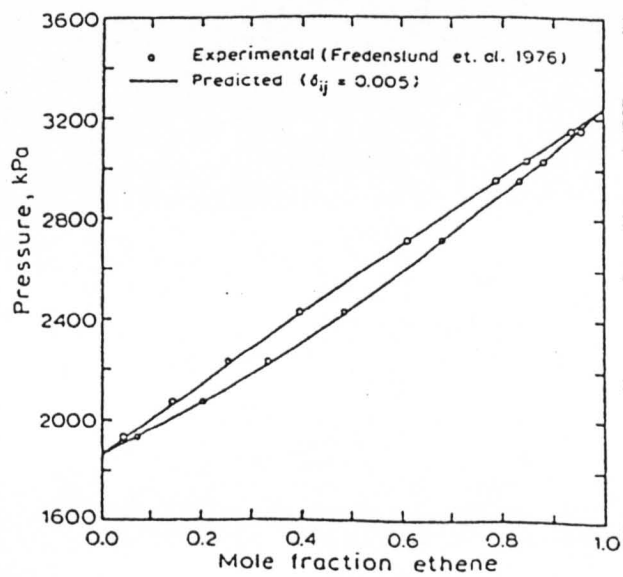

Figure 5.11. Pressure equilibrium phase-composition diagram for ethene-ethane at 263.15 K.

a method for extending Van der Waals type equations of state to highly polar and hydrogen bonding fluids. He reported a three-parameter RKS EOS that fits vapour pressures for polar fluids much better than the original equation. Fredenslund et al.[86] reported a procedure based on RKS equation of state to predict accurately phase behaviour of heavy oils encountered in petroleum mixtures.

Vidal and co-authors at the Institut Francais du Petrole have extensively studied RKS and PR EOS for the past ten years. Vidal et al.[87] in 1978 reported correlations for six halocarbon binary systems as part of a broad investigation on new refrigerants to improve COP of heat pumps (Chapter 1, section 1.7). Figures 5.12, 5.13 and 5.14 display some bubble and dew pressures obtained for $CCl_2F_2/CClF_3$ and CF_4/CHF_3 systems. Later, Vidal and co-workers[88] correlated temperature dependent k_{ij} values for phase equilibrium of H_2 and hydrocarbon mixtures. They applied both RKS and PR methods to several other light gases[89] extending to pressures of 130 atm for CH_4 and H_2S and to 300 atm for H_2 and N_2. Figure 5.15 illustrates a binary system of H_2 - CH_4 correlated by them.

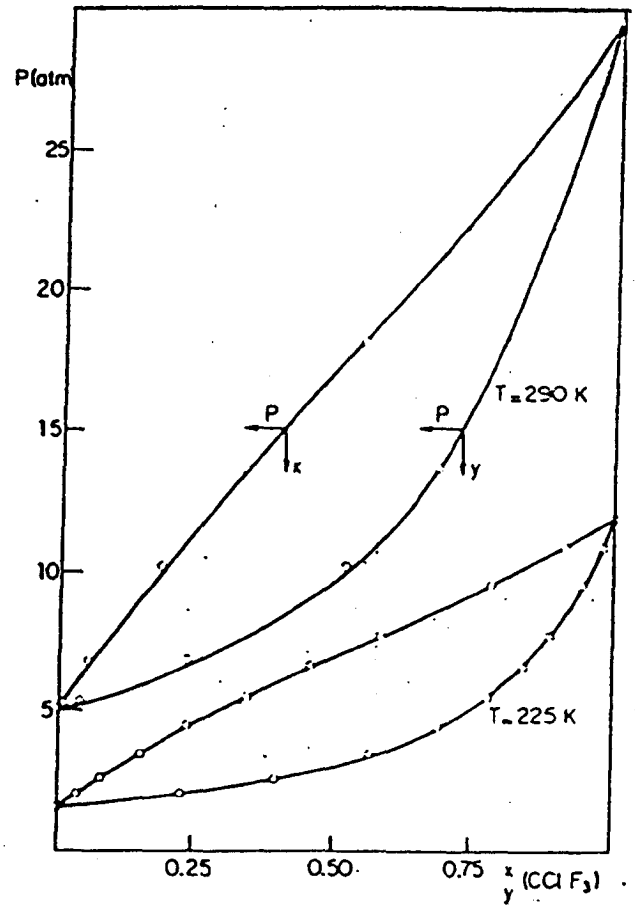

Figure 5.12. Pressure-composition diagram for CCl_2F_2/CCl_2F_3 system
O Experimental data[11]: --- Correlation

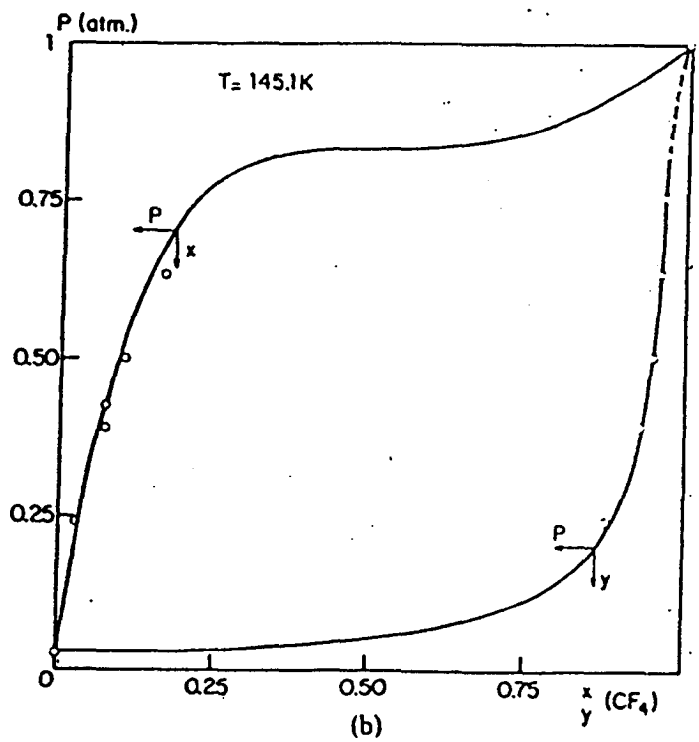

Figure 5.13. Pressure-composition diagram for CF_4/CHF_3 system.
O Experimental data[12]; --- Correlation

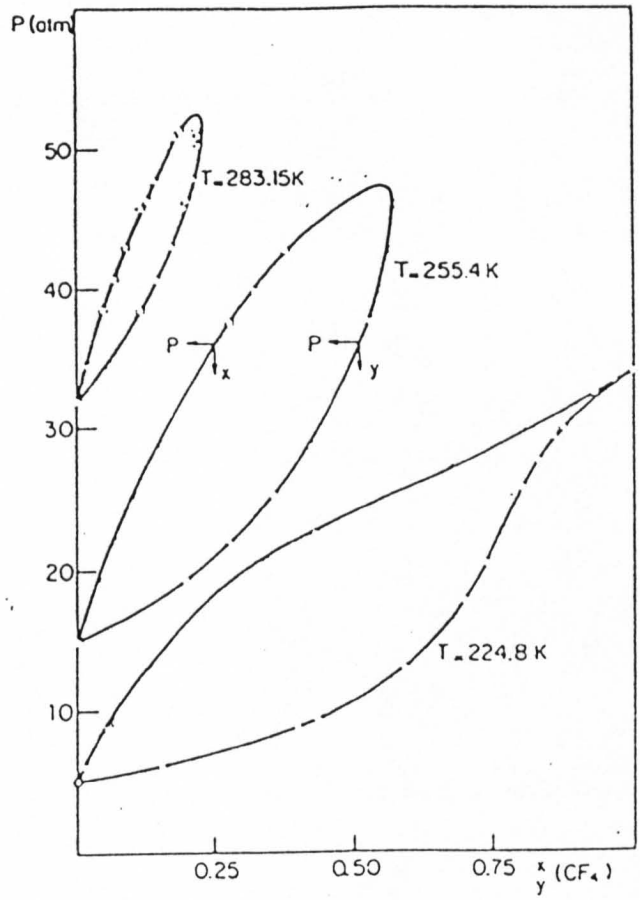

Figure 5.14. Vapour-liquid equilibria of CF_4/CHF_3 system.

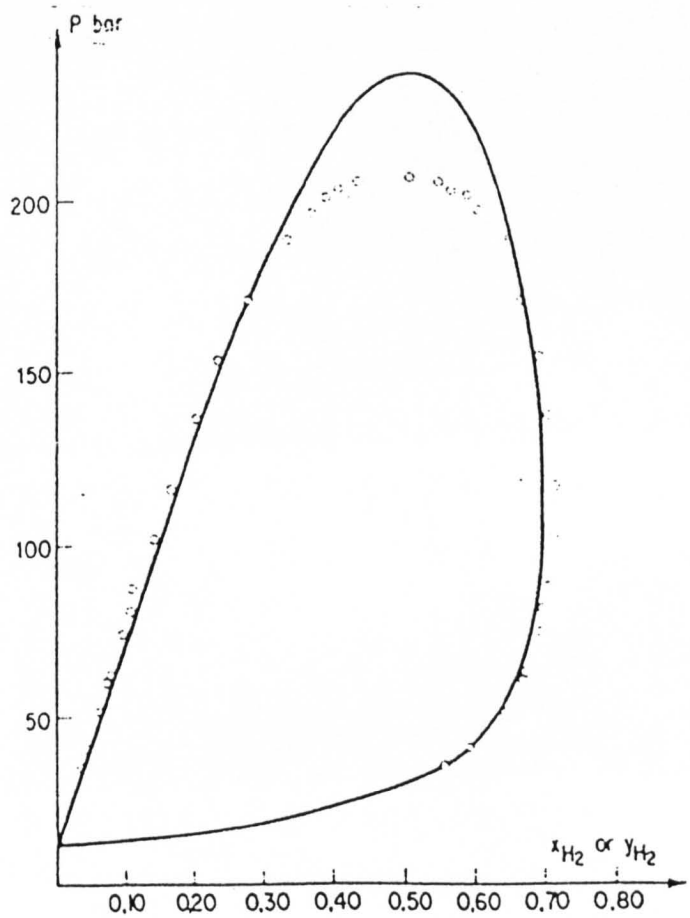

Figure 5.15. Vapour liquid equilibria of the system H_2CH_4 at 153.21 K. Calculated curve using the PR method (K_{12} = 0.069). The RKS method (K_{12} = 0.012) would give nearly the same curve. 0 Experimental data[11].

Knapp et al.[90] have presented a comprehensive monograph on the calculation of vapour-liquid equilibria by using an equation of state. Knapp considered four equations of state (Lee-Kesler, Benedict-Webb-Rubin, Peng and Robinson and Redlich-Kwong-Soave) for comparison of their ability to predict vapour-liquid equilibria of binary mixtures currently encountered in petroleum technology. He found overall that the Benedict-Webb-Rubin did not perform as well as the others. Furthermore, he concluded that, of the four equations used, one particular equation was not distinctly superior to the others.

On the grounds of a fruitful discussion with Professor J. Vidal, Professor H. Knapp from the Institut für Thermodynamik und Anlagentechnik of the Technische Universität, Berlin and Dr.K.C. Chao (co-editor of "Equations of State: Theories and Applications", ACS Symp.Series of Amer.Chem.Soc.) during the IUPAC conference in Paris in 1985, the author opted to use Redlich-Kwong-Soave EOS throughout this research project. One of the main reasons that RKS was preferred to the PR EOS lies in the fact that k_{ij} (interaction parameters) are more available for Soave's in the literature. Better prediction of liquid densities by the Peng and Robinson correlation was not a bonus in favour of this method since VLE parameters and calorimetric properties (e.g. enthalpy, entropy) were the core of the research.

5.6. MIXING RULES RELATED TO VAN DER WAALS TYPE EQUATIONS OF STATE

Calculating vapour-liquid equilibria by applying the same equation of state to both phases was first suggested by Van der Waals many years ago. When applying this method, the contribution of each component present in the mixture should be computed. This is expressed by mixing rules, i.e. by the variation of equation of state constants with composition. Since Van der Waals' time, the geometric mean assumption has been widely used to calculate a, the intermolecular attraction parameter. The co-volume b of the mixture, which compensates for the volume occupied by the molecules, has been chosen to be a linear average of the molecular volumes of each component.

The so-called classical mixing rules may be stated as follows:

$$a = \sum_{i=1}^{m} \sum_{j=1}^{m} x_i \, x_j \, a_{ij}$$

where

$$a_{ij} = \sqrt{a_i \, a_j} \qquad \text{for } i \neq j$$

and

$$b = \sum_{i=1}^{m} x_i \, b_i$$

Those relations were established on strictly empirical grounds by Berthelot in the late nineteenth century[6].

To match experimental data more precisely, an adjustable binary interaction parameter (k_{ij}) was introduced in the geometric average rule. Therefore a_{ij} may be written:

$$a_{ij} = \sqrt{a_i\, a_j}\ (1 - k_{ij})$$

This is sometimes called the combining rule. The binary interaction parameter k_{ij} is determined by seeking the optimum value for all experimental points on the pressure-liquid composition (P-x) curve of each isothermal binary mixture. Optimum binary interaction parameters have been calculated by Knapp et al.[93] for a large number of substances using the Lee and Kesler equation of state. However, the more constants the equation of state has, the more mixing rules are required and more data are needed for evaluating the pure component parameters. This partly explains the popularity of the two-constant equations of state.

Many mixing rules have been suggested in recent years. Panagiotopoulos and Reid[94] proposed an empirical modification ofthe combining rule relaxing the assumption $k_{ij} = k_{ji}$ and introducing a second interaction parameter per binary as follows:

$$a_{ij} = \sqrt{a_i\, a_j}\ [1 - k_{ij} + (k_{ij} - k_{ji})\ x_i]$$

They correlated polar systems including CO_2 - H_2O, ethanol-H_2O, CO_2-acetone and a ternary CO_2-acetone-H_2O. Figure 5.16 presents their correlation for the system ethanol-water using the Peng and Robinson EOS.

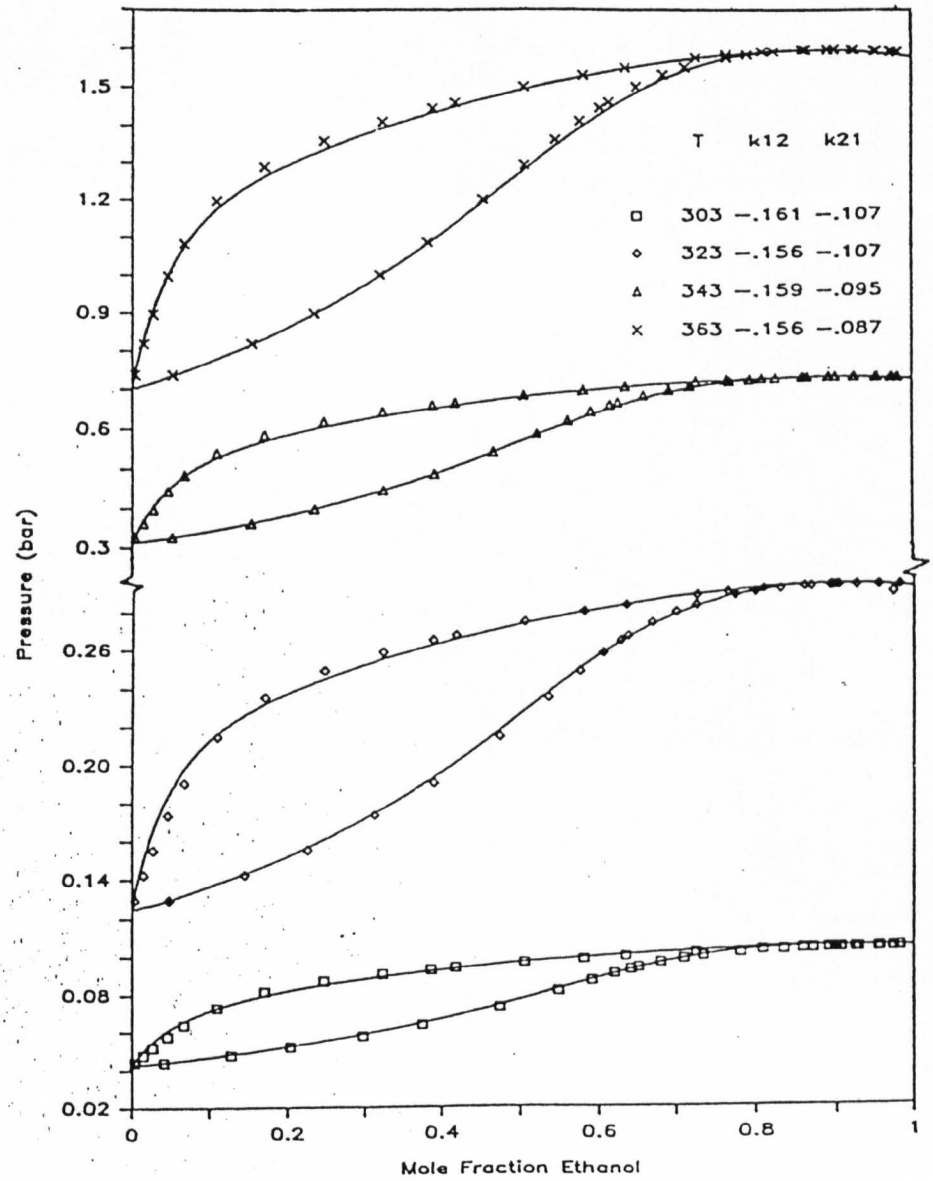

Figure 5.16. Experimental and predicted phase equilibrium behaviour for ethanol-water system.

Another similar alternative to the so-called "classical" mixing rule was developed by Stryjek and Vera[95] and is written as follows:

$$a_{ij} = (a_i\, a_j)^{0.5}\, (1 - x_i\, k_{ij} - x_j\, k_{ji})$$

where $a_{ij} = a_{ji}$ but $k_{ij} \neq k_{ji}$.]

They reported that this composition dependent mixing rule gives consistently better results than other methods for highly polar systems such as water-alcohols and alkane/alcohols.

Later Stryjek and Vera[95] correlated $HC\ell-H_2O$ systems using the Peng and Robinson EOS. Table 5.3. extracted from their article shows for several temperatures a comparison between experimental and calculated pressures.

T(K)	k_{12}	k_{21}	x_{az}	P_{az}(kPa)	
				Experimental	Calculated PRSV
298.15	−0.2250	−1.3656	0.1381	1.719	1.741
303.15	−0.1790	−1.3749	0.1365	2.342	2.367
313.15	−0.0928	−1.3882	0.1333	4.213	4.248
323.15	−0.0151	−1.3961	0.1300	7.413	7.354
343.15	0.1041	−1.3928	0.1236	20.57	20.02
373.15	0.1394	−1.3319	0.1139	74.26	73.50

Table 5.3. Binary parameters and azeotropic data for the system hydrogen chloride-water[95].

Radosz, Lin and Chao[96] used conformal mixing rules in the RKS equation. Their mixing rules were:

$$a\, b^{-0.25} = \sum_{i=1}^{m} \sum_{j=1}^{m} x_i\, x_j\, a_{ij}\, b_{ij}^{-0.25}$$

$$b = \sum_{i=1}^{m} \sum_{j=1}^{m} x_i\, x_j\, b_{ij}$$

$$b_{ij} = [(b_i^{1/3} + b_j^{1/3})]^3$$

$$a_{ij}\, b_{ij}^{-0.25} = (1 - x_{ij}) \left[a_i\, a_j\, (b_i\, b_j)^{-0.25}\right]^{-0.5}$$

The authors claim that SRLC predict k-values better than Soave's EOS with classical mixing rules for organic binary mixtures containing as solute H_2, CH_4 and CO_2. Lüdeche and Prausnitz[97] introduced a density dependent correction to the usual (density independent) quadratic mixing rule in an equation of state of the Van der Waals form to represent vapour-liquid and liquid-liquid equilibria in binary particularly aqueous mixtures. They obtained the following expression for "Van der Waals a":

$$a = \sum_i^m \sum_j^m x_i x_j (a_{ij} a_{ji})^{1/2} (1 - k_{ij}) + \frac{\rho}{RT} \sum_i^m \sum_{j \neq i}^m x_i x_j$$

$$(x_i c_{i(j)} + x_j c_{j(i)})$$

for a binary mixture it becomes:

$$a = x_1^2 a_{11} + x_2^2 a_{22} + 2x_1x_2 [(a_{11}a_{22})^{1/2} (1 - k_{12})$$

$$+ (\rho/RT) (x_1 c_1c_2) + x_2 c_2c_1)]$$

where

$c_{i(j)}$ is a binary parameter that reflects noncentral forces when molecule j is infinitely dilute, surrounded by molecules i. Adachi and Sugie[98] proposed the following Redlich-Kwong (RK) type mixing rule in the modified Van der Waals (MVDW) developed by Adachi and Lu[53].

$$a_m = \sum_i x_i a_i + \Sigma \Sigma x_i x_j [A + B(x_i - x_j)$$

$$+C(x_i - x_j)^2 + D(x_i - x_j)^3]$$

with a linear mixing rule for the co-volume parameter b_m

$$b_m = \sum_i x_i b_i$$

They concluded that no advantage is gained for binary mixtures by introducing more than two interaction parameters. Later[99] they modified a_m to a two-parameter RK type mixing rule:

$$a_m = \sum_{i=1}^{m} x_i a_i + \sum_{i=1}^{m} \sum_{j=1}^{m} x_i x_j [A + B(x_i - x_j)$$

to obtain the following form:

$$a_m = \sum_{i}^{m} \sum_{j}^{m} x_i x_j a_{ij}$$

$$a_{ij} = (1 - k_{ij}) (a_i - a_j)^{1/2}$$

$$k_{ij} = l_{ij} + m_{ij} (x_i - x_j)$$

where the parameters l_{ij} and m_{ij} can be obtained from parameters A and B by means of the following translations

$$l_{ij} = -[(a_i^{1/2} - a_j^{1/2})^2 + A]/2(a_i a_j)^{1/2}$$

$$m_{ij} = - B/2(a_i a_j)^{1/2}$$

to be used in VLE calculations for strongly polar substances. Values for l_{ij} and m_{ij} were reported for several binary systems containing methanol, ethanol and water.

Mansoori[100] developed a statistical mechanical nonformal solution method to derive mixing rules for cubic equations of state. Although he reported new mixing rules for the Van der Waals, Redlich-Kwong and Peng-Robinson EOS very few have been tried. Benmekki and Mansoori[101] correlated water-ketone, water-alcohol, alcohol-ketone and other complex mixtures by these rules and found that these were more accurate than the original form of Peng-Robinson EOS with

classical mixing rules. They treated these systems with the following version of PR EOS:

$$z = \frac{V}{V - b} - \frac{(\frac{c}{RT}) + d - 2\sqrt{(\frac{cd}{RT})}}{(V + b) + (b/V)(V - b)}$$

where

$$c = a(T_c)\ (1 - k)^2$$

$$d = a(T_c)\ k^2/RT_c$$

where parameters b and d are proportional to (molecular length)^3 or ($b \propto h$ and $d \propto h$) while parameter c is proportional to (molecular length)^3(molecular energy) or ($c \propto fh$). The mixing rules being quadratic are in the classical case:

$$c = \sum_i^m \sum_j^m x_i\ x_j\ c_{ij}$$

$$b = \sum_i^m \sum_j^m x_i\ x_j\ b_{ij}$$

$$d = \sum_i^m \sum_j^m x_i\ x_j\ d_{ij}$$

So far only classical mixing rules have been used here since the binary mixtures of interest which are systems of hydrocarbon-organometallic and hydrocarbon-hydrocarbon compounds, can be adequately described by a cubic EOS at high pressure with one binary interaction parameter for the former and without any for the latter[63]. Should any slightly polar system (e.g. amines) be investigated, Panagiotopoulos and Reid's mixing rules will probably be the most indicated to use due to its simplicity and accuracy.

It is perhaps interesting and also reassuring to some extent to close this section by quoting a recent review on mixing rules by Copeman and Mathias[102]. "The capability of equations of state to describe asymmetric mixtures has improved substantially over the past five years. The old rule of thumb that one must use activity coefficient models for mixtures with polar components is beginning to fade away.....".

5.7. THE REDLICH-KWONG-SOAVE EQUATION OF STATE

This equation is a modification proposed by Soave[69] to the original two parameter equation of Redlich-Kwong[62].

The original Redlich-Kwong equation of state is:

$$P = \frac{RT}{V - b} - \frac{a}{T^{1/2}\, V(V+b)}$$

In the modification proposed by Soave the term $a/T^{1/2}$ was replaced by a more general temperature dependent a(T) hence:

$$P = \frac{RT}{V - b} - \frac{a}{V(V + b)} \qquad (5.5)$$

Letting

$$V = z\,\frac{RT}{P}$$

$$A = \frac{aP}{R^2T^2}$$

$$B = \frac{bP}{RT}$$

Equation (5.5) can be expressed as follows:

$$Z^3 - Z^2 + (A - B - B^2)Z - AB = 0 \qquad (5.6)$$

For a pure substance, the modified Soave equation satisfies the thermodynamic stability criteria at the critical point, i.e.

$$\left\{\frac{\partial P}{\partial V}\right\}_{T_c} = 0 \qquad \text{and} \qquad \left\{\frac{\partial^2 P}{\partial V^2}\right\}_{T_c} = 0$$

We then obtain that for a pure substance at the critical point:

$$a_i\ (T_{ci}) = a_{ci} = \frac{\Omega_a\ R^2 T_{ci}^2}{P_{ci}}$$

and

$$b_{ii} = \frac{\Omega_b\ RT_{ci}}{P_{ci}}$$

where the values of constants Ω_a and Ω_b are defined as follows:

$$\Omega_a = \frac{1}{[9\ (2^{1/3} - 1)]}$$

$$\Omega_b = \frac{(2^{1/3} - 1)}{3}$$

At temperatures other than the critical, Soave proposed that:

$$a_{ii}^{(T)} = a_{ci}\ \alpha_{mi}^{(T)}$$

where α_{mi} is a correlation factor.

The fugacity coefficient of a pure component can be calculated from the following equation:

$$\ln \frac{f}{P} = (z - 1) - \ln(z-B) - \frac{A}{B} \ln \left(\frac{z + B}{z}\right) \qquad (5.7)$$

At the saturation condition $f_i^L = f_i^V$, Soave, using experimental vapour pressures and equation (5.7) determined values for $a_i(T)$ and hence $\alpha_{mi}(T)$. By plotting values of $\alpha_i^{0.5}$ against $T_r^{0.5}$ where T_r is the reduced temperature, he obtained straight lines of the form:

$$\alpha_{mi}^{0.5} = 1 + m_i \ (1 - T_{ri}^{0.5})$$

The slopes m_i can be connected directly with the acentric factor ω_i of each substance and were correlated by Soave as:

$$m_i = 0.48 + 1.574\omega_i - 0.176 \ \omega_i^2$$

For hydrocarbons, according to Graboski and Daubert[91]:

$$m_i = 0.48508 + 1.55171\omega_i - 0.15613 \ \omega_i^2$$

and for hydrogen, according to Graboski and Daubert[92]:

$$\alpha_i = 1.202 \exp.(-0.30288 \ T_{ri})$$

5.8. RESIDUAL PROPERTIES FROM THE REDLICH-KWONG-SOAVE EQUATION OF STATE

The following expressions for departure functions of enthalpies and entropies can be found in reference [23], pp.509-512.

$$P = \frac{RT}{V - b} - \frac{a\alpha}{V(V + b)} \qquad \text{Soave's equation of state}$$

where $$\alpha = \left\{1 + m\left(1 - \sqrt{\frac{T}{T_c}}\right)\right\}^2$$

$$\left\{\frac{\partial P}{\partial T}\right\}_V = \frac{R}{V - b} - a\,\frac{d\alpha}{dT} \cdot \frac{1}{V(V + b)}$$

$$\frac{d\alpha}{dT} = -\,m\sqrt{\frac{\alpha}{TT_c}} = -\,\frac{m}{T}\sqrt{a\,\frac{T}{T_c}}$$

$$\Delta H' = RT\left[1 - Z + \frac{a}{bRT}\left(\alpha - T\,\frac{d\alpha}{dT}\right) \ln\left(1 + \frac{b}{V}\right)\right]$$

and for entropy we get:

$$\Delta S' = -R\left[\ln\left[Z\left(1 - \frac{b}{V}\right)\right] + \frac{a}{bR} \cdot \frac{d\alpha}{dT} \ln\left(1 + \frac{b}{V}\right)\right]$$

The above are residual properties for pure components. For mixtures, we have:

$$D_i = -\,T\,\frac{d(a\alpha)_i}{dT} = \left[\, m\,(a\alpha)\sqrt{\frac{T}{T_r\alpha}}\right]_i$$

$$D = \sum_i \sum_j y_i\, y_j\, m_j\,(1 - k_{ij})\sqrt{a_i\,\alpha_i}\sqrt{a_j(T/T_c)_j}$$

$$\Delta H' = RT\left[(1 - Z) + \frac{A}{B}\left(1 + \frac{D}{a\alpha}\right) \ln\left(1 + \frac{B}{Z}\right)\right] \qquad (5.8)$$

$$\Delta S' = -R\left[\ln\,(Z - B) + \frac{AD}{Ba\alpha} \ln\left(1 + \frac{B}{Z}\right)\right] \qquad (5.9)$$

where $A = \frac{aP}{(RT)^2}$ and $B = \frac{bP}{RT}$

5.8.1. Liquid and Vapour Enthalpy and Entropy

5.8.1.1. Liquid Enthalpy and Entropy

The liquid phase enthalpy for a mixture is given by:

$$H_{mix}(T,P) = \left[H^{Res}_{mix}(T,P) - H^{Res}_{mix}(T,O)\right] - H^{Ideal}_{mix}(T,O) \qquad (5.10)$$

The first term on the RHS of Eqn.5.10 is the enthalpy departure function for mixtures which for the Soave equation is given by Eqn.5.8. The latter term is the enthalpy of an ideal gas and is obtained from zero pressure heat capacities of the pure components. The final value $H_{mix}{}^{Ideal}$ is calculated taking into account the liquid mole fractions of each component.

Zero pressure heat capacities are a function of temperature and can be written in a polynomial form as follows:

$$C^{o}_{Pi} = A + BT + CT^2 + DT^3 + \ldots\ldots$$

with C^{o}_{Pi} in J/mol'K

so that:

$$H^{Ideal}(T,O) = \int_{T_o}^{T} C^{o}_{Pi}\, dT$$

Substituting for the zero pressure heat capacity equation we have:

$$H_i^{Ideal}(T,O) = A_i(T - T_o) + \frac{B_i}{2}(T^2 - T_o^2) + \frac{C_i}{3}(T^3 - T_o^3)$$

$$+ \frac{D_i}{4}(T^4 - T_o^4)$$

Finally,

$$H_{mix}^{Ideal} = \sum_i^n x_i H_i^{Ideal}$$

where x_i is the vapour mole fraction of component i. The values for A_i, B_i, C_i and D_i were obtained from THERPROP data bank[103]. T_o, the reference temperature, is fixed and equal to 0°C in accordance with I.C.I.'s reference value (at 0°C h_f = 100 kJ/kg, s_f = 1 kJ/kg°K).

The procedure for normalising enthalpy values is as follows:

1. Calculate the Bubble pressure at 0°C.
2. Calculate Enthalpy at Bubble point of 0°C. Letting this value be X then make a correction constant such that h_f = 100 kJ/kg at 0°C.

$$X + X_{correction} = 100$$

then

$$X_{correction} = 100 - X$$

Now, for any other point,

$$h_f = h + X_{correction}.$$

Similarly, for the entropy of a liquid mixture:

$$S_{mix}(T,P) = \left[S^{Res}_{mix}(T,P) - S^{Res}_{mix}(T,O)\right] - S^{Ideal}_{mix}(T,O) + S_{mix} \quad (5.11)$$

and as before, the first term on the RHS of equation (5.11) is the entropy departure function which for the Soave equation of state is given by Equation (5.9). The second term is the entropy of an ideal gas and is obtained as follows:

$$S^{Ideal}(T,O) = \int_{T_o}^{T} \frac{C^o_{Pi}}{T}\, dT$$

or

$$S^{Ideal}_i = A_i \ln (T/T_o) + B_i (T - T_o) + \frac{C_i}{2}(T^2 - T_o^2) + \frac{D_i}{3}(T^3 - T_o^3) + R \ln \frac{P_i}{P_o}$$

where T_o is the same as above and P_o a reference pressure being given by the bubble pressure of the mixture calculated at 0°C. The final value $S_{mix}{}^{Ideal}$ is obtained taking into account the liquid mole fractions of each component as follows:

$$S^{Ideal}_i = \sum_i x_i S^{Ideal}_i$$

where x_i is the liquid mole fraction of component i.

The final term S_{mix} is the entropy of mixing which is given by:

$$S_{mix} = - \sum_i^m x_i \ln x_i$$

The procedure for normalising entropy values is similar to that for enthalpy values.

1. Calculate the Bubble pressure at 0°C.

2. Calculate entropy at bubble point of 0°C. Letting this value by Y then make correction constant such that:

S_f = 1 kJ/kg°K at 0°C. This is as follows:

$$Y + Y_{correction} = 1$$

then

$$Y_{correction} = 1 - Y$$

Now, for any other point,

$$S_f = S + Y_{correction}$$

5.8.1.2. Vapour Enthalpy and Entropy

Similarly, for the vapour state, entropy and enthalpy are estimated by the same procedure used in the liquid state.

Residual properties and ideal gas contributions are calculated using vapour mole fractions and liquid compressibilities instead.

Finally, a note should be added here concerning the accuracy of cubic equations of state in the prediction of departure functions. Adachi and Sugie[104] in a recent article investigated the dependence of the enthalpy departure calculation for a cubic EOS for three sets of cohesion and co-volume parameters. They concluded that an equation of state which gives good PVT predictions is found to be able to predict enthalpy departures well, and the PR EOS would be a good choice. Mather[105] compared the ability of Redlich-Kwong-Soave (RKS), Peng-Robinson (PR), BWR Starling and Lee-Kesler (LK) equations of state and Leach-Leland corresponding states principle of enthalpy prediction. Mather investigated hydrocarbons up to C_8, nitrogen and carbon dioxide. The results are summarised in Table 5.4. The numbers are average absolute deviations between calculated and experimental values in kJ/kg.

RKS	PR	BWRS	LK	LL
3.0	4.4	2.6	4.4	2.3

Table 5.4.

On this basis the RKS EOS appears to be the most accurate of the popular cubic equations and only marginally inferior to the more complex equations of state.

REFERENCES

1. Reid, R.C. 1983. Fluid Phase Equilibria, Vol.14, pp.225-234.

2. Treybal. "Mass Transfer Operations". McGraw-Hill, New York, 1955.

3. Laddha and Degaleesan. "Transport Phenomena in Liquid Extraction". McGraw-Hill, New Delhi, 1976.

4. Prausnitz, J.M. "State-of-the-Art Review of Phase Equilibria". ACS Symp. Series, Vol.60,1977.

5. Pitzer, K.S. J. Am. Chem. Soc., Vol.77, 3427, 1955.

6. Prausnitz, J.M. "Molecular Thermodynamics of Fluid-Phase Equilibria". Prentice-Hall International Series, New Jersey, 1969.

7. Prausnitz, J.M., Eckert, C.A., Orye, R.V., and O'Connell, J.P. "Computer Calculations for Multicomponent Vapour-Liquid Equilibria". Prentice-Hall International Series, New Jersey, 1980.

8. Hala, E, Pick, J., Fried, V. and Vilim, O. "Vapour-Liquid Equilibrium", 2nd Ed. Pergamon Press, 1967.

9. Margules, M. Sitzber Akad. Wiss Wein, Math. Naturn. Kl.II, Vol.104, 1243, 1895.

10. Wilson, G.M. J. Am. Chem. Soc., Vol.86, 127, 1964.

11. Orye, R.V. and Prausnitz, J.M. Ind. Eng. Chem. Vol.57, No.5, 19, 1965.

12. Renon, H. and Prausnitz, J.M. A.I.Ch.E. Journal, Vol.14, 135, 1968.

13. Abrams, D.S. and Prausnitz, J.M. A.I.Ch.E. Journal, Vol.121, pp.116-128, 1975.

14. Maurer, G. and Prausnitz, J.M. Fluid Phase Equilibria, Vol.2, p.91, 1978.

15. Fredenslund, A., Rasmussen, P. and Mollerup, J. "Thermophysical and Transport Properties for Chemical Process Design". Instituttet for Kemiteknik, Danmarks Tekniske Hojskole, DK2800 Lyngby, Denmark.

16. Kojima, K, and Tochigi, K. "Prediction of Vapour-Liquid Equilibria by the ASOG Method". Kodansha-Elsevier, Tokyo, 1979.

17. Fredenslund, A., Jones, R.L. and Prausnitz, J.M. A.I.Ch.E. Journal, Vol.21, 1086, 1975.

18. Fredenslund, A., Gmehling, J. and Rasmussen, P. "Vapour-Liquid Equilibria using UNIFAC, Elsevier, 1979.

19. Gmehling, J. Rasmussen, P. Skjold-Joergensen, S, Kolbe, B. Ind. Eng. Chem. Proc. Des. Dev. Vol.18, 714, 1979.

20. Kehiaian, H.V. and Sandler, S.I. Fluid Phase Equilibria, Vol.27, 139, 1984.

21. Kehiaian, H.V., Bravo, R., Barral, Pais de Andrade, M., Guieu, R and Grolier, J.P. Fluid Phase Equilibria, Vol.17, 187, 1984.

22. Kehiaian, H.V. and Marongin, B. Fluid Phase Equilibria, Vol.2l, 197, 1985.

23. Walas, S.M. "Phase Equilibria in Chemical Engineering". Butterworths, 1985.

24. Heidemann, R.A. and Fredenslund, A. "Vapour-Liquid Equilibria in Complex Mixtures" I.Chem.E. Symp. Series, No.104,, 1987.

25. Benedict, M., Webb, G.B. and Rubin, L.C. J.Chem.Physics, Vol.8, 334, 1940: Vol.10, 747, 1942, Chem. Eng. Prog. Vol.47, 419, 195l.

26. Beattie, J.A. and Bridgemann, O.C. J.Am.Chem.Soc., Vol.50, No.12, 1928.

27. Starling, K.E. "Fluid Thermodynamic Properties for Light Petroleum Systems". Gulf Publishing Co., Houston Texas, 1973.

28. Lin,C.J. and Hopke, S.W. A.I.Ch.E. Symp.Series, Vol.70, No.140, 37, 1974.

29. Bender, E. Cryogenics, Vol.13, ll, 1973.

30. Bender, E. Cryogenics, Vol.15, 667, 1975.

31. Bishnoi, P.R. and Robinson, D.B. Canadian J. Chem.Eng., Vol.50. pp.101-107, 1972.

32. Bishnoi, P.R. and Robinson, D.B. Hydrocarbon Processing, Vol.5l, No.ll, pp.152-156, 1972.

33. Nishiumi, H. J.Chem.Eng. Japan, Vol.13, pp.74-76,1980.

34. Nishiumi, H. J.Chem.Eng., Japan, Vol.13, pp.178-183, 1980.

35. Lewis, G.N. and Randall, M. "Thermodynamics", 2nd Ed. (Revised by K.S. Pitzer and L.Brewer) McGraw-Hill Book Co., New York, 1961.

36. Pitzer, K.S. J. Chem. Phys. Vol.7, 583, 1939.

37. Pitzer, K.S. Origin of the accentric factor. T.S. Storrick and S.I. Sandler (Editors). Phase Equilibria and Fluid Properties in the Chemical Industry 1-10 ACS Symp.Series 60, Am. Chem.Soc., 1977.

38. Lee, B.I. and Kesler, M.G. A.I.Ch.E. Journal, Vol.21, 510, 1975.

39. Smith, I.K. Procs. of National Physical Laboratory Conf. Chemical Thermodynamic Data on Fluids and Fluid Mixtures, their correlation, estimation and use, Sept.1978.

40. Plöcker, U., Knapp, H., Prausnitz, J.M. Ind. Eng. Chem. Process Des. Dev., Vol.17, No.3, pp.324-332, 1978.

41. Beret, S. and Prausnitz, J.M. A.I.Ch.E., Journal, Vol.21, 1123, 1975.

42. Donohue, M.D. and Prausnitz, J.M. A.I.Ch.E. Journal, Vol.24, 849, 1978.

43. Carnahan, N.F. and Starling, K.E. J.Chem.Physics, Vol.51, 636, 1969.

44. Alder, B.J., Young, D.A. and Mark, M.A. J.Chem.Physics, Vol.56, 3013, 1972.

45. Chien, C.H., Greenkorn, R.A. and Chao, K.C. A.I.Ch.E., Journal, Vol.29, p.560, 1983.

46. Lin, H.M., Kim, H., Guo, T.M. and Chao, K.C. Fluid Phase Equilibria, Vol.13, p.143, 1983.

47. Masouuka, H. and Chao, K.C. IEC Fundum, Vol.23, 24, 1984.

48. Kim, H., Lin, H.M. and Chao, K.C. IEC Fundam, Vol.25, 75, 1986.

49. Leet, W.A., Lin, H.M. and Chao, K.C. Ind.Eng.Chem.Fundam. Vol.25, 695, 1986.

50. Van der Waals, J.D. "Over de Continuiteit van den Gas en Vloeistoftoestand". Thesis Disseration. Leyden, Holland, 1873.

51. Abbott, M.M. A.I.Ch.E. Journal, Vol.19, 596, 1973.

52. Abbott, M.M. Adv.Chem.Series, No.182, 47-70, 1979.

53. Adachi, Y, Benjamin, C.Y Lu and Sugie, H. Fluid Phase Equilibria, Vol.11, 29, 1983.

54. Freze, R., Chevalier, J.L., Peneloux, A., and Rauzy, E. Fluid Phase Equilibria, Vol.15, 33, 1983.

55. Behar, E, Simonet, R. and Rauzy, E. Fluid Phase Equilibria, Vol.21, 237, 1985.

56. Toghiani, H. and Viswanath, D.S. Ind.Eng.Chem. Process Des.Deve., Vol.25, 531, 1986.

57. Valderrama, J.O. and Cisternas, L.A. Fluid Phase Equilibria, Vol.29, 431, 1986.

58. Tavares, N. Ph.D. Thesis, Renssalar Poly.Inst., 1986.

59. Trebble, N.A. Ph.D.Thesis, University of Calgary, 1986.

60. Martin, J.J. Ind.Eng.Chem. Fundamentals, Vol.18, 81-97, 1979.

61. Vidal, J. Fluid Phase Equilibria, Vol.13, 15-33, 1983.

62. Redlich, O., and Kwong, J.N.S. Chem.Rev., Vol.44, 233, 1949.

63. Tsonopoulos, C and Heidman, J.L. Fluid Phase Equilibria, Vol.24, 1-23, 1985.

64. Levelt Sengers, J.M.H., Greer, W.L. Senger,J.V. J.Phys.Chem. Ref.Data, (5) 1, 1, 1976.

65. Van Ness, H.C. A.I.Ch.E. Journal, Vol.1, 100-104, 1955.

66. Zudkevitch, D. and Joffe, J. A.I.Ch.E. Journal, Vol.16, 112-119, 1970.

67. Wilson, G.M. Adv.Cryogen.Eng., Vol.9, 168-176, 1966.
Ibid, Vol.11, 392-400, 1969.

68. Riedel, L. Chem.Ing.Tech., Vol.26, 679, 1954.

69. Soave, G. Chem.Eng.Science, Vol.27, 1197-1203, 1972.

70. Peng, D.Y. and Robinson, D.B. Ind.Eng.Chem. Fundamentals, Vol.15, 59-64, 1976.

71. Skogestad, S. Fluid Phase Equilibria, Vol.13, 179-188, 1983.

72. Vera, J.H., Huron, M.J. and Vidal, J. Chem.Eng.Commun. Vol.26, 311-318, 1984.

73. Schmidt, G. and Wenzel, H. Chem.Eng.Sci., Vol.35, 1503, 1980.

74. Harmens, A, and Knapp, H. Ind.Eng.Chem. Fundamentals, Vol.19, 291-294, 1980.

75. Clausius, R. Ann der Phys. Vol.9, 337,1880.

76. Kubie, W.L. Fluid Phase Equilibria, Vol.9, 79-97, 1982.

77. Joffe, J. Ind.Eng.Chem.Process Des.Deve., Vol.20, 168-172, 1981.

78. Gundersen, T. Computer and Chemical Eng. Vol.6, No.3, pp.245-255, 1982.

79. Peneloux, A, Rauzy, E. and Freze, R. Fluid Phase Equilibria, Vol.8, 7-23, 1982.

80. Soave, G. Chem.Eng.Sci. Vol.39, 357-369, 1984.

81. Stryjek, R. and Vera, J.H. 189 ACS National Meeting, Miami, April-May, 1985.

82. Chang, T, Rousseau, R.W. and Ferrell, J.K. Ind.Eng.Chem.Process Des.Dev., Vol.22, 462, 1985.

83. Robinson, D.B., Peng, D.Yu and Chung S.Y.K. Fluid Phase Equilibria, Vol.24, 25, 1985.

84. Lin, H.M., Fluid Phase Equilibria, Vol.16, 151, 1984.

85. Yesavage, V.F. Fluid Phase Equilibria, Vol.31, 273, 1986.

86. Pedersen, K.S, Thomassen, P. and Fredenslund, A. Fluid Phase Equilibria, Vol.14, 209-218, 1983.

87. Asselineau, L., Bogdanic, G. and Vidal, J. Chem.Eng.Sci., Vol.33, 1269-1276, 1978.

88. Moysan, J.M., Huron, M.J. Paradowski, H. and Vidal, J. Chem.Eng.Sci., Vol.38, 1085, 1983.

89. Moysan, J.M., Paradowski, H. and Vidal, J. Chem.Eng.Sci. Journal Vol.41, 2069, 1986.

90. Knapp, H. Döring, R., Oellrich, L., Plöcker, U. and Prausnitz, J.M. Chemistry Data Series, Vol.VI: VLE for Mixtures of Low Boiling Substances. D.Behrens and R.Eckerman (Eds.) DECHEMA, Frankfurt, W.Germany, 1982.

91. Graboski, M.S. and Daubert, T.E. Ind.Eng.Chem.Process Des.Dev., Vol.17, 443, 1976.

92. Graboski, M.S. and Daubert, T.E. Ind.Eng.Chem.Process Des.Dev. Vol.18, 300, 1979.

93. Knapp, H., Plöcker, U., Oellrich, L. and Prausnitz, J.M. Internat.Chem.Eng., Vol.21, No.1, pp.1-16, 1981.

94. Panagiotopoulos, A.Z. and Reid, R.C. 189 ACS National Meeting, Miama, April-May, 1985. Also see same article in "Equations of State: Theories and Applications" Editors K.C. Chao and R.L. Robinson Jr., ACS Symp.Series No.300, Amer.Chem.Soc. Washington, D.C. p.571, 1986.

95. Stryjek, R. and Vera, J.H. IUPAC Conference, Paris, Sept.1985.

96. Radosz, Lin and Chao. IUPAC Conference Paris, Sept.1985.

97. Luedecke, D. and Prausnitz, J.M. Fluid Phase Equilibria, Vol.22, 1-19, 1985.

98. Adachi, Y. and Sugie, H. Fluid Phase Equilibria, Vol.24, 353-362,. 1985.

99. Adachi, Y. and Sugie, H. Fluid Phase Equilibria, Vol.28, 103-118, 1986.

100. Mansoori, G.A. in "Equations of State: Theories and Applications". Eds. K.C.Chao and R.L. Robinson Jr., ACS Symp.Series No.300, Amer.Chem.Soc., Washington, D.C. p.314, 1986.

101. Benmekki, E.H. and Mansoori, G.A. Fluid Phase Equilibria, Vol.32, 139, 1987.

102. Copeman, T.W. and Mathias, P.M. in "Equations of State: Theories and Applications" Eds.K.C. Chao and R.L.Robinson Jr., ACS Symp.Series, No.300, Amer.Chem.Soc., Washington, D.C. p.352, 1986.

103. Smith, I.K. THERPROP Data Bank. The City University, London, 1982.

104. Adachi, Y. and Sugie, H. Fluid Phase Equilibria, Vol.34, pp.203-208, 1987.

105. Mather, A.E. 71st Annual A.I.Ch.E. Meeting, Miami, 1978.

CHAPTER 6

COMPUTER CALCULATIONS OF VAPOUR-LIQUID EQUILIBRIA (VLE)

6.1. EQUATION OF STATE METHOD

The method adopted here uses the Redlich-Kwong-Soave cubic equation of state together with classical mixing rules applied to both phases. At a given temperature, pressure and composition, the roots of the RKS equation are calculated from equation (5.6) in Chapter 5 (which is cubic in volume V or compressibility Z). Figure 6.1 shows how both liquid and vapour volumes may be reproduced with a single cubic equation of state (EOS). The equation is continuous and gives a smooth transition from liquid to vapour volumes through the two-phase region. This is of course not according to nature where there is a discontinuity followed by a linear change of volume between the bubble and dew points dependent only on the dryness fraction. Since the Redlich-Kwong-Soave EOS is of the third degree in volume (or in compressibility factor Z), any subcritical isotherm has three real roots, whereas supercritical isotherms have only one real root.

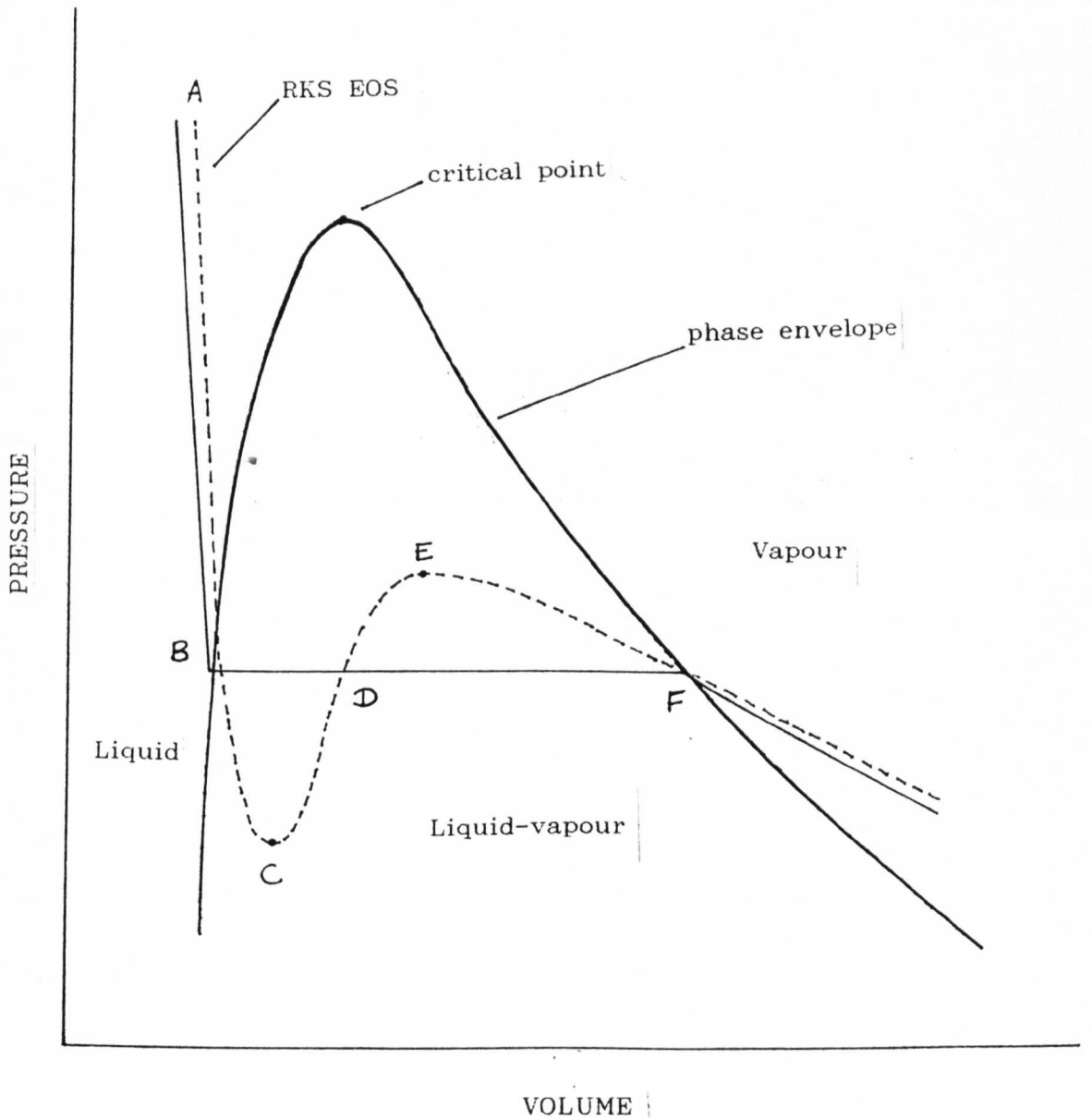

BC metastable superheated liquid
CDE physically meaningless region
EF metastable subcooled vapour

Figure 6.1. P-V diagram of an RKS EOS isotherm.

Portions BC and EF of the curve ABCDEF in Figure 6.1 represent metastable conditions that have been realized experimentally but portion CDE is not physically possible since it corresponds to changes of pressure and volume in the same direction at fixed temperature[1]. The volumetric behaviour of a cubic EOS inside the two-phase region is constrained to obey Maxwell's equal-area rule (see Figure 6.2). Maxwell's rule comes from the criterion of equal fugacities in both phases for a pure substance or mixture at VLE. When there are three real roots, the strategy is therefore to pick up the largest root interpreted as the specific volume of a vapour phase, the smallest root as the specific volume of a liquid phase and the intermediate one as physically meaningless.

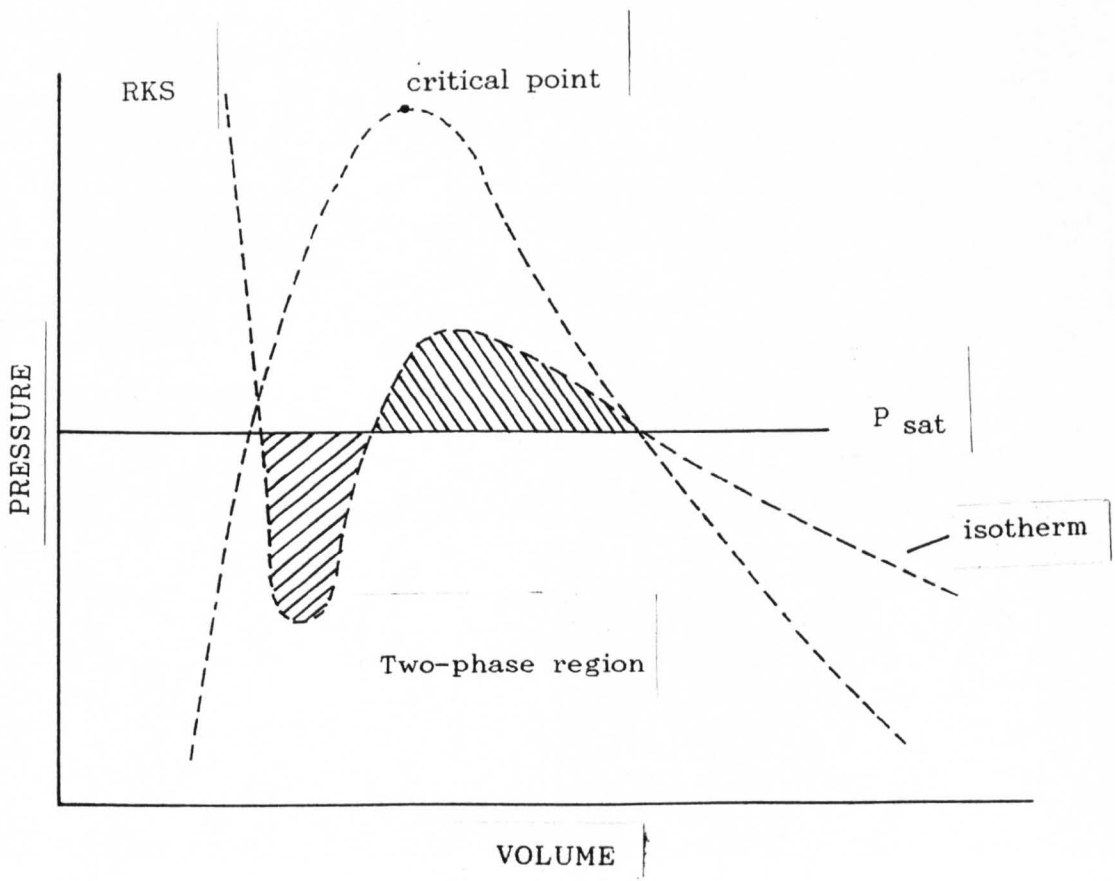

Figure 6.2. P-V diagram of Maxwell's equal area rule.

6.2. EQUILIBRIUM EQUATIONS

The vapour-liquid equilibrium calculations may be stated as follows:

$$f_i^L = f_i^V \qquad (i = 1,.....,N) \tag{6.1}$$

and when an equation of state is applied to both phases, equation (6.1) becomes:

$$\phi_i^L \cdot x_i = \phi_i^V \cdot y_i \tag{6.2}$$

with the fugacity coefficient of component i ϕ_i (liquid or vapour) for SRK EOS given by:

$$\ln \phi_i = \frac{b_i}{b}(Z-1) - \ln(Z-B) - \frac{A}{B}\left[2\sum_j \frac{w_j a_{ij}}{a} - \frac{b_i}{b}\right].\ln\left(1 + \frac{B}{Z}\right) \tag{6.3}$$

where

$$A = \frac{aP}{R^2T^2} \quad \text{and} \quad B = \frac{bP}{RT} \quad \text{with } w_j = \text{either liquid or vapour mole fractions}$$

The vapour phase fugacity coefficient ϕ_I^V is calculated by using the vapour phase compressibility root Z^V in equation (6.3) and the liquid phase fugacity coefficient ϕ_I^L by replacing the liquid compressibility root Z^L in the same equation.

Further we have the stoichiometric equations:

$$\sum_i x_i = 1 \qquad \text{and} \qquad \sum_i y_i = 1 \tag{6.4}$$

There are N liquid-phase mole fractions, N vapour-phase mole fractions, the pressure P and the temperature T. Since there are 2N+2 variables in this list and only N+1 may be independently specified, the other N+1 must be determined by the solution of N equilibrium relationships and 1 stoichiometric relation:

GIVEN	FIND	
P, $x_1, x_2, \ldots\ldots x_N$	T, $y_1, y_2, \ldots y_N$	(Bubble Temperature)
P, $y_1, y_2, \ldots\ldots y_N$	T, $x_1, x_2, \ldots x_N$	(Dew Temperature)
T, $x_1, x_2, \ldots\ldots x_N$	P, $y_1, y_2, \ldots y_N$	(Bubble Pressure)
T, $y_1, y_2, \ldots\ldots y_N$	P, $x_1, x_2, \ldots x_N$	(Dew Pressure)

The four types of calculation, bubble and dew pressure and bubble and dew temperatures, are solved using the same model but slightly different calculation techniques.

6.3. COMPUTER METHOD OF SOLUTION

Two computer programs were written for this purpose. One calculates bubble and dew pressures and the other bubble and dew temperatures. When KEY is set to 1 in both programs bubble calculations are made. When KEY is set to 2 in both programs dew calculations are carried out. Flow charts and listings for these four types of calculation are given in Appendix B.

6.3.1. Bubble Pressure Calculation

In the bubble pressure calculation, the unknown variables are the pressure P and the vapour mole fractions y_i's. The program starts off by calling subroutine INPUT to provide the initial value of pressure, and all the data required by the main program. Next the value of KEY is read in and in this case it will be 1. On the next line the temperature at which the calculation is to be performed is read in. On the following line the liquid mole fractions are read in. These, in turn, are stored in the dummy array XORY(I) and then transferred to array X(I). Subroutine INIT is then called up to provide an initial estimate of the vapour mole fractions y_i's by making use of Raoult's law with the saturation vapour pressure PSAT(I) evaluated with Antoine's equation. Further the pseudo mixture critical temperature is calculated by using the following equations:

$$\Phi_j = \frac{y_j \, V_{cj}}{\sum_i y_i \, V_{ci}} \qquad (6.5)$$

and

$$T_{cT} = \sum_j \Phi_j \, T_{cj} \qquad (6.6)$$

where

y_j = mole fraction of component j

V_{cj} = critical volume of j

T_{cj} = critical temperature of j

T_{cT} = pseudo critical temperature

and the critical volume for RKS equation of state is as follows:

$$V_{cj} = 0.33 \; R \; T_{cj}/P_{cj} \qquad (6.7)$$

where

P_{cj} = critical pressure of component j.

The pseudo mixture critical pressure is also evaluated by the following equations:

$$P_{cT} = P^* \left[1.0 + (5.808 + 4.93\omega)\left(\frac{T_{cT}}{T^*} - 1\right)\right] \qquad (6.8)$$

where

$$P^* = \sum_j y_j P_{cTj}$$

$$T^* = \sum_j y_j T_{cTj}$$

$$\omega = \sum_j y_j \omega_j$$

where P_{cTj} = critical pressure of component j

ω_j = accentric factor of component j.

After initialisation, an estimation of the vapour and liquid phase fugacity coefficients is made by calling subroutine PHI. (This subroutine contains equation 6.3) and subroutine RKSEQN which contains the roots (compressibility factor roots) of Redlich-Kwong-Soave EOS. Next, the liquid phase fugacity f_I^L is calculated as follows:

$$f_i^L = x_i \, \phi_i^L \, P \qquad (6.9)$$

Subroutine NEWRAF is then called up to update the fugacity coefficient ϕ_i^V. A new estimate of P is made by using either the Secant or the Bisection Method (Appendix C).

The new value of the pressure P is now checked with the old value and if the two are not (within tolerance) equal then a further estimate of the pressure is made.

When the two successive values of P are found to have converged a check is made on the stoichiometric equation

$\sum_i y_i = 1$. If the SUMXY (here $\sum_i y_i$) is not equal to unity

then the vapour phase fugacity coefficient ϕ_i^V is recalculated and a new estimate of the vapour phase mole fractions y_i's is made. When the recalculated values of pressure have converged and SUMXY is equal to unity (within tolerance) then the simultaneous equations have been satisfied and the calculated value for P and the vapour mole fractions y_i's are the required results. When SUMXY (which is also the error) and SUMXYP (previous error) have opposite signs, the iteration process is then executed by the Bisection method (see Appendix C). Although slow, this root-finding procedure was found to be safer than the Secant method for some calculations.

6.3.2. Dew Pressure Calculation

The dew pressure calculation is carried out in a similar manner. Input data are now the temperature and the vapour mole fractions y_i's.

6.3.3. Bubble Temperature Calculations

In the bubble temperature calculation, initial estimation for the fugacity coefficients, the liquid phase fugacity f_i^L and the vapour mole fractions y_i's are made in a similar manner to the bubble pressure calculation. Initialisation consists now of the temperature T (since P is fixed) and the liquid mole fraction x_i's by calling, as before, subroutine INIT. After initialisation has been completed, an estimation of the vapour and liquid phase fugacity coefficients is made. Compressibility factor Z's (roots of the cubic equation of state) are calculated by using NAG routine CO2AEF.

Next, the value of SUMXY ($\sum_i y$) is checked to see if it equals unity. If it doesn't, then the temperature is adjusted by either using the Secant or the Bisection method and the whole process is repeated until SUMXY is constant and equal to unity (within tolerance).

6.3.4. Dew Temperature Calculation

In the dew temperature calculation the liquid mole fractions x_i's are replaced by the vapour mole fraction y's as input data.

6.4. DIFFICULTIES WITH COMPLEX ROOTS

During the process of iteration, complex roots of equation (5.6) numerically sound but physically meaningless, may be encountered

even when the VLE is being performed away from the critical point. The reason why VLE calculations fail at high pressure has been found to be either the lack of good initial estimates of phase composition or combinations of pressure and temperature approaching the true critical point of the mixture, or both[2]. Asselineau et al.[3] demonstrated that when below the pseudo critical point, a root of equation (5 .6) can be unequivocally assigned to either the liquid or vapour phase by comparing the calculated volume with the pseudo critical volume V_{pc}

$$\text{where } V_{pc} = R(\sum_i x_i T_{ci}/P_i)/3 \text{ and } V = ZRT/P.$$

The root is of a liquid-phase type when $V < V_{pc}$ and vapour-phase type when $V > V_{pc}$. However, no simple method was given to avoid or replace complex roots. References [2] and [4] present numerical techniques to overcome this computational problem. The method adopted here makes use of what is known as the Van der Waals' spinodal curve. It consists of finding a curve which represents the loci of maxima and minima of all subcritical isotherms of a cubic equation of state on a P-V plane. (The spinodal curve for the Redlich-Kwong-Soave EOS is presented in Appendix D). The Van der Waals' spinodal curve is a polynomial of the fourth degree in volume. When there are three or four positive real roots only two must be retained since negative roots which correspond to negative volumes are obviously physically meaningless: These are the liquid-phase fictitious root and the vapour-phase fictitious root. The criterion for choosing the suitable real roots is as follows. The repulsive term in any cubic EOS yields a singularity at V = b. It was found that only the real volume roots greater than the co-volume b were "successful

fictitious roots". Thus the singularity was avoided. For tested roots, smaller than b, the program never converged. In the bubble and dew pressure calculations the spinodal roots are fixed since VLE is evaluated at constant T while in the bubble and dew temperature calculations they vary in each iteration. Although this numerical technique never failed, except near the critical point where both the cubic equations of state and spinodal curve yield complex roots, no thermodynamic justification was found for this method by the author.

Whenever a pair of complex roots from eqn.(5.6) is detected, subroutine SPIN is called up to provide the master program with fictitious real roots. This is realised as follows: the real root from the cubic equation of state is retained while the pair of complex roots are dropped out. The other real root is provided by the spinodal curve. The spinodal curve being a polynomial of the fourth degree (see Appendix C) yields four roots. Only positive roots are kept since negative roots are devoid of physical meaning. It was observed that one of the "spinodal roots" is always negative. Also among the remaining three roots, only those which are greater than BMIX (co-volume b for mixtures) are selected. This is because a root smaller than BMIX yields a "numerical singularity". The procedure is then to test the equation of state real root for phase, i.e. its value is compared to the "spinodal roots". If the real root is greater than the "spinodal roots", it is a vapour volume real root (V^V) and the smaller of the "spinodal roots" is used as the fictitious liquid volume root (V^L). And vice versa, if the real root from the cubic equation of state is smaller than the "spinodal roots", then it must be a liquid volume root (V^L). The vapour volume root (V^L) is assigned by picking up the largest of the "spinodal roots".

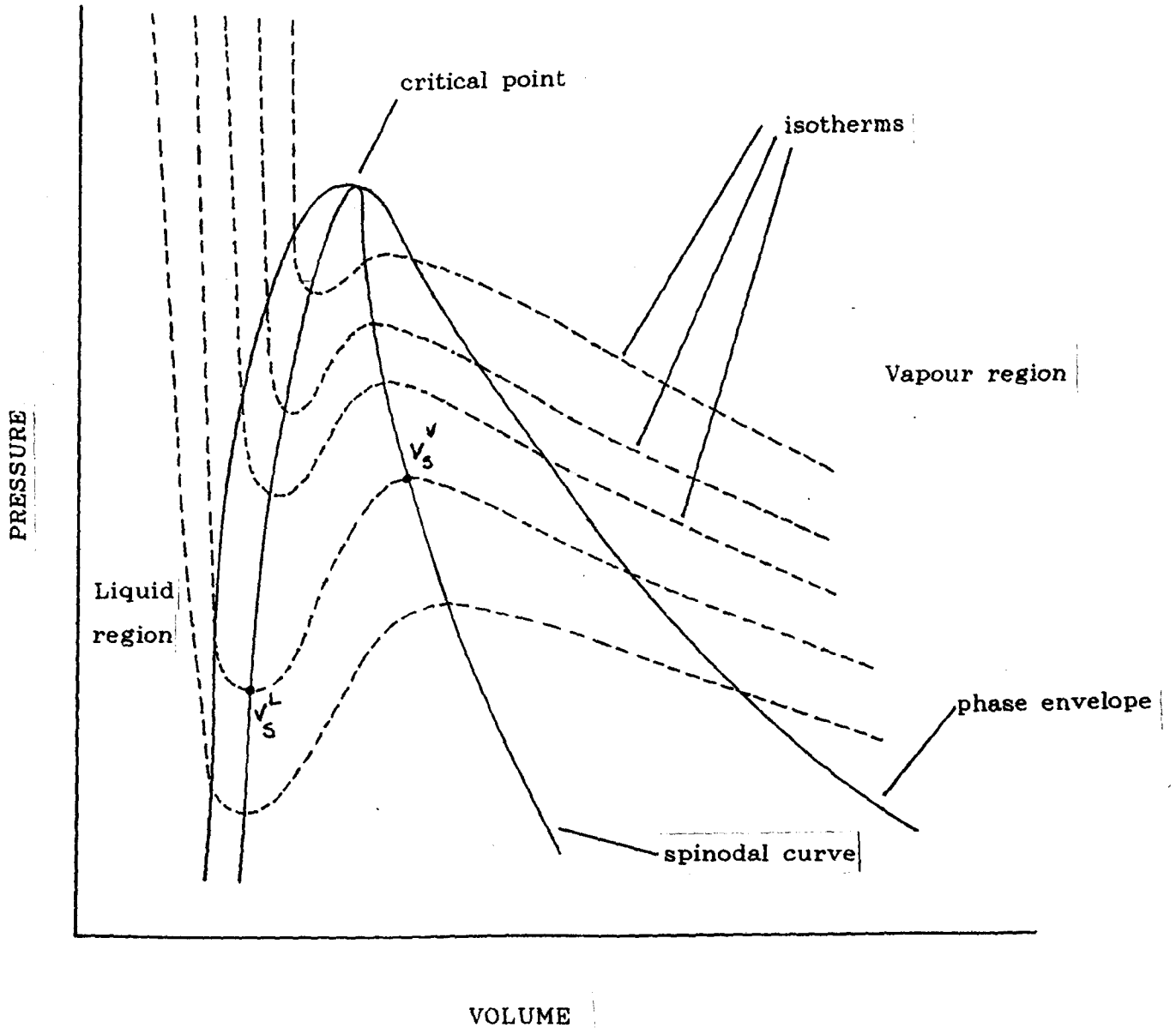

V_s^L and V_s are the spinodal roots

Figure 6.3. P-V diagram of spinodal curve.

The spinodal curve technique is illustrated in Figure 6.3. Finally, it should be noted that although numerically sound, the "spinodal roots" are fictitious and therefore the final iteration (the one yielding the VLE final value) is always to be performed with the equation of state roots.

6.5. ENTROPY AND ENTHALPY CALCULATIONS

In order to calculate the entropy and enthalpy of the binary mixtures subroutines ENTROP and ENTHAL are called up after the bubble or dew points and mole fractions are determined. These subroutines contain respectively the residual entropy and enthalpy relations presented in Section 5.8 of Chapter 5.

6.6. CONVERGENCE PROBLEMS

Several convergence difficulties were encountered. It was found that the algorithm is very sensitive to the initial guess of either temperature or pressure in both bubble and dew point calculations. This is related to the inability of Raoult's Law (subroutine INIT) to predict good initial values of either liquid or vapour mole fractions at moderate and (specially) high pressures. A somewhat ad hoc procedure was introduced. Steps of 10 kPa were either subtracted or added to the pressure (in Raoult's Law) to force the sum of mole fractions to be never greater than 10 or smaller than an arbitrary value set equal to 0.1. Similarly, when the calculation involved bubble or dew temperature points, steps of 5 K were either added or subtracted in order to modify PSAT(I) forcing Raoult's Law to produce mole fractions never greater than 1.0 or smaller than 0.1.

Although successful for the mixtures studied, it is not inconceivable that this procedure may fail to produce thermodynamically coherent values to initialize the program. Thus, convergence difficulties may arise particularly when one of the components is highly supercritical. The Antoine vapour pressure equation in this case becomes too artificial to be used.

6.7. SOME VAPOUR-LIQUID EQUILIBRIUM (VLE) RESULTS

Some sample results of refrigerant (freon) and hydrocarbon binary mixtures are shown. These were primarily intended to test the algorithm. A mixture of trifluorochloromethane (R.13) and dichlorodifluoromethane (R.12) was studied (see pages 172-176). A maximum error of 2.7% in predicting bubble pressures over an entire range of composition was found when these values were compared with experimental data of Mollerup and Fredenslund[5]. However, the prediction of vapour mole fractions was less good with errors for a couple of points of 5%. Nevertheless, the vapour-liquid equilibria representation for this system may be considered fair for engineering calculations when using the Redlich-Kwong-Soave equation of state.

The algorithm was also tested for bubble and dew temperature calculations. A mixture of n-pentane + n-heptane was chosen for this purpose. Bubble temperatures were compared with experimental data of Cummings, Stones and Volante[6]. The Redlich-Kwong-Soave predictions are in excellent agreement with the exception of the vapour mole fractions. However, one should not jump to the

conclusion that the equation of state is poor. Quality of experimental values often varies from one set of data to another. For the isobar of 3060 kPa studied by Volante et al.[6], convergence was not achieved for x = 0.255, x = 0.3 and x = 0.4 of n-pentane. For these compositions the isobar was very near the measured critical pressure for this system[7].

No interaction parameter k_{ij} was used for the n-pentane + n-heptane mixture since k_{ij} values for hydrocarbon mixtures are very small and often neglected. For the refrigerant binary system k_{ij} was found in [8]. k_{ij} values are determined by the Marquart minimization procedure through the bubble pressure vapour-liquid equilibrium calculation method with the following objective function:

$$OF = \sum_{i=1}^{M} \left[\frac{P_{(exp)} - P_{(cal)}}{P_{(exp)}} \right]_i^2$$

where M is the number of experimental data considered, $P_{(exp)}$ is the experimental pressure and $P_{(cal)}$ is the calculated pressure. From the above equation the average deviation in pressure can be expressed as:

$$\frac{DP}{P} = \left[\frac{OF}{M} \right]^{1/2}$$

Similarly, it is also possible to determine k_{ij} by minimizing an objective function based on vapour mole fractions as follows:

$$OF = \sum_{i=1}^{M} \left[\frac{y_{(exp)} - y_{(cal)}}{y_{(exp)}} \right]_i^2$$

with the average deviation expressed by:

$$\frac{dy}{y} = \left[\frac{OF}{M} \right]^{1/2}$$

REFRIGERANT BINARY MIXTURE

Chlorotrifluoromethane (R.13)
Dichlorodifluoromethane (R.12)

Temperature = 255.0 K

Source: Mollerup & Fredunslund[5]

Bubble Pressure (kPa) Experimental[5]	Bubble Pressure (kPa) Theoretical(RKS)	Error $\frac{\text{Exp-RKS}}{\text{Exp.}} \times 100$ %	Liquid mole fraction R.13	Vapour Mole fraction Experimental R.13[5]	Vapour Mole fraction Theoretical (RKS) R.13	Error $\frac{\text{Exp-RKS}}{\text{Exp}} \times 100$ %
214.50	210.65	1.79	0.036	0.2301	0.2492	-8.3
272.1	267.35	1.74	0.0791	0.3985	0.4233	-6.2
356.7	359.74	-0.85	0.1535	0.5653	0.5914	-4.6
449.1	458.54	-2.10	0.2392	0.6862	0.6985	-1.79
561.2	572.3	-1.97	0.3461	0.7793	0.7790	0.04
674.4	685.28	-1.61	0.4602	0.8401	0.8357	0.52
785.9	802.16	-2.0	0.5841	0.8877	0.8810	0.76
972.3	988.58	-1.67	0.7817	0.9460	0.9389	0.75
1105.1	1121.6	-1.49	0.9123	0.9794	0.9748	0.47

REFRIGERANT BINARY MIXTURE

Chlorotrifluoromethane (R.13)
Dichlorodifluoromethane (R.12)

Temperature = 290.0 K

Source: Mollerup and Fredunslund[5]

Bubble Pressure (kPa) Experimental[5]	Bubble Pressure (kPa) Theoretical	Error Exp-RKS / Exp. x100 %	Liquid mole fraction R.13	Vapour Mole fraction Experimental R.13[5]	Vapour Mole fraction Theoretical (RKS) R.13	Error Exp-RKS / Exp x 100 %
541.4	542.93	-0.28	0.0079	0.0380	0.042	-10.5
693.4	674.8	2.68	0.0569	0.2376	0.2419	-1.8
1038.5	1010.0	2.74	0.1890	0.5220	0.5199	-0.40
1385.4	1359.5	1.87	0.3382	0.6817	0.6710	1.57
1836.0	1825.3	0.58	0.5486	0.8090	0.7946	1.78
2249.0	2258.1	-0.40	0.7388	0.8919	0.8782	1.69
2656.2	2676.1	-0.75	0.9004	0.9566	0.9491	0.78
2783.1	2820.0	-1.32	0.9494	0.9774	0.9730	0.45

HYDROCARBON BINARY MIXTURE

n-Pentane (C_5H_{12})
n-Heptane (C_7H_{16})

Pressure = 1013.25 kPa

Source: Cummings, Stones and Volante[6]

Bubble Temperature (K) Experimental[6]	Bubble Temperature (K) Theoretical	Error Exp-RKS / Exp. x100 %	Liquid mole fraction n-Pentane	Vapour Mole fraction Experimental[6] n-Pentane	Vapour Mole fraction Theoretical (RKS) n-Pentane	Error Exp-RKS / Exp x 100 %
463.95	463.48	0.10	0.1	0.236	0.2109	10.6
453.35	453.52	-0.03	0.2	0.408	0.3859	5.4
443.85	444.28	-0.09	0.3	0.545	0.5292	2.9
435.35	435.77	-0.09	0.4	0.656	0.6457	1.57
427.75	427.97	-0.05	0.5	0.745	0.7399	0.68
420.85	420.84	0.00	0.6	0.818	0.8161	0.23
414.75	414.33	0.10	0.7	0.875	0.8775	-0.28
409.15	408.38	0.18	0.8	0.923	0.9272	-0.45
404.05	402.93	0.27	0.9	0.964	0.9674	-0.35

HYDROCARBON BINARY MIXTURE

n-Pentane (C_5H_{12})
n-Heptane (C_7H_{16})

Pressure = 2026.50 kPa

Source: Cummings, Stones and Volante[6]

Bubble Temperature (K) Experimental[6]	Bubble Temperature (K) Theoretical	Error $\frac{\text{Exp-RKS}}{\text{Exp.}} \times 100$ %	Liquid mole fraction n-Pentane	Vapour Mole fraction Experimental[6] n-Pentane	Vapour Mole fraction Theoretical (RKS) n-Pentane	Error $\frac{\text{Exp-RKS}}{\text{Exp}} \times 100$ %
509.05	508.91	0.03	0.1	0.169	0.1524	9.8
499.25	499.58	-0.06	0.2	0.320	0.2943	8.0
489.95	490.45	-0.10	0.3	0.456	0.4244	6.9
481.25	481.59	-0.07	0.4	0.576	0.5421	5.8
472.85	473.03	-0.04	0.5	0.680	0.6474	4.8
465.05	464.84	0.04	0.6	0.765	0.7404	3.2
457.75	457.06	0.15	0.7	0.835	0.8214	1.6
450.85	449.73	0.25	0.8	0.897	0.8910	0.67
444.15	442.85	0.29	0.9	0.951	0.9501	0.09

HYDROCARBON BINARY MIXTURE

n-Pentane (C_5H_{12})
n-Heptane (C_7H_{16})

Pressure = 3060 kPa

Source: Cummings, Stones and Volante[6]

Bubble Temperature (K) Experimental[6]	Bubble Temperature (K) Theoretical(RKS)	Error $\frac{\text{Exp-RKS}}{\text{Exp.}} \times 100$ %	Liquid mole fraction n-Pentane	Vapour Mole fraction Experimental[6] n-Pentane	Vapour Mole fraction Theoretical (RKS) n-Pentane	Error $\frac{\text{Exp-RKS}}{\text{Exp}} \times 100$ %
526.65	-	-	0.255	0.255	-	-
521.95	-	-	0.300	0.331	-	-
512.65	-	-	0.400	0.457	-	-
503.85	506.11	-0.45	0.500	0.573	0.5333	6.9
495.45	497.05	-0.32	0.600	0.676	0.6435	4.8
487.25	488.30	-0.21	0.700	0.770	0.7434	3.4
479.45	478.80	-0.07	0.800	0.853	0.8352	2.0
471.75	471.37	0.08	0.900	0.935	0.9214	1.45

REFERENCES

1. Callen, H.B. "Thermodynamics", John Wiley & Sons, New York, 1960.

2. Gunderson, T. "Numerical Aspects of the Implementation of Cubic Equations of State in Flash Calculation Routines". Computers & Chemical Engineering, Vol.6, No.3, pp.245-255, 1982.

3. Asselineau, L., Bogdanic, G., and Vidal, J. Fluid Phase Equilibria, Vol.3, 273, 1979.

4. Polling, B.E., Grens II, E.A. and Prausnitz, J.M. Ind. Eng. Chem. Process Des. Dev., Vol.20, 127-130, 1981.

5. Mollerup, J. and Fredenslund, A. J.of Chem.& Eng.Data, Vol.21, pp.299-301, (1976).

6. Cummings, L.W.T., Stones, F.W. and Volante, M.A. Indust. & Eng.Chem., Vol.25, No.7, pp.728-732 (1933).

7. Hicks, C.P. and Young, C.L. Chemical Reviews, Vol.75, No.2, pp. (1975)

8. Knapp, H., Döring, R., Ocllrich, L., Plöcker, U. & Prausnitz, J.M. Chemistry Data Series, Vol. VI, VLE for Mixtures of Low Boiling Substances, D. Behrens & R. Eckerman (Eds.), DECHEMA, Frankfurt a M., (1982).

CHAPTER 7

ORGANIC WORKING FLUID MIXTURES

7.1. STRUCTURE OF THE T-S DIAGRAM

Given a set of thermodynamic property values such as internal energy, enthalpy and entropy one can subsequently calculate the heat and work effects of various processes and determine equilibrium conditions in a variety of systems. Although such a set of properties can be readily incorporated in a computer program to make design calculations or to simulate plant performance it is also convenient to represent thermodynamic properties in diagrams for preliminary cycle calculations.

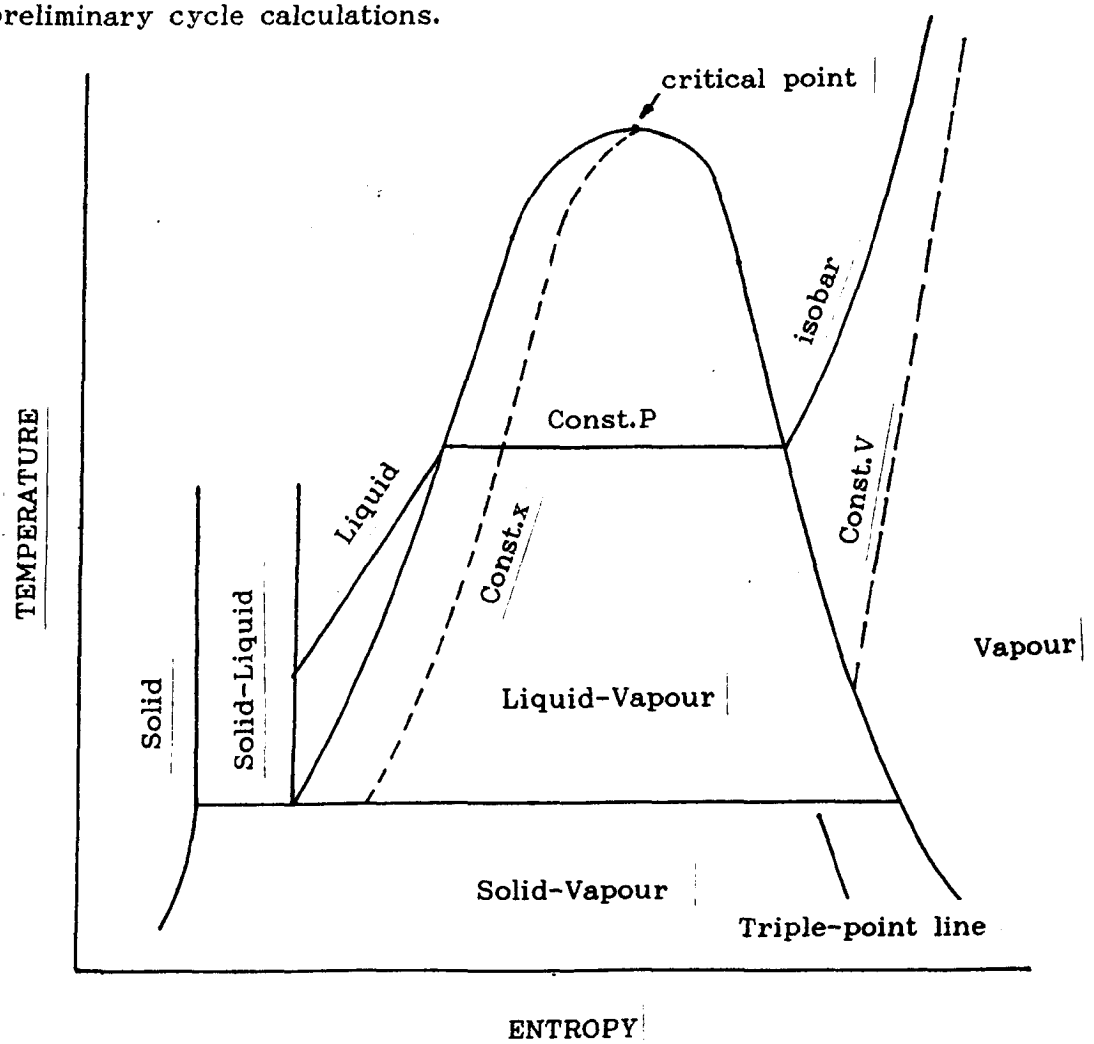

Figure 7.1. A General T-s diagram.

Normally the thermodynamic properties are plotted against directly measurable quantities such as temperature, pressure or volume. However, the T-s diagram is particularly useful when heat transferred and cycle efficiency are to be evaluated for cycle analysis and this is illustrated in Figure 7.1 in its most complete form.

Since our major concern here is the study of processes involved in a thermodynamic cycle a more convenient T-s diagram would include liquid, liquid-vapour and vapour regions only as displayed in Figure 7.2.

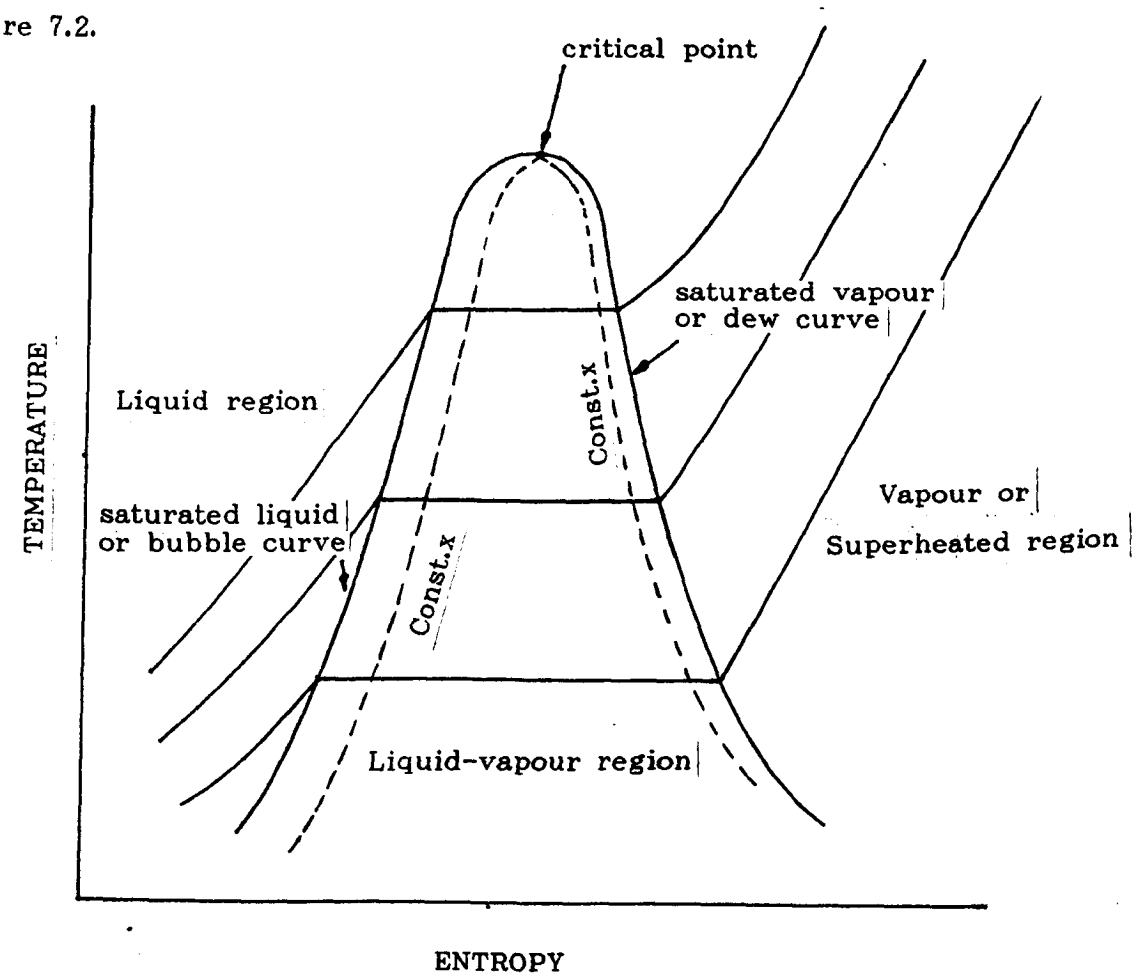

Figure 7.2. Usual T-s diagram.

The choice of a suitable working fluid mixture for the Trilateral Flash Power Plant involves the shape of the T-s diagram saturation line as was explained in Chapter 3. One of the major control parameters is the slope of the dew curve boundary between the two-phase and the vapour regions. Therefore we should proceed to examine how the slope varies with other working fluid characteristics such as chemical composition, molecular weight, and boiling point. To illustrate this, consider water, the commonest working fluid for which the T-s diagram is shown in Figure 7.3.

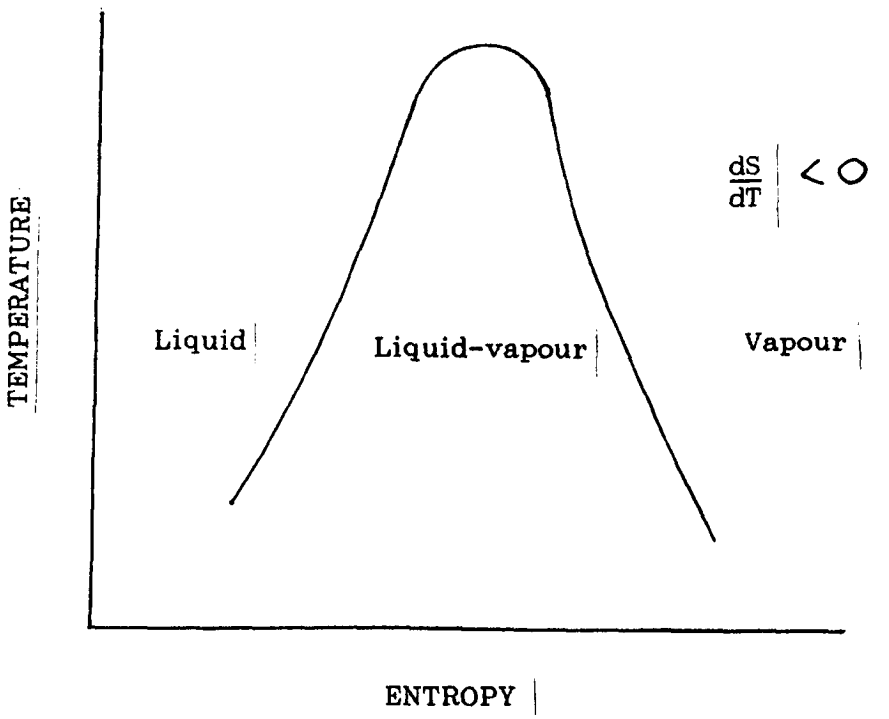

Figure 7.3. A T-s diagram of a negative slope saturation line.

The slope of the dew curve is negative that is:

$$\frac{ds}{dT} < 0$$

This means that when saturated steam expands isentropically (e.g. in a steam turbine) from point A to point B the steam becomes wet. In practice care must be taken that point B is not excessively wet to avoid turbine blade erosion and loss of efficiency.

Figure 7.4 displays a T-s diagram for a typical organic fluid such as iso-Butane commonly used in supercritical Rankine cycles in geothermal fields (see Chapter 1). The slope is approximately zero.

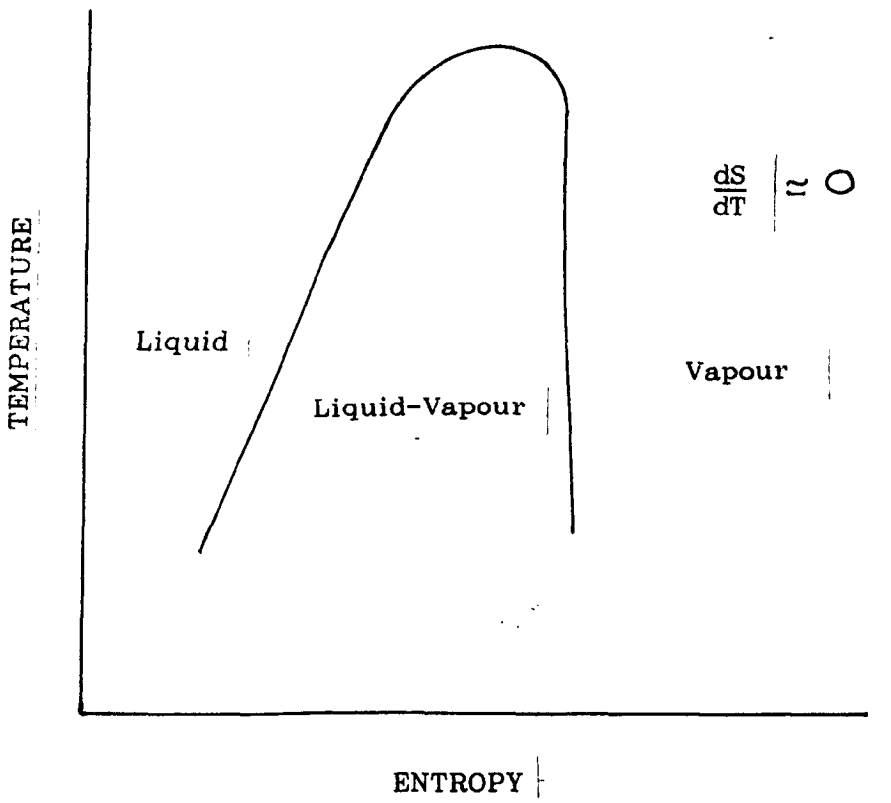

Figure 7.4. T-s diagram of an isentropic saturation line.

The organic working fluid expands as dry (or mainly dry) saturated vapour throughout the turbine. For yet higher molecular weight organic fluids (e.g. n-Heptane) $^{ds}/_{dT}$ appears to become positive as shown in Figure 7.5.

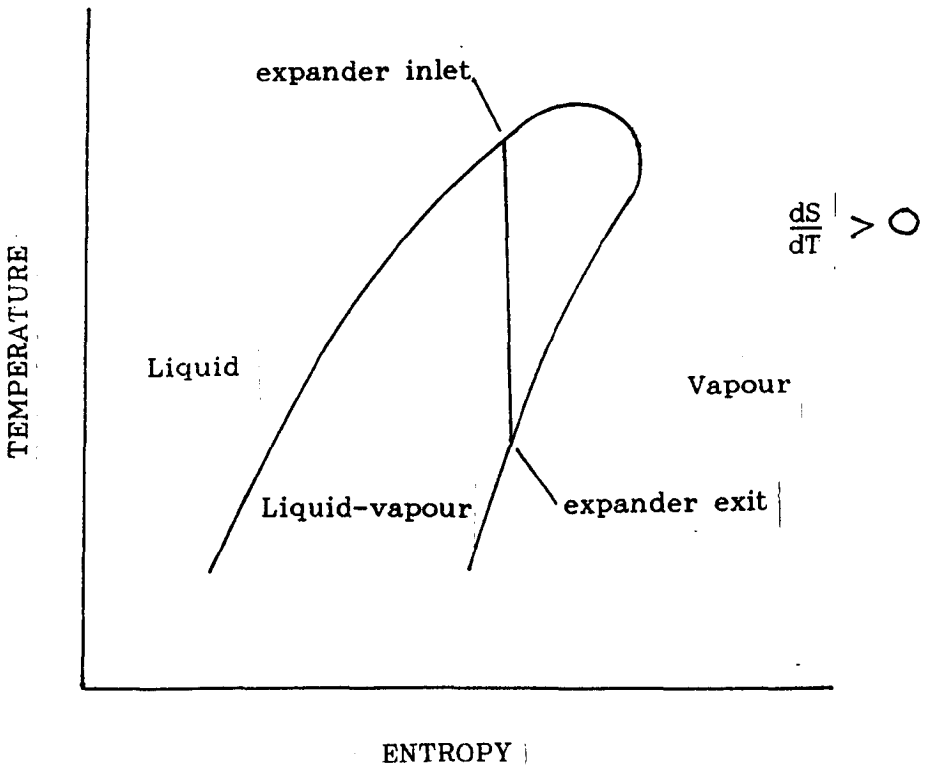

Figure 7.5. T-s diagram of a positive slope saturation line.

This shape of saturation line is of particular interest. As pointed out in Chapter 3, an ideal organic fluid mixture for the Trilateral cycle should expand isentropically from saturated liquid to an exhaust temperature (approximately 35°C) such that the fluid reaches nearly dry vapour conditions. The evaluation of the slope of the saturated vapour line is too complex to enable simple procedures to be established to estimate its value accurately*. A simpler approach is therefore to find out the connection, if it exists, between $^{ds}/_{dT}$ and other fluid characteristics such as molecular weight or boiling point. The search for good candidates to form the binary mixture then becomes to a large extent an empirical exercise.

---

* This is evaluated by forcing a cubic equation of state to obey Maxwell's equal area rule (equality of fugacities) to obtain bubble and dew temperatures and corresponding entropy values - see Chapter 6).

For a pure organic fluid Goldstein[2] demonstrated that the slope of the saturated vapour line, to a first approximation, seems to be independent of the nature of the substance but rather (dependent) on the number of atoms in the molecule. He derived from first principles a thermodynamically exact relation for the reciprocal of the slope of the dew curve. This is as follows:

$$\left(\frac{\partial T}{\partial s}\right)_{\sigma} = \frac{1}{\frac{Cp}{T} - \left(\frac{\partial V}{\partial T}\right)_{T} \left(\frac{\Delta H_V}{T\Delta V}\right)}$$

where

ΔH_V is the heat of vaporization of the pressure of the saturated vapour at atmospheric boiling temperature T.

ΔV is the change in volume on evaporation.

Cp is the heat capacity at constant pressure.

If sufficient data on the vapour and liquid are available, it is possible to calculate the slope exactly. He, then, considered the ideal gas equation and obtained a simpler relation:

$$\left(\frac{\partial T}{\partial s}\right)_{\sigma} = \frac{T}{Cp - \frac{\Delta H_V}{T}}$$

For normal liquids at their boiling point $^{\Delta H V}/_{T}$ is about 21 J/mol·K and the slope of the saturated vapour curve is positive or negative according to whether Cp is greater or less than 21 J/mol·K.

Therefore the magnitude of the specific heat of the vapour is decisive. To estimate the specific heat of a substance three modes of motion are to be considered: translational, rotational and vibrational.

The first two modes are classically excited at room temperature and contribute 3R to Cp. The contribution of the vibrational mode is given by 3n - 6 where n is the number of atoms per molecule. Quantum restrictions tend to reduce this contribution except at higher temperatures. He then concluded that roughly speaking Cp tends to be greater, for a greater number of atoms in a molecule.

It was decided then to retain Goldstein's simple relation as a guide for the selection of good candidates to form the binary mixture.

7.1.1. Influence of Binary Mixtures on T-s Diagrams

Little is known about the effect of binary mixtures on the saturation line of a T-s diagram. No published material was found on this matter. Critical temperatures are normally shifted or lowered in a linear fashion and are dependent on the number of atoms in a molecule[3]. Critical pressures combine non-linearly and available correlations[3] give large errors when the number of atoms in each molecule differ appreciably. Generally speaking, the critical pressure of the binary mixture tends to be higher than the component's highest critical pressure. This gives rise to a higher back pressure at the condensing temperature (30 - 35°C) as long as the critical temperature remains not too high (not above 250°C). This may be considered as a bonus since it helps keep the expander small.

The advantage of using mixtures rather than pure compounds stems from the fact that although pure fluids already exist, (e.g.

n-Hexane or n-Heptane) none show the same drying out characteristics for adiabatic expansion from the saturated liquid condition starting at temperatures in the 150 - 180°C range or below it. If such a fluid were to be found, screw turbine combinations for large power outputs would be possible even when recovering power from lower temperature resources. Furthermore binary mixtures include the possibility of "tuning" the properties of the working fluid to the existing external conditions by adjusting the composition of the mixture (e.g. the critical temperature of the mixture may be adjusted according to the source temperature).

Having stressed the utility of binary mixtures, the author also finds it important to point out their limitations. The desirable characteristics of the working fluid mixture include a small difference between the bubble and dew temperatures in order to keep condensation nearly isothermal (and minimize condenser cost per unit of heat transfer area which is an increasing function of ΔT). This can only be partially achieved when the number of atoms per molecule of each component present does not differ appreciably and therefore drastically reduce the possible combinations. Also, each component should mix in all proportions with one another. Complete solubility is only guaranteed when components are chemically similar in nature.

When the various requirements of the ideal fluid listed in section 2.2 are considered it is clear that some of the different desirable characteristics are incompatible and a process of trading-off a loss or gain in requirements seems to be unavoidable to produce the most acceptable compromise.

7.2. ORGANIC WORKING FLUIDS FROM THE THERPROP DATA BANK

The THERMOPROP Data Bank[4] developed at the Department of Mechanical Engineering of The City University, was used to obtain T-s diagrams of single compounds. It uses the Lee-Kesler EOS to predict thermodynamic and transport properties of fluids. The Data Bank initially comprised over 91 fluids and was later extended by the author to 120 compounds. Thirty-six fluids were analysed as possible candidates to form the binary mixture. The criteria adopted for the selection of fluids was based on the desirable characteristics presented in section 2.2 and the overwhelming majority of fluids selected were hydrocarbons and cyclic hydrocarbons. These fulfil several of the working fluid mixture requirements. Alkenes and alkynes were eventually ruled out due to thermal instability at the critical region. Amines and halocarbons were also studied.

7.2.1. Case Studies

The following pages describe the family characteristics of compounds and present T-s diagrams for relevant fluids.

Halocarbon group

Halocarbon or halogenated hydrocarbons have been used as refrigerants for a long period of time. These substances are stable (at normal temperature), non-flammable, and non-toxic. However, in recent years[5] these fluids are thought to be responsible for the depletion of the ozone layer. Although chemical reactions in the upper atmosphere are not well-established[6] R.11 (trichloro-

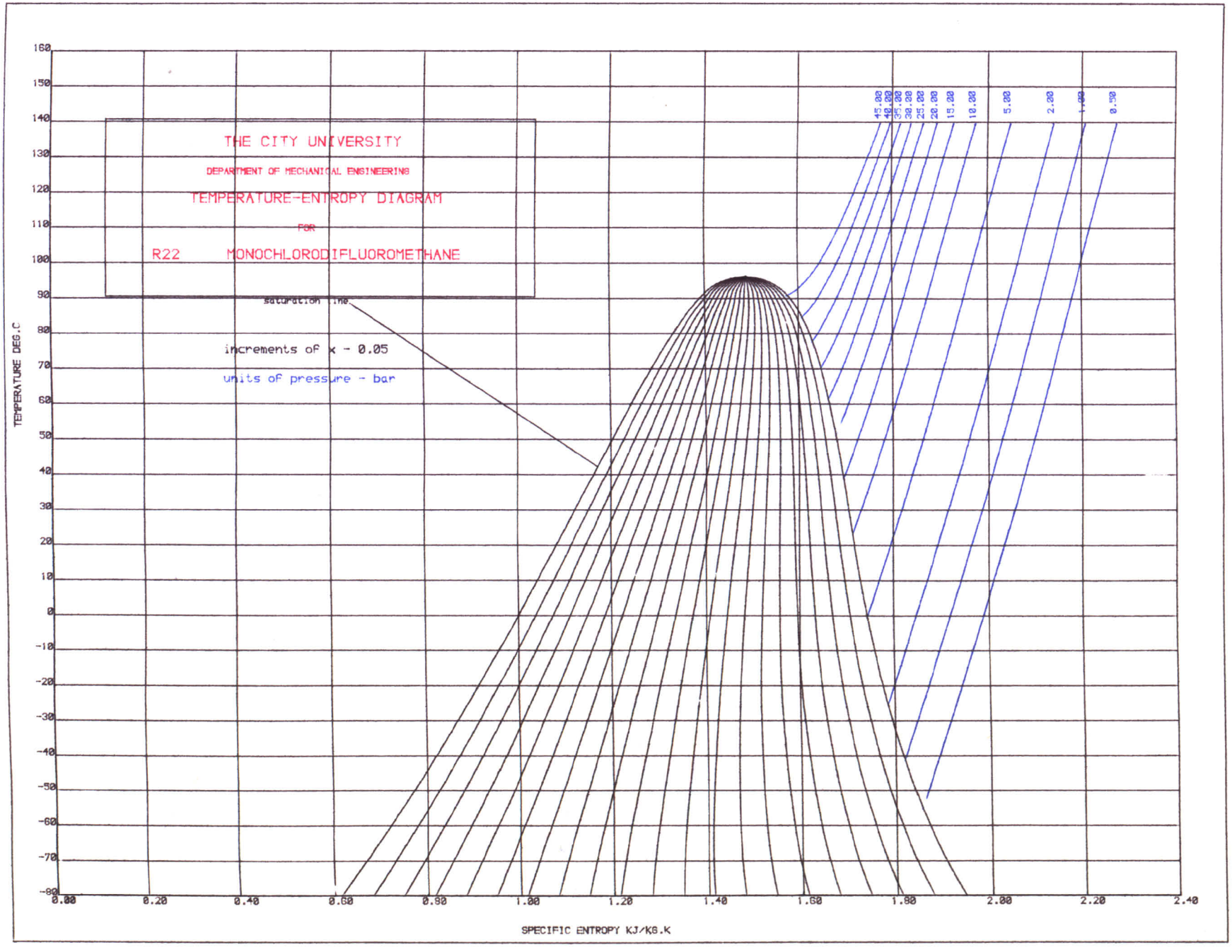
THE CITY UNIVERSITY
DEPARTMENT OF MECHANICAL ENGINEERING
TEMPERATURE-ENTROPY DIAGRAM
FOR
R22 MONOCHLORODIFLUOROMETHANE
saturation line
increments of x - 0.05
units of pressure - bar
45.00
40.00
35.00
30.00
25.00
20.00
15.00
10.00
5.00
2.00
1.00
0.50
TEMPERATURE DEG.C
160
150
140
130
120
110
100
90
80
70
60
50
40
30
20
10
0
-10
-20
-30
-40
-50
-60
-70
-80
0.00
0.20
0.40
0.60
0.80
1.00
1.20
1.40
1.60
1.80
2.00
2.20
2.40
SPECIFIC ENTROPY KJ/KG.K

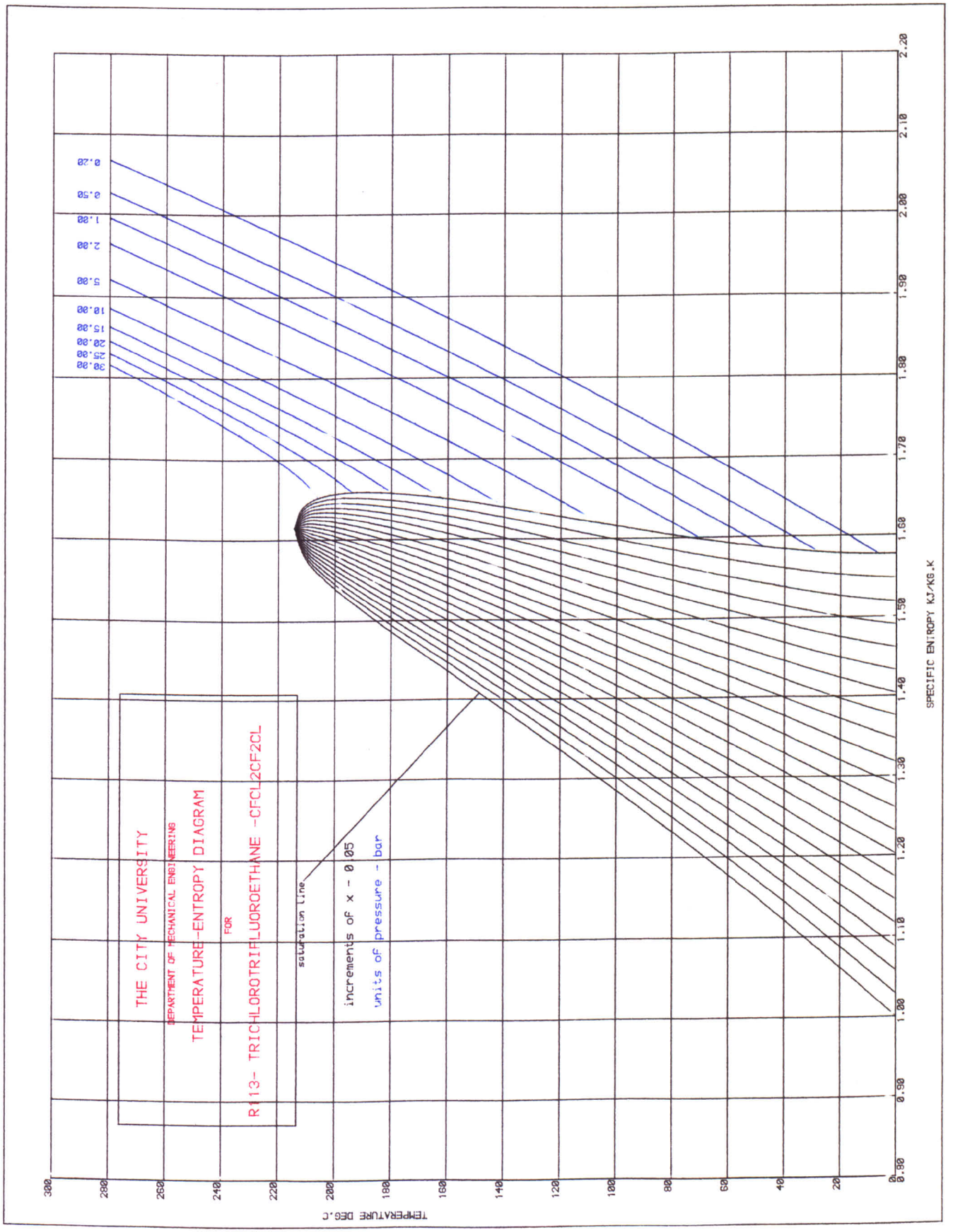
THE CITY UNIVERSITY
DEPARTMENT OF MECHANICAL ENGINEERING
TEMPERATURE-ENTROPY DIAGRAM
FOR
R113- TRICHLOROTRIFLUOROETHANE -CFCL2CF2CL
saturation line
increments of x - 0.05
units of pressure - bar
0.20
0.50
1.00
2.00
5.00
10.00
15.00
20.00
25.00
30.00
TEMPERATURE DEG.C
SPECIFIC ENTROPY KJ/KG.K

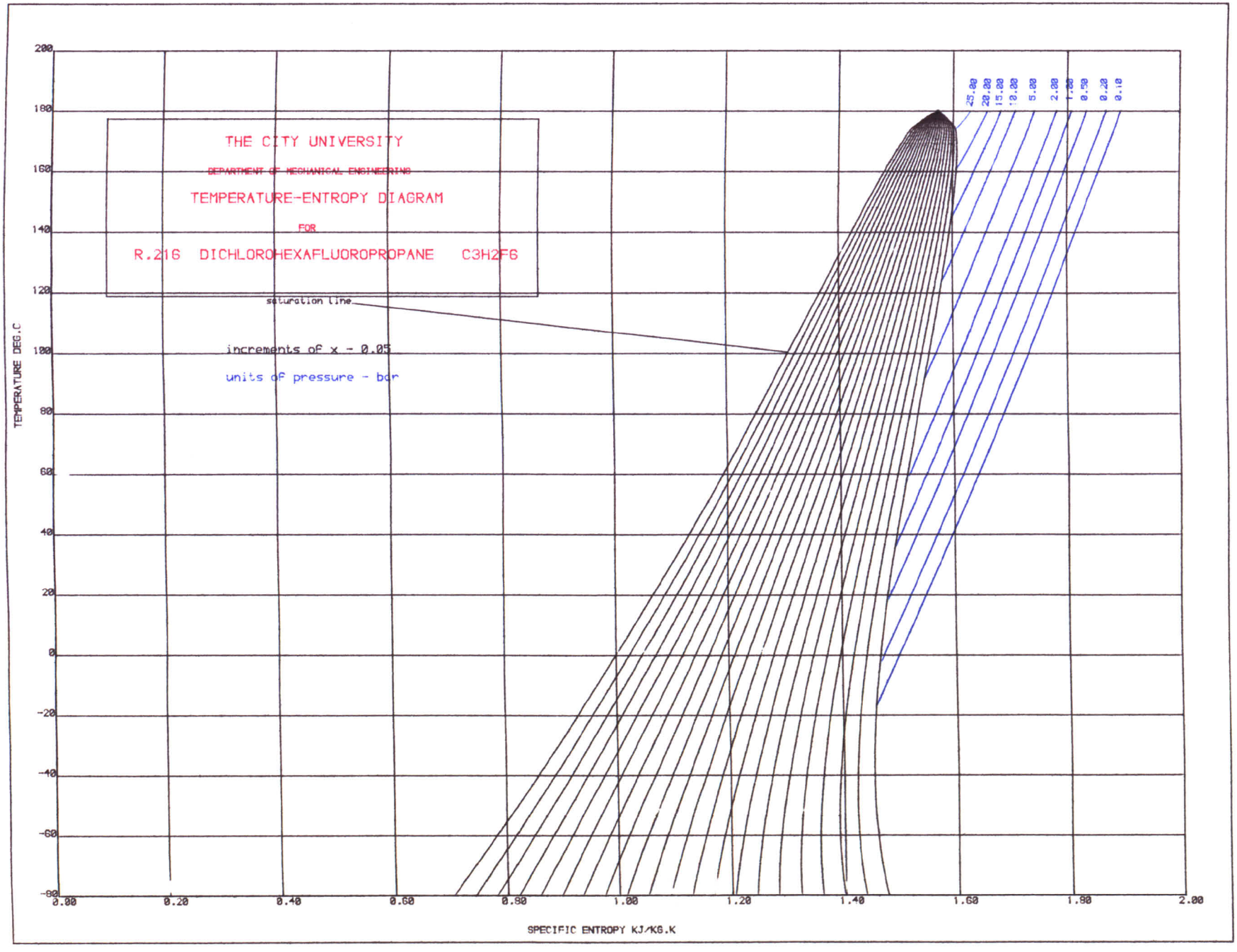
THE CITY UNIVERSITY
DEPARTMENT OF MECHANICAL ENGINEERING
TEMPERATURE-ENTROPY DIAGRAM
FOR
R.216 DICHLOROHEXAFLUOROPROPANE C3H2F6
saturation line
increments of x - 0.05
units of pressure - bar
25.00
20.00
15.00
10.00
5.00
2.00
1.00
0.50
0.20
0.10
TEMPERATURE DEG.C
200
180
160
140
120
100
80
60
40
20
0
-20
-40
-60
-80
0.00
0.20
0.40
0.60
0.80
1.00
1.20
1.40
1.60
1.80
2.00
SPECIFIC ENTROPY KJ/KG.K

fluoromethane), R.12 (dichlorofluoromethane) and R.13 (trichloro-fluoroethane) were banned in the United States. Halocarbons have been synthetically produced, particularly for their refrigerating properties, by substitution of a halogen for one or more of the hydrogen atoms in methane, ethane, or propane. The halogens used are fluorine, chlorine, and sometimes bromine. The American Society of Heating, Refrigerating and Air-Conditioning Engineers (ASHRAE)[7] has developed a numerical system for designation of different refrigerants. The last digit in the designation (the one on the right) indicates the number of fluorine atoms in the molecule formed. The second digit from the right is one more than the number of hydrogen atoms remaining, and the third digit is one less than the number of carbon atoms i.e. blank indicating methane structure, 1 ethane structure, and 2 propane structure. If bromine is used, this designation is followed by a B with the number of bromine atoms after the B.

T-s diagrams of R.22, R.113, and R.216 are presented. Only R.216 (dichlorohexafluoropropane) has proved to be useful, as the working fluid does dry out at condensing temperatures (30-35°C). However, it was eventually discarded due to its heavy molecular weight. Although suitable for some organic Rankine cycle systems halocarbons are not suitable for the majority of TFC systems.

Cyclic hydrocarbon group

Cycloalkanes have the general formula C_nH_{2n} and are isomeric with alkenes. Their boiling points are 10 to 20° higher than those of the corresponding alkanes[8]. Their chemical and physical

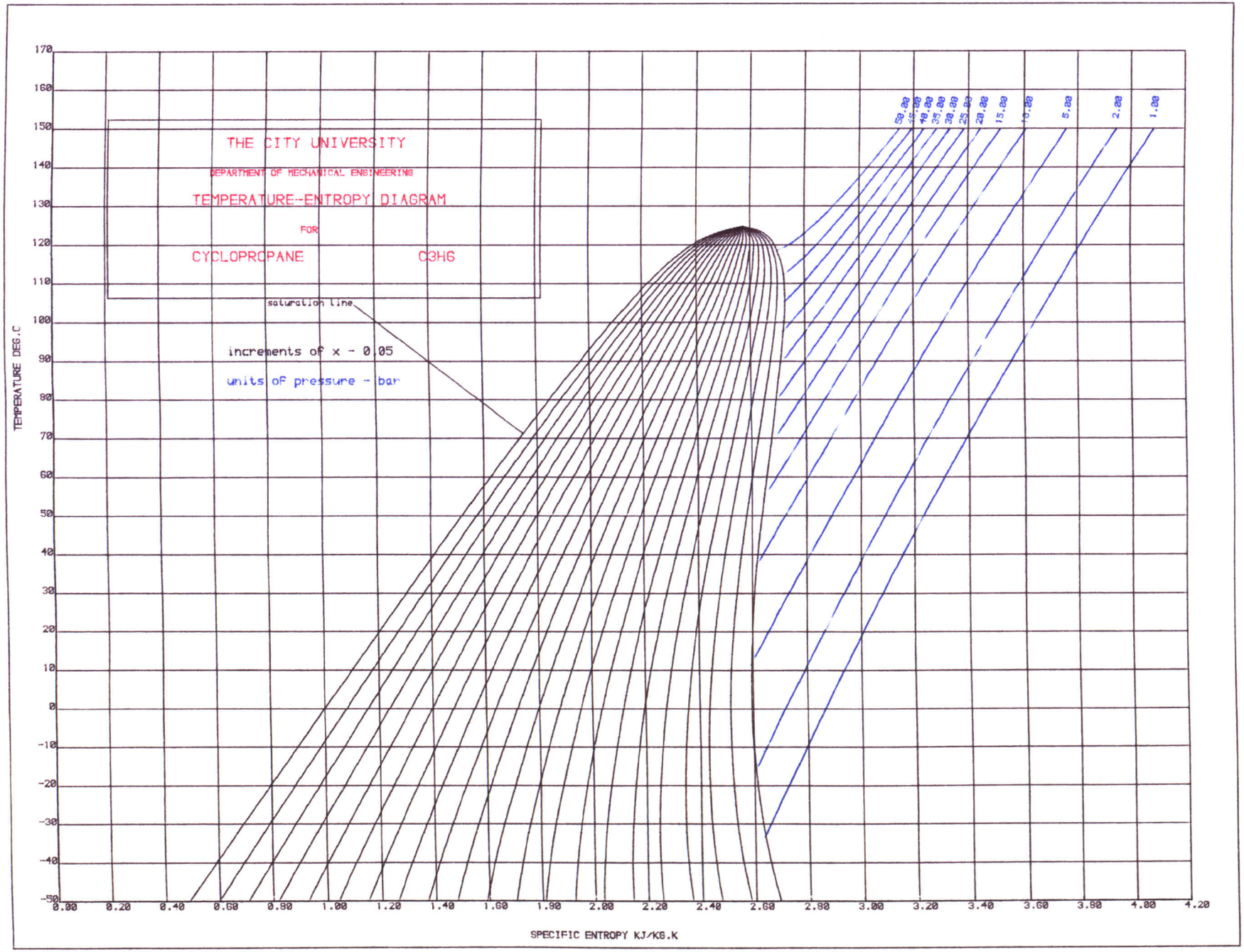
THE CITY UNIVERSITY
DEPARTMENT OF MECHANICAL ENGINEERING
TEMPERATURE--ENTROPY DIAGRAM
FOR
CYCLOPROPANE C3H6
saturation line
increments of x - 0.05
units of pressure - bar
50.00
40.00
35.00
30.00
25.00
20.00
15.00
10.00
5.00
2.00
1.00
TEMPERATURE DEG.C
SPECIFIC ENTROPY KJ/KG.K

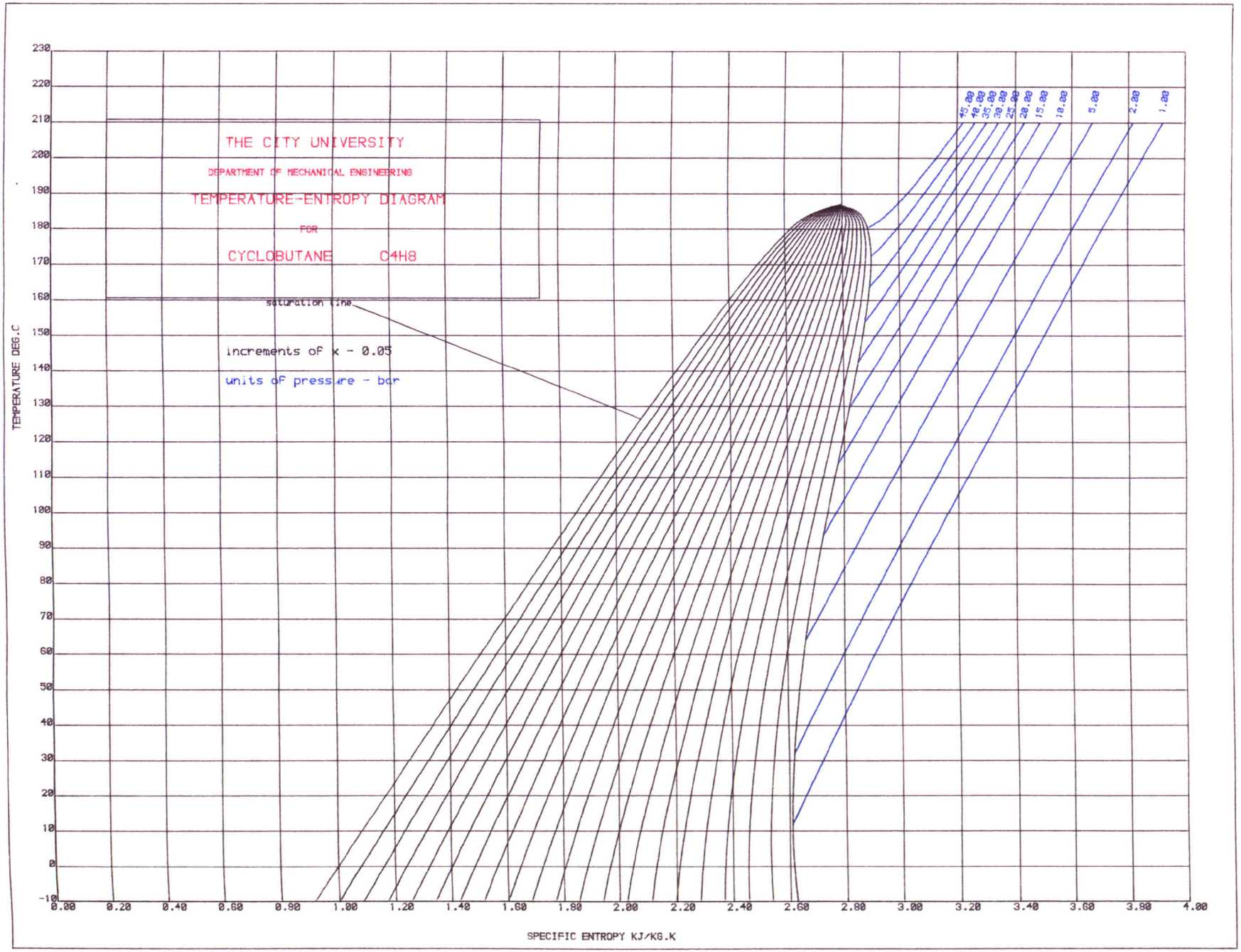
THE CITY UNIVERSITY
DEPARTMENT OF MECHANICAL ENGINEERING
TEMPERATURE-ENTROPY DIAGRAM
FOR
CYCLOBUTANE C4H8
saturation line
increments of x - 0.05
units of pressure - bar
45.00
40.00
35.00
30.00
25.00
20.00
15.00
10.00
5.00
2.00
1.00
TEMPERATURE DEG.C
SPECIFIC ENTROPY KJ/KG.K

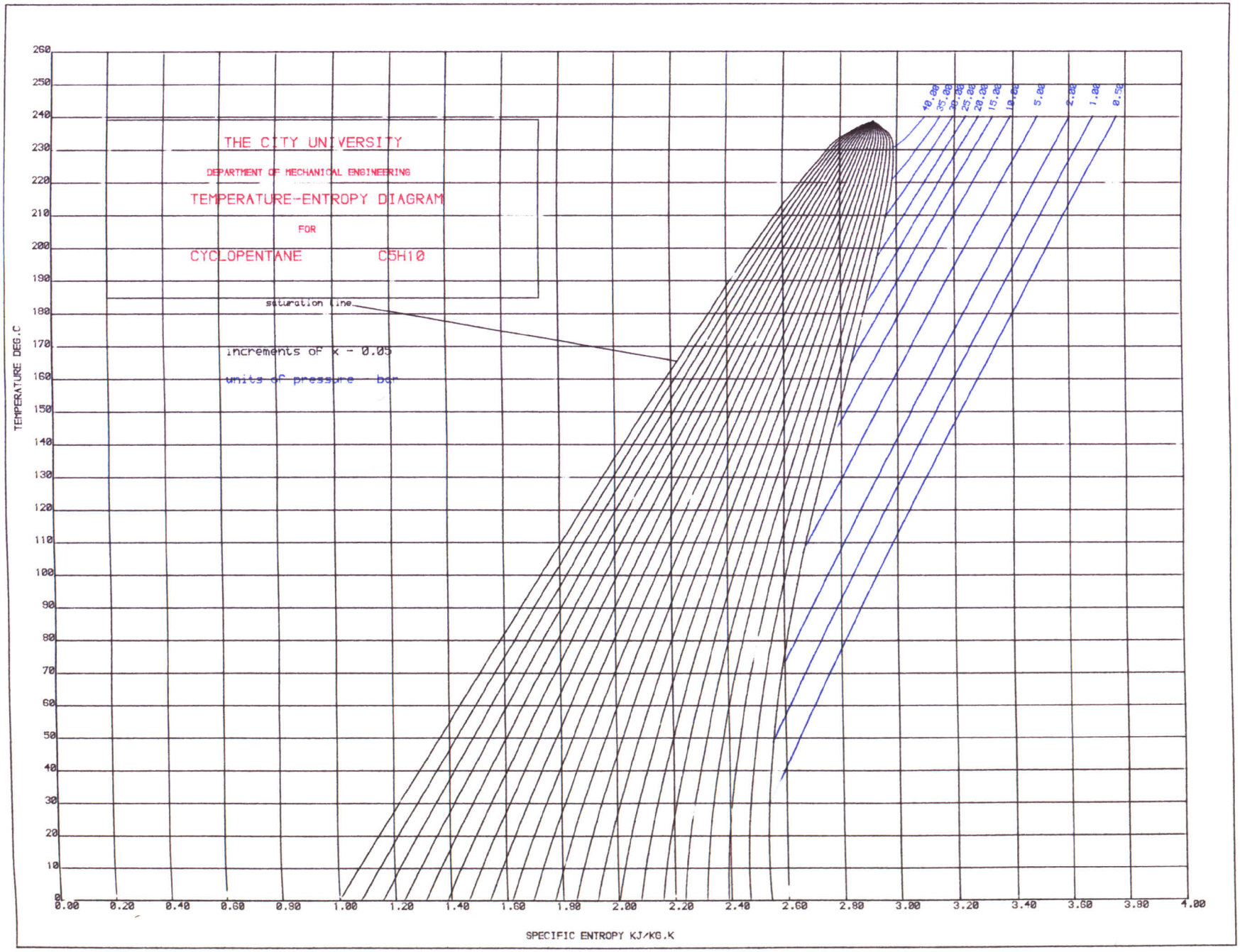
THE CITY UNIVERSITY
DEPARTMENT OF MECHANICAL ENGINEERING
TEMPERATURE-ENTROPY DIAGRAM
FOR
CYCLOPENTANE C5H10
saturation line
increments of x - 0.05
units of pressure bar
40.00
35.00
30.00
25.00
20.00
15.00
10.00
5.00
2.00
1.00
0.50
TEMPERATURE DEG.C
SPECIFIC ENTROPY KJ/KG.K

properties are similar to those of the acyclic compounds except that cyclopropane and cyclobutane are slightly more reactive than propane and butane owing to strain in the ring system. Cyclic hydrocarbons are of particular interest since these compounds are thermally stable in the critical region.

T-s diagrams of cyclopropane, cyclobutane and cyclopentane are shown. As can be seen, these compounds have high critical pressures (particularly useful to obtain high back pressure to keep the expander compact) but none of them present the dry out characteristics required.

Aldehydes and ketones group

The aldehydes and ketones are isomeric and are known as carbon compounds as both contain the carbonyl group $>C=O$. In aldehydes this group is linked to a hydrogen atom (to two hydrogen atoms in the simplest member of the series, methanol), whereas in ketones the carbonyl carbon atom is always linked to two hydrocarbon groups. The general formulae are thus:

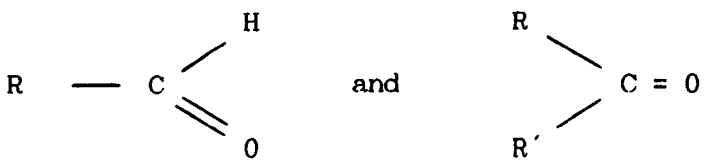

aldehydes ketones

where R and R´ are either alkyl or aryl groups.

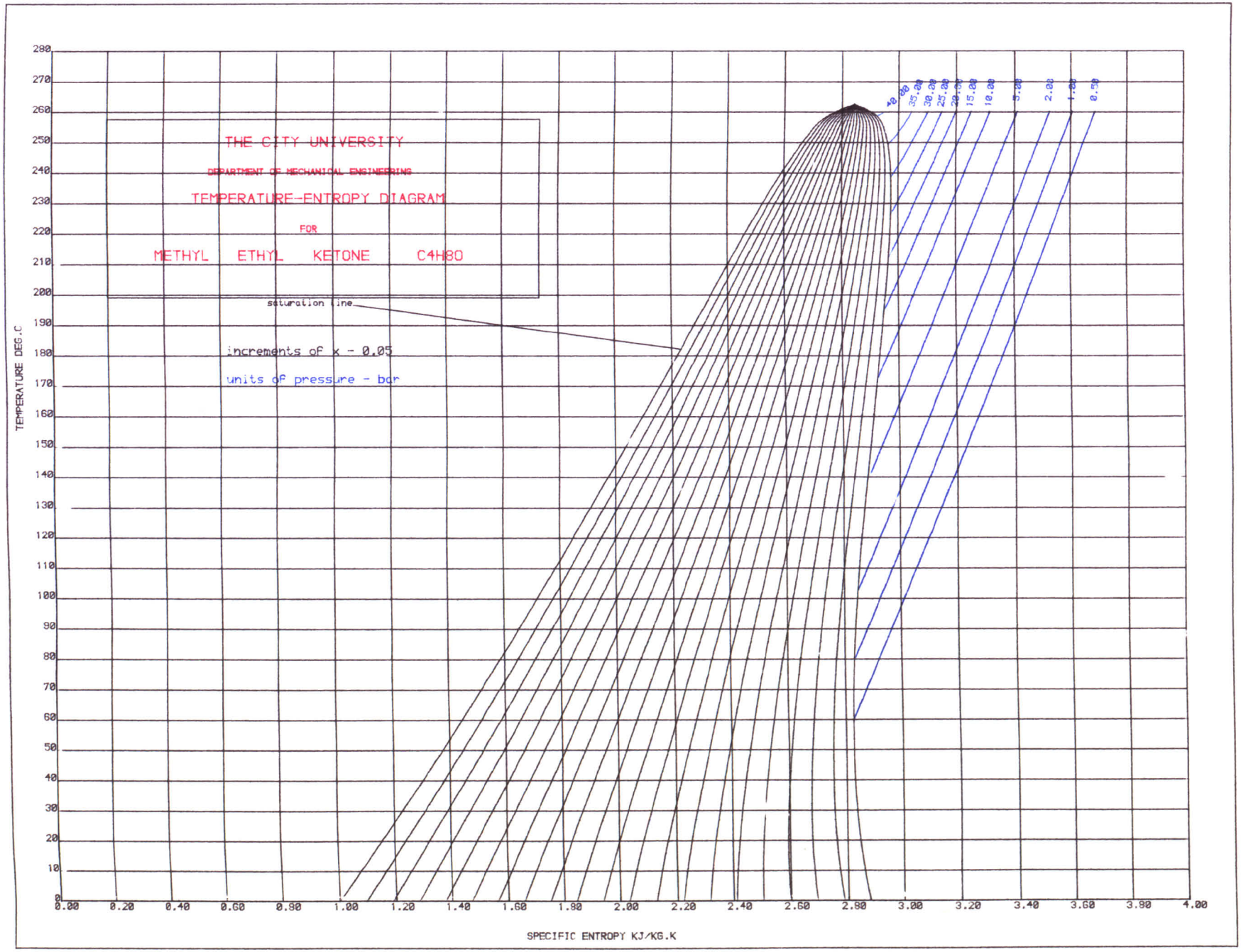
THE CITY UNIVERSITY
DEPARTMENT OF MECHANICAL ENGINEERING
TEMPERATURE-ENTROPY DIAGRAM
FOR
METHYL ETHYL KETONE C4H8O
saturation line
increments of x - 0.05
units of pressure - bar
TEMPERATURE DEG.C
SPECIFIC ENTROPY KJ/KG.K

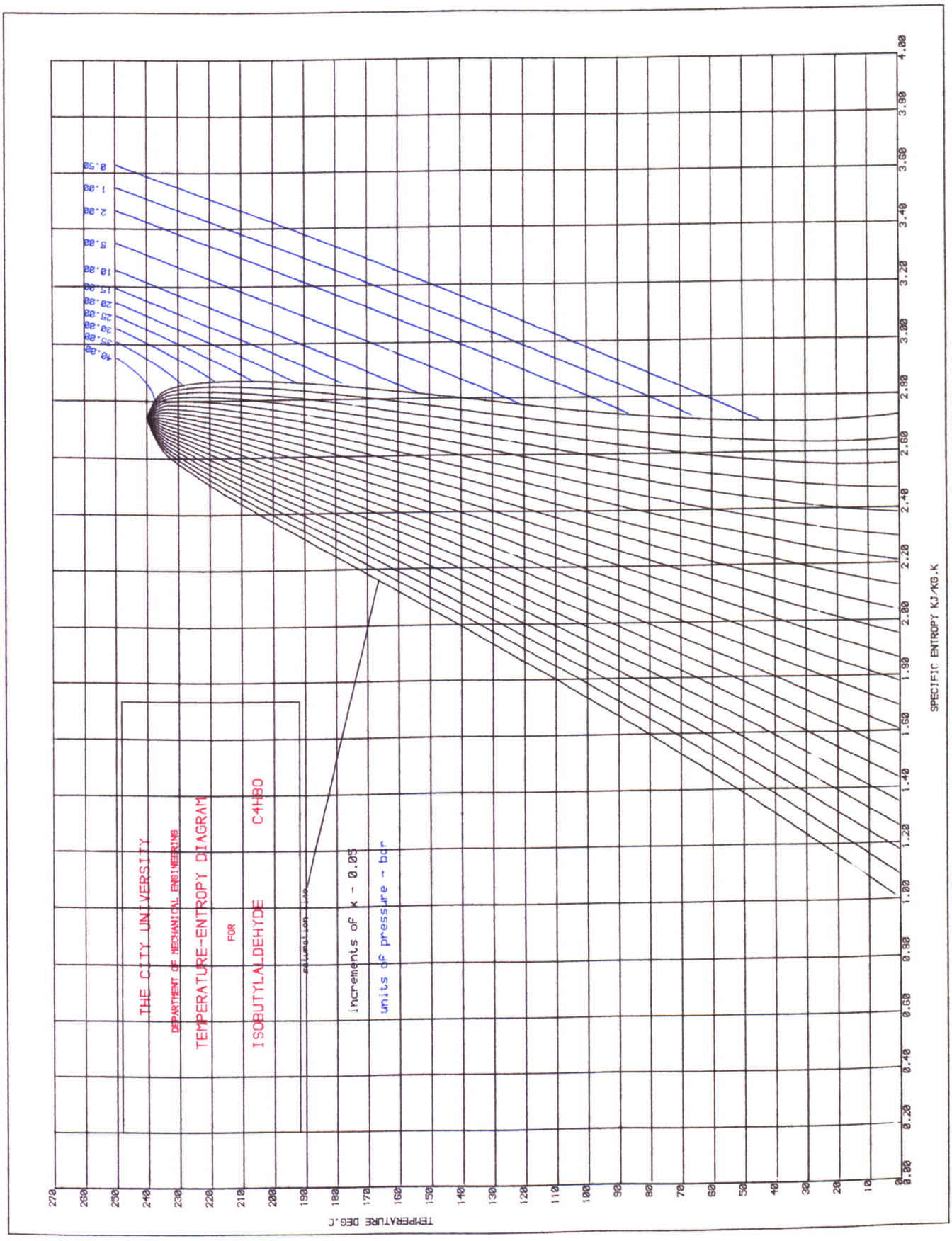
THE CITY UNIVERSITY
DEPARTMENT OF MECHANICAL ENGINEERING
TEMPERATURE-ENTROPY DIAGRAM
FOR
ISOBUTYLALDEHYDE C4H8O
saturation line
increments of K - 0.05
units of pressure - bar
8.50
1.00
2.00
5.00
10.00
15.00
20.00
25.00
30.00
35.00
40.00
TEMPERATURE DEG.C
SPECIFIC ENTROPY KJ/KG.K

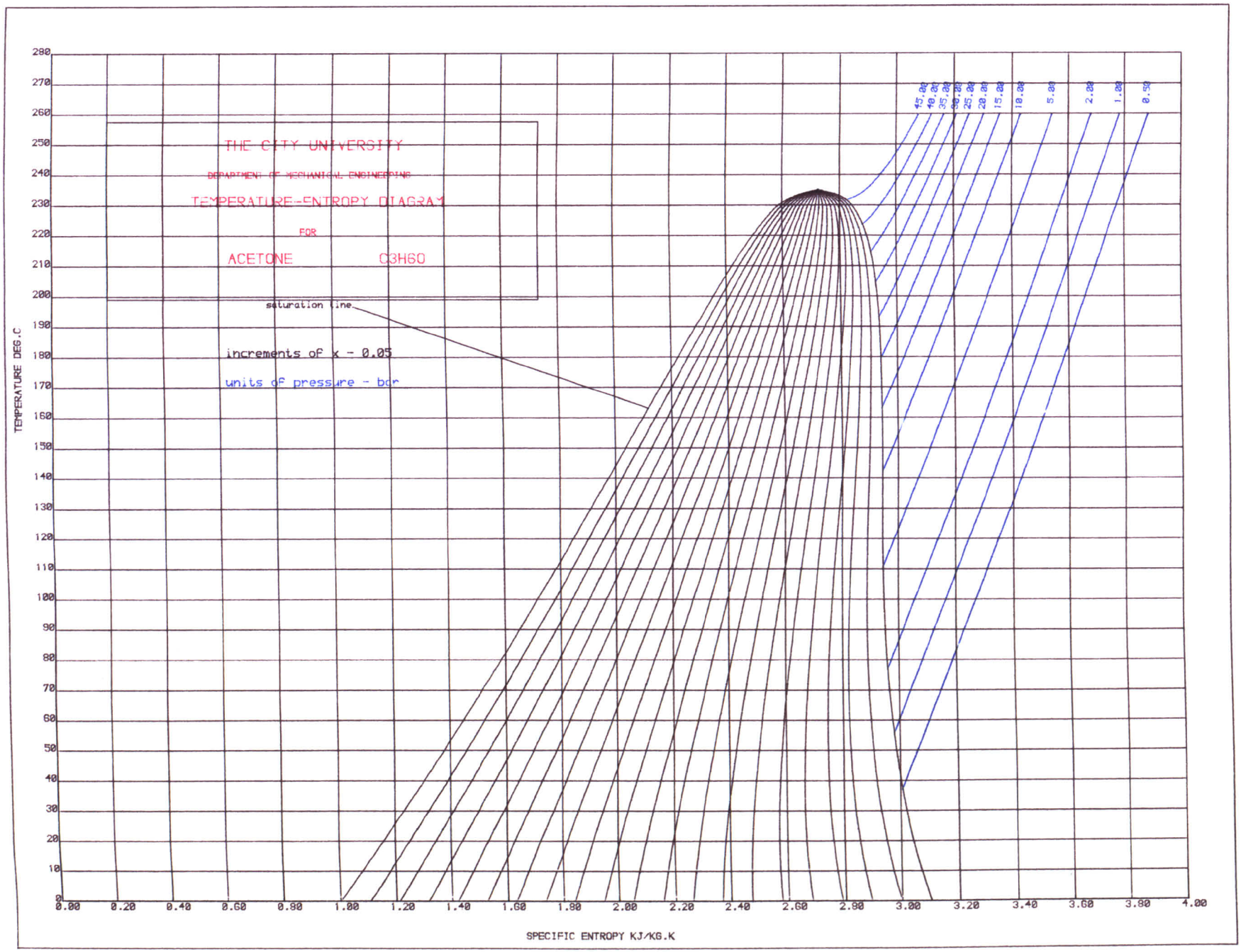
THE CITY UNIVERSITY
DEPARTMENT OF MECHANICAL ENGINEERING
TEMPERATURE-ENTROPY DIAGRAM
FOR
ACETONE C3H6O
saturation line
increments of x - 0.05
units of pressure - bar
TEMPERATURE DEG.C
SPECIFIC ENTROPY KJ/KG.K
45.0a
40.0a
35.0a
30.0a
25.0a
20.0a
15.0a
10.0a
5.0a
2.0a
1.0a
0.5a

T-s diagrams of methyl ethyl ketone (C_4H_8O) isobutylaldehyde (C_4H_8O) and acetone (C_3H_6O) are shown. None of them present the drying out characteristics required. Furthermore, aldehydes and ketones are thermally unstable.

Amine group

Amines may be regarded as derivatives of ammonia in which one or more of the hydrogen atoms in the ammonia molecule have been replaced by an alkyl or aryl group.

Functional group	Aliphatic amine	Class	Hydrogen atoms replaced
$-NH_2$	RNH_2	primary	1
NH	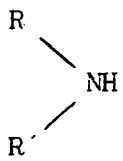	secondary	2
$-N$	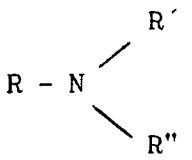	tertiary	3

CH_3NH_2 methylamine

$(C_2H_5)_2NH$ diethylamine

$(CH_3)_3N$ trimethylamine.

They are slightly polar fluids. Amines are also:

i) thermally stable

ii) readily available

iii) lower alkylamines are gases with ammoniacal "fishy" odour

iv) dissolve in organic solvents and are very soluble in water

v) aliphatic amines are flammable.

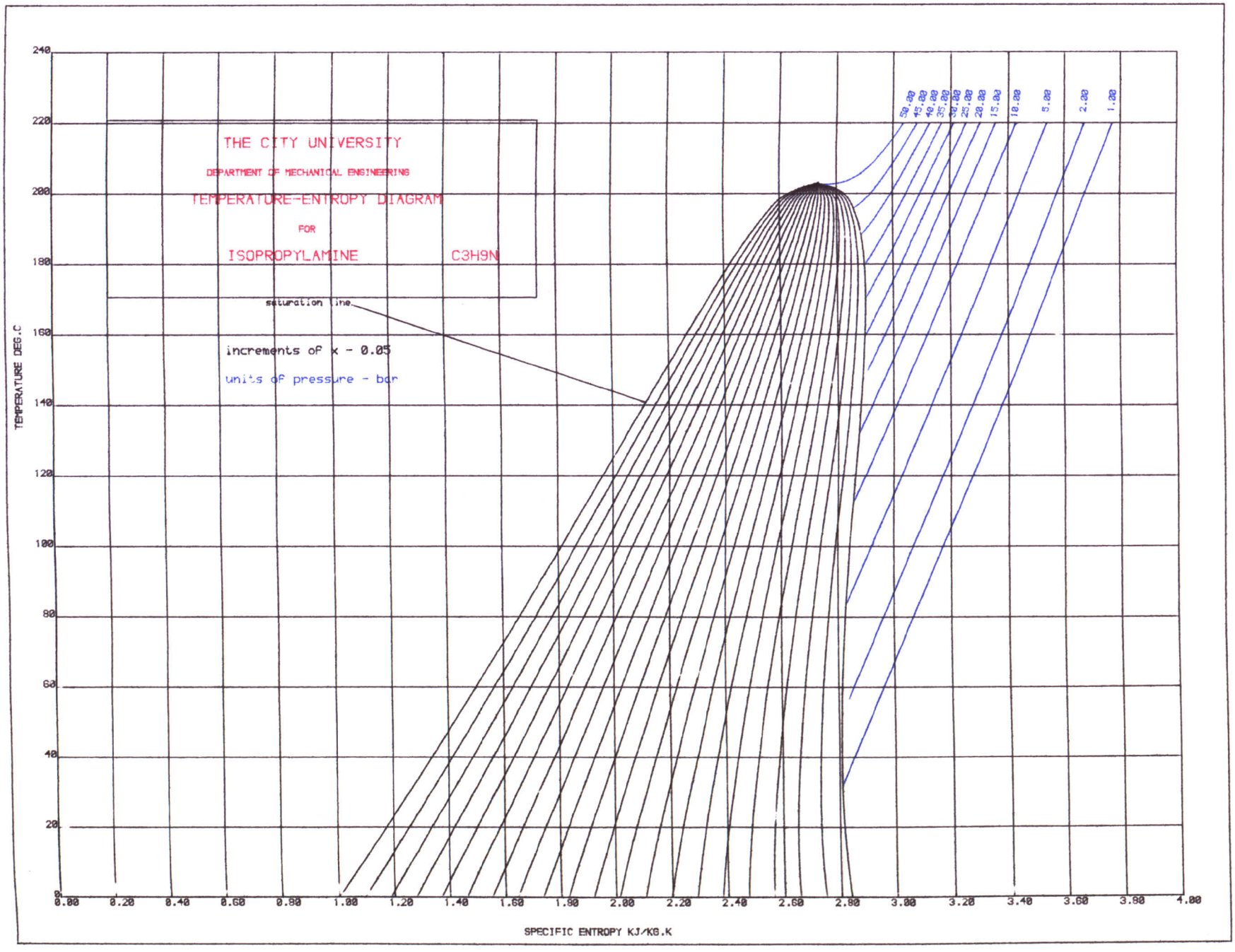
THE CITY UNIVERSITY
DEPARTMENT OF MECHANICAL ENGINEERING
TEMPERATURE-ENTROPY DIAGRAM
FOR
ISOPROPYLAMINE C3H9N
saturation line
increments of x - 0.05
units of pressure - bar
50.00
45.00
40.00
35.00
30.00
25.00
20.00
15.00
10.00
5.00
2.00
1.00
TEMPERATURE DEG.C
SPECIFIC ENTROPY KJ/KG.K

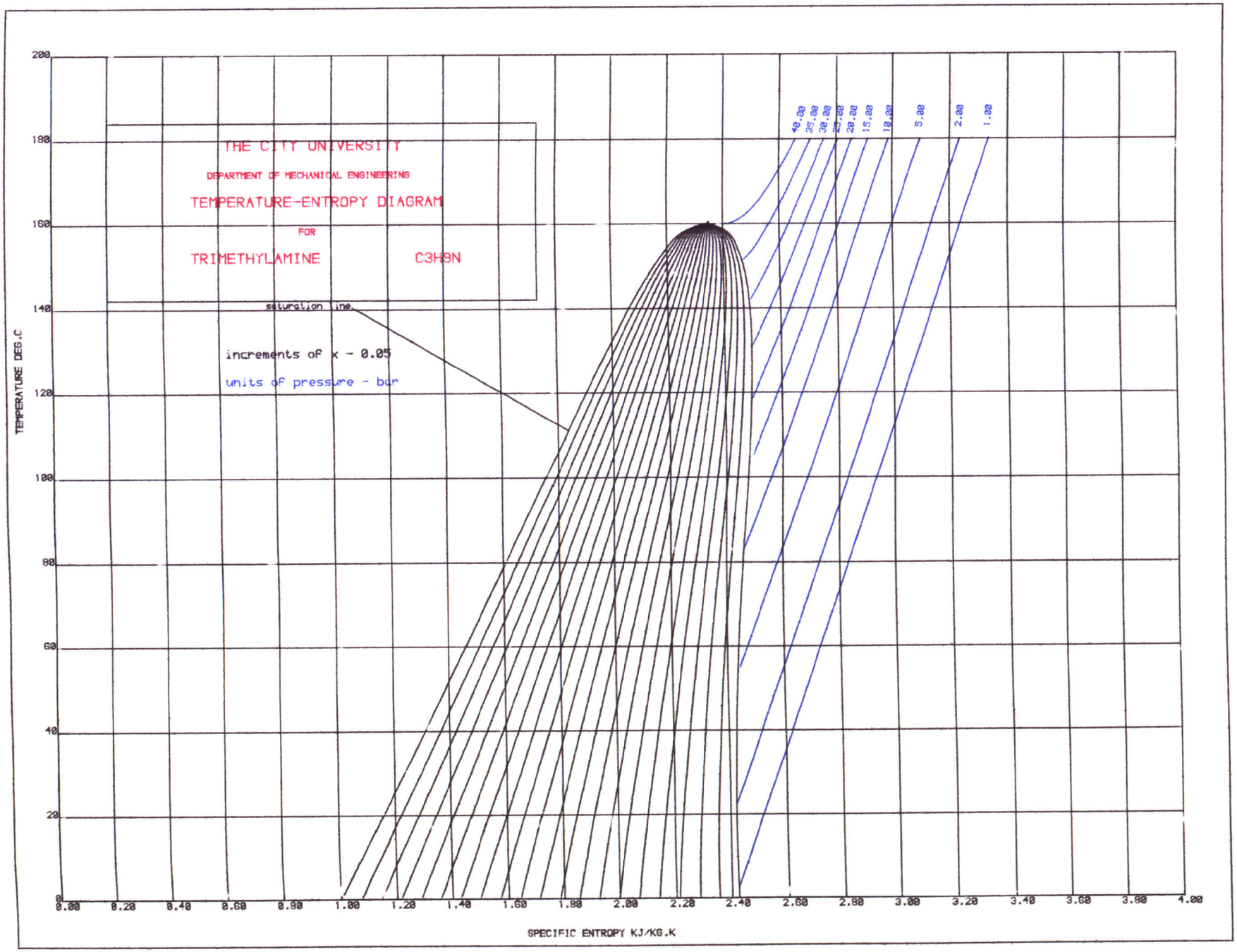
THE CITY UNIVERSITY
DEPARTMENT OF MECHANICAL ENGINEERING
TEMPERATURE-ENTROPY DIAGRAM
FOR
TRIMETHYLAMINE C3H9N
saturation line
increments of x - 0.05
units of pressure - bar
40.00
35.00
30.00
25.00
20.00
15.00
10.00
5.00
2.00
1.00
TEMPERATURE DEG.C
SPECIFIC ENTROPY KJ/KG.K

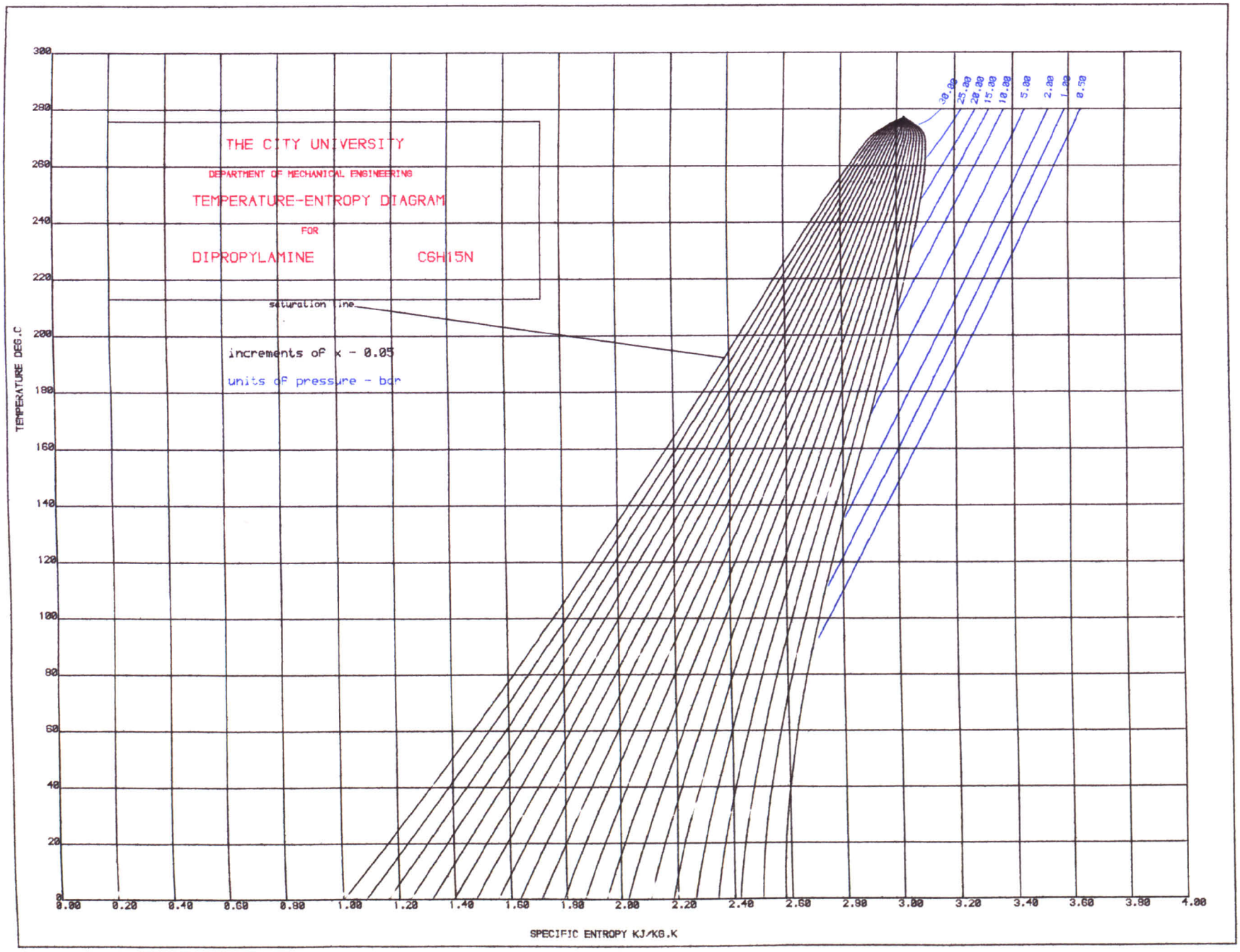
THE CITY UNIVERSITY
DEPARTMENT OF MECHANICAL ENGINEERING
TEMPERATURE-ENTROPY DIAGRAM
FOR
DIPROPYLAMINE
C6H15N
saturation line
increments of x - 0.05
units of pressure - bar
30.00
25.00
20.00
15.00
10.00
5.00
2.00
1.00
0.50
TEMPERATURE DEG.C
SPECIFIC ENTROPY KJ/KG.K
0
20
40
60
80
100
120
140
160
180
200
220
240
260
280
300
0.00
0.20
0.40
0.60
0.80
1.00
1.20
1.40
1.60
1.80
2.00
2.20
2.40
2.60
2.80
3.00
3.20
3.40
3.60
3.80
4.00

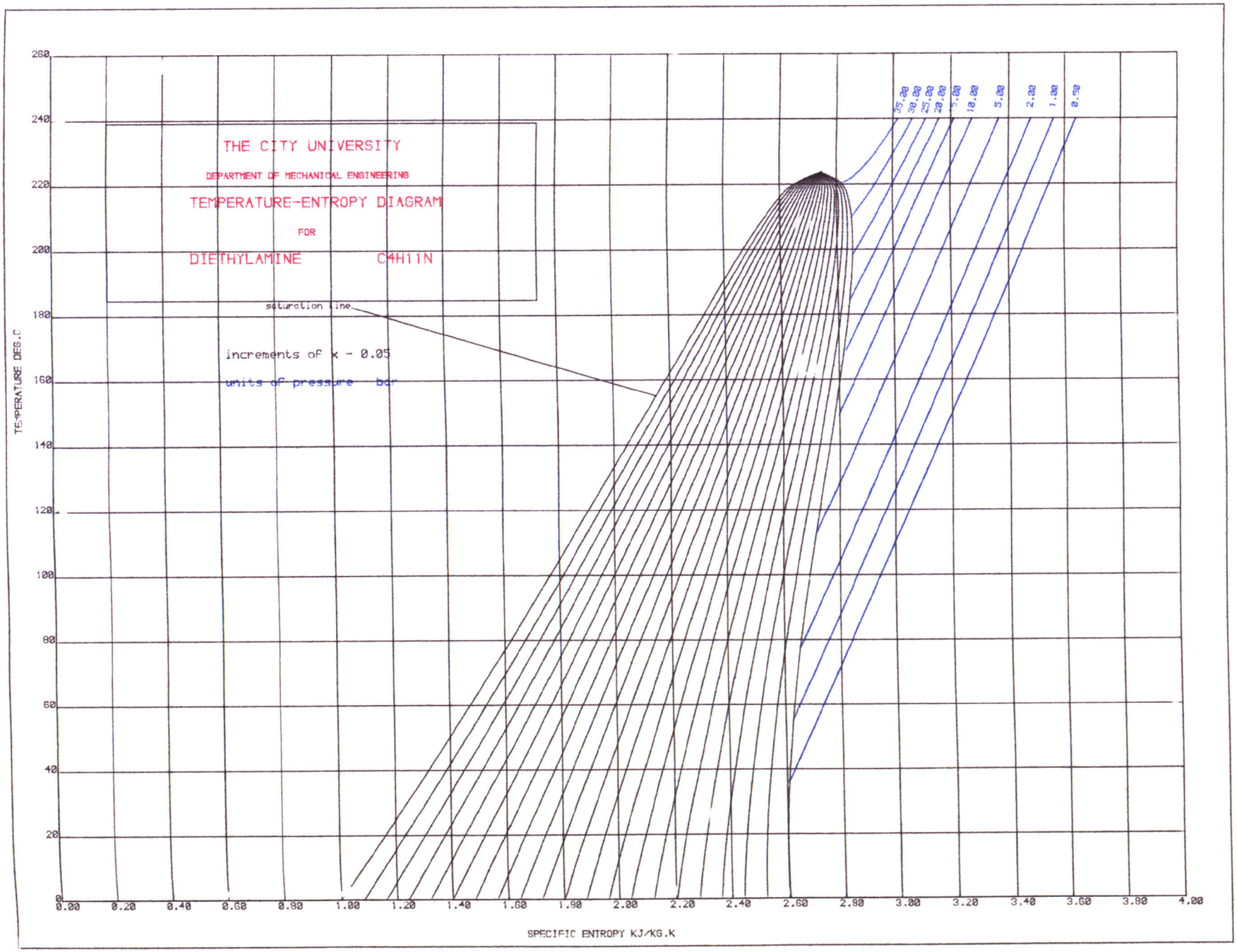
THE CITY UNIVERSITY
DEPARTMENT OF MECHANICAL ENGINEERING
TEMPERATURE-ENTROPY DIAGRAM
FOR
DIETHYLAMINE C4H11N
saturation line
increments of x - 0.05
units of pressure bar
35.00
30.00
25.00
20.00
15.00
10.00
5.00
2.00
1.00
0.50
TEMPERATURE DEG.C
SPECIFIC ENTROPY KJ/KG.K

T-s diagrams of isopropylamine (C_3H_9N), trimethylamine (C_3H_9N), dipropylamine ($C_6H_{15}N$) and diethylamine ($C_4H_{11}N$) are presented in the following pages. None of them can be considered as a good candidate. Trimethylamine although possessing a high critical pressure at lower temperature has an isentropic saturated vapour line which makes it unsuitable as a potential candidate.

Alkane, alkene and alkyne groups

The alkanes are the simplest of all organic compounds. They are saturated hydrocarbons, that is, contain only carbon-carbon and carbon-hydrogen single bonds. The general formula of the alkanes is C_nH_{2n+2}. Methane (b.p. -162°C), ethane (b.p. -89°C), propane (b.p. -42°C) and butane (b.p. -0.5°C) are colourless, odourless gases at room temperature. The boiling points of the unbranched chain alkanes increase steadily throughout the homologous series. The alkanes from pentane (b.p. 36°C) are colourless liquids at ordinary temperatures, while higher homologues are waxy solids. Other physical properties of the alkanes (such as viscosity) also vary uniformly with molecular mass. This family of hydrocarbons are important raw materials for the large-scale preparation of both aliphatic and aromatic compounds.

Alkanes are particularly attractive fluids. They have low molecular weight and therefore high sonic velocity. They are readily available and cheap. Higher alkanes from pentane upwards possess a strong rightward slope. Several n-alkanes were considered. It is interesting to observe that the slope of the saturation vapour curve

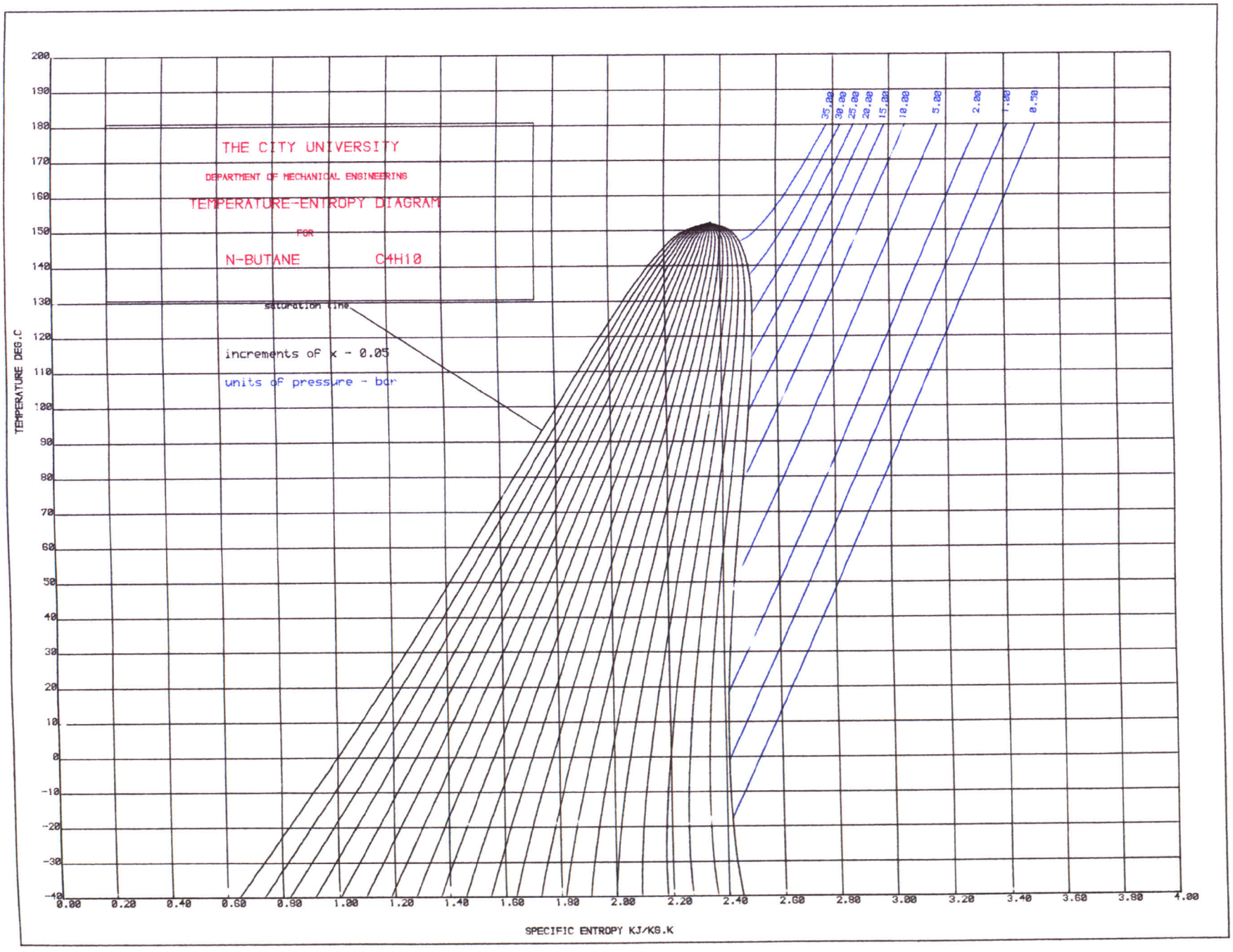
THE CITY UNIVERSITY
DEPARTMENT OF MECHANICAL ENGINEERING
TEMPERATURE-ENTROPY DIAGRAM
FOR
N-BUTANE C4H10
saturation line
increments of x - 0.05
units of pressure - bar
35.00
30.00
25.00
20.00
15.00
10.00
5.00
2.00
1.00
0.50
TEMPERATURE DEG.C
200
190
180
170
160
150
140
130
120
110
100
90
80
70
60
50
40
30
20
10
0
-10
-20
-30
-40
0.00
0.20
0.40
0.60
0.80
1.00
1.20
1.40
1.60
1.80
2.00
2.20
2.40
2.60
2.80
3.00
3.20
3.40
3.60
3.80
4.00
SPECIFIC ENTROPY KJ/KG.K

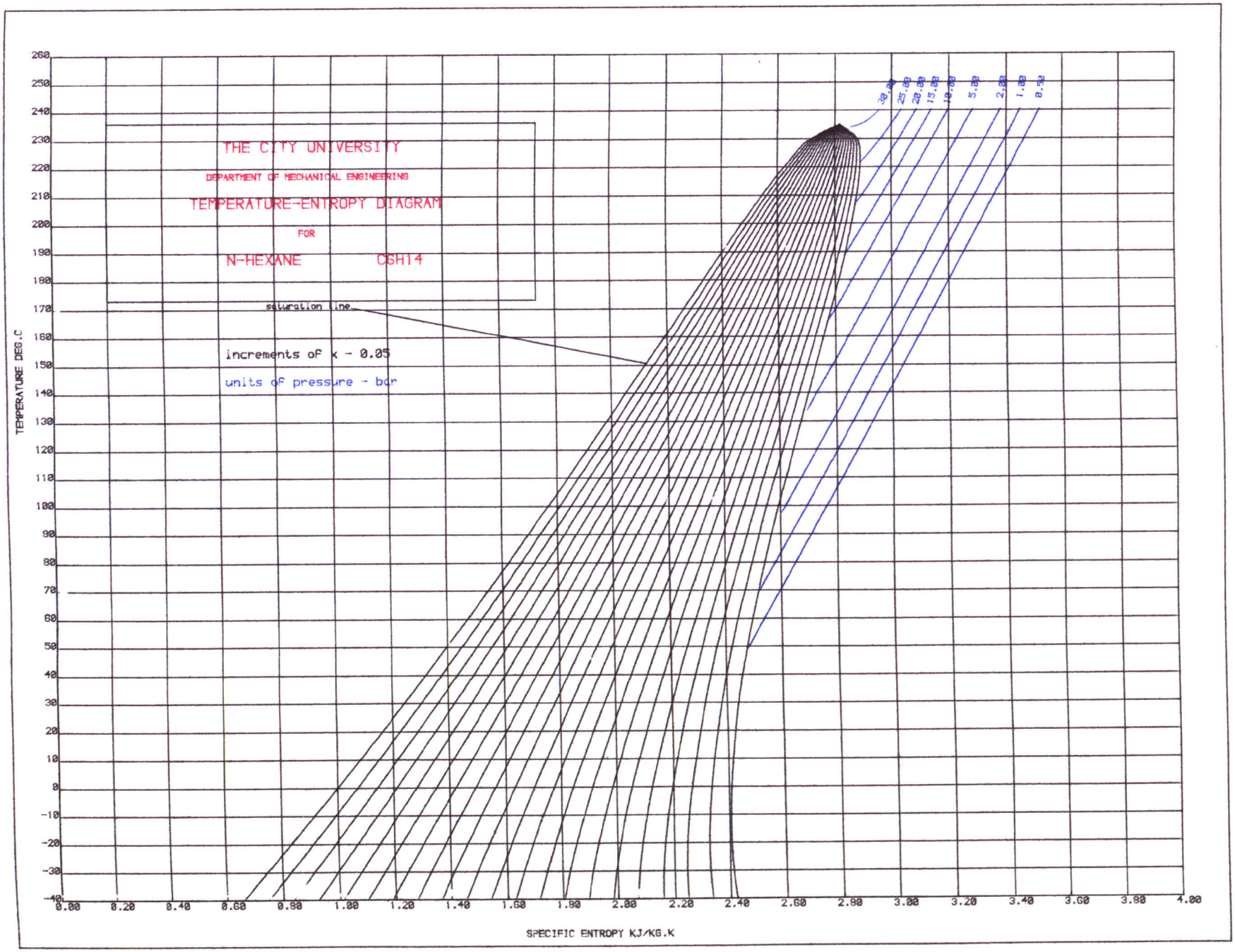
THE CITY UNIVERSITY
DEPARTMENT OF MECHANICAL ENGINEERING
TEMPERATURE-ENTROPY DIAGRAM
FOR
N-HEXANE C6H14
saturation line
increments of x - 0.05
units of pressure - bar
30.0
25.0
20.0
15.0
10.0
5.0
2.0
1.0
0.5
TEMPERATURE DEG.C
SPECIFIC ENTROPY KJ/KG.K

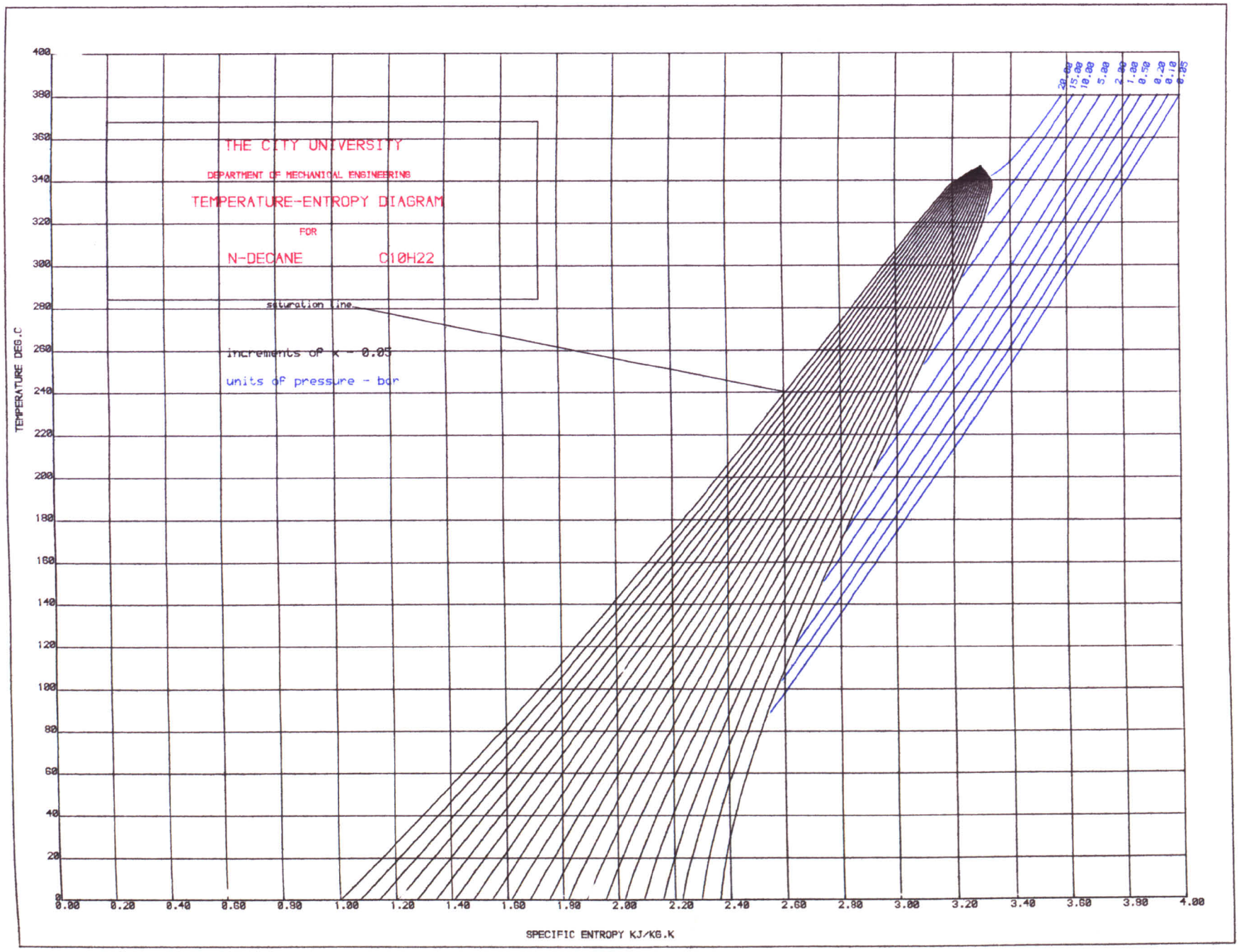
THE CITY UNIVERSITY
DEPARTMENT OF MECHANICAL ENGINEERING
TEMPERATURE-ENTROPY DIAGRAM
FOR
N-DECANE C10H22
saturation line
increments of x - 0.05
units of pressure - bar
20.00
15.00
10.00
5.00
2.00
1.00
0.50
0.20
0.10
0.05
TEMPERATURE DEG.C
SPECIFIC ENTROPY KJ/KG.K

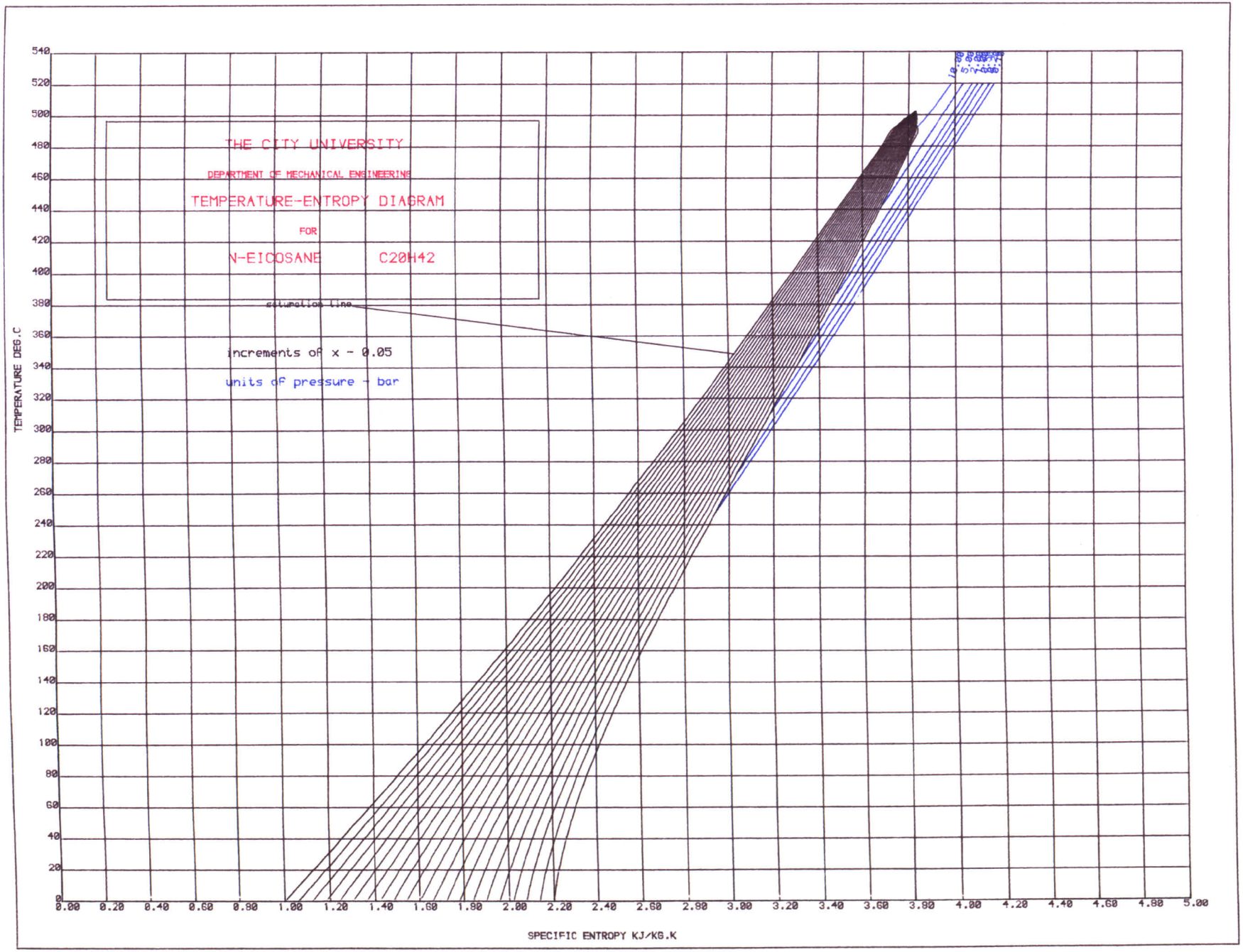
THE CITY UNIVERSITY
DEPARTMENT OF MECHANICAL ENGINEERING
TEMPERATURE-ENTROPY DIAGRAM
FOR
N-EICOSANE C20H42
saturation line
increments of x - 0.05
units of pressure - bar
TEMPERATURE DEG.C
SPECIFIC ENTROPY KJ/KG.K
0 20 40 60 80 100 120 140 160 180 200 220 240 260 280 300 320 340 360 380 400 420 440 460 480 500 520 540
0.00 0.20 0.40 0.60 0.80 1.00 1.20 1.40 1.60 1.80 2.00 2.20 2.40 2.60 2.80 3.00 3.20 3.40 3.60 3.80 4.00 4.20 4.40 4.60 4.80 5.00

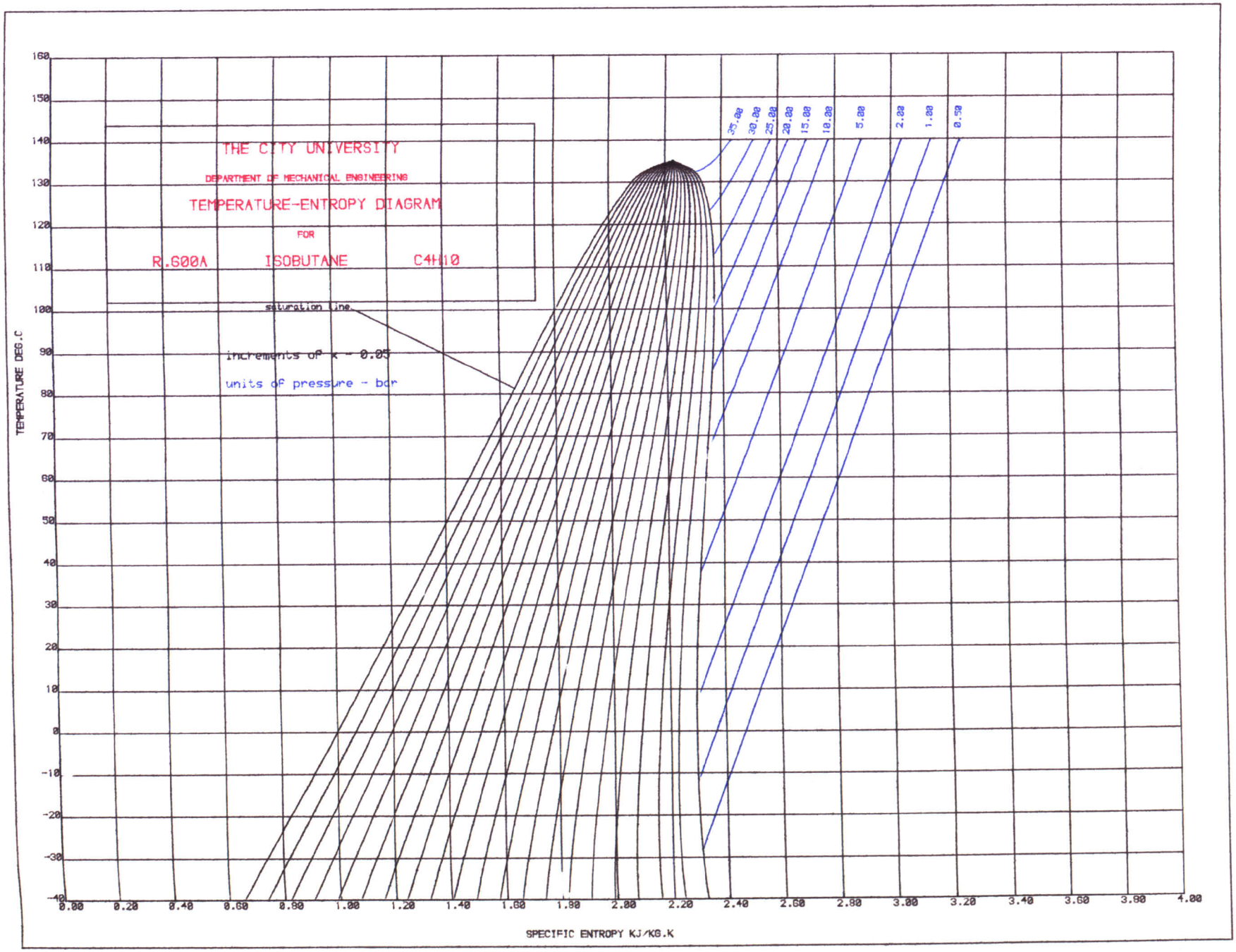
THE CITY UNIVERSITY
DEPARTMENT OF MECHANICAL ENGINEERING
TEMPERATURE-ENTROPY DIAGRAM
FOR
R.600A ISOBUTANE C4H10
saturation line
increments of x - 0.05
units of pressure - bar
35.00
30.00
25.00
20.00
15.00
10.00
5.00
2.00
1.00
0.50
TEMPERATURE DEG.C
SPECIFIC ENTROPY KJ/KG.K

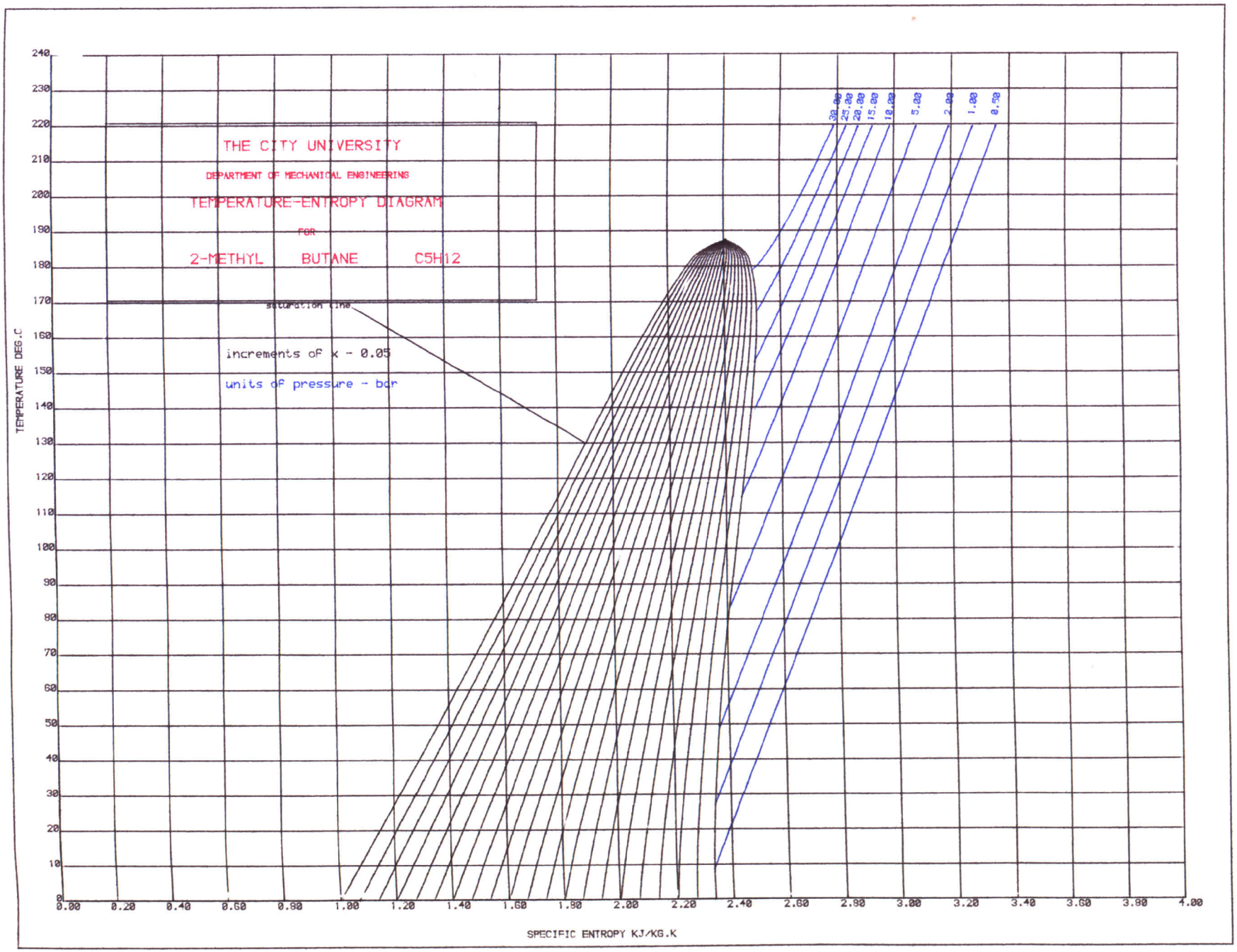
THE CITY UNIVERSITY
DEPARTMENT OF MECHANICAL ENGINEERING
TEMPERATURE-ENTROPY DIAGRAM
FOR
2-METHYL BUTANE C5H12
saturation line
increments of x - 0.05
units of pressure - bar
30.00
25.00
20.00
15.00
10.00
5.00
2.00
1.00
0.50
TEMPERATURE DEG.C
SPECIFIC ENTROPY KJ/KG.K

does become very positive with increasing number of atoms in a molecule. This is illustrated by the T-s diagrams for n-butane, n-hexane, n-decane and n-eicosane. However, none of them present desirable drying out characteristics over the required temperature range. The author then turned to examine their isomers bearing in mind that the number of atoms per molecule should not exceed 20. This figure was deduced on entirely empirical grounds. Molecules containing more than 20 atoms normally yield "too high" critical temperatures (over 250°C). As a consequence if the expansion process starts, say, at 150°C, the fluid does not dry out. Isobutane (2-methyl-propane C_4H_{10}), isopentane (2-methyl-butane C_5H_{12}) and neopentane (2-2-dimethyl-propane) were investigated. Neopentane was found to be the most suitable candidate as we shall see in the next section.

Alkenes and alkynes were also considered. Alkenes are unsaturated compounds and contain one or more carbon-carbon double bonds. Alkynes are highly unsaturated and contain a carbon-carbon triple bond. Alkenes and alkynes tend to follow the saturation line pattern of homologous alkanes. However, due to their double and triple bonds these fluids start to decompose near the critical region. Therefore these two families of hydrocarbons were discarded. As an illustration T-s diagrams of 1-butyne, 1-pentyne, 3-methyl-1-butene, 1-butene and 1-pentene are displayed.

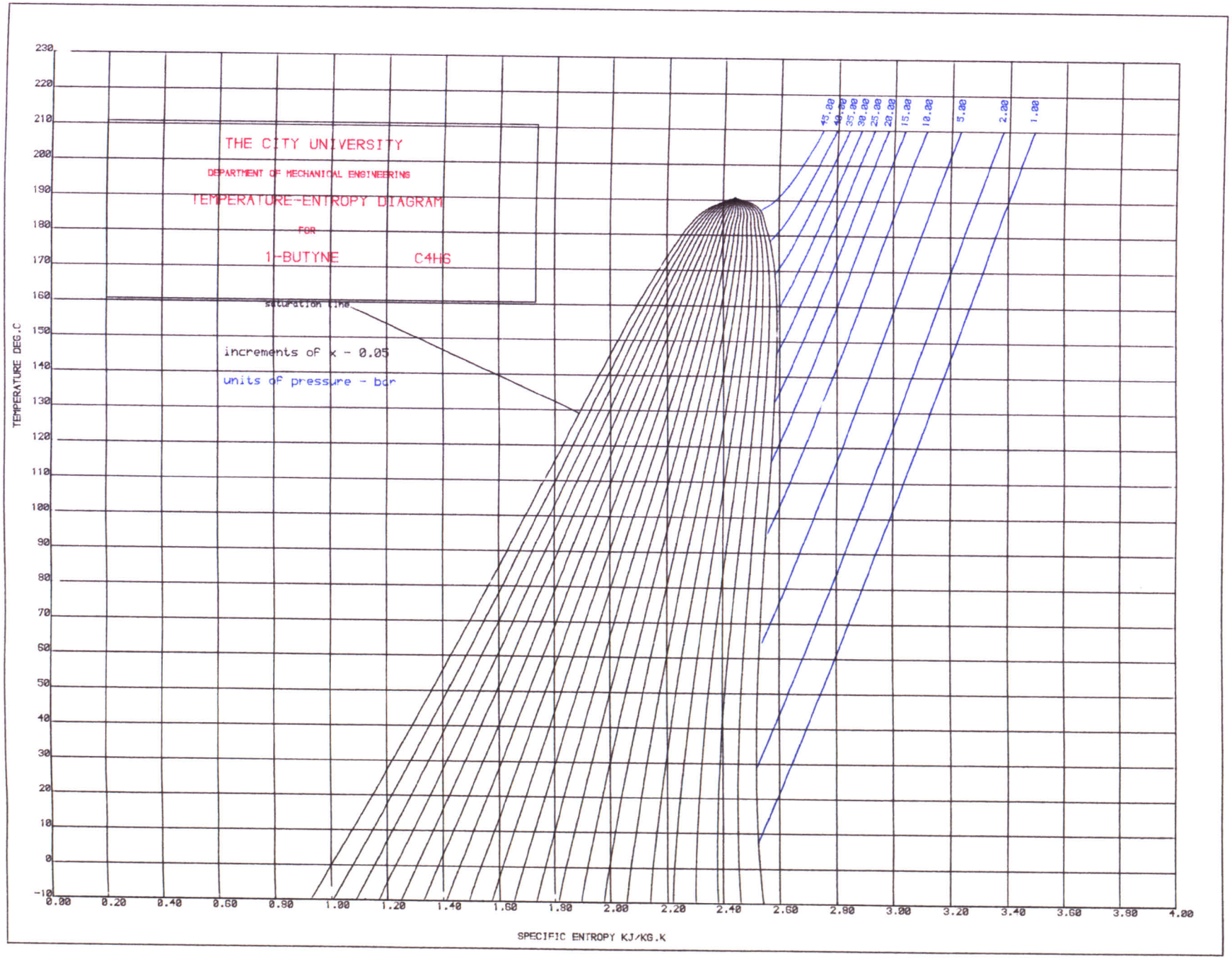
THE CITY UNIVERSITY
DEPARTMENT OF MECHANICAL ENGINEERING
TEMPERATURE-ENTROPY DIAGRAM
FOR
1-BUTYNE C4H6
saturation line
increments of x - 0.05
units of pressure - bar
45.00
40.00
35.00
30.00
25.00
20.00
15.00
10.00
5.00
2.00
1.00
TEMPERATURE DEG.C
230
220
210
200
190
180
170
160
150
140
130
120
110
100
90
80
70
60
50
40
30
20
10
0
-10
0.00
0.20
0.40
0.60
0.80
1.00
1.20
1.40
1.60
1.80
2.00
2.20
2.40
2.60
2.80
3.00
3.20
3.40
3.60
3.80
4.00
SPECIFIC ENTROPY KJ/KG.K

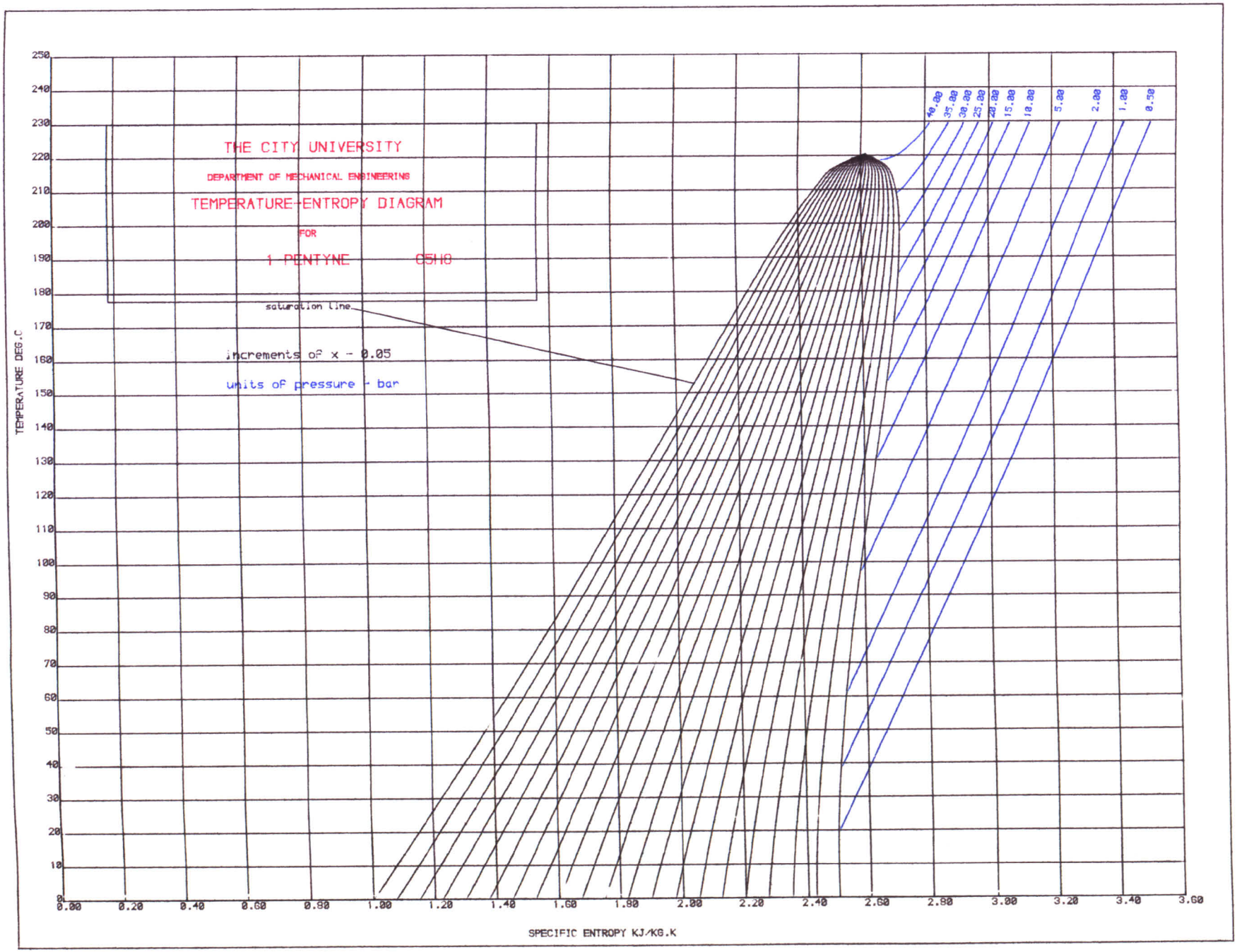
THE CITY UNIVERSITY
DEPARTMENT OF MECHANICAL ENGINEERING
TEMPERATURE-ENTROPY DIAGRAM
FOR
1-PENTYNE C5H8
saturation line
increments of x - 0.05
units of pressure - bar
TEMPERATURE DEG.C
SPECIFIC ENTROPY KJ/KG.K
40.00
35.00
30.00
25.00
20.00
15.00
10.00
5.00
2.00
1.00
0.50

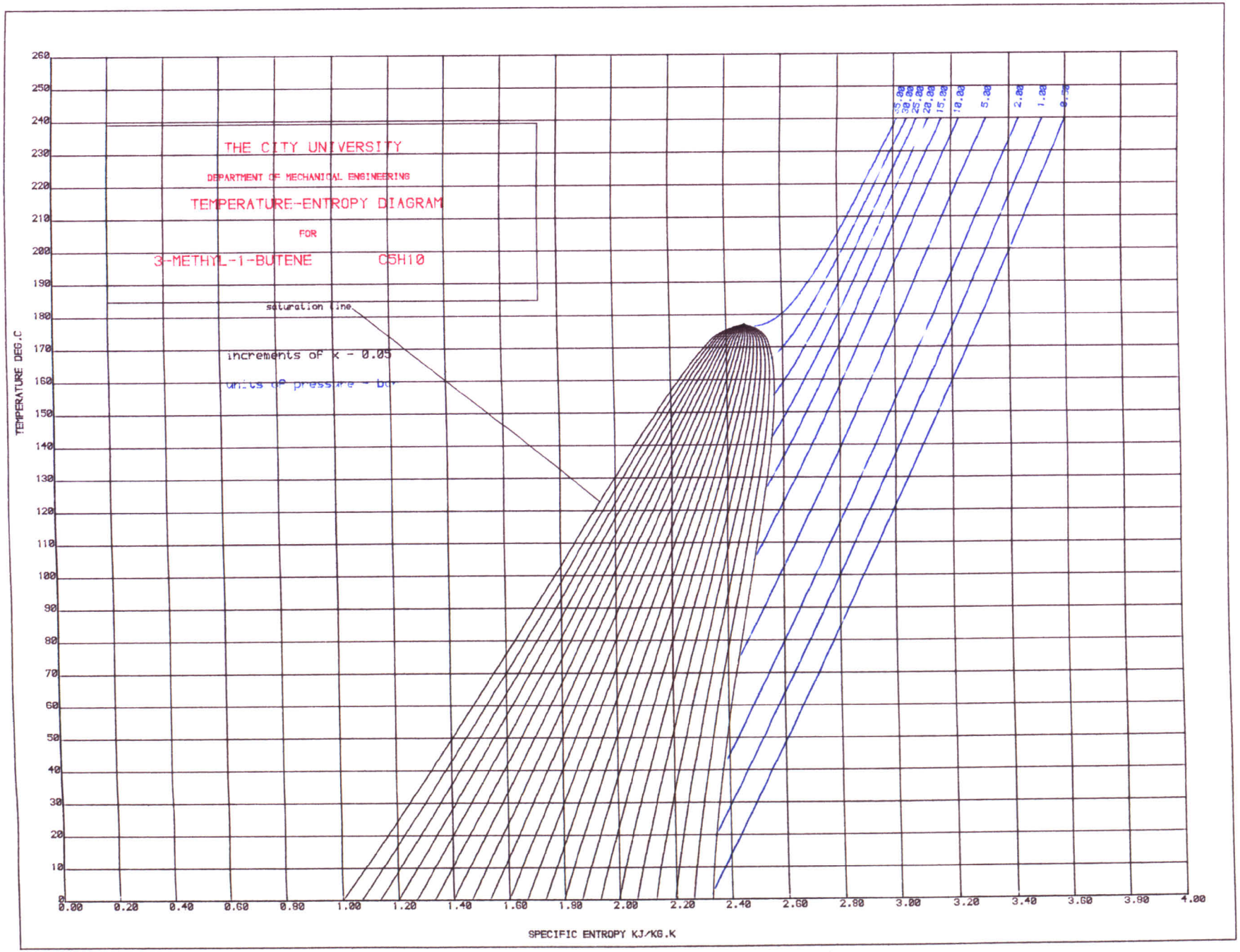
THE CITY UNIVERSITY
DEPARTMENT OF MECHANICAL ENGINEERING
TEMPERATURE-ENTROPY DIAGRAM
FOR
3-METHYL-1-BUTENE C5H10
saturation line
increments of x - 0.05
units of pressure - bar
35.0a
30.0a
25.0a
20.0a
15.0a
10.0a
5.0a
2.0a
1.0a
0.5a
TEMPERATURE DEG.C
SPECIFIC ENTROPY KJ/KG.K
260
250
240
230
220
210
200
190
180
170
160
150
140
130
120
110
100
90
80
70
60
50
40
30
20
10
0
0.00
0.20
0.40
0.60
0.80
1.00
1.20
1.40
1.60
1.80
2.00
2.20
2.40
2.60
2.80
3.00
3.20
3.40
3.60
3.80
4.00

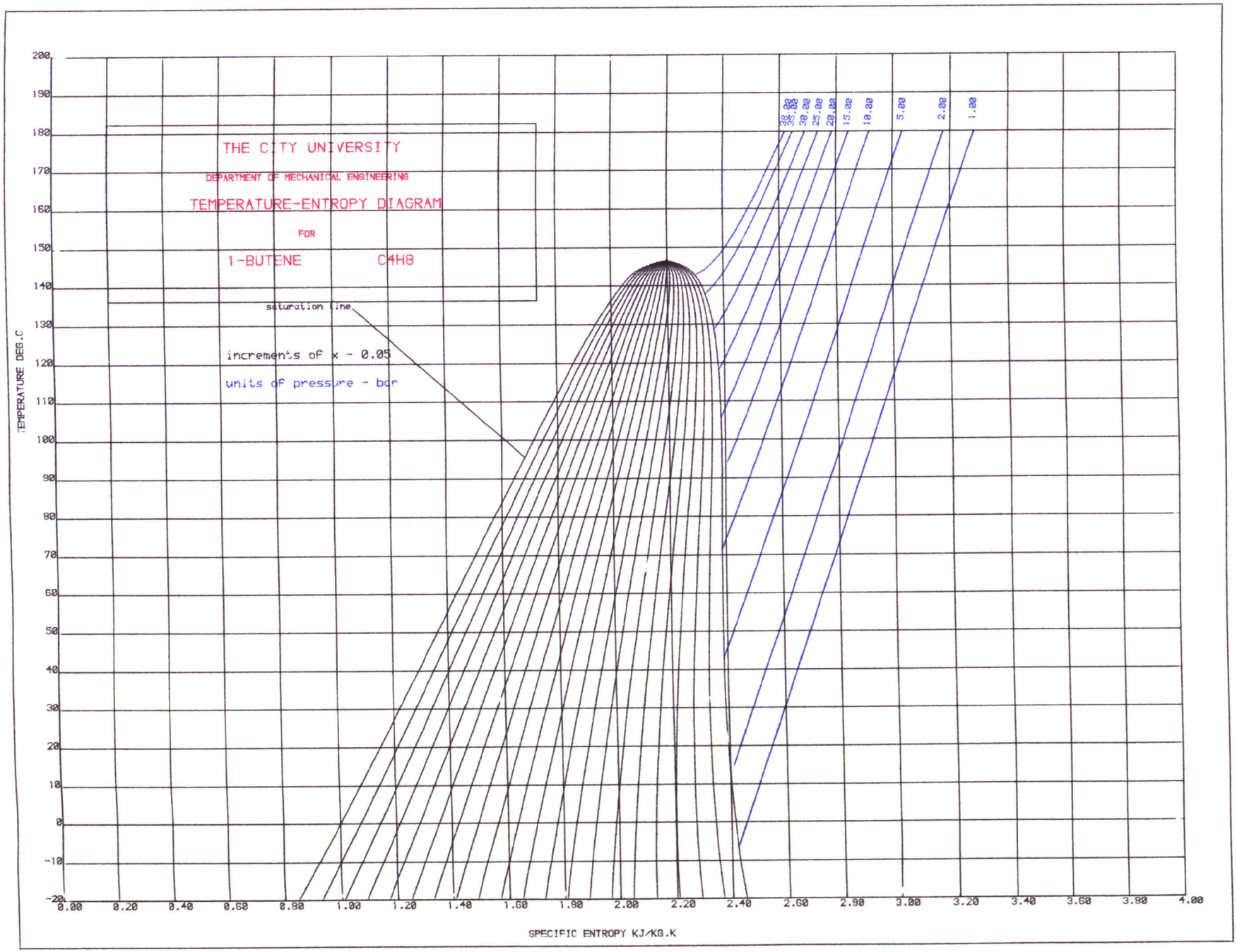
THE CITY UNIVERSITY
DEPARTMENT OF MECHANICAL ENGINEERING
TEMPERATURE-ENTROPY DIAGRAM
FOR
1-BUTENE C4H8
saturation line
increments of x - 0.05
units of pressure - bar
TEMPERATURE DEG.C
SPECIFIC ENTROPY KJ/KG.K
200
190
180
170
160
150
140
130
120
110
100
90
80
70
60
50
40
30
20
10
0
-10
-20
0.00
0.20
0.40
0.60
0.80
1.00
1.20
1.40
1.60
1.80
2.00
2.20
2.40
2.60
2.80
3.00
3.20
3.40
3.60
3.80
4.00
35.00
30.00
25.00
20.00
15.00
10.00
5.00
2.00
1.00

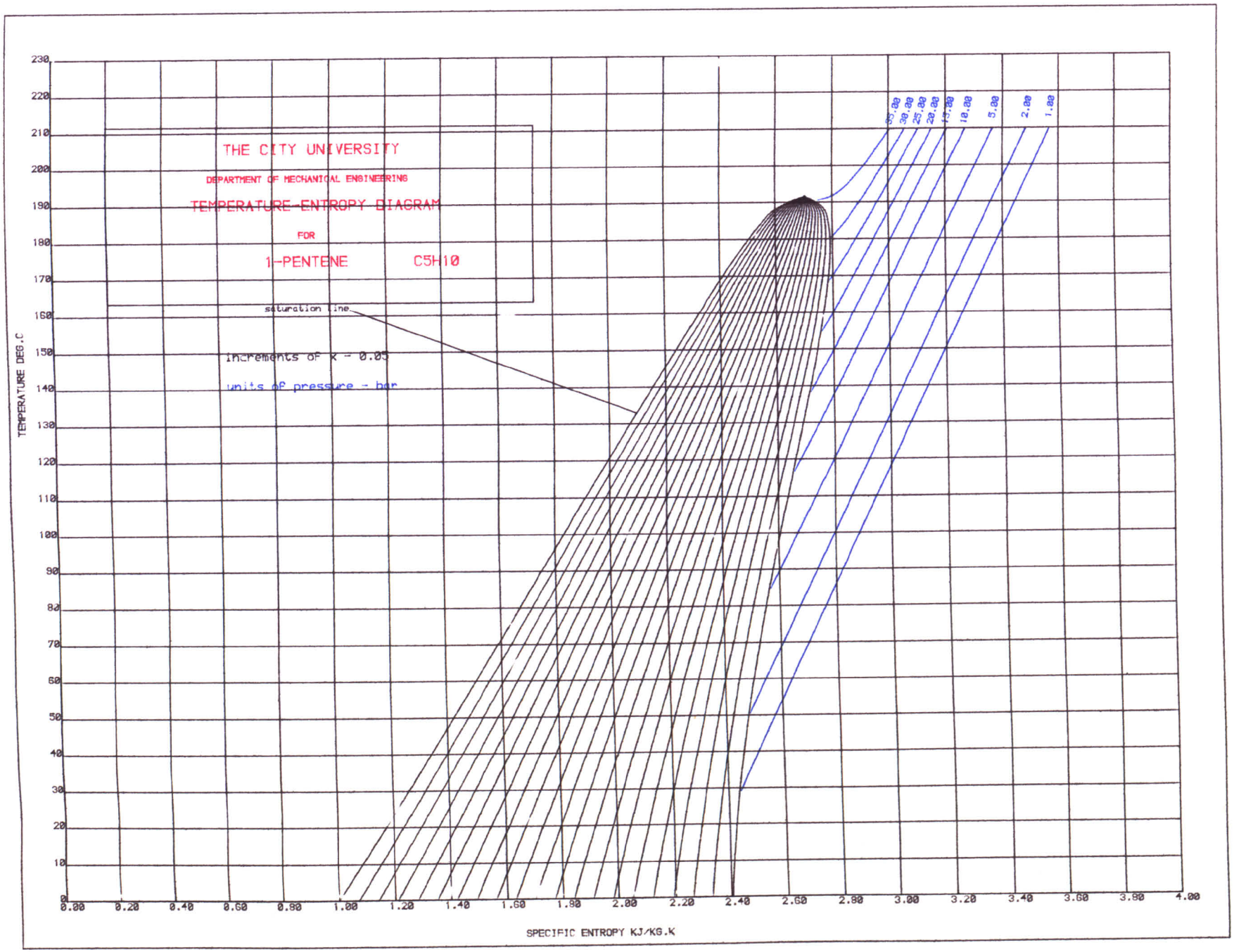
THE CITY UNIVERSITY
DEPARTMENT OF MECHANICAL ENGINEERING
TEMPERATURE-ENTROPY DIAGRAM
FOR
1-PENTENE C5H10
saturation line
increments of x = 0.05
units of pressure - bar
35.00
30.00
25.00
20.00
15.00
10.00
5.00
2.00
1.00
TEMPERATURE DEG.C
SPECIFIC ENTROPY KJ/KG.K

7.3. THE ORGANIC WORKING FLUID BINARY MIXTURE

The study of many organic compounds led the author to choose neopentane (2-2-dimethyl propane) and n-pentane as the most suitable fluids to form the working fluid mixture. Neopentane appeared to fulfil most of the desirable characteristics better than any other fluid. The results of a program written to evaluate drying out characteristics of fluids are displayed in Tables 7.1 and 7.2. A listing of the program is given in Appendix B.

As can be seen from Table 7.1, 2-2-dimethyl propane after isentropic expansion comes nearly dry at temperatures of 150°C. Another important feature is a high back pressure obtained at a condensing temperature of 30°C at approximately 2 bar. Also low volume ratios (VOLR) may be noted for this fluid; these will keep the expander very compact.

In Table 7.2, n-pentane is examined. For this fluid desirable drying out characteristics are obtained at higher temperatures as expected. A combination of both fluids seems to be the best possible choice for an application where the geothermal fluid is at a temperature of around 180 - 190°C. Another advantage of such a mixture is related to the fact that neopentane is an isomer of n-pentane, the two fluids should mix in all proportions to yield a homogeneous mixture. This was a particular concern at the beginning of the project since the use of binary mixtures may involve partial solubility.

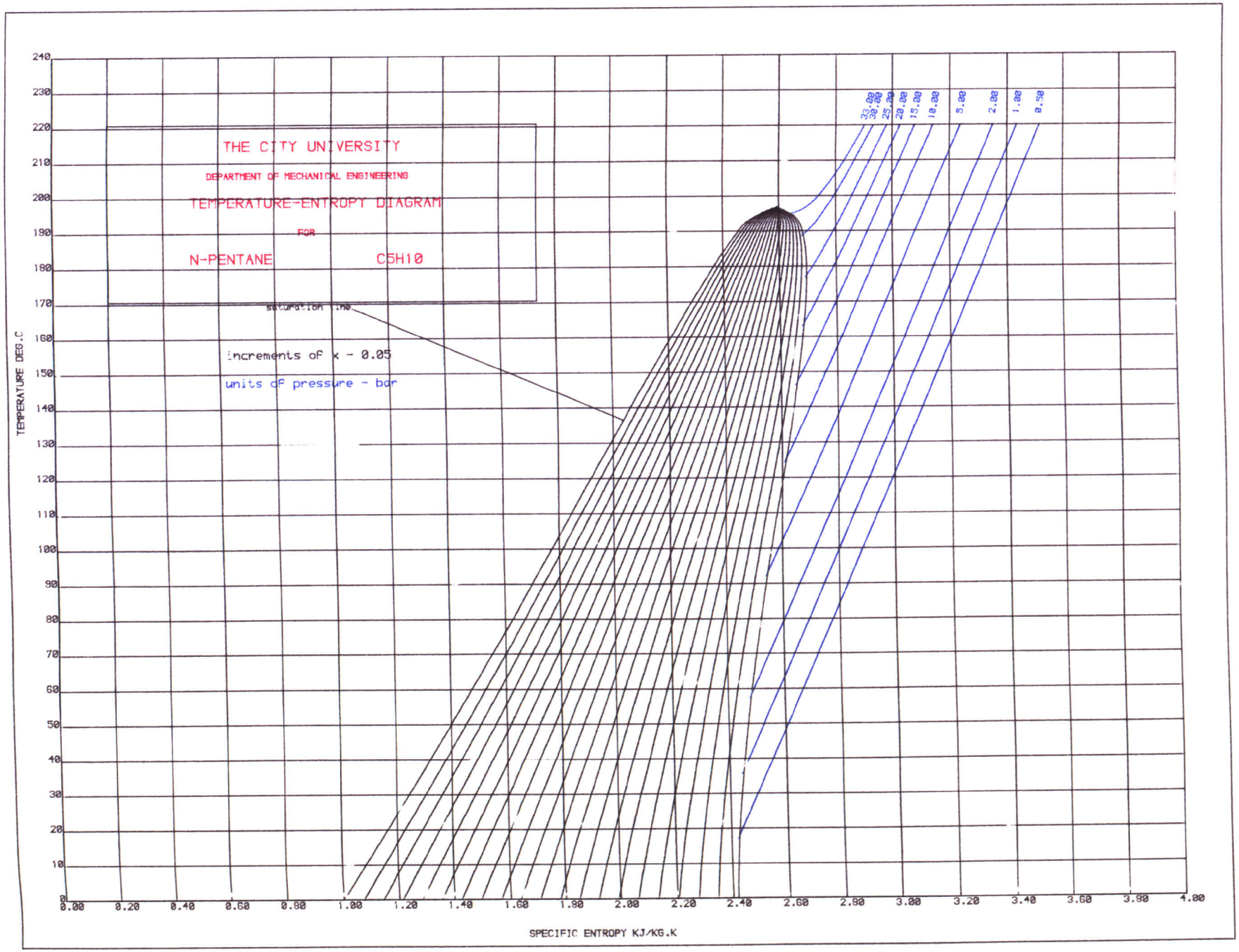
THE CITY UNIVERSITY
DEPARTMENT OF MECHANICAL ENGINEERING
TEMPERATURE-ENTROPY DIAGRAM
FOR
N-PENTANE C5H10
saturation line
increments of x - 0.05
units of pressure - bar
33.00
30.00
25.00
20.00
15.00
10.00
5.00
2.00
1.00
0.50
TEMPERATURE DEG.C
SPECIFIC ENTROPY KJ/KG.K

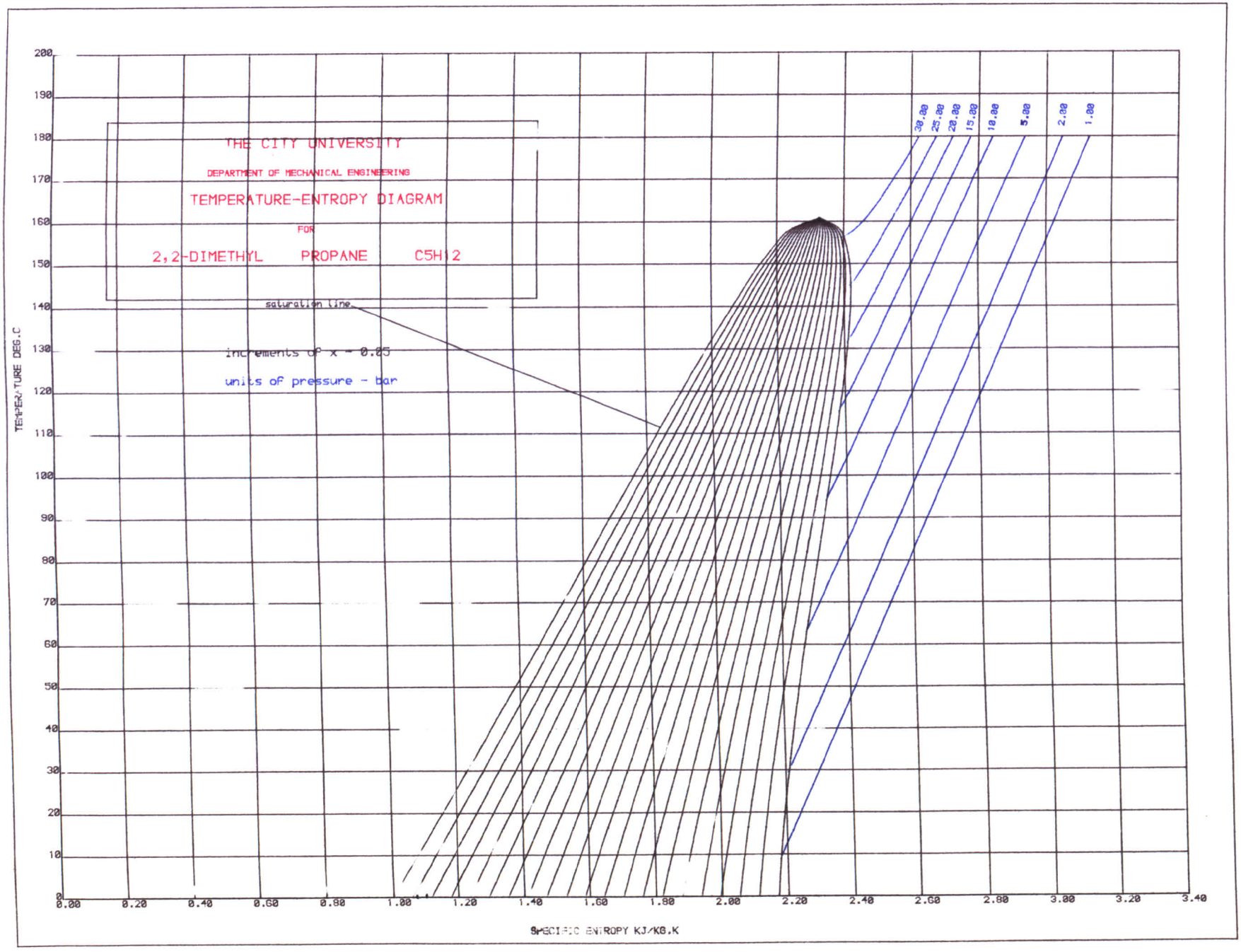
THE CITY UNIVERSITY
DEPARTMENT OF MECHANICAL ENGINEERING
TEMPERATURE-ENTROPY DIAGRAM
FOR
2,2-DIMETHYL PROPANE C5H12
saturation line
increments of x - 0.05
units of pressure - bar
30.00
25.00
20.00
15.00
10.00
5.00
2.00
1.00
TEMPERATURE DEG.C
SPECIFIC ENTROPY KJ/KG.K
0
10
20
30
40
50
60
70
80
90
100
110
120
130
140
150
160
170
180
190
200
0.00
0.20
0.40
0.60
0.80
1.00
1.20
1.40
1.60
1.80
2.00
2.20
2.40
2.60
2.80
3.00
3.20
3.40

Condensing Temperature = 30°C

Inlet Temp. (°C)	Inlet Pressure (bar)	Exit Pressure (bar)	Exit Dryness Fraction	Enthalpy Drop (kJ/kg)	Expansion Volume ratio
150	27.06	2.01	0.981	48.86	57.69
145	24.96	2.01	0.931	44.19	57.76
140	22.99	2.01	0.884	40.01	57.18
135	21.15	2.01	0.839	36.19	56.19
130	19.43	2.01	0.796	32.65	54.90
125	17.82	2.01	0.754	29.35	53.38

Table 7.1. Drying out characteristics for 2,2-dimethyl propane

Condensing Temperature = 30°C

Inlet Temp. (°C)	Inlet Pressure (bar)	Exit Pressure (bar)	Exit Dryness Fraction	Enthalpy Drop (kJ/kg)	Expansion Volume ratio
180	26.18	0.81	0.987	71.46	156.5
175	24.20	0.81	0.950	66.24	156.5
170	22.35	0.81	0.913	61.39	155.5
165	20.60	0.81	0.878	56.85	153.7
160	18.97	0.81	0.844	52.56	151.5
155	17.43	0.81	0.810	48.50	148.7
150	15.99	0.81	0.777	44.65	145.6
145	14.65	0.81	0.744	40.98	142.1
140	13.39	0.81	0.711	37.80	138.3
135	12.21	0.81	0.679	34.18	134.2

Table 7.2. Drying out characteritics for n-pentane.

A tentative molecular structure which yields good candidates was found. This was established on empirical grounds based on the neopentane molecule where the central atom is replaced by any chemical element of group IV of the periodic table. These are:

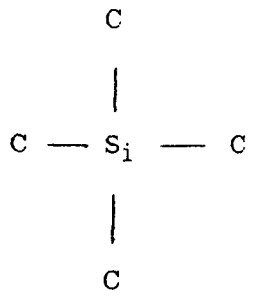

tetramethylsilane $Si(CH_3)_4$

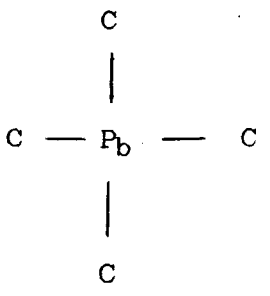

tetramethyl lead $Pb(CH_3)_4$

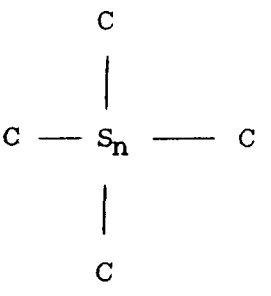

tetramethyl tin $Sn(CH_3)_4$

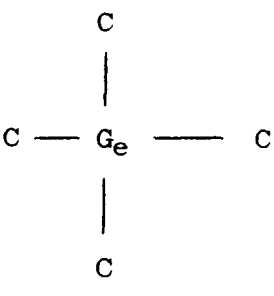

tetramethyl germanium $Ge(CH_3)_4$

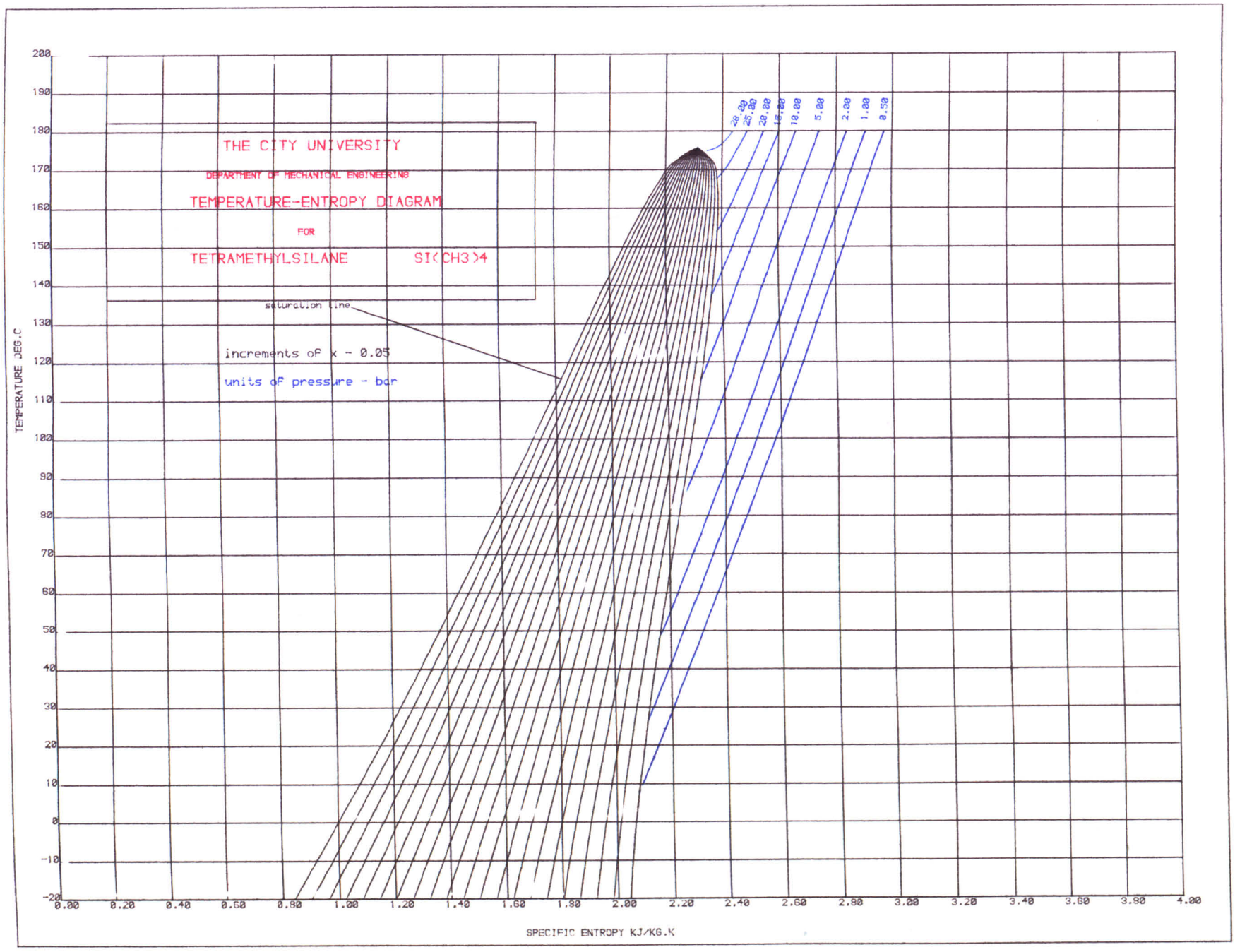
THE CITY UNIVERSITY
DEPARTMENT OF MECHANICAL ENGINEERING
TEMPERATURE-ENTROPY DIAGRAM
FOR
TETRAMETHYLSILANE SI(CH3)4
saturation line
increments of x - 0.05
units of pressure - bar
TEMPERATURE DEG.C
SPECIFIC ENTROPY KJ/KG.K
200
190
180
170
160
150
140
130
120
110
100
90
80
70
60
50
40
30
20
10
0
-10
-20
0.00
0.20
0.40
0.60
0.80
1.00
1.20
1.40
1.60
1.80
2.00
2.20
2.40
2.60
2.80
3.00
3.20
3.40
3.60
3.80
4.00
30.00
25.00
20.00
15.00
10.00
5.00
2.00
1.00
0.50

A T-s diagram of tetramethylsilane is shown. As can be seen this fluid could also be used. T-s diagrams for tetramethyl tin, tetramethyl lead and tetramethyl germanium were not obtained due to lack of critical properties and ideal heat capacity data. Tetramethyl lead, although obtainable in bulk, was discarded due to its toxicity. Tetramethyl tin and tetramethyl germanium are rare compounds and even if they were suitable fluids their utilization would be prohibitive on the grounds of cost.

T-s diagrams of n-pentane+neopentane were obtained for several compositions. The expansion process for an isentropic efficiency of 80% for condensing temperature of 35°C is also shown for each composition. A listing of the program written for plotting binary mixtures is given in Appendix B.

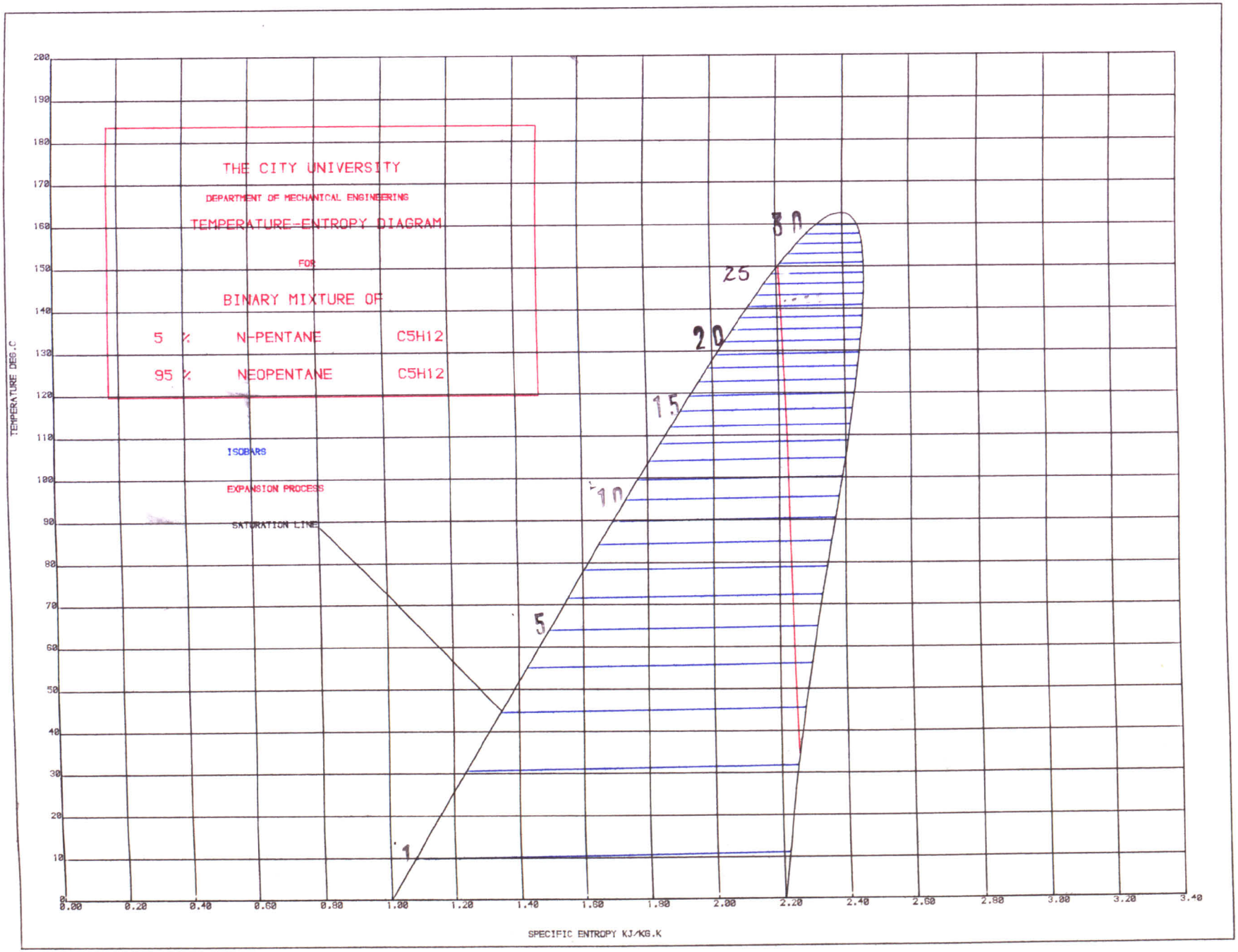
THE CITY UNIVERSITY
DEPARTMENT OF MECHANICAL ENGINEERING
TEMPERATURE-ENTROPY DIAGRAM
FOR
BINARY MIXTURE OF
5 % N-PENTANE C5H12
95 % NEOPENTANE C5H12
ISOBARS
EXPANSION PROCESS
SATURATION LINE
TEMPERATURE DEG.C
SPECIFIC ENTROPY KJ/KG.K
1
5
10
15
20
25
30

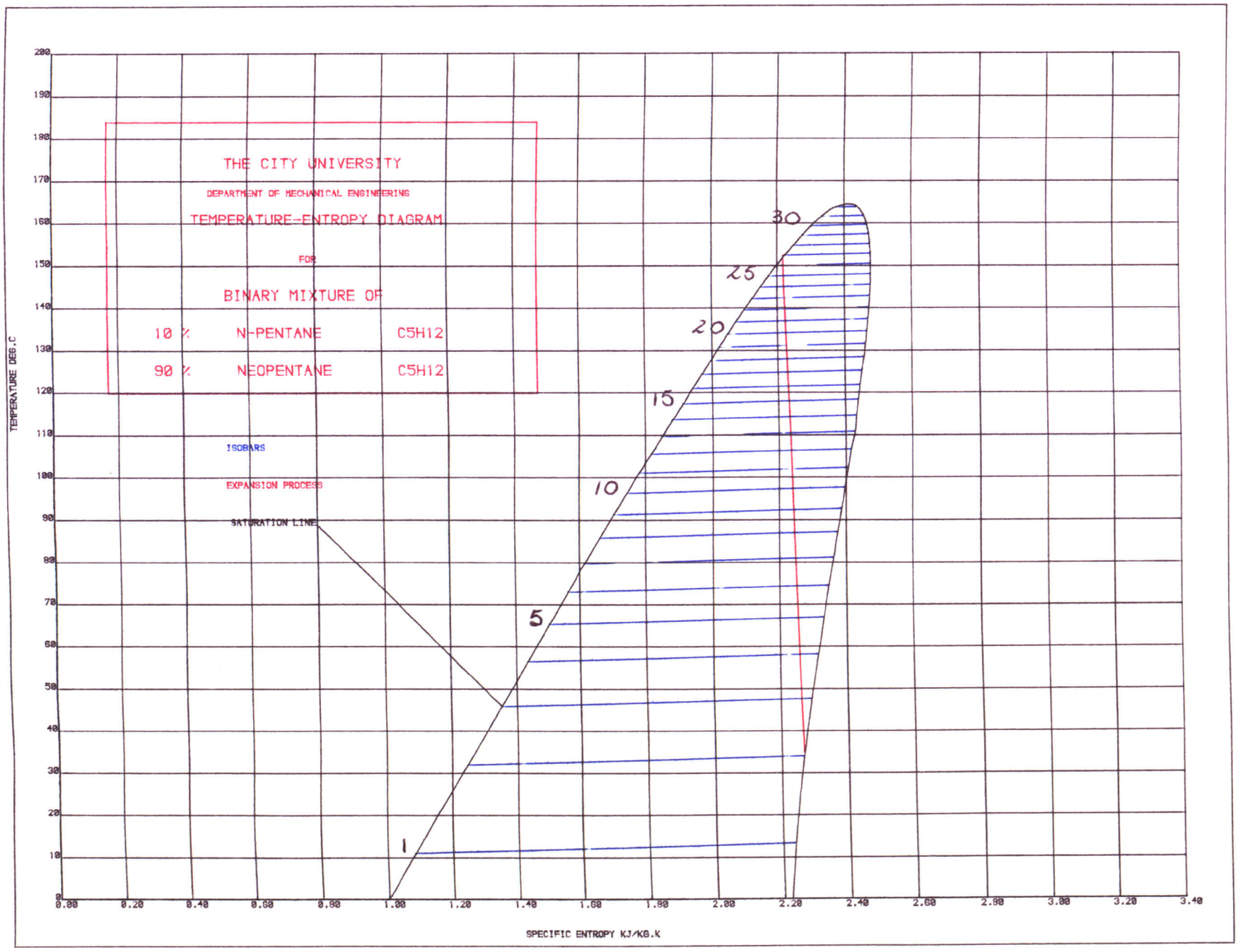
THE CITY UNIVERSITY
DEPARTMENT OF MECHANICAL ENGINEERING
TEMPERATURE-ENTROPY DIAGRAM
FOR
BINARY MIXTURE OF
10 % N-PENTANE C5H12
90 % NEOPENTANE C5H12
ISOBARS
EXPANSION PROCESS
SATURATION LINE
30
25
20
15
10
5
1
TEMPERATURE DEG.C
SPECIFIC ENTROPY KJ/KG.K

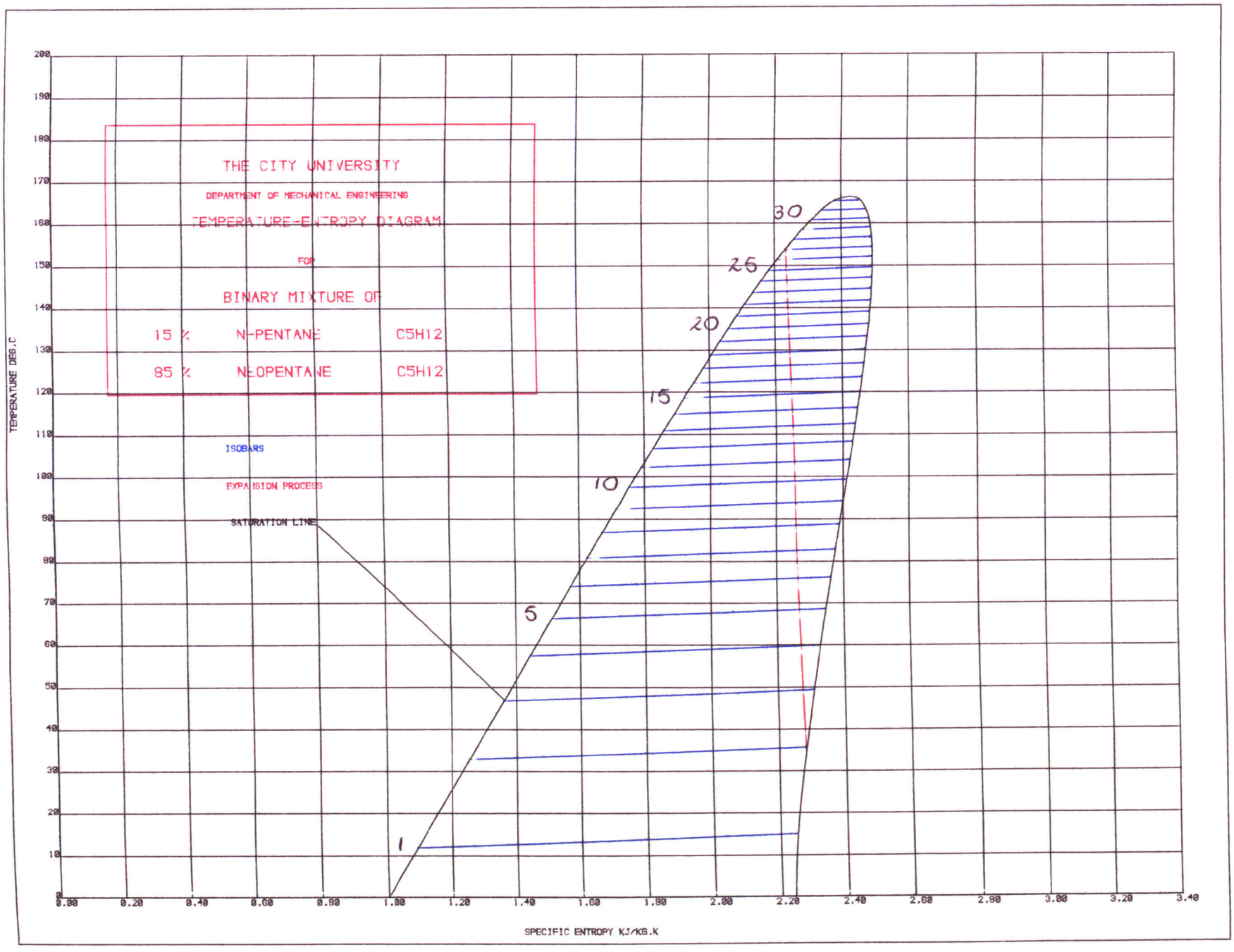
THE CITY UNIVERSITY
DEPARTMENT OF MECHANICAL ENGINEERING
TEMPERATURE-ENTROPY DIAGRAM
FOR
BINARY MIXTURE OF
15 % N-PENTANE C5H12
85 % NEOPENTANE C5H12
ISOBARS
EXPANSION PROCESS
SATURATION LINE
TEMPERATURE DEG.C
SPECIFIC ENTROPY KJ/KG.K
1
5
10
15
20
25
30
0.00
0.20
0.40
0.60
0.80
1.00
1.20
1.40
1.60
1.80
2.00
2.20
2.40
2.60
2.80
3.00
3.20
3.40

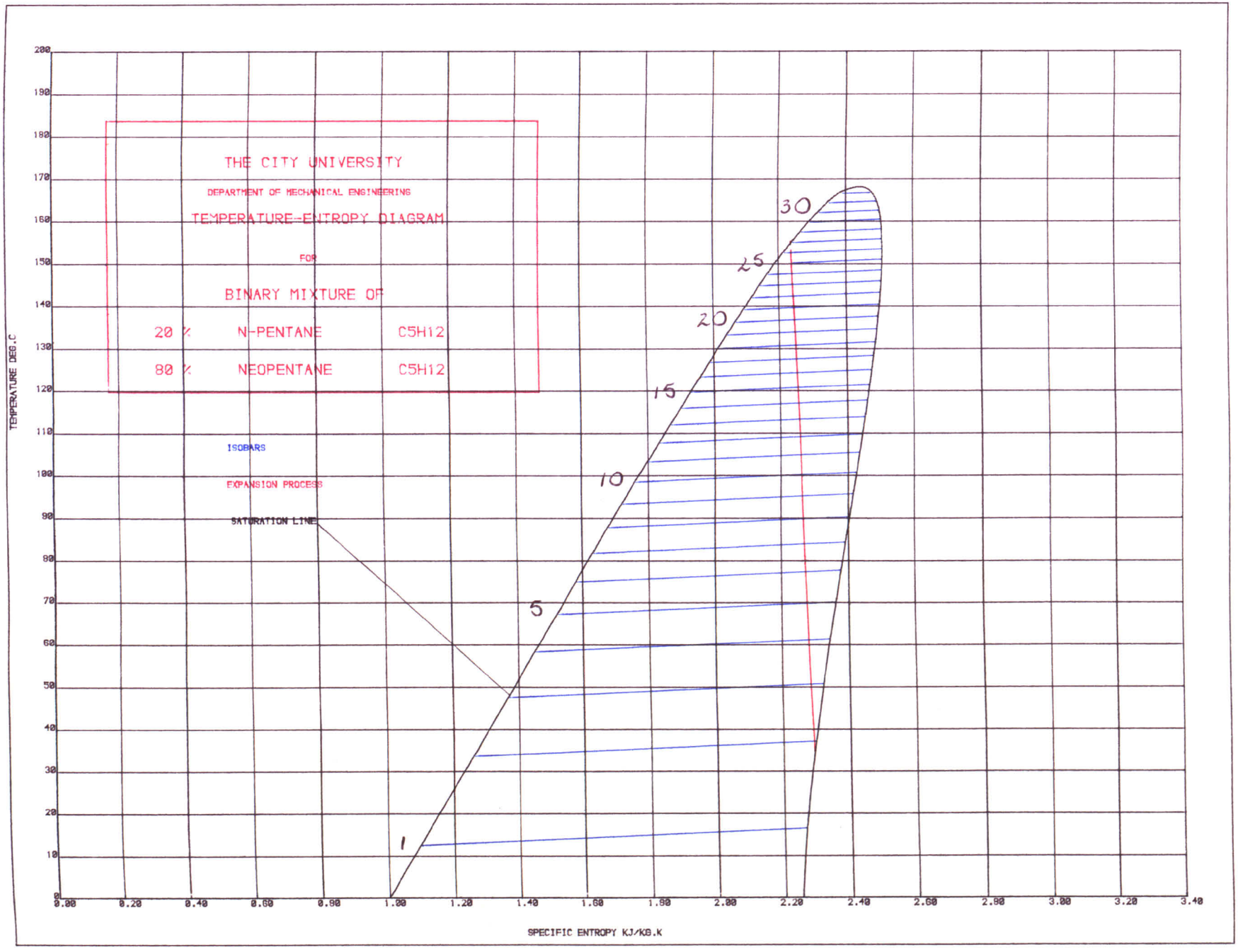
THE CITY UNIVERSITY
DEPARTMENT OF MECHANICAL ENGINEERING
TEMPERATURE-ENTROPY DIAGRAM
FOR
BINARY MIXTURE OF
20 % N-PENTANE C5H12
80 % NEOPENTANE C5H12
ISOBARS
EXPANSION PROCESS
SATURATION LINE
30
25
20
15
10
5
1
TEMPERATURE DEG.C
SPECIFIC ENTROPY KJ/KG.K
0.00
0.20
0.40
0.60
0.80
1.00
1.20
1.40
1.60
1.80
2.00
2.20
2.40
2.60
2.80
3.00
3.20
3.40

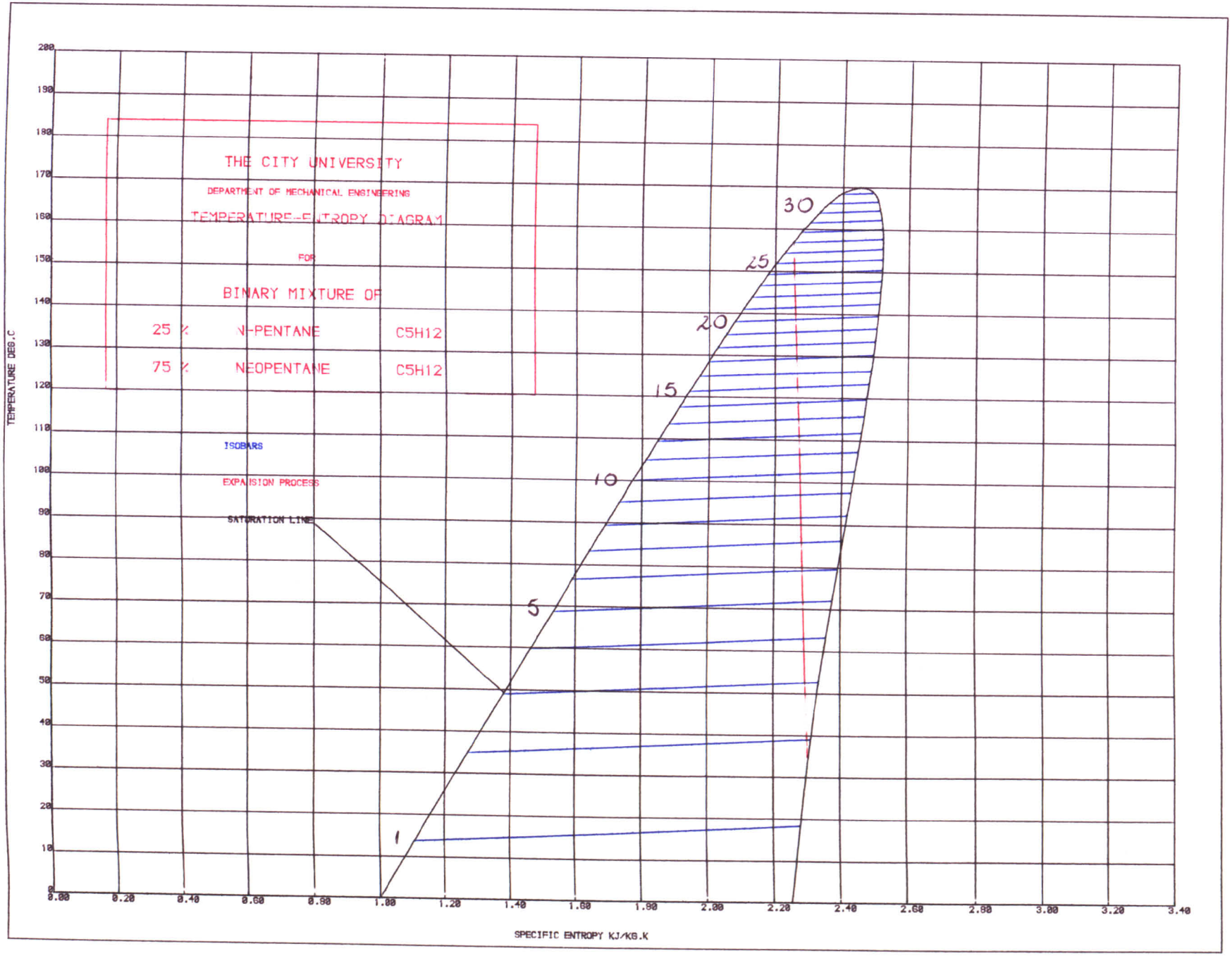
THE CITY UNIVERSITY
DEPARTMENT OF MECHANICAL ENGINEERING
TEMPERATURE-ENTROPY DIAGRAM
FOR
BINARY MIXTURE OF
25 % N-PENTANE C5H12
75 % NEOPENTANE C5H12
ISOBARS
EXPANSION PROCESS
SATURATION LINE
TEMPERATURE DEG.C
SPECIFIC ENTROPY KJ/KG.K
30
25
20
15
10
5
1

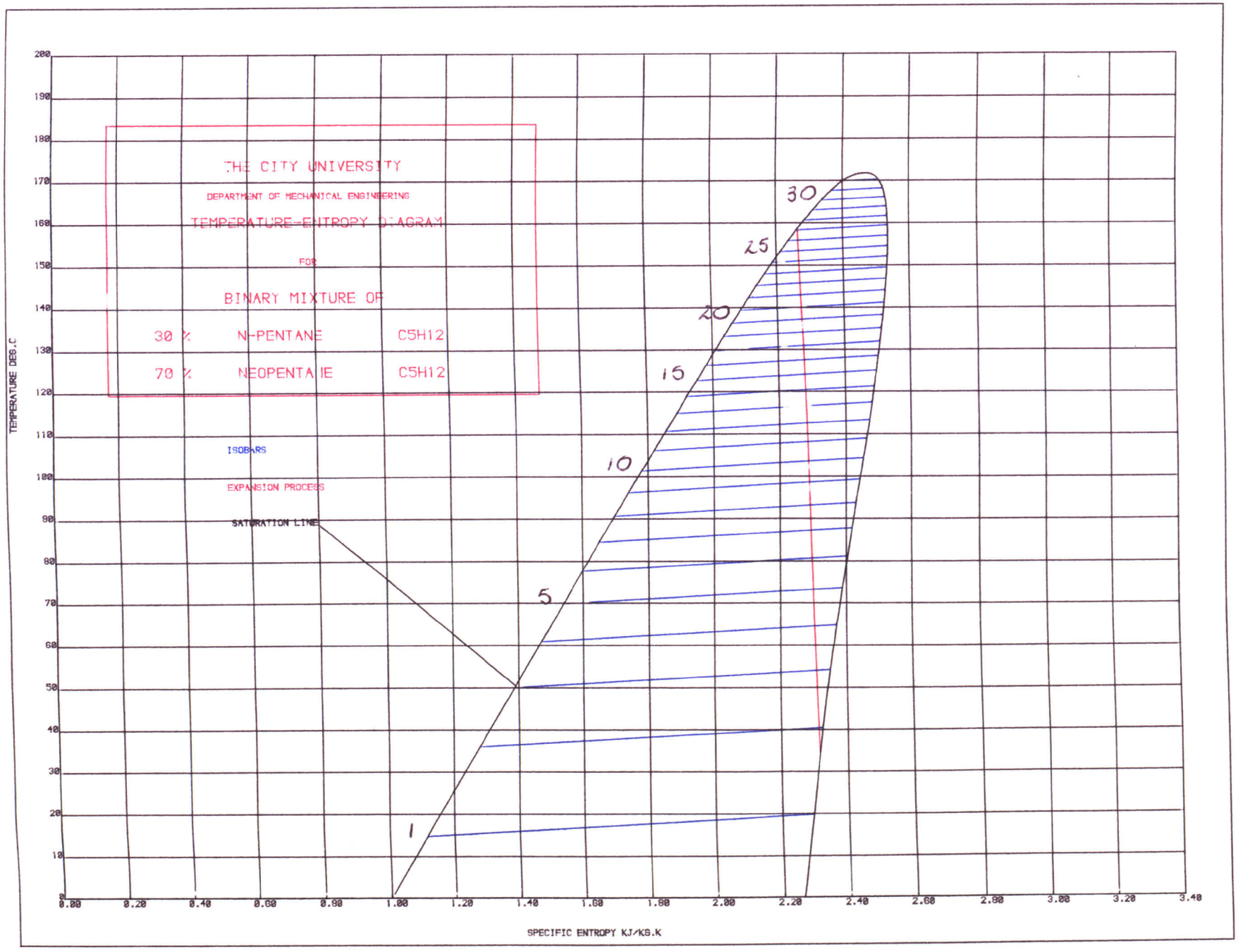
THE CITY UNIVERSITY
DEPARTMENT OF MECHANICAL ENGINEERING
TEMPERATURE-ENTROPY DIAGRAM
FOR
BINARY MIXTURE OF
30 % N-PENTANE C5H12
70 % NEOPENTANE C5H12
ISOBARS
EXPANSION PROCESS
SATURATION LINE
TEMPERATURE DEG.C
SPECIFIC ENTROPY KJ/KG.K
1
5
10
15
20
25
30

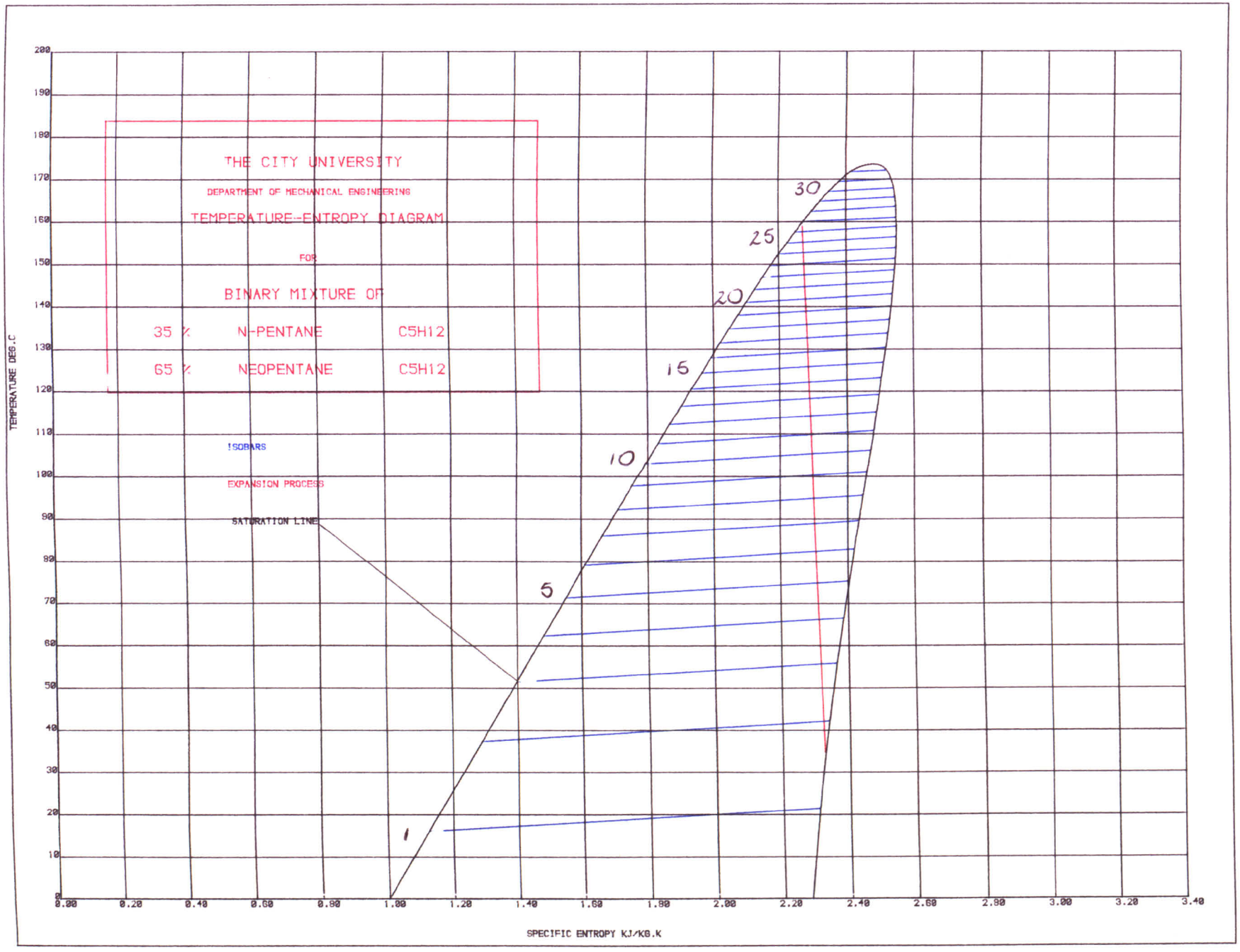
THE CITY UNIVERSITY
DEPARTMENT OF MECHANICAL ENGINEERING
TEMPERATURE--ENTROPY DIAGRAM
FOR
BINARY MIXTURE OF
35 % N-PENTANE C5H12
65 % NEOPENTANE C5H12
ISOBARS
EXPANSION PROCESS
SATURATION LINE
30
25
20
15
10
5
1
TEMPERATURE DEG.C
SPECIFIC ENTROPY KJ/KG.K

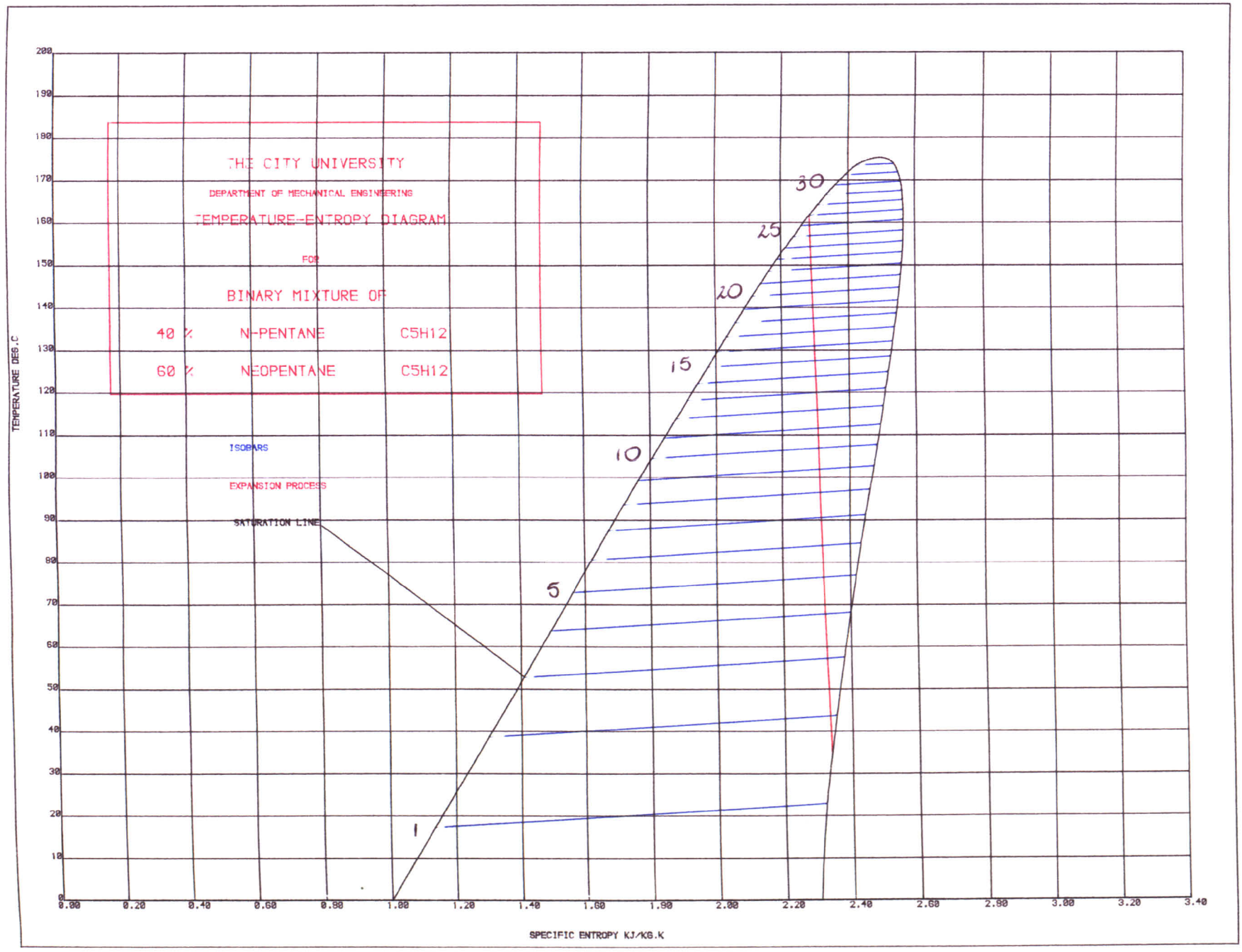
THE CITY UNIVERSITY
DEPARTMENT OF MECHANICAL ENGINEERING
TEMPERATURE-ENTROPY DIAGRAM
FOR
BINARY MIXTURE OF
40 % N-PENTANE C5H12
60 % NEOPENTANE C5H12
ISOBARS
EXPANSION PROCESS
SATURATION LINE
1
5
10
15
20
25
30
TEMPERATURE DEG.C
SPECIFIC ENTROPY KJ/KG.K
0
10
20
30
40
50
60
70
80
90
100
110
120
130
140
150
160
170
180
190
200
0.00
0.20
0.40
0.60
0.80
1.00
1.20
1.40
1.60
1.80
2.00
2.20
2.40
2.60
2.80
3.00
3.20
3.40

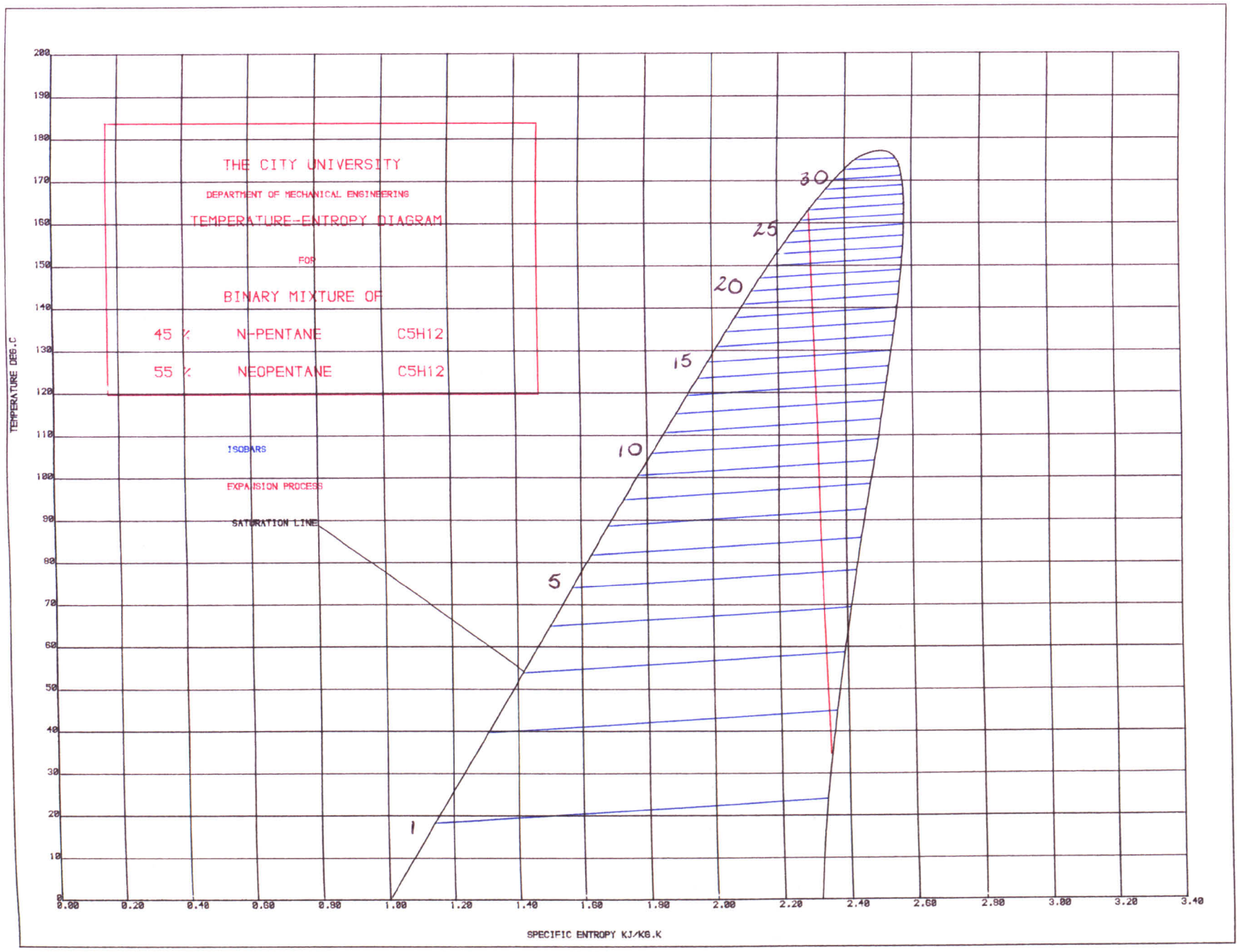
THE CITY UNIVERSITY
DEPARTMENT OF MECHANICAL ENGINEERING
TEMPERATURE-ENTROPY DIAGRAM
FOR
BINARY MIXTURE OF
45 % N-PENTANE C5H12
55 % NEOPENTANE C5H12
ISOBARS
EXPANSION PROCESS
SATURATION LINE
1
5
10
15
20
25
30
TEMPERATURE DEG.C
SPECIFIC ENTROPY KJ/KG.K
0
10
20
30
40
50
60
70
80
90
100
110
120
130
140
150
160
170
180
190
200
0.00
0.20
0.40
0.60
0.80
1.00
1.20
1.40
1.60
1.80
2.00
2.20
2.40
2.60
2.80
3.00
3.20
3.40

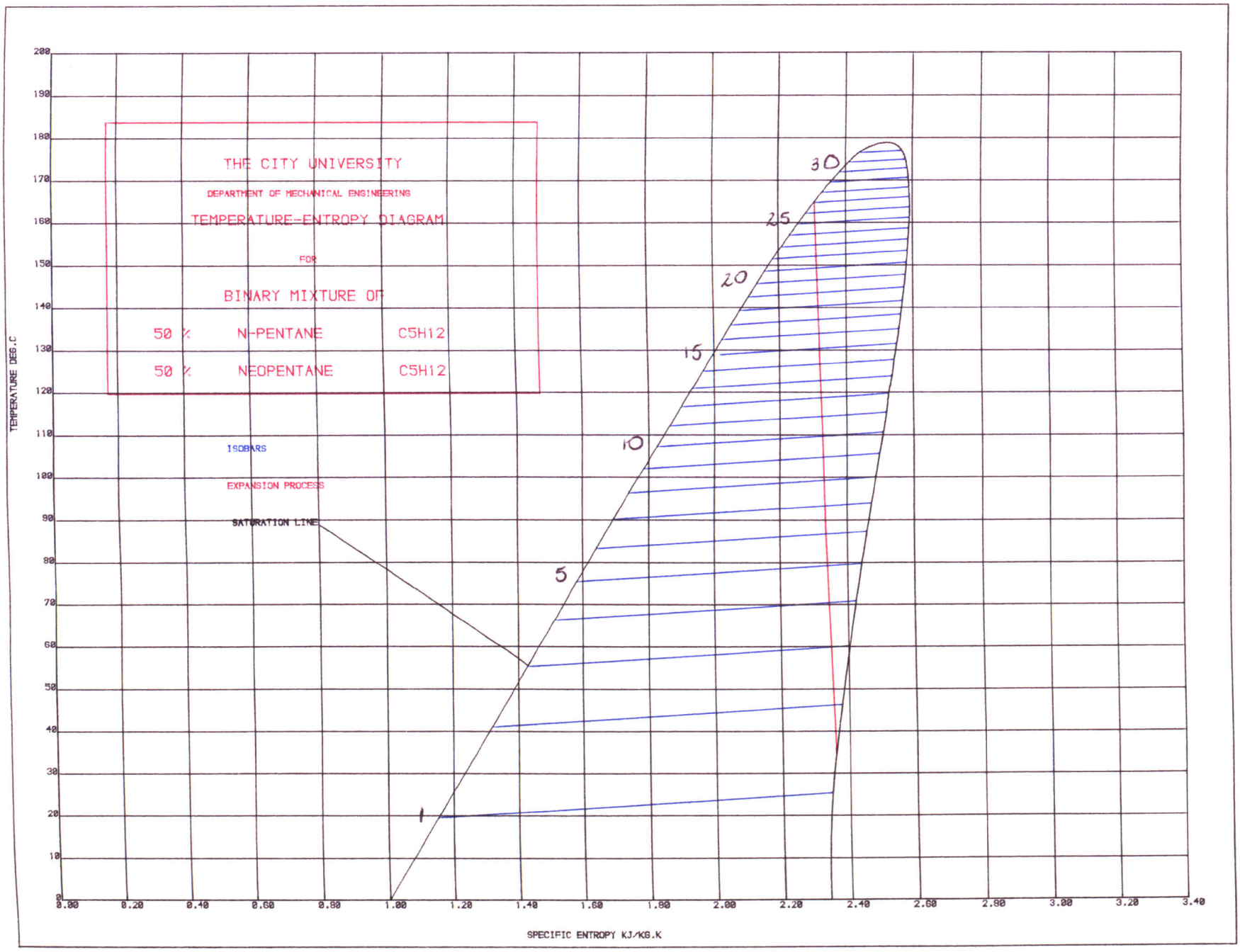
THE CITY UNIVERSITY
DEPARTMENT OF MECHANICAL ENGINEERING
TEMPERATURE-ENTROPY DIAGRAM
FOR
BINARY MIXTURE OF
50 % N-PENTANE C5H12
50 % NEOPENTANE C5H12
ISOBARS
EXPANSION PROCESS
SATURATION LINE
1
5
10
15
20
25
30
TEMPERATURE DEG.C
SPECIFIC ENTROPY KJ/KG.K
0
10
20
30
40
50
60
70
80
90
100
110
120
130
140
150
160
170
180
190
200
0.00
0.20
0.40
0.60
0.80
1.00
1.20
1.40
1.60
1.80
2.00
2.20
2.40
2.60
2.80
3.00
3.20
3.40

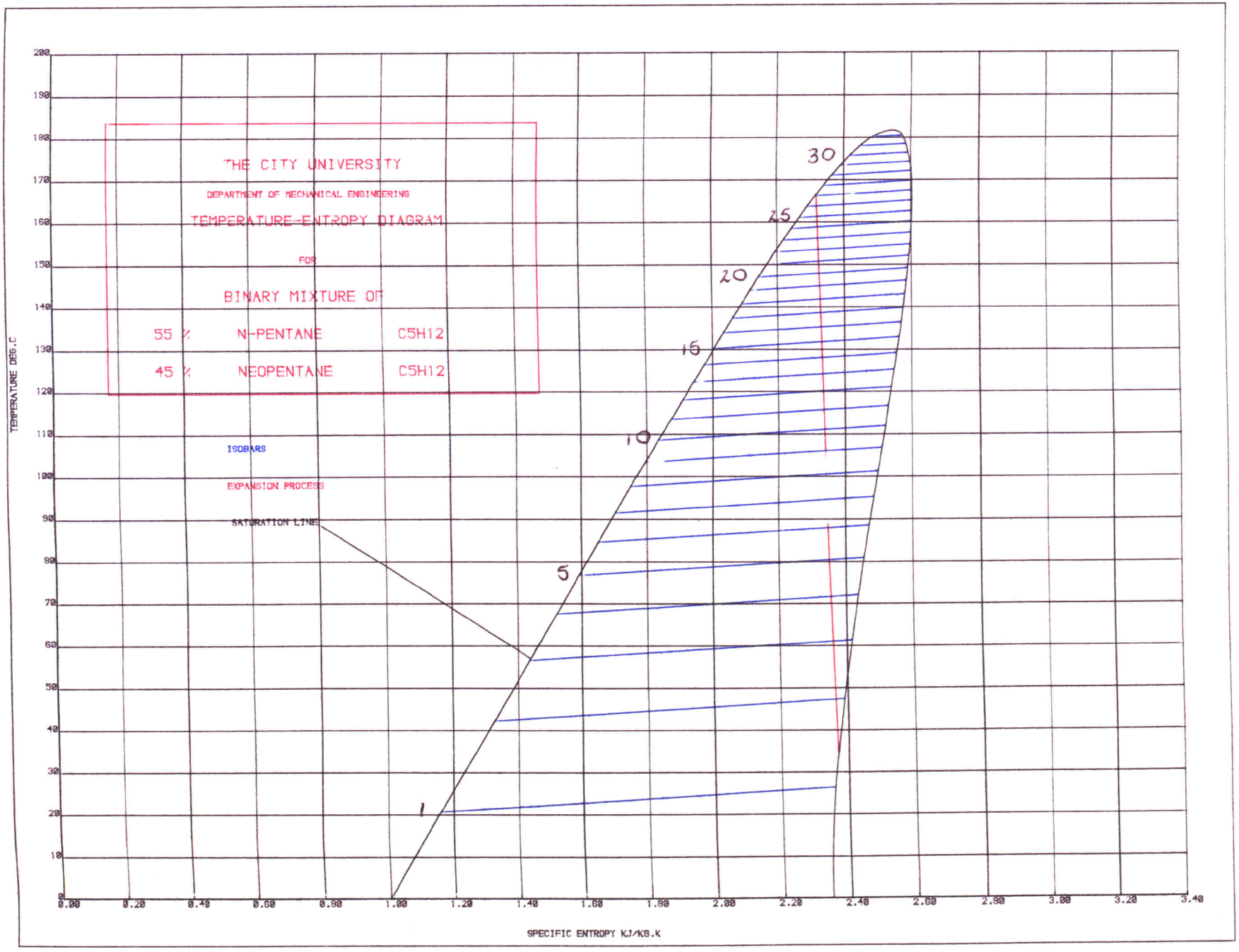
THE CITY UNIVERSITY
DEPARTMENT OF MECHANICAL ENGINEERING
TEMPERATURE-ENTROPY DIAGRAM
FOR
BINARY MIXTURE OF
55 % N-PENTANE C5H12
45 % NEOPENTANE C5H12
ISOBARS
EXPANSION PROCESS
SATURATION LINE
30
25
20
15
10
5
1
TEMPERATURE DEG.C
SPECIFIC ENTROPY KJ/KG.K

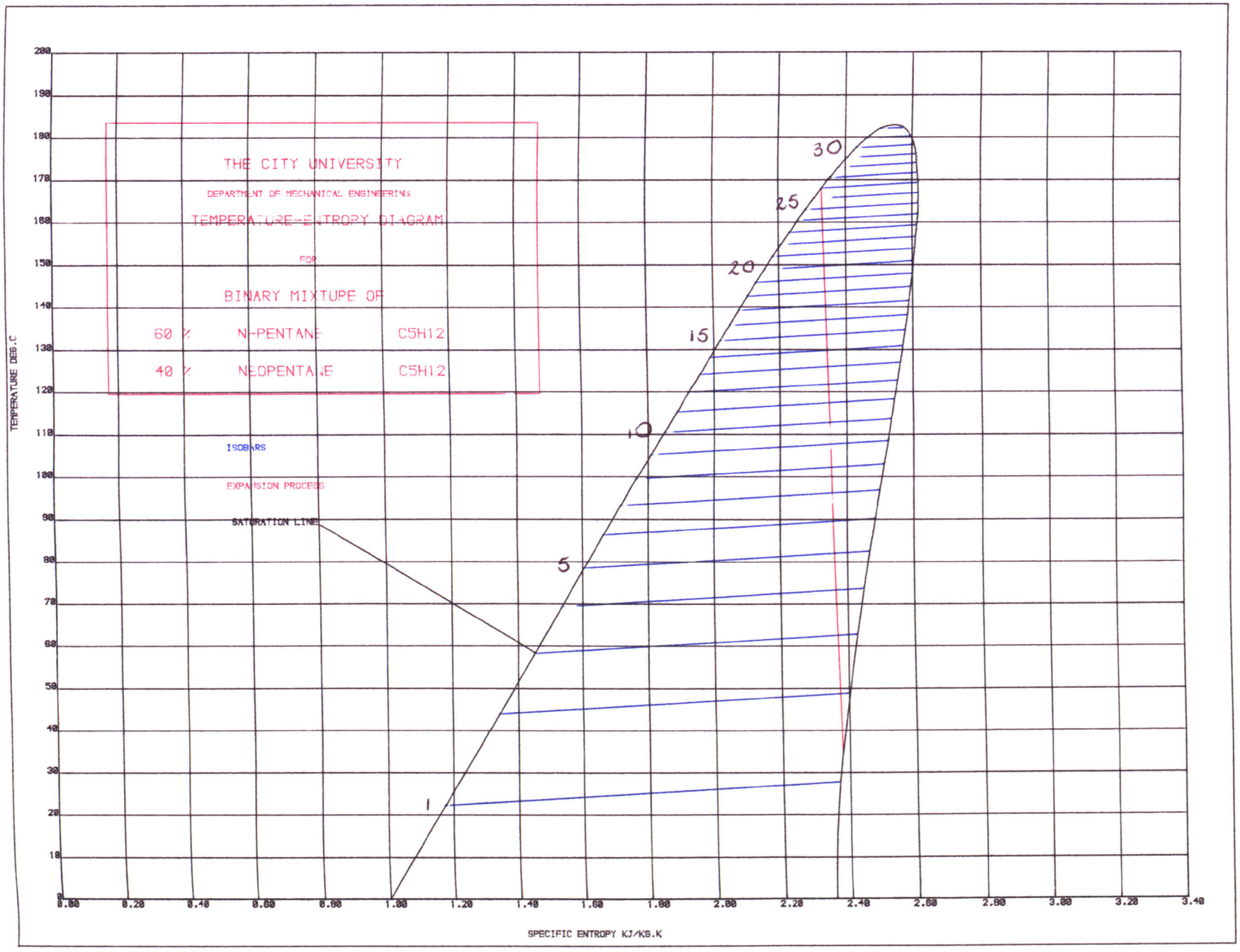
THE CITY UNIVERSITY
DEPARTMENT OF MECHANICAL ENGINEERING
TEMPERATURE-ENTROPY DIAGRAM
FOR
BINARY MIXTUPE OF
60 % N-PENTANE C5H12
40 % NEOPENTANE C5H12
ISOBARS
EXPANSION PROCESS
SATURATION LINE
TEMPERATURE DEG.C
SPECIFIC ENTROPY KJ/KG.K
1
5
10
15
20
25
30

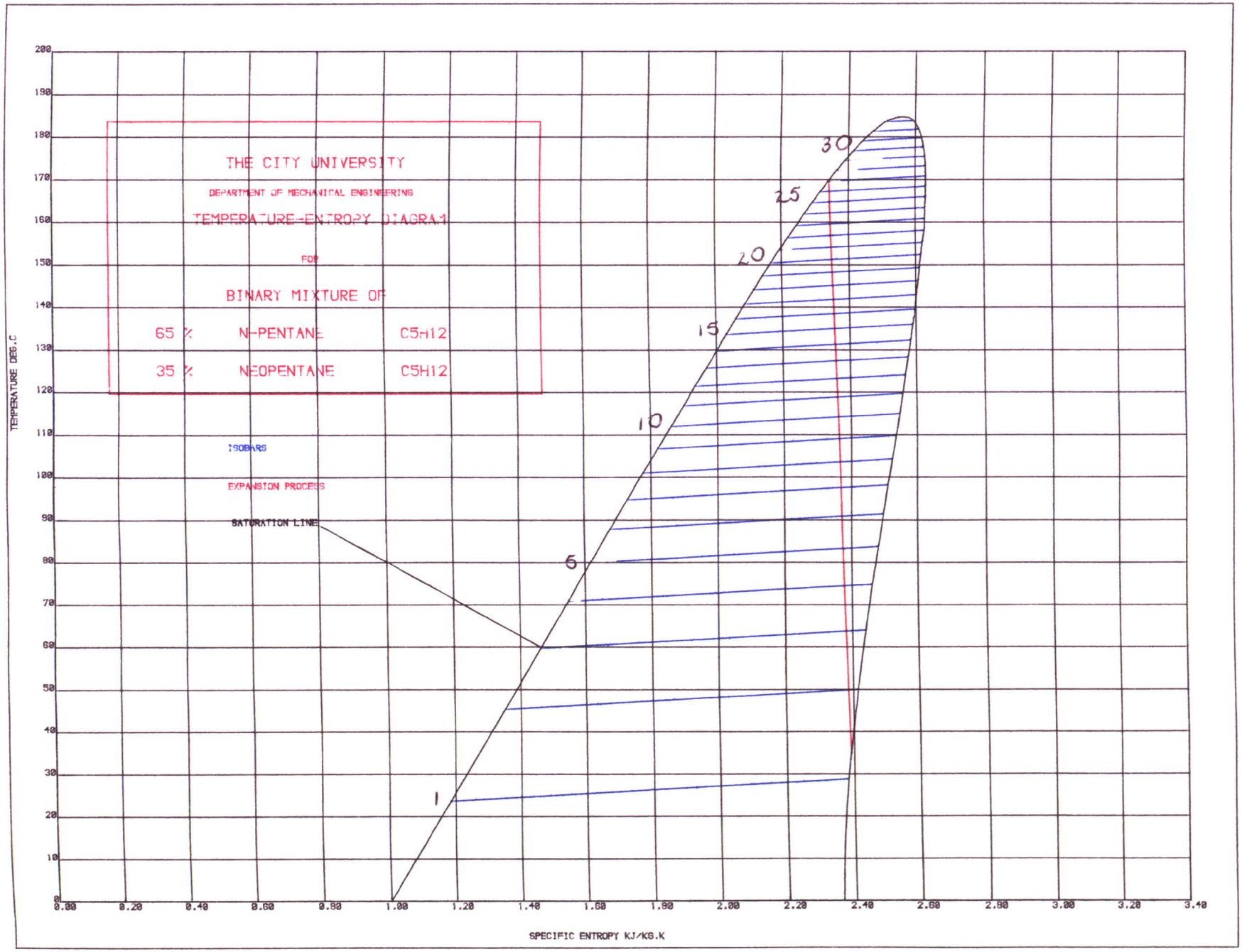
THE CITY UNIVERSITY
DEPARTMENT OF MECHANICAL ENGINEERING
TEMPERATURE-ENTROPY DIAGRAM
FOR
BINARY MIXTURE OF
65 % N-PENTANE C5H12
35 % NEOPENTANE C5H12
ISOBARS
EXPANSION PROCESS
SATURATION LINE
30
25
20
15
10
5
1
TEMPERATURE DEG.C
SPECIFIC ENTROPY KJ/KG.K
0.00
0.20
0.40
0.60
0.80
1.00
1.20
1.40
1.60
1.80
2.00
2.20
2.40
2.60
2.80
3.00
3.20
3.40

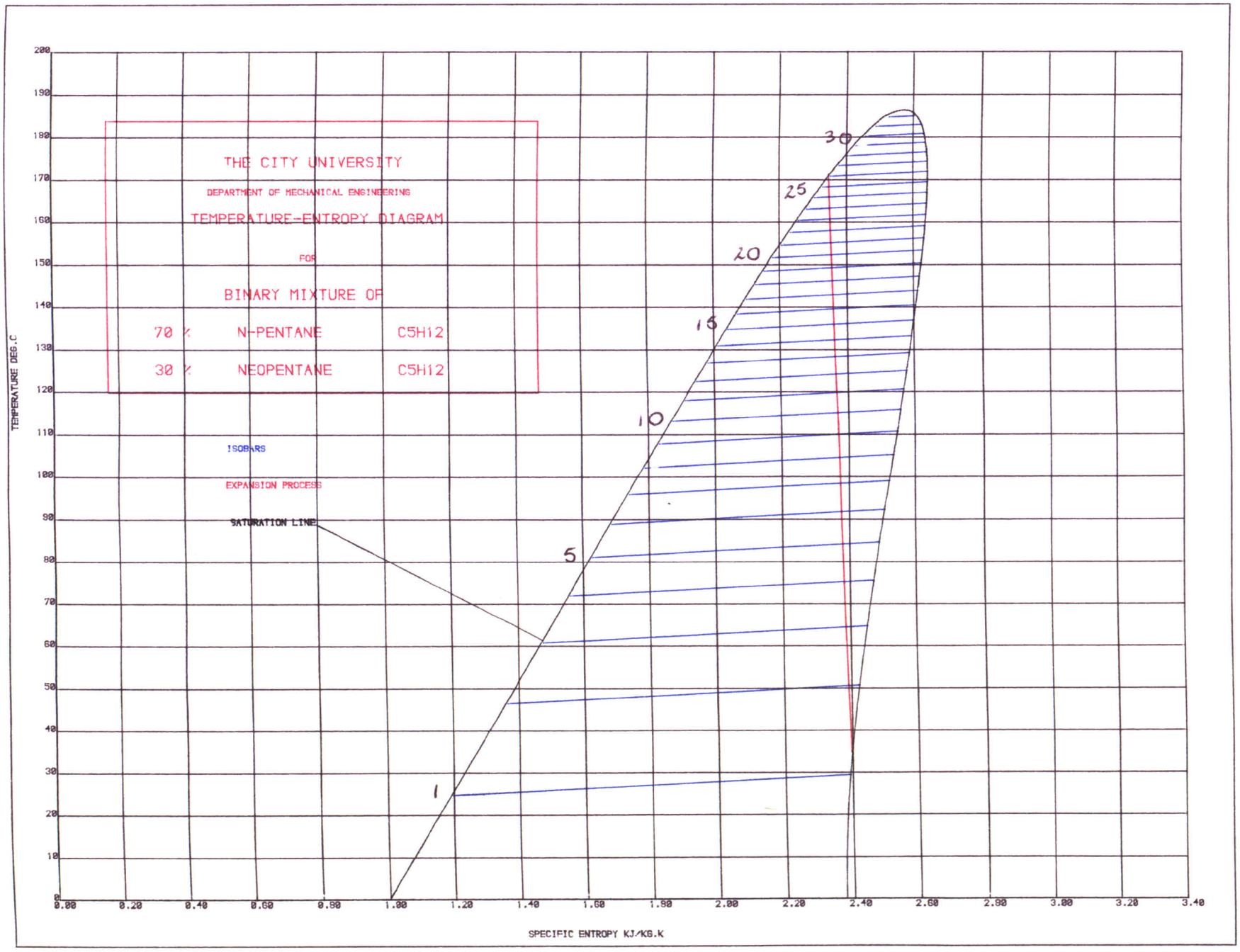
THE CITY UNIVERSITY
DEPARTMENT OF MECHANICAL ENGINEERING
TEMPERATURE-ENTROPY DIAGRAM
FOR
BINARY MIXTURE OF
70 % N-PENTANE C5H12
30 % NEOPENTANE C5H12
ISOBARS
EXPANSION PROCESS
SATURATION LINE
30
25
20
15
10
5
1
TEMPERATURE DEG.C
SPECIFIC ENTROPY KJ/KG.K

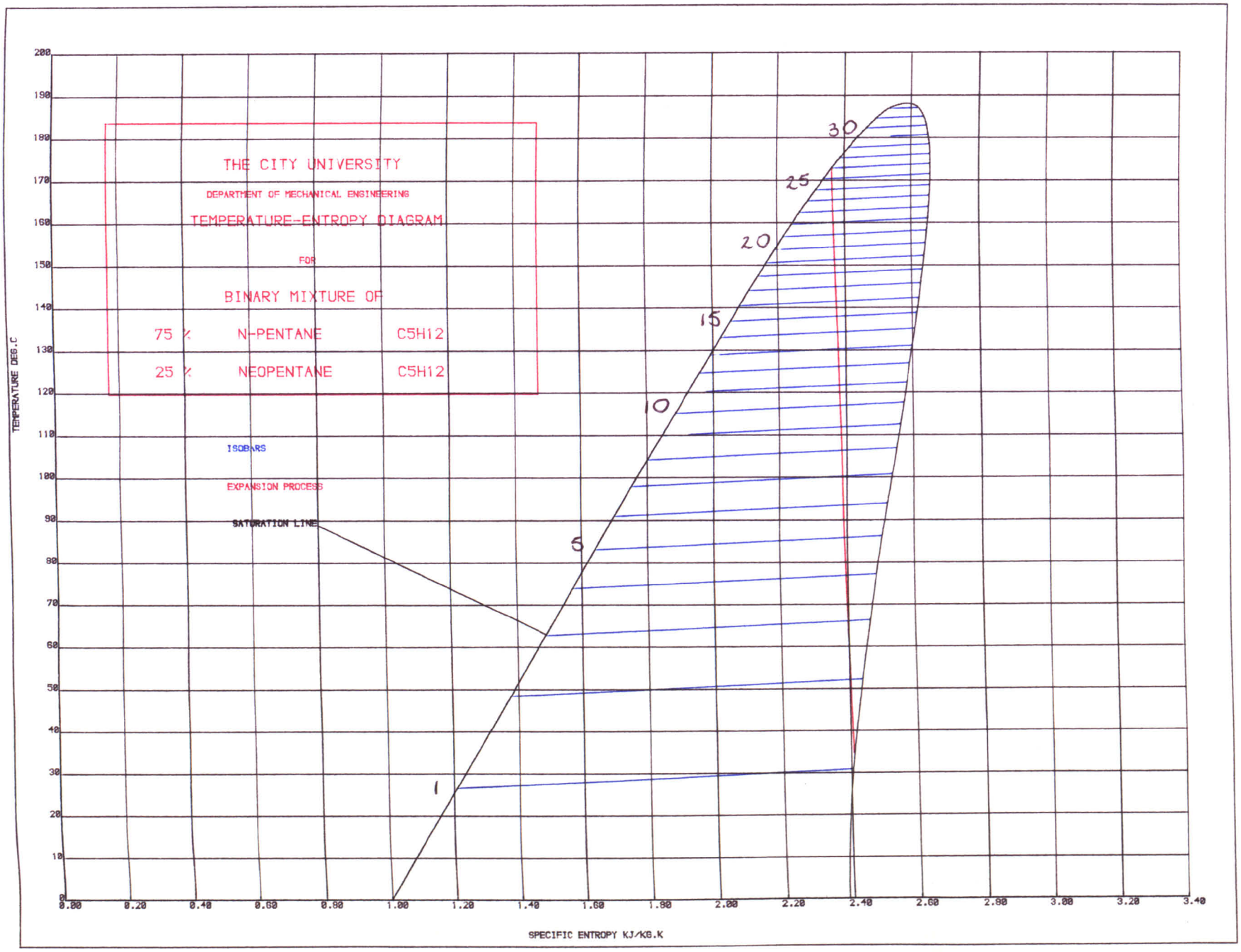
THE CITY UNIVERSITY
DEPARTMENT OF MECHANICAL ENGINEERING
TEMPERATURE-ENTROPY DIAGRAM
FOR
BINARY MIXTURE OF
75 % N-PENTANE C5H12
25 % NEOPENTANE C5H12
ISOBARS
EXPANSION PROCESS
SATURATION LINE
30
25
20
15
10
5
1
TEMPERATURE DEG.C
SPECIFIC ENTROPY KJ/KG.K

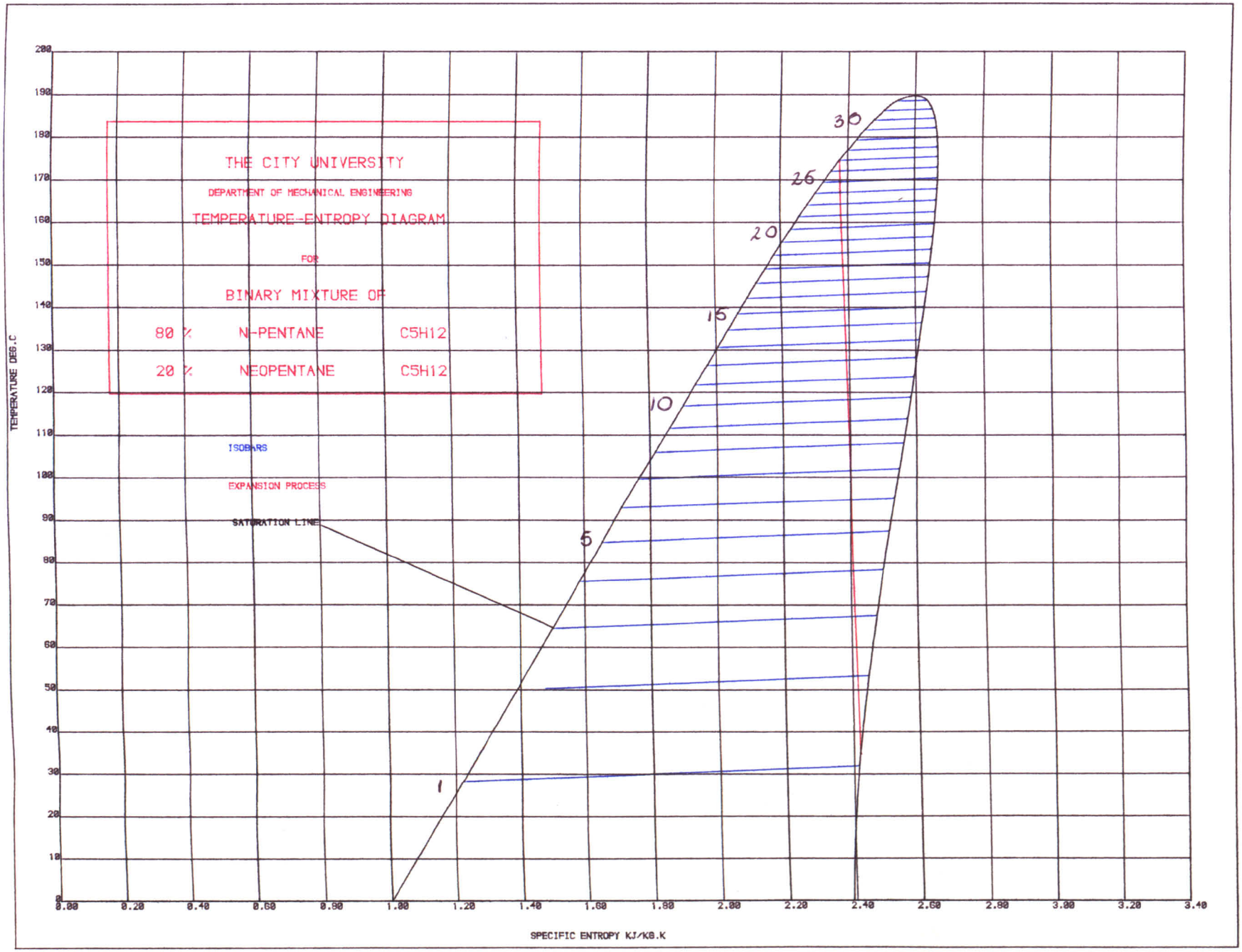
THE CITY UNIVERSITY
DEPARTMENT OF MECHANICAL ENGINEERING
TEMPERATURE-ENTROPY DIAGRAM
FOR
BINARY MIXTURE OF
80 % N-PENTANE C5H12
20 % NEOPENTANE C5H12
ISOBARS
EXPANSION PROCESS
SATURATION LINE
30
26
20
15
10
5
1
TEMPERATURE DEG.C
SPECIFIC ENTROPY KJ/KG.K
0.00
0.20
0.40
0.60
0.80
1.00
1.20
1.40
1.60
1.80
2.00
2.20
2.40
2.60
2.80
3.00
3.20
3.40

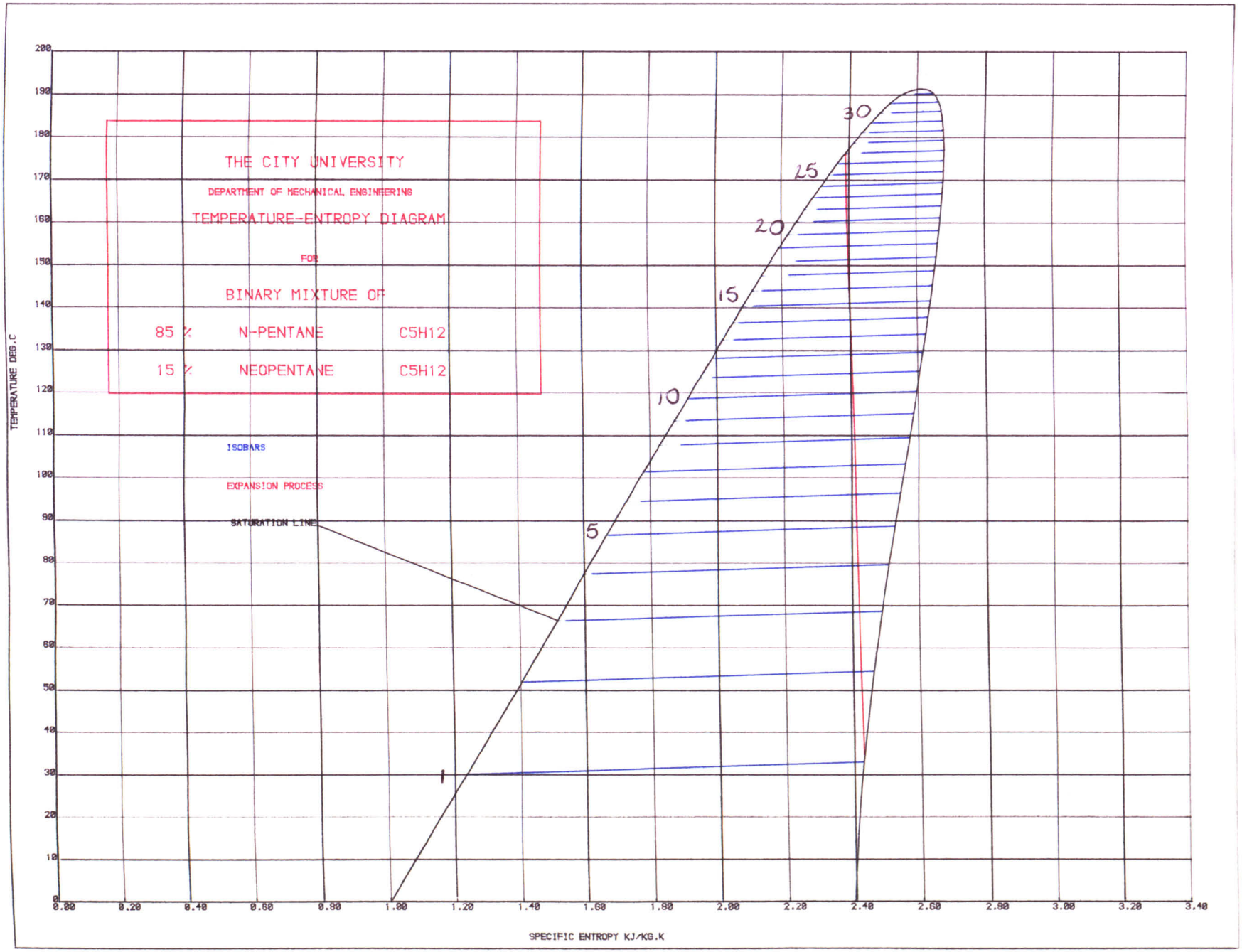
THE CITY UNIVERSITY
DEPARTMENT OF MECHANICAL ENGINEERING
TEMPERATURE-ENTROPY DIAGRAM
FOR
BINARY MIXTURE OF
85 % N-PENTANE C5H12
15 % NEOPENTANE C5H12
ISOBARS
EXPANSION PROCESS
SATURATION LINE
TEMPERATURE DEG.C
SPECIFIC ENTROPY KJ/KG.K
1
5
10
15
20
25
30

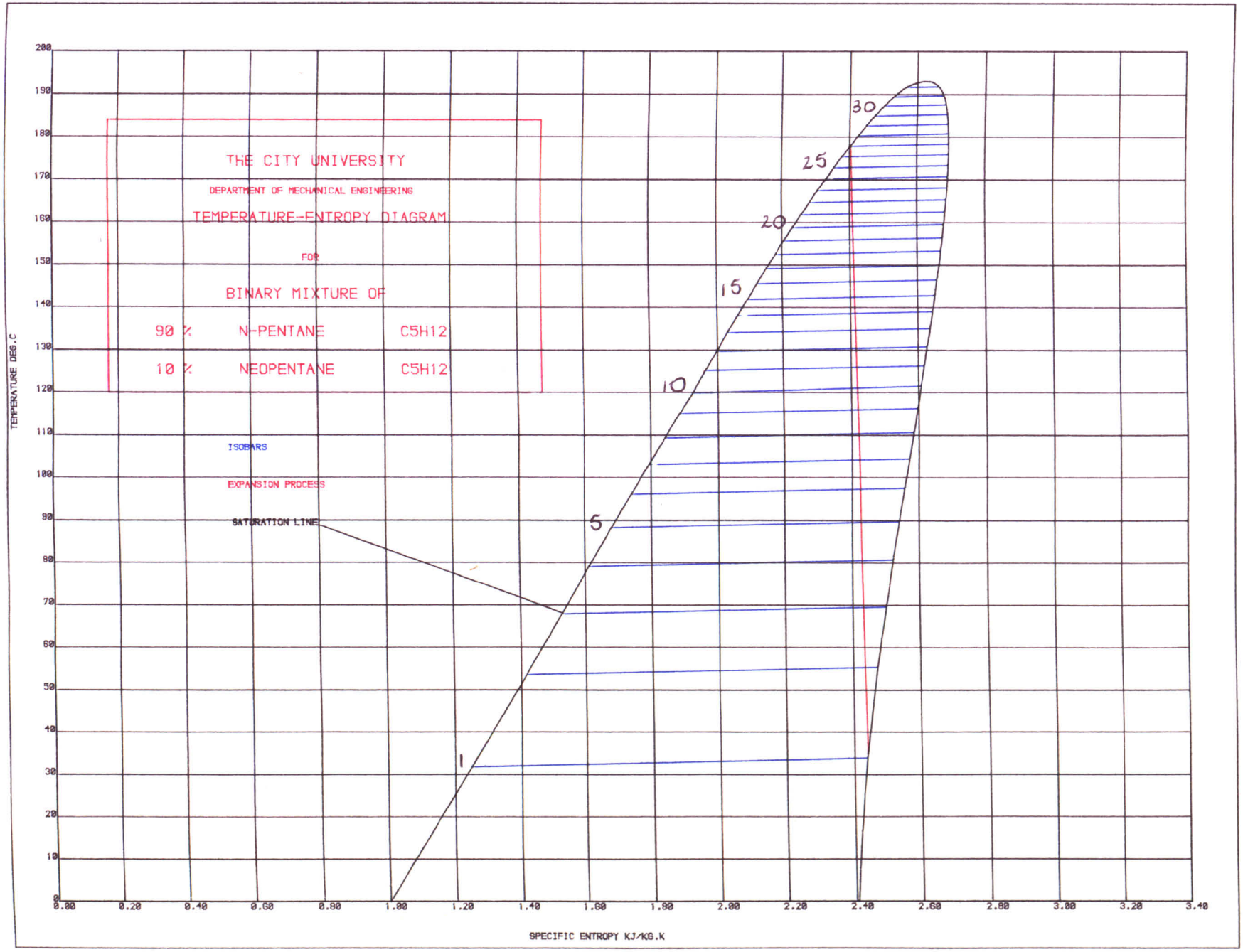
THE CITY UNIVERSITY
DEPARTMENT OF MECHANICAL ENGINEERING
TEMPERATURE-ENTROPY DIAGRAM
FOR
BINARY MIXTURE OF
90 % N-PENTANE C5H12
10 % NEOPENTANE C5H12
ISOBARS
EXPANSION PROCESS
SATURATION LINE
1
5
10
15
20
25
30
TEMPERATURE DEG.C
SPECIFIC ENTROPY KJ/KG.K

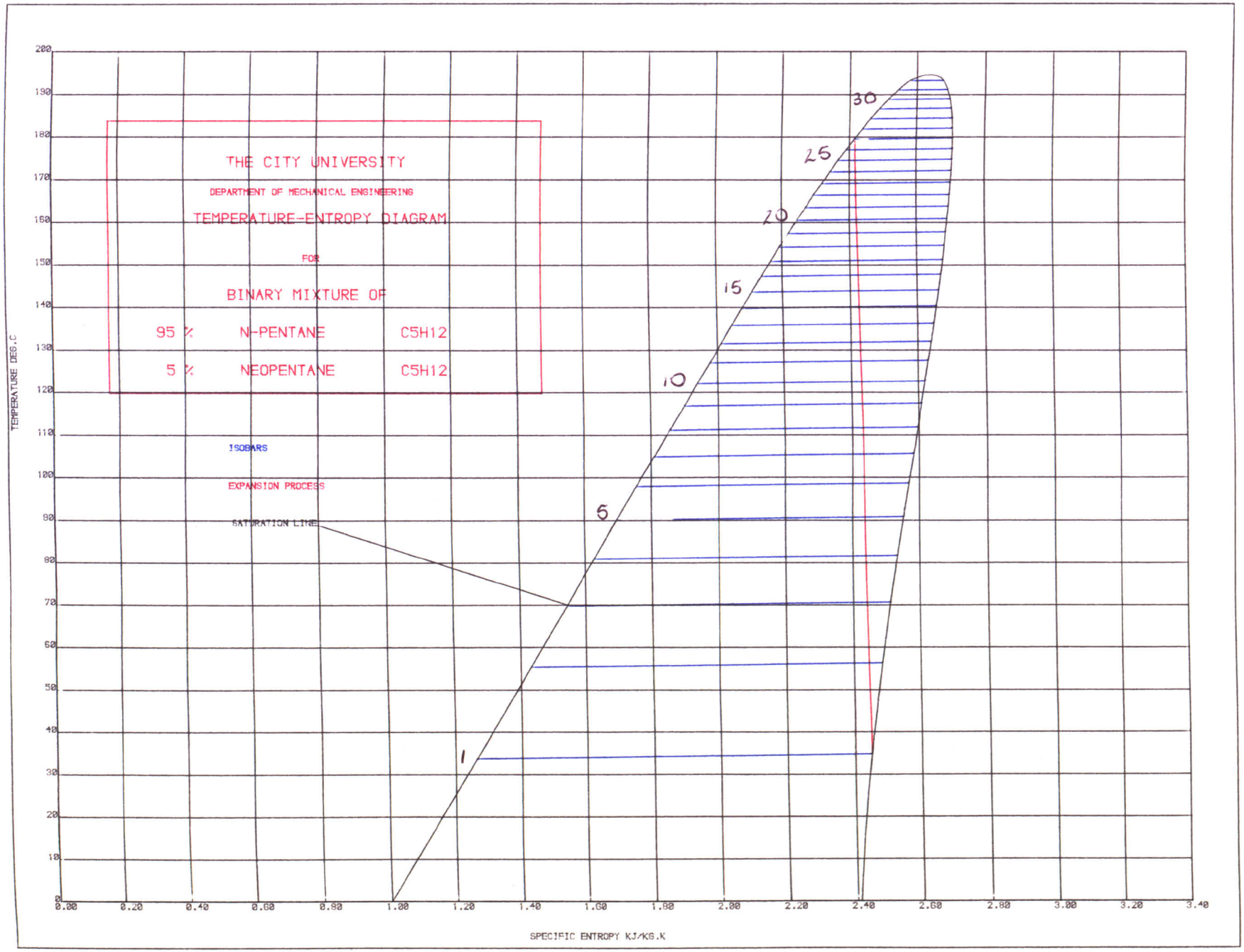
THE CITY UNIVERSITY
DEPARTMENT OF MECHANICAL ENGINEERING
TEMPERATURE-ENTROPY DIAGRAM
FOR
BINARY MIXTURE OF
95 % N-PENTANE C5H12
5 % NEOPENTANE C5H12
ISOBARS
EXPANSION PROCESS
SATURATION LINE
TEMPERATURE DEG.C
SPECIFIC ENTROPY KJ/KG.K
1
5
10
15
20
25
30

REFERENCES

1. Abbott and Van Ness. "Thermodynamics". Schaum Collection, McGraw-Hill, 1972.

2. Tabor, H. and Bronicki, L. "Establishding Criteria for Fluids for Small Vapour Turbines" see Appendix A by M. Goldstein, SAE National Transportation, Power plant and Fuels and Lubricants Meeting, Oct.1964.

3. Reid, R.C., Prausnitz, J.M. and Sherwood, T.K. "Properties of Gases and Liquids". McGraw-Hill, New York, 1977.

4. Smith, I.K. "THERPROP Data Bank" The City University, 1981.

5. Newsweek Magazine. "Mother Nature's Revenge. The Depletion of the Ozone Threatens our Climate". March 12, 1987.

6. Stratospheric Ozone Depletion by Halocarbons: Chemistry and Transport (National Academy of Sciences, Washington, D.C.), 1979.

7. ASHRAE Handbook of Fundamentals. American Society of Heating, Refrigerant and Air-Conditioning Engineers, New York, 1972.

8. Pine, S. "Organic Chemistry" 5th Ed., McGraw-Hill, 1987.

CHAPTER 8

EQUIPMENT AND EXPERIMENTAL PROCEDURES

8.1. INTRODUCTION

The experimental part of this work was carried out at the Department of Chemistry, University College, London. All experimental procedures used were in accordance with those previously utilized by Sanchez[1].

The aim of the experimental work was to determine the bubble and dew pressures of a mixture of n-pentane + 2,2-dimethylpropane (neopentane) for five different compositions. This was intended to verify the usefulness of the Redlich-Kwong-Soave equation of state to predict vapour-liquid equilibrium of the aforementioned mixture. Vapour pressures of pure n-pentane and neopentane were also measured. In order to test the accuracy of the isothermal static apparatus, the critical point of 2,2-dimethylpropane was measured.

The apparatus, the experimental method and temperature and pressure measurements are described. A detailed description of the way the samples were prepared is given in Section 8.9.

8.2. DYNAMIC TECHNIQUES

When a liquid boils in an open vessel its vapour pressure roughly equals that of the atmosphere. If the boiling process is

carried out under reflux and pressure allowed to vary, the measurement of the vapour pressure of the liquid can be made very accurately. A technique of measurement of vapour pressures of pure compounds and mixtures is known as ebulliometry[2]. This is normally grouped in two categories: (a) where the pressure is directly measured and (b) the comparative method which involves the determination of the unknown vapour pressure relative to the known vapour pressure of a reference substance normally water or mercury. Depending on which of these methods is used the recirculating apparatus contains one or two ebulliometers. The major disadvantage of these techniques is the difficulty in ensuring that equilibrium is precisely reached.

A large number of recirculating stills have been designed over the years and some have been reviewed by Fowler[3]. Modern equilibrium stills incorporate a Cottrell[4] vapour lift pump and a vapour hold-up trap first introduced by Sameshima[5].

According to Williamson[6], one of the most successful stills of the liquid recirculating type is due to Brown[7] shown in Figure 8.1. Several refinements incorporated in the design ensure that at equilibrium, compositions of the condensate and liquid samples are accurately reflected at a well-defined temperature and pressure. In Brown's still, a liquid is boiled in the heater A. To promote nucleation, the boiler is coated with a layer of finely powdered glass thus reducing surges of pressure and temperature fluctuations.

The two-phase mixture boiled at a particular pressure pumps up the Cottrell vapour lift pump B and flows over a thermometer well. The two-phases are then separated, with each phase being collected by a hold-up trap F. A system of baffles ensures that no liquid droplet is carried over with vapour. The vapour phase condenses at E and E′. The condensate returns via trap G. The hold-up traps are fitted with magnetic ball valves in such a way that once the still has reached the steady-state both samples are isolated for analysis before the apparatus is turned off.

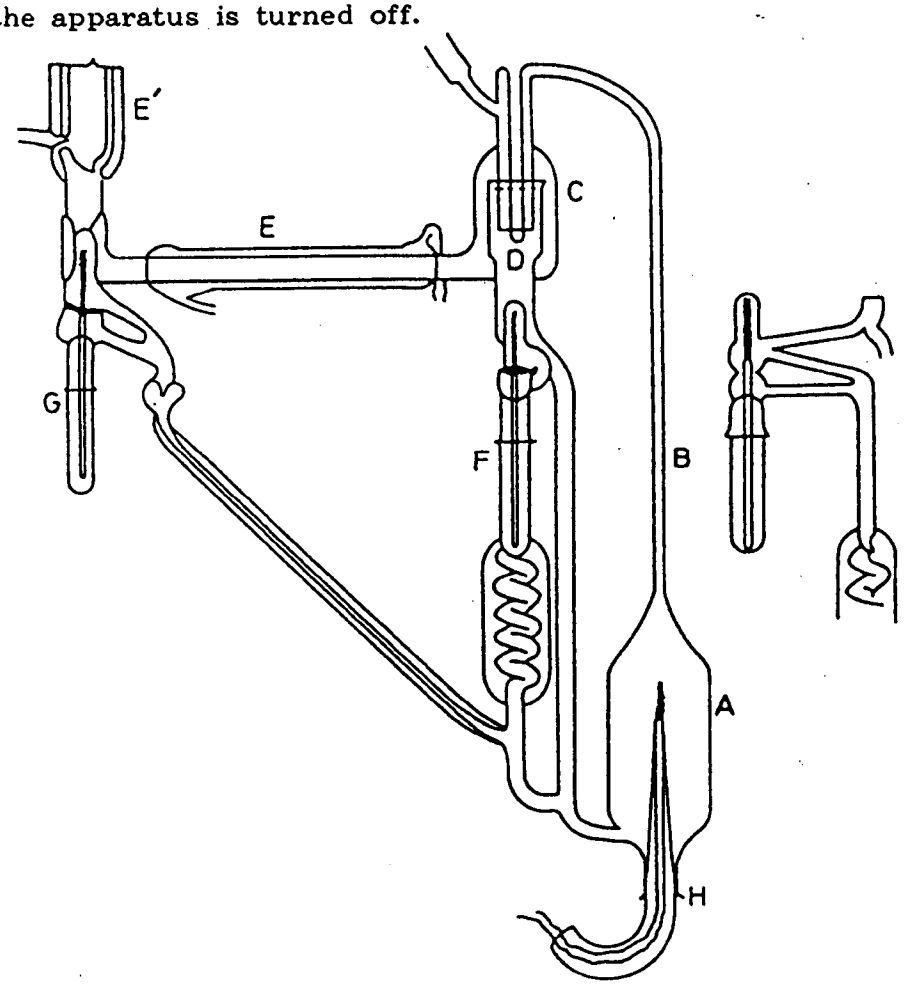

Figure 8.1. Brown's still.

8.3. STATIC TECHNIQUES

While dynamic methods are usually successful when the relative volatility of the components are not too high, static techniques are preferred when one of the components is virtually involatile. Brown's recirculating equilibrium still, for example, is normally employed for mixtures whose relative volatilities are of 1 to 14. Static phase apparatus for vapour pressure measurements have been reviewed by Williamson[6] and will not be discussed here.

An important type of static equipment for studying vapour liquid equilibrium at high pressures is the bubble and dew point apparatus. In this apparatus the sample of the mixture is confined over the mercury in the sealed end of a thick glass tube. The glass tube is connected to a pressure line (oil and/or nitrogen) provided with an oil-balance for pressure measurements. It is then inserted in a metal block thermostat at a desired temperature. The appearance and disappearance of the meniscus can be observed through a slit illuminated by a beam of light. The chief difficulty with static methods is that it is of fundamental importance to remove all air from the system. The degassing of the system and samples is the major experimental difficulty. Another form of the static method consists of introducing a two-phase mixture in the experimental cell at a controlled temperature and agitating the mixture. After the equilibrium has been reached, the sample is removed for analysis. If no provision is made for keeping the pressure constant this technique can lead to large errors.

Tsiklis and co-workers[8] built several static apparatuses which operate at pressures over 100 MPa to study the so-called "gas-gas" immiscibility phenomenon. The basic design consists of a high pressure cylinder containing a piezometer, mercury and the sample of known composition. The pressure transmitting liquid is forced into the cylinder by hydraulic oil acting on a pressure intensifier. This causes the mercury to enter the piezometer and compress the sample. After the system has been allowed to reach equilibrium, samples are carefully withdrawn for analysis while pressure is kept constant by pumping mercury into the piezometer. No visualisation of the equilibrium cell is possible.

Lindroos and Dodge[9] designed an apparatus for studying the barotropic effect observed in the ammonia + nitrogen system at about 200 MPa and 370 K. Their system could be operated at pressures up to 400 MPa. No provision was made to maintain the pressure constant after samples of each phase were extracted to be analysed. However, the authors argued that the average pressure drop (0.6% of the initial pressure) had negligible effect on the composition except in the critical region.

Several high pressure static apparatus provided with an optical system for visualisation of the cell have been built. Thodos and co-workers[10] designed an apparatus where the contents of the cell could be viewed through a glass window to investigate the system n-heptane + ethane. In more sophisticated cells, for the study of

fluid behaviour at higher pressures, no glass is used in the optical system. A particular complicated cell has been developed by Alwani and Schneider[11]. It was constructed from Nimonic 90 steel. The phase transitions are observed in the cell through a window made of synthetic sapphire. To stir the fluid mixture, the cell is provided with a magnetic ring which can be moved back and forward by means of an alternating polarity solenoid.

A bubble and dew point isothermal static apparatus was used here to study the phase behaviour of n-pentane + neopentane system. In this apparatus, a sample of known composition is entirely expanded in the gaseous phase at constant temperature and by slowly applying pressure, a small amount of liquid will eventually appear, i.e., the dew point. If the pressure is further increased, the sample will entirely condense except for a small trace of gas, i.e. the bubble point. There are two disadvantages associated with the bubble and dew point apparatus; firstly, the sample is in contact with mercury at relatively high temperatures (isothermal experiments were carried out at temperatures of up to 433.15 K). This drawback is overcome by subtracting the vapour pressure of the mercury from the final value of the pressure. Secondly, the co-existing vapour and liquid phases cannot be analysed.

Figure 8.2 displays a general view of the test rig. Temperatures were measured by a platinum resistance thermometer and pressures were measured by an oil-pressure balance specially designed for this purpose.

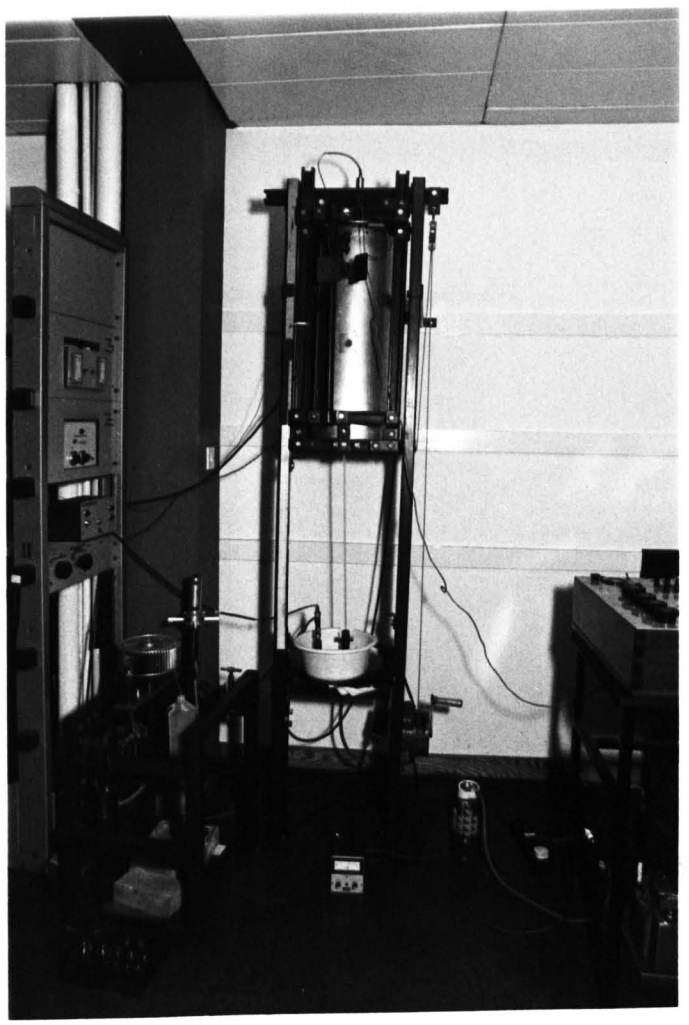

Figure 8.2. General View of the Test Rig.

8.4. THE OVEN

The metal-block thermostat was a cylinder of aluminium alloy ("duralumin") 450 mm long and 100 mm in diameter. It was designed and built by Ambrose et al.[12] at the National Physical Laboratory.

An axial hole (8 mm diameter) allowed the sample tube to be inserted and accommodate the platinum resistance thermometer. A horizontal hole (9 mm diameter) located at half height of the cylinder block was drilled to observe the sample. At the one end of the hole, a light bulb was installed, at the other a telescope was fixed to the frame which supports the thermostat. The bulb and the telescope allowed a clear visualisation of the sample. A brass tube running through the axis of the cylinder block accommodated the heater. Excessive heating loss was avoided by a series of saw cuts milled at each end of the brass tube. The oven is shown in Figure 8.3.

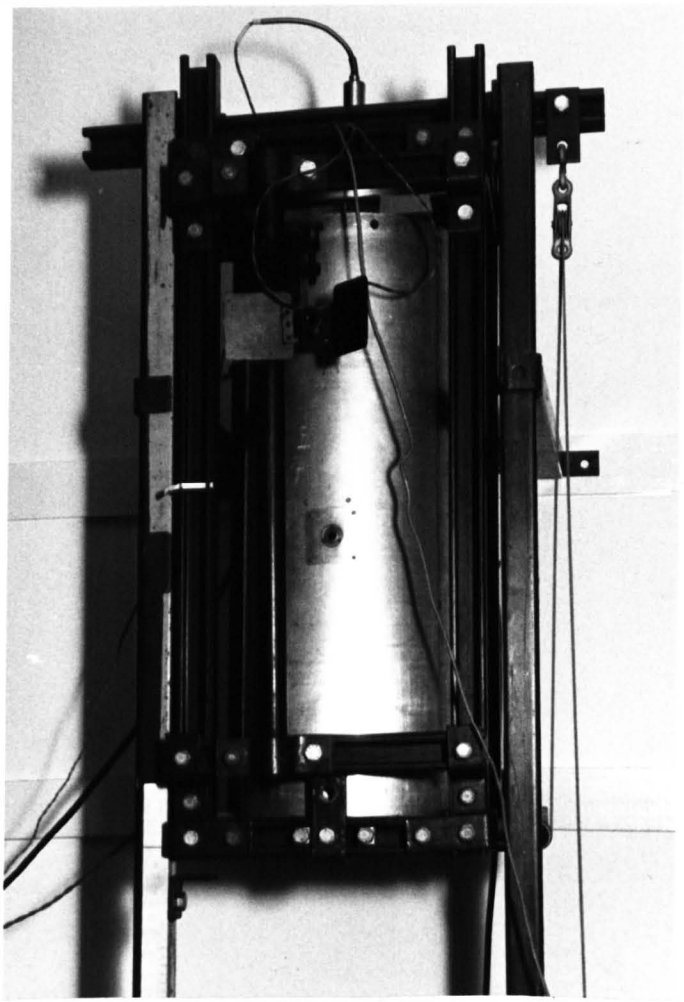

Figure 8.3. The Oven

The metal block was insulated with a layer of pre-formed pipe lagging (made of calcium silicate) wrapped with aluminium-covered corrugated asbestos paper. The whole assembly was suspended in a frame so that it could be lowered or lifted by means of tension cables and a crank. The sample tube which was sitting in the U-tube of the base plate was centred along the axis of the metal block. Care was taken to avoid contact between the sample tube and the oven which could result in breaking the glass sample tube.

8.5. TEMPERATURE GRADIENTS AND TEMPERATURE CONTROL

The temperature controller 'Thermotrol' (Hallikainen Instruments Ltd.) had two channels each of which could be attached to a heater. It was calibrated for the interval of temperature where the measurements were made (333.15 - 433.15 K). The coarse dial was used to reproduce accurately the temperature of the oven when set to a pre-estabilised value. The fine dial had to be adjusted manually to reach a desired temperature which corresponded to a value of resistance in the D.C. bridge (Croydon Precision Instruments).

The temperature inside the oven was kept constant to ±2 mK for periods of up to 10 hours. This was more than adequate to carry out all the required experiments.

Temperature gradients along the sample tube affect the measured pressures and therefore the values of bubble and dew points.

Sanchez[1] reduced the amount of sample present to keep temperature gradient effects to a minimum. He reported a maximum temperature gradient of 35 mK or less over lengths of up to 6 cm. This was considered satisfactory even when measuring dew pressures where volumes occupied by the sample exceeded 6 cm.

8.6 TEMPERATURE MEASUREMENTS

Measurements of temperature were carried out by a platinum resistance thermometer (Rosemount Engineering Model WS104), the resistance of which was measured by a D.C. bridge (Croydon Precision Instruments) operating at 1 mA and a 100 Ω resistor; the precision was better than 1 mK (see Figure 8.4). The thermometer was calibrated on the International Practical Temperature Scale (IPTS-68).

The temperature on IPTS-68[2] was calculated as follows:

$$T = t + 273.15\ K$$

where

$$t = t' + 0.045(t'/100^{\circ}C)[(t'/100^{\circ}C)-1][t/419.58^{\circ}C-1][(t'/630.74^{\circ}C)-1]$$

and t' was given by:

$$t' = (w(t') - 1)/\alpha + \delta(t'/100^{\circ}C)[(t/100^{\circ}C)-1]$$

the resistance ratio was defined by:

$$w(t') = R(t')/R(0^{\circ}C)$$

The relations above yield a quadratic polynomial which was solved analytically in t'. The constants $R(0^{\circ}C)$, α and δ were determined from measurements of R at the triple point of water and the normal melting temperatures of tin and zinc. These constants which were used throughout this work are:

$R = 25.5093\ \Omega$

$\delta = 1.49314\ K$

$\alpha = 0.00392306\ K^{-1}$

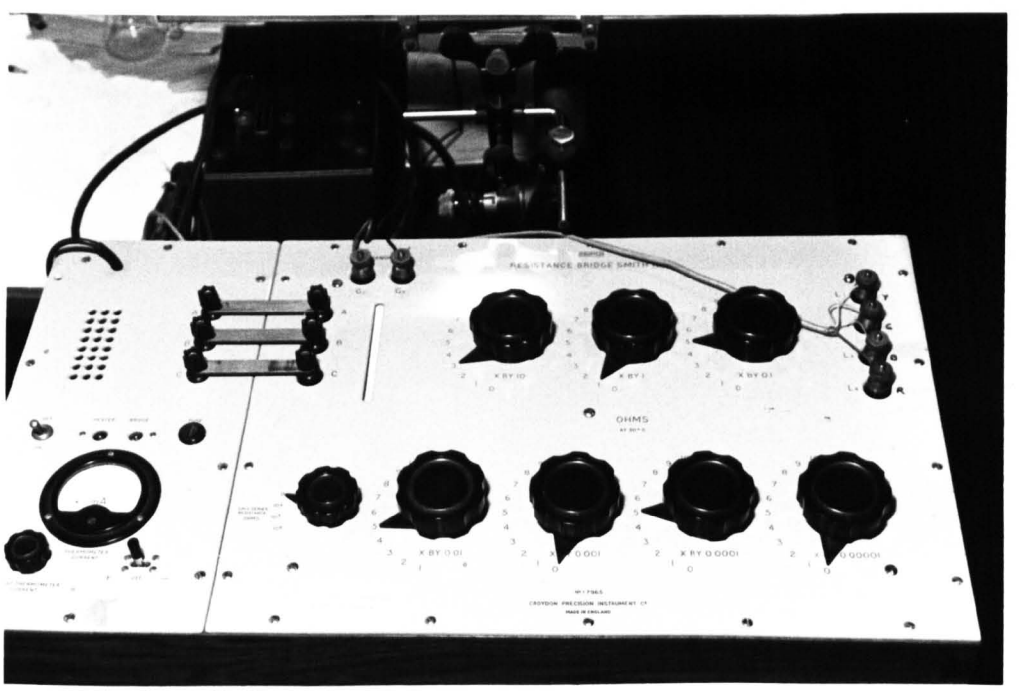

Figure 8.4. The D.C. Bridge

8.7. MEASUREMENT AND CALCULATION OF PRESSURE

The pressure line was supplied with oil as pneumatic fluid; the pressure was roughly controlled by a system of valves. Rough measurements were made on a sight gauge. Precise measurements of pressure were carried out by an oil-pressure balance manufactured by Budenberg Gauge Co. (Model CS3). Fine adjustments to the pressure were made by a hydraulic piston screw incorporated in the gauge.

The oil-pressure balance is of a simple type[13]. It consists of a high precision machined piston (nominal area A_o = 129.032 mm^2) sliding on a cylinder jacket. Due to a clearance between piston and cylinder, oil leaks out and is collected in a flask when pressure is applied. Pressure exerted by the balance is achieved by loading it with known brass and dead-weights and its value calculated from the effective area of the piston. The balance is also provided with a table with blades which rotates by means of a continuous jet of compressed air. This is to minimise friction between the piston and the cylinder jacket.

The pressure p exerted by the sample was calculated by the following equation:

$$p = \frac{W}{A} + p_a + h_o \rho_o g - h_m \rho_m g - h_\ell \rho_\ell g - p_m$$

The terms W/A and p_a are the pressures exerted by the balance and the atmosphere respectively. Corrections were made for

variation of temperature and pressure in the nominal area A of the piston. The following equation expresses the effective area of the piston as a function of the applied pressure p at a temperature T.

$$A = A_o\ (1 + \alpha p)\ [1 + \lambda(T - 293.15\ K)]$$

with

α = 4.1 x 10^{-9} kPa

λ = 2.3 x 10^{-5} K^{-1}

A_o = 129.032 mm^2 at reference T = 293.15 K.

The value of the downward force W exerted by the weights was also subjected to corrections to account for the effect of upthrust of the air as follows:

$$W = \sum_i M_i\ g\ (1 - \rho_a/\rho_w)$$

where

M_i are the masses of the dead-weights, the piston and the table with blades. Table 8.1 lists these masses as weighed by Sanchez[1]. The local value acceleration of free fall is 9.811856 m/s^2. ρ_a and ρ_w are the densities of air and dead-weights (8 g cm^{-3}) respectively.

The atmospheric pressure p_a was measured with a mercury-in-glass barometer; corrections were made due to expansivity of the mercury and brass scale. The uncertainty in the measurement of the atmospheric pressure is approximately 0.02 kPa.

TABLE 8.1.

THE MASSES M_i OF THE DEAD-WEIGHTS

Weights marked as	M_i (in grams)	Weights marked as	M_i (in grams)
100,1	5669.10	50,1	2834.65
100,2	5669.44	20,1	1133.85
100,3	5670.00	15,1	849.95
100,4	5669.27	10,1	566.77
100,5	5669.41		
100,6	5669.33	piston	347.375
100,7	5669.38	table with	
100,8	5669.95	blades	261.248
100,9	5669.97		
100,10	5669.23		
mean value	5669.51		

The terms containing $h\varrho g$ are the hydrostatic heads exerted by a column of fluid of height h, density ϱ, and the local acceleration of free fall g.

The subscripts o, m and ℓ denote oil, mercury and liquid sample respectively. The vapour pressure p_m of the mercury at the temperature of the sample was subtracted from the calculated pressure. Figure 8.5 shows the heights used to calculate the hydrostatic heads.

On the left-hand side of the U-tube two electrical probes (A & B) were installed to help locate the initial level of the mercury.
When the level of mercury is too high, it touches the bottom of probe B switching the red light on in the mercury level indicator box. In such an event, a rotary pump connected to the right-hand side of the U-tube (at D in Figure 8.5) may drain the excess mercury. If neither the red light nor the green light (bottom of probe A in Figure 8.5) are switched on the level of mercury is too low. No experiment should be attempted and mercury must be added until the green light is on. For the bubble and dew point measurements where the length of the sample tube had to be increased in order to determine the dew pressures, the initial level of mercury was kept at the bottom of probe B. Once the sample tube has been mounted in the U-tube, and all experiments were made, the initial height of mercury could be determined. This was done by lowering the column of mercury at the right-hand side of the U-tube until the green light switched on. The initial height of mercury is represented by h_3 in Figure 8.5.

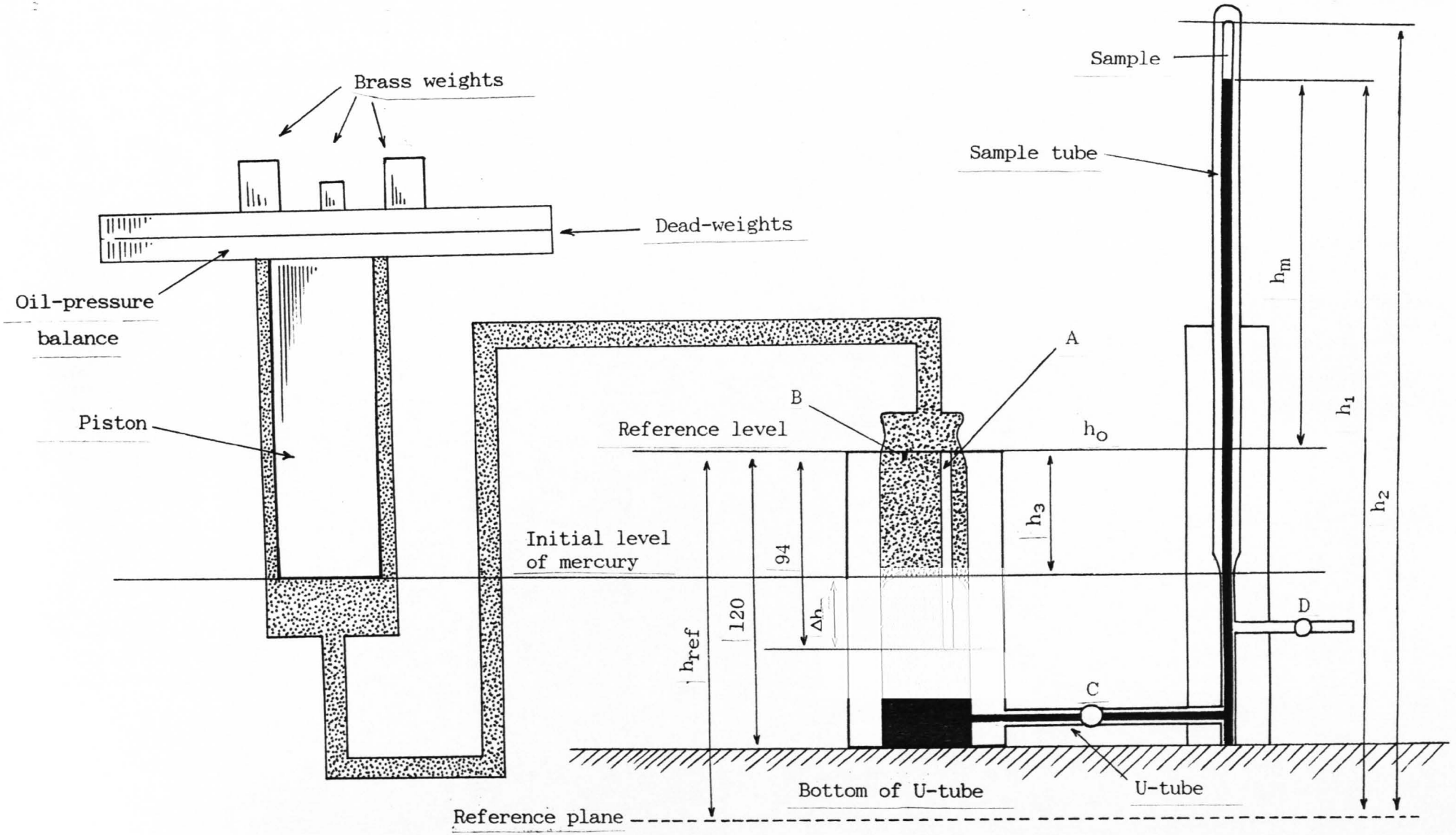

Figure 8.5. Heights used in the calculation of hydrostatic heads. The oil-balance, the sample tube and U-tube are also shown.

Once the initial height of mercury has been established a correction due to the expansivity of the sample had to be determined. The displacement of the mercury is calculated using the relation between the volume of the sample tube and the volume of the left-hand side of the U-tube. This is given by:

$$\Delta h_u \frac{1}{4} \pi d^2_u = \Delta h_s \frac{1}{4} \pi d^2_s \qquad (8.1)$$

where the subscripts of u and s refer to left-side mercury filled U-tube and sample respectively. The diameter d_u is 1.175 cm (measured with a vernier) while the internal diameter of the precision-bore capilllary d_s = 0.25 cm. When these values are inserted in equation 8.1, the displacement of the mercury is given by:

$$\Delta h_u = 0.04527\ \Delta h_s$$

The displacement of the mercury Δh_s was measured by a cathetometer. The uncertainty in Δh_s taking into account temperature gradients in the mercury is 1 mm. The height of mercury $h_{\acute{m}}$ was determined by difference between two values:

$$h_{\acute{m}} = h_1 - h_{ref}$$

where

h_1 and h_{ref} are heights measured by a cathetometer from a given reference plane (represented by a dotted line in Figure 8.5). The final value of h_m in the term $h_m \rho_m g$ in equation 8.2 is as follows:

$$h_m = h_{\acute{m}} + h_3 + \Delta h_u \qquad (8.2)$$

The density of mercury ρ_m was calculated according to Hugill[14] who divided the column of mercury in the right-hand side of the U-tube into three parts. The section outside the oven, the section within the insulation of the oven where the sample is located and the section inside the metal block down to the bottom of the oven. The mercury density for this zone is evaluated by an arithmetic mean of the densities in the other sections.

The uncertainties in the measurements of h_1, h_{ref}, and h_3 for evaluation of the hydrostatic head of the mercury are approximately 0.3 kPa.

The hydrostatic head of oil is calculated by taking the density of oil as 878 kg m^{-3} (Shell Tellus 27). The contribution of the hydrostatic head of oil for the final value of the pressure was never greater than 1.5 kPa.

In the calculation of the hydrostatic head of the liquid $h\rho g$, the height of the liquid ($h_\ell = h_2 - h_1$) was never greater than 10 mm in all measurements. The density of the liquid was always taken to be that at reference temperature (293.15 K). With this assumption, the hydrostatic head of the liquid was always less than 0.1 kPa. In the calculation of dew pressures, the hydrostatic head of the liquid is replaced by that of the vapour. The density of the vapour was evaluated by taking into account the mass of the sample and its volume when totally expanded in the gaseous phase.

The vapour pressure of the mercury was evaluated by the Chebyshev equation given by Ambrose and Sprake[14]. The contribution of the vapour pressure of the mercury was never greater than 0.6 kPa.

The uncertainty δp in pressure came mainly from three sources: (i) the hydrostatic head of mercury (approximately 0.3 kPa), (ii) the uncertainty in the area of the piston of the pressure balance which contributed to about 5×10^{-4} p (pressure balance value), and (iii) the uncertainty in locating the level of mercury on the left-hand side of the U-tube (approximately 4 kPa).

8.8. MATERIALS

8.8.1. n-Pentane

The n-pentane was obtained from Aldrich Chemicals with a mole fraction purity of 0.9995 (research grade). The substance was used without any further purification.

8.8.2. 2,2-dimethylpropane (neopentane)

The neopentane was obtained from Argo International with a mole fraction purity of 0.99. The impurities according to the manufacturer, consisted of less than 0.01 of n-butane and traces of cis-2-butene. The substance was further purified by means of 5A molecular sieves placed in a flask which was left overnight before

use. Both n-pentane and neopentane were degassed by freezing with liquid nitrogen and pumping off the non-condensables. The freezing-melting process was repeated six times.

8.9. PREPARATION OF SAMPLES

The samples of pure n-pentane, pure neopentane, and of mixtures were prepared at the Department of Chemistry, City University, London. A vacuum line shown in Figure 8.6 was used for the transfer of small quantities of each component to the sample tube. It consisted of a one-piece glass tube with incorporated arms. The sample tube, flasks, and the calibrated capillary tube were connected to the arms by vacuum "Young" joints and vacuum taps.

Small quantities of n-pentane in a flask were transfered to the sample tube after the vacuum line was degassed over a period of one hour. Similarly, when samples of neopentane were required the flask

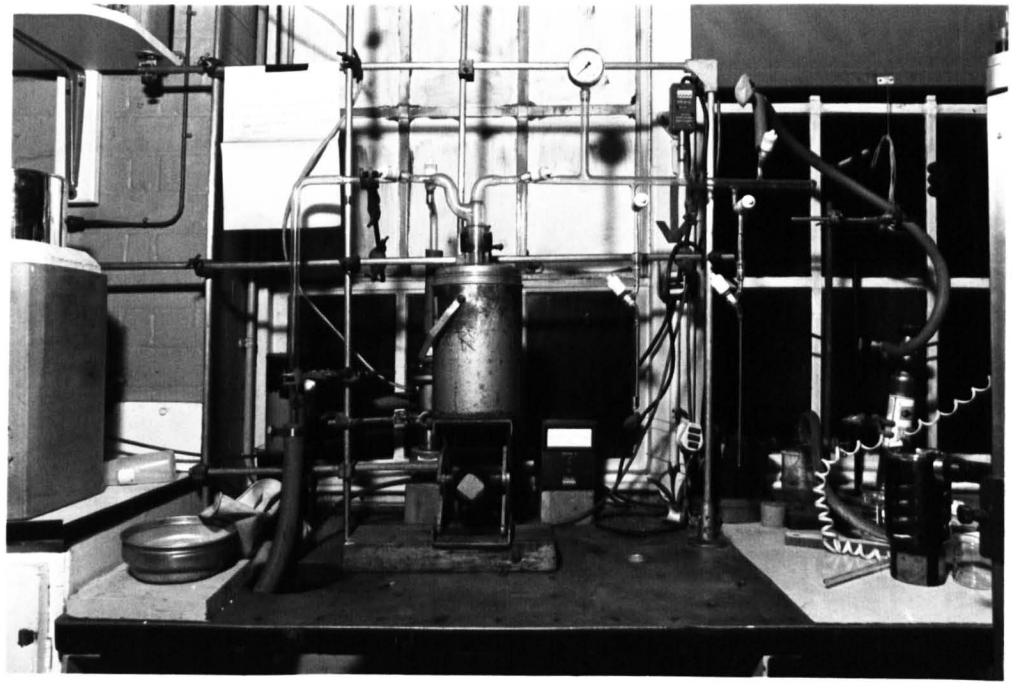

Figure 8.6. The vacuum line.

was replaced by one containing neopentane. The amount of substance used never exceeded 30 mm^3. After the sample tube had been filled, it was sealed off at the lower end by a torch.

8.9.1. Calibrated Capillary Method

For preparing mixtures a 10 mm bore precision capillary as shown in Figure 8.7 was used. Once the vacuum line had been degassed small quantities of pentane and neopentane were transferred to the capillary tube. The height was then measured by a cathetometer reading 0.01 mm. The sample was then transferred to the sample tube cooled under liquid nitrogen.

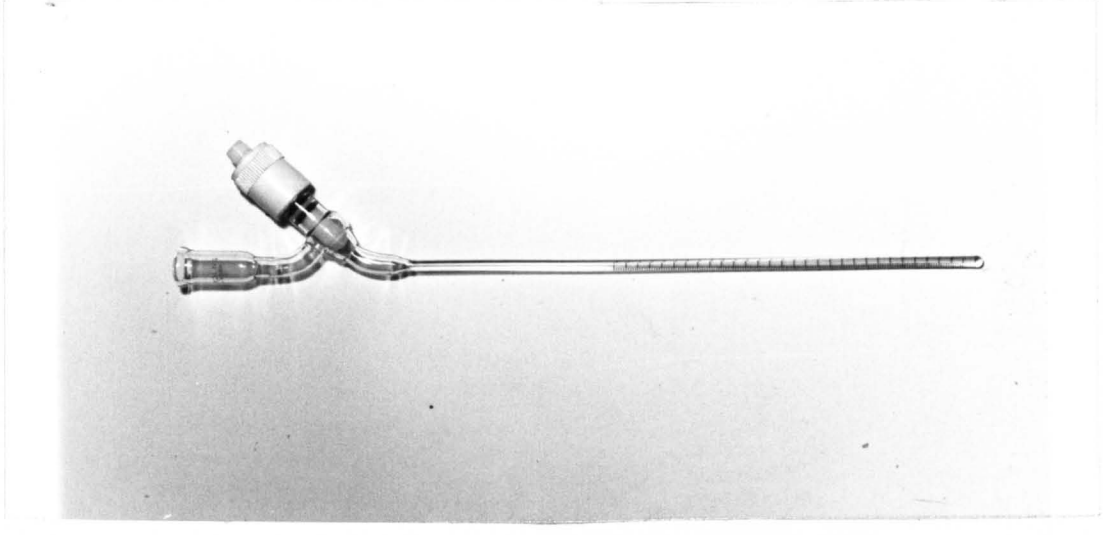

Figure 8.7. The 10 mm i.d. calibrated capillary tube used for the samples of binary mixtures.

The amounts of each component present were determined as follows:

$$m\ (C_5H_{12}) = h\ \rho\ (C_5\ H_{12})\ A/M\ (C_5H_{12})$$

where

m = mass of either component

h = the height measured

A = the cross-sectional area of the capillary tube

M = the molar mass of either pentane or neopentane.

The random uncertainty of this method of preparing mixtures is given by:

$$d_m/m(C_5H_{12}) = \{d\rho/\rho(C_5H_{12})\}^2 + (dA/A)^2 + (dh/h)^2 + \{dM/M(C_5H_{12})\}^2$$

The uncertainty in dA/A given by the manufacturer was 7×10^{-3}. The value of $d\rho/\rho$ for both pentane and neopentane was kept to a minimum by maintaining the capillary tube in a large beaker of water at controlled temperature. The dominant term was always dh/h but the uncertainty in preparing the sample was less than 0.01.

8.10. THE PROCEDURE FOR MOUNTING THE SEALED SAMPLE TUBE IN THE U-TUBE

8.10.1. The U-Tube

The U-tube was situated below the oven inside a plastic bucket. At the top of the left-hand side the mercury probe was firmly tightened. The pressure line was also connected to this side of the U-tube. Two valves were incorporated; valve C situated between the two arms roughly controlled the flow of mercury and valve D on the right-hand side of the U-tube connected it to a vacuum pump. Figure 8.8 shows schematically a glass-to-metal union incorporated in the U-tube for mounting the sample tube.

8.10.2. The Mounting of the Sample Tube

The sample tube was made of borosilicate glass tube about 72 cm long before filling (see Figure 8.9). The bottom (8 cm long) made of thin-walled glass allowed breaking of the tube with relative ease. The lower end of this thin-walled glass was provided with a swelling to locate a metal washer and an O-ring to accomplish the breaking. The remaining 64 cm was a thick-walled capillary (i.d. = 2.5 mm and o.d. 7.2 mm) which was sealed at the top. The lower end of this part was also provided with a swelling to accommodate 3 elastomer rubber rings and a ring made of PTFE as shown in Figure 8.8. In the original design, the upper part of the sample tube (about 10 cm long) had a larger internal diameter (i.d. = 3 mm) where all the expansions, compressions, and measurements took place. This design of the sample tube was not possible in the modified version of the oven used for this work.

The mounting of the sample tube was as follows: with valve D closed, a rotary vacuum pump was connected to the U-tube and was left switched on for more than 2 hours. The pressure was then measured with a Pirani gauge. The vacuum attained was approximately 5×10^{-2} Pa.

With valve C open to the atmosphere, the U-tube was filled with tripled-distilled mercury until its level reached approximately the entrance of valve D. The level of mercury on the left-hand side of

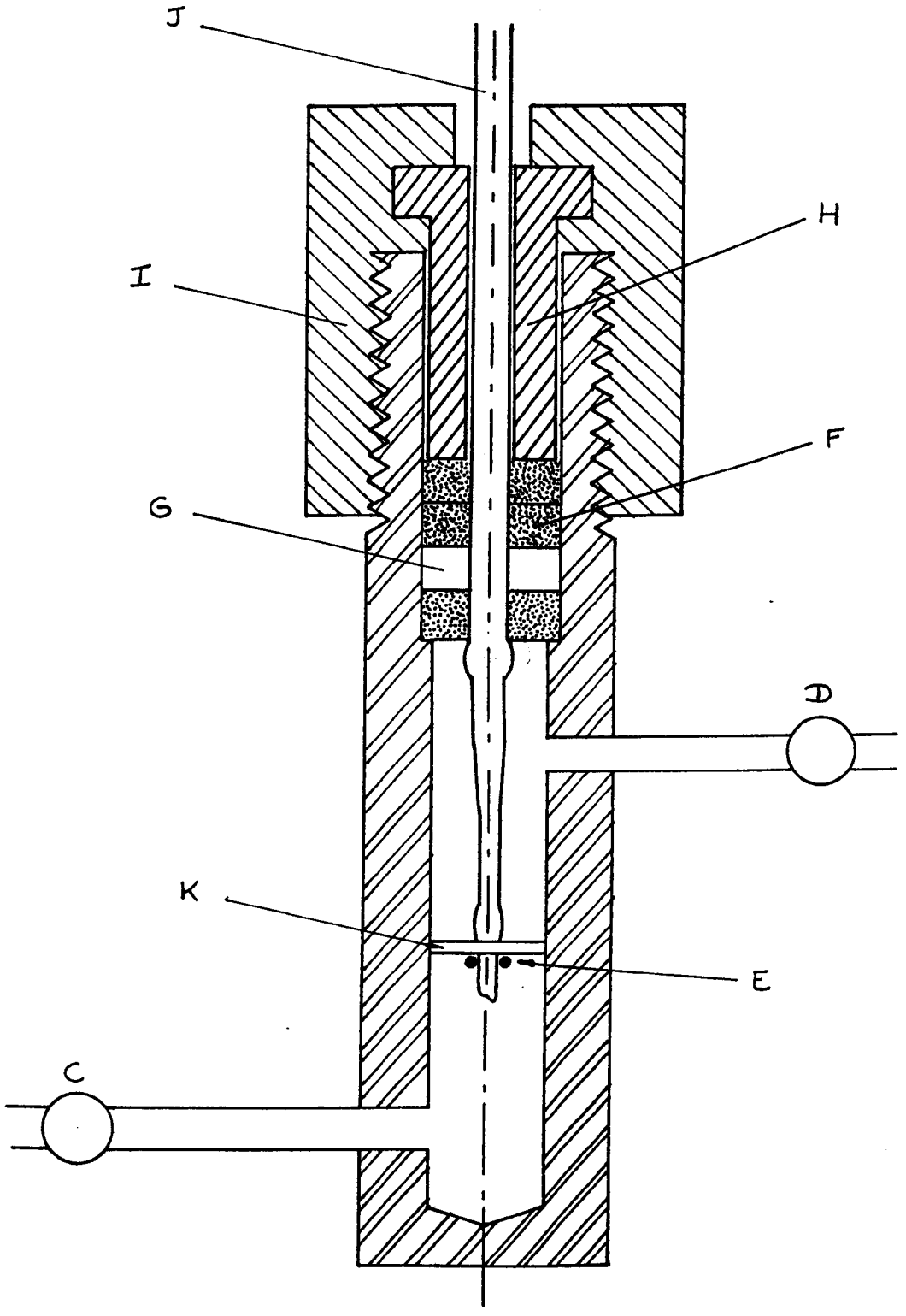

Figure 8.8. Glass-to-metal pressure-tight union

E = O-ring
F = elastomer rubber sealing rings
G = PTFE spacer
H = gland
I = cap screw
J = sample tube.
k = washer

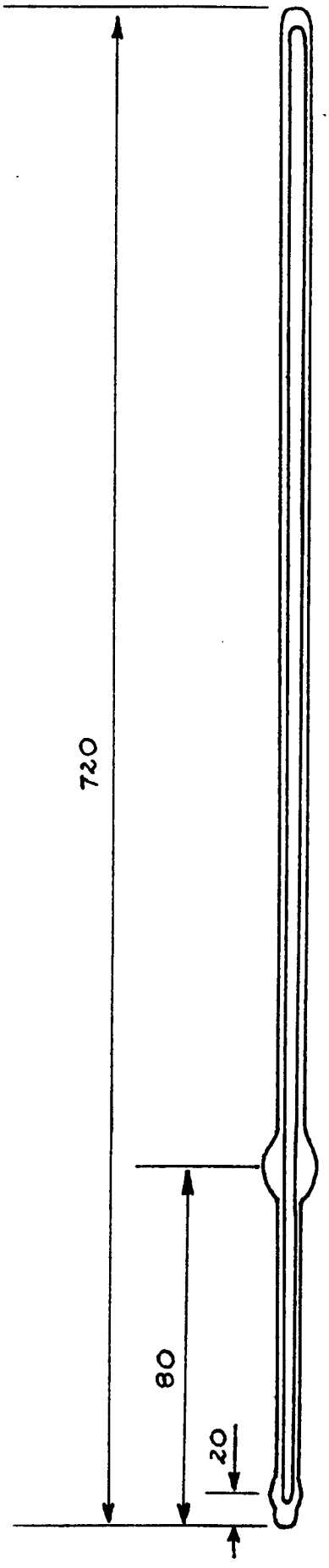

Figure 8.9. A sealed sample tube (not drawn to scale). (i.d. = 2.5 mm and o.d. = 7.1 mm)

the U-tube was indicated by the red light on at mercury level indicator box. With valve C closed, the oil-pressure line was then connected to the left-hand side of the U-tube and tested for leaks.

After the PTFE spacer and rings had been held in place as illustrated in Figure 8.8 a cut was made in the sample tube at approximately 2 cm below the upper swelling to accomplish the breaking. The top of the sample tube was then immersed in liquid nitrogen to freeze the sample.

With the sample tube held in place, gland H, and cap nut I, were inserted and hand-tightened very gently. The sample was kept frozen by pouring small quantities of liquid nitrogen on top of a glove-like cloth.

With valve C shut and valve D opened, to evacuate the space between rings and the mercury, the sample tube was gently rocked until breakage. Valve D was then shut and valve C quickly opened while mercury rose up the sample tube trapping the sample at the top. The cap nut was tightened further. The glove-like cloth was removed and the sample tube allowed to be defrosted.

The sample tube was aligned properly by means of shims placed under the plate base below the plastic bucket. The oven was then very carefully lowered over the sample tube.

Having taken all these precautions it was important to test the system for leaks.

REFERENCES

1. Sanchez, C.J. Ph.D. Thesis, University College, London, (1987).

2. Ambrose, D. "Vapour Pressures" Pure & Applied Chemistry Experimental Thermodynamics, Vol.II, IUPAC, Editors, B.Le Neindre and B. Vodar. Butterworths. (1975).

3. Fowler, L, Trump, W.N. and Vogler, C.E. J.Chem.Eng.Data. Vol.13, 209, (1968).

4. Cottrell, F.G. J.Am.Chem.Soc., Vol.41, 721, (1919).

5. Sameshima, J. J.Am.Chem.Soc., Vol.40, 1483, (1918).

6. Williamson, A.G. in Experimental Thermodynamics Vol.II, Editors, Le Neindre and Vodar. Butterworths, Chp.16, (1975).

7. Brown, I. Aust.J.Sci Research, A5, 530, (1952).

8. Tsiklis, D.S. and Rott, L.A. Russ.Chem.Rev., Vol.36, 351, (1967).

9. Lindroos, A.E. and Dodge, B.F. Chem.Eng.Prog.Symp., Vol.148, No.3, 10, (1953).

10. Thodos, G. and Ekiner, O. J.Chem. & Eng.Data, Vol.11, 154, and 457 (1966).

11. Alwani, Z. and Schneider, G.M. Ber.Bunsengesellschaft Phys.Chem., Vol.73, 294, (1969).

12. Ambrose, D., Broderick, B.E. & Townsend, R. J.Chem.Soc., A., 633, (1967).

13. Lewis, S. & Peggs, G.N. "The Pressure Balance, a Practical Guide to its use". NPL, London (1979).

14. Ambrose, D. & Sprake, C.H.S. J.Chem. Thermodynamics, Vol.4, 603-620, (1972).

15. Hugill, J.A. Ph.D. Thesis, University of Exeter (1978).

CHAPTER 9

RESULTS AND DISCUSSION

9.1. VAPOUR PRESSURES OF PURE n-PENTANE AND PURE 2,2-DIMETHYLPROPANE

9.1.1. Vapour pressures of n-pentane

Previous measurements of the vapour pressures of n-pentane have been made by several authors [1], [2], [3], [4] covering a large range of temperatures. Osborn and Douslin[1] correlated their results in terms of Cox vapour pressure equation. A fair agreement was found for the range of temperatures covered by Beattie et al[4]. However, they pointed out that the agreement with Messerly and Kennedy[2] measurements was poor in the temperature range 283 to 298 K.

It was the intention of the author to repeat some of those measurements to become familiar with the methods of preparing samples and with the apparatus. The range of temperatures covered (333 to 433 K) was chosen more or less arbitrarily. Indeed, the aim of the experimental work was rather to test the usefulness of the Redlich-Kwong-Soave equation of state than to measure vapour pressures. That range of temperatures was found more adequate for this purpose.

The results of measurements of the vapour presure of pure n-pentane are shown in Table 9.1. These were correlated in terms of Lee and Kesler and Wagner vapour pressure equations. These equations are as follows:

Fluid n-Pentane (research grade) Temperature	Experimental vapour pressures	Lee & Kesler vapour pressures equation	Error $\frac{\text{Exp-Theo}}{\text{Exp}}$ x100	Wagner vapour pressure equation	Error $\frac{\text{Exp-Theo}}{\text{Exp}}$ x100
K	kPa	kPa	%	kPa	%
333.145	218.7	215.7	1.37	214.19	2.1
353.145	371.5	371.3	0.05	367.47	1.09
373.149	598.9	598.4	0.08	591.8	1.2
393.155	917.3	914.5	0.30	905.26	1.3
413.153	1347.1	1339.4	0.57	1327.85	1.4
433.154	1898.8	1896.9	0.10	1885.9	0.68

Remarks: Uncertainty in all measurements with n-Pentane was ± 4 kPa

Table 9.1. Vapour pressure measurements of n-Pentane (C_5H_{12})

$$\ln P_{vpr} = f^{(o)}(T_r) + \omega f^{(1)}(T_r)$$

$$f^{(o)} = 5.92714 - \frac{6.09648}{T_r} - 1.28862 \ln T_r + 0.169347 T_r^6$$

$$f^{(1)} = 15.2518 - \frac{15.6875}{T_r} - 13.4721 \ln T_r + 0.43577 T_r^6$$

(Lee & Kesler)

$$\ln P_{vp} = \frac{a\tau + b\tau^{1.5} + c\tau^3 + d\tau^6}{T_r}$$

(Wagner)

where $\tau = 1 - T_r$. Values of a, b, c and d were from Reid et al.[5]. As can be seen from Table 9.1 experimental results are in very good agreement with theoretical predictions.

9.1.2. Vapour pressures of 2,2-dimethylpropane (neo-pentane)

Beattie, Douslin and Levine[6] have measured the vapour pressure of neopentane from 323.15 K to the critical point. Aston and Messerly[7] covered experimental pressures in the range 258 to 283 K while Osborn and Douslin[1] measured the vapour pressures in the intermediate range 267 to 313 K.

Although the vapour pressures of neopentane were measured at the same temperature range as with the n-pentane the main purpose here was to determine its critical point. This allowed to test the accuracy of the apparatus. the critical temperature of the 2, 2-dimethylpropane was found to be in excellent agreement with the literature value[6]. The critical temperature, however was 0.81 degrees lower than the accepted value, possibly due to impurities (mainly n-butane C_4H_6) in the sample.

Fluid neo-Pentane (99% pure*) Temperature	Experimental vapour pressures	Lee & Kesler vapour pressures equation	Error Exp-Theo / Exp x100	Wagner vapour pressure equation	Error Exp-Theo / Exp x100
K	kPa	kPa	%	kPa	%
333.150	468.33	463.1	1.11	460.95	1.60
353.149	742.58	739.9	0.36	736.94	0.76
373.149	1128.5	1121.4	0.63	1118.86	0.86
393.155	1640.64	1631.2	0.57	1630.7	0.61
413.153	2324.33	2299.7	1.06	2299.78	1.06
433.15	not measured	3169.7		3161.7	

* further purified using 5Δ molecular sieves)

Table 9.2. Vapour pressures of 2, 2-dimethylpropane (C_5H_{12}) and its critical point value.

Critical point of 2,2-dimethylpropane (C_5H_{12})

	Literature value[6]	This Work	
P_c	3200	3202.1	kPa
T_c	432.99	433.80	K

Vapour pressures of neo-pentane are given in Table 9.2 and were correlated as before with Less and Kesler and Wagner vapour pressure equations. The constants for the Wagner equation were found in [5].

9.2. BUBBLE AND DEW PRESSURES OF n-PENTANE + 2,2-DIMETHYLPROPANE $\{(1-x)C_5H_{12} + xC_5H_{12}\}$

The only previous vapour-liquid equilibria data found on the mixture $\{(1-x)C_5H_{12} + xC_5H_{12}\}$ were those of Hoepfner, Kreibich and Schaefer[6]. Vapour pressures were measured for 10 different compositions at five different temperatures (253.15 K, 263.15 K, 273.15 K, 283.15 K, and 293.15 K). The critical point for n-pentane + 2,2-dimethylpropane system was also measured for 4 different compositions by Partington, Rowlinson and Weston[7]. Table 9.3 shows a comparison between measured and predicted values (theoretical values were those for which convergence was achieved) using the Redlich-Kwong-Soave equation of state. These are in excellent agreement with experimental data.

Liquid mole fraction n-pentane	Experimental Literature values[7] T_c (K)	Theoretical Predictions This Work T_c (K)
0.175	440.6	440.14
0.350	447.4	446.68
0.576	455.5	454.80
0.791	462.7	462.40

Table 9.3. Comparison between measured and predicted values of the critical point of $\{(1-x)C_5H_{12} + xC_5H_{12}\}$ system for 4 different compositions.

The 60 experimental bubble and dew presures from this work started at 333.15 K up to 433.15 K in steps of 20 K. Five different compositions were studied. Tables 9.4, 9.5, 9.6, 9.7 and 9.8 present bubble and dew pressures measured along with predicted RKS values.

9.3. FURTHER COMMENTS

Measurements of vapour pressure of neopentane by Levine et al[4] have shown a maximum error of 0.33%. These which appear to be at first sight better than those obtained by the author were correlated by a specific vapour pressure equation. For n-pentane no comparisons were possible. Douslin[1] used the Cox vapour pressure equation but only gives a graphical representation of the derivations. In addition, the range of temperatures covered by this work (333 - 433°K) were not measured before.

Temperature	Experimental bubble pressure	RKS equation of state	Error $\frac{\text{Exp-RKS}}{\text{Exp}}$ x 100	Experimental dew pressure	RKS equation of state	Error $\frac{\text{Exp-RKS}}{\text{Exp}}$ x 100
K	kPa	kPa	%	kPa	kPa	%
333.153	277.8	264.42	4.81	233.4	241.87	-3.6
353.149	458.46	441.9	3.61	398.7	414.38	-3.9
373.149	719.3	703.35	2.21	648.8	666.5	-2.7
393.155	1075.03	1060.8	1.32	996.7	1018.1	-2.14
413.153	1548.4	1536.2	0.78	1472.3	1490.4	-1.23
433.154	2167.13	2149.9	0.79	2085.3	2106.0	-1.00

Remarks: Uncertainty in all measurements ± 4kPa

Table 9.4. Bubble and dew pressures of $\{(1-x)\ C_5H_{12} + x\ C_5H_{12}\}$ for x = 0.2017

Temperature	Experimental bubble pressure	RKS equation of state	Error $\frac{\text{Exp-RKS}}{\text{Exp}}$ x 100	Experimental dew pressure	RKS equation of state	Error $\frac{\text{Exp-RKS}}{\text{Exp}}$ x 100
K	kPa	kPa	%	kPa	kPa	%
333.153	368.25	363.04	1.41	327.4	321.3	1.84
353.149	601.34	591.91	1.57	546.6	538.4	1.51
373.149	922.67	913.58	0.98	861.3	849.65	1.35
393.155	1361.83	1347.7	1.03	1291.4	1276.6	1.14
413.153	1928.32	1914.2	0.73	1862.3	1842.8	1.05
433.154	2649.63	2631.8	0.67	2596.4	2574.4	0.84

Remarks: Uncertainty in all measurements ± 4 kPa

Table 9.5. Bubble and dew pressures of $\{(1-x)C_5H_{12} + xC_5H_{12}\}$ for x = 0.6043

	Bubble Pressure pressure in kPa	RKS equation of state pressure in kPa	Error in %	Dew Pressure pressure in kPa	RKS equation of state pressure in kPa	Error in %
Temperature °C	Experimental	Theoretical	$\frac{\text{Exp-RKS}}{\text{Exp}}$ x100	Experimental	Theoretical	$\frac{\text{Exp-RKS}}{\text{Exp}}$ x100
333.153	427.2	413.6	-3.2	368.4	382.9	3.7
353.149	683.7	668.5	-2.2	617.8	630.06	1.9
373.149	1026.4	1023.9	-0.24	936.6	979.0	4.3
393.153	1491.7	1500.4	0.58	1452.1	1407.5	3.0
413.153	2098.7	2118.7	0.94	2013.5	2072.8	2.8
433.154	2886.3	2897.9	0.40	2822.2	2868.4	1.61

Uncertainty in all measurements were ±4 kPa.

Table 9.6. Bubble and dew pressures of {(1-x) C_5H_{12} + x C_5H_{12}} for x = 0.8089

	Bubble Pressure pressure in kPa	RKS equation of state pressure in kPa	Error in %	Dew Pressure pressure in kPa	RKS equation of state pressure in kPa	Error in %
Temperature °K	Experimental	Theoretical	$\frac{\text{Exp-RKS}}{\text{Exp}}$ x100	Experimental	Theoretical	$\frac{\text{Exp-RKS}}{\text{Exp}}$ x100
333.153	479.8	441.14	-8.76	393.76	425.07	7.3
353.149	741.54	710.37	-4.3	687.3	690.6	0.47
373.149	1060.3	1084.6	2.2	975.3	1061.9	8.1
393.155	1593.35	1585.1	-0.52	1497.72	1561.2	4.0
413.153	2228.9	2233.6	0.21	2117.8	2211.8	4.2
433.154	3051.4	3050.5	-0.03	2980.6	3040.1	1.9

Uncertainty in all measurements were ± 4 kPa.

Table 9.7. Bubble and dew pressures of {(1-x) C_5H_{12} + x C_5H_{12}} for x = 0.9185

Temperature	Experimental bubble pressure	RKS equation of state	Error $\frac{\text{Exp-RKS}}{\text{Exp}}$ x 100	Experimental dew pressure	RKS equation of state	Error $\frac{\text{Exp-RKS}}{\text{Exp}}$ x 100
K	kPa	kPa	%	kPa	kPa	%
333.153	338.2	311	8.04	283.3	274.21	3.2
353.149	540.97	513.7	5.0	474.2	465.7	1.8
373.149	828.2	801.8	3.1	716.9	743.3	-3.7
393.155	1220.5	1194.6	2.1	1159.3	1127.9	2.7
413.153	1733.75	1711.7	1.27	1596.8	1641.9	-2.8
433.154	2400.3	2372.2	1.17	2329.5	2309.6	0.85

Remarks: Uncertainty in all measurements ± 4 kPa

Table 9.8. Bubble and dew pressures of $\{(1-x)C_5H_{12} + x\ C_5H_{12}\}$ for x = 0.3919

Sets of experimental VLE data are normally tested for thermodynamic consistency. For the data to be consistent an integral test developed by Chueh et al[8] is usually employed. This consistency test requires vapour mole fractions and liquid phase densities but these values were not obtained experimentally. An attempt to estimate liquid phase densities by an equation of state could introduce large errors and falsify the test. However, for practical engineering applications, the Redlich-Kwong-Soave equation of state in the case of light hydrocarbons is generally accepted to be adequate to predict accurately thermodynamic properties and vapour-liquid equilibria[9]. Therefore the author concluded that the phase equilibria behaviour of the binary system considered in this study can reliably be predicted from mixture P-V-T data using RKS equation of state with classical mixing rules.

REFERENCES

1. Osborn, A.G. and Douslin, D. J.of Chemical and Eng.Data., Vol.19, No.2, (1979).

2. Messerly, G.H. and Kennedy, R.M. J.of Amer.Chemical Soc., Vol.65, 803, (1943).

3. Willingham, C.B., Taylor, W.J. Pignocco, J.M. and Rossini, F.D. J.Res.Nat.Bur.Stand., Vol.35, 219, (1945).

4. Beattie, J.A., Levine, S.W. and Douslin, D.R. J.Amer.Chem.Soc., Vol.58, 2355, (1936).

5. Reid, R., Prausnitz, J.M. and Poling, B. "The Properties of Gases and Liquids", McGraw-Hill, 4th Ed., (1987).

6. Hoepfner, A., Kreibich, U.T. and Schaefer, K. Ber.Bunsenges, Phys., Chemie, Vol.74, 1016, (1970).

7. Partington, E.J., Rowlinson, J.S. and Weston, J.F. Trans.Faraday Soc., Vol.56, 479, (1960).

8. Chueh, P.L., Muirbrook, N.K., and Prausnitz, J.M. Multicomponent vapour-liquid equilibria at high pressures. J.of Amer.Inst.of Chem.Eng., Vol.11, 1092-1102, (1965).

9. West, E.H. and Erbar, J.H. Procs.52nd Annual Convention of the NGPA, pp.50-61, Natural Gas Proc.Assoc., Tulsa (1973).

CHAPTER 10

CONCLUSIONS

The search for a working fluid for a TFC system in which condensation would take place at approximately 35°C after adiabatic expansion with approximately 80% efficiency led to the following conclusions:

1. No fluid could be found to begin expansion as saturated liquid at temperatures below 150°C and exhaust as substantially dry vapour.

2. If the inlet temperature were raised to 150° - 180°C, three pure fluids could be used. These were 2,2-dimethylpropane (neopentane), 3-methyl-1-butene and tetramethylsilane.

3. A mixture of n-pentane and neopentane whose proportions could be varied according to the inlet temperature was found to be the most suitable and could effectively cover the entire 150° - 180°C range.

4. The use of such a mixture permits conventional low cost high efficiency radial inflow turbines to be used as a final expansion stage in TFC systems at lower inlet temperatures than was previously thought possible. This extends the scope of TFC power plant to higher unit power outputs at lower geothermal resource temperatures and lower costs than is possible with Lysholm twin screw expanders alone.

5. The Redlich-Kwong-Soave cubic equation of state is a reliable means of predicting both the thermodynamic properties and phase equilibrium states of hydrocarbon mixtures up to near critical conditions.

APPENDIX A

Suggested Flammability and Toxicity of Organic Working Fluids

Fluid	Chemical formula	Flash point °C	Ignition Temp. °C	Suggested Hazard Flam.	Health	TLV-WA p.p.m.
Trichlorofluoromethane (R11)	CCl_3F					1000
Dichlorodifluoromethane (R12)	CCl_2F_2					1000
Monobromotrifluoromethane (R13B1)	$CBrF_3$					1000
Dichlorofluoromethane (R21)	$CHCl_2F$					1000
Monochlorofluoromethane (R21)	$CHClF$					1000
Trichlorotrifluoroethane (R113)	$CCl_2FCCl F_2$					1000
Dichlorotrifluoroethane (R114)	$C_2Cl_2F_4$					1000
Monochloropentafluoroethane (R115)	$CClF_2CF_3$					1000
Octafluorocylclobutane (RC318)	$C\text{-}C_4F_8$					
Azeotrope (R12/152a 73.8/26.2 wt.%)	CCl_2F_2/CH_3CHF_2					
Azeotrope (R22/115 48.851.2 wt.%)	$CHClF_2/CClF_2CF_3$					
Perfluoro-n-hexane	C_6F_{14}					
Perfluoromethylcyclohexane	C_7F_{14}					
Perfluoro (1,3 dimethylcyclohexane)	C_8F_{14}					
Perfluorodicalin	$C_{10}F_{18}$					
Biphenyl	$C_{12}H_{10}$	112.8	540	1	2	
Monoisopropylbiphenyl (MIPB)	$C_{15}H_{16}$					
Benzene	C_6H_6	-11	560	3	2	25
Toluene	$C_6H_5CH_3$	4.5	480	3	2	100
Monochlorbenzene	C_6H_5Cl					
Hexafluorobenzene	C_6F_6					

Fluid	Chemical formula	Flash point C	Ignition Temp. C	Suggested Hazard Flam.	Health	TLV-WA p.p.m.
Pyridine	m-C_5H_5	20	482	3	2	5
Thiophene	C_4H_4S	-1.1		3	2	
Dowtherm A (biphenyl-biphenyl oxide eutectic 26.5/73.5 wt.%)		124	617			
Dowtherm E (O-dichlorobenzene)	$C_6H_4Cl_2$	66.1	648	2	2	50
Dichorotetrafluorobenzene (DCTFB)	$C_6F_4Cl_2$					
Perfluoro-2-butyltetrahydrofuran (FC75)	$C_8F_{16}O$					
Acetaldehyde	CH_3CHO	-38	175	4	2	100
Butane	C_4H_{10}		405	4	1	
1-chloroapthalene	$C_{10}H_7Cl$	132	>558#	1	1	
Dibromodifluoromethane	CBr_2F_2					
Ethane	C_2H_6		515	4	1	
Ethylamine	$C_2H_5NH_2$	-18	403	4	3	
Ethylchloride	C_2H_5Cl	-50	519	4	2	1000
Ehtyl ether	$(C_2H_5)_2O$	45	160	4	2	400
Ehtylene oxide	C_2H_4O	-18	429	4	2	50
Isobutane	C_4H_{10}		460	4	1	
Isopentane	C_5H_{12}	-51	420	4	1	
Neopentane	C_5H_{12}		450	4	1	
Methyl bromide	CH_3Br		537	0	3	15
Methyl chloride	CH_3Cl		632	4	2	100
Methyl formate	$C_2H_4O_2$	-19	465	4	2	100
Methyl mercaptan	CH_3SH	-18		4	2	10
3 methyl-1 butene	C_5H_{10}	-7	365	4	2	
Methylene chloride	CH_2Cl_2		615	0	2	250
2 methyl pyridine	$CH_3C_6H_4N$	39	538	2	2	
Monobromobenzene	C_6H_5Br			2	2	
O ethyl toluene	$C_2H_5C_6H_4CH_3$		440	2		
O xylene	$C_6H_4(CH_3)_2$	32.2	465	3	2	100
pentane	C_5H_{12}	-40	260	4	1	500
Perfluorocyclopentane	C_5F_{10}					
Propane	C_3H_8		450	4	1	1000

Notes on Appendix A

i) Flash Point is the minimum temperature at which a liquid gives off sufficient vapour to form an ignitable mixture with air near the surface of the liquid or within the vessel used.

ii) Ignition Temperature is the minimum temperature required to initiate or cause self sustained combustion independently of the heating or heating element.

iii) Suggested Hazard - Flammability

Notation identifies the hazards of a material in order of severity.

4 - severe hazard 0 - no special hazard.

4. Very flammable gases or very volatile liquids. Shut off flow and keep cooling water streams on exposed tanks or containers.

3. Materials which can be ignited under almost all normal temperature conditions. Water may be ineffective because of the low flash point.

2. Materials which must be moderately heated before ignition will occur. Water may be used to extinguish the fire because the material can be cooled below its flash point.

1. Materials that must be preheated before ignition can occur. Water may cause frothing if it gets below the surface of the liquid and turns to steam. However water fog gently applied to the surface will cause a frothing which will extinguish the fire.

0. Materials that will not burn.

Notes on Appendix A

The Threshold Limit Values are divided into three categories according to the American Conference on Governmental Hygienists (ACGHIH) as follows:

a) Threshold Limit Value-Time Weighted Average (TLV-TWA) the time-weighted average concentration for a normal 8-hour work day or 40-hour work week, to which nearly all workers may be repeatedly exposed, day after day, without adverse effect.

b) Threshold Limit Value Short Term Exposure Limit (TLV-STEL) the maximal concentration to which workers can be exposed for a period up to 15 minutes continuously without suffering from (1) intolerable irritation (2) chronic or irreversible tissue change or (3) narcosis of sufficient degree to increase accident proneness, impair self-rescue or materially reduce work efficiency, provided that no more than four excursions per day are permitted, with at least 60 minutes between exposure periods and provided that the daily TLV-TWA) also is not exceeded.

c) Threshold Limit Value Ceiling (TLV-C) the concentration that should not be exceeded even instantaneously.

The exposure, the threshold limit value is expressed in parts per million (p.p.m.) and the highest value assigned to any chemical (except CO_2) is 1000 p.p.m.

iv) Suggested Hazards - Health

4. Materials too dangerous to health to exposure firefighters. A few whiffs of the vapour could cause death or the vapour or liquid could be fatal on penetrating the firefighters normal full protective clothing. The normal full protective clothing and breathing apparatus available to the average fire department will not provide adequate protection against inhalation or skin contact with these materials.

3. Materials extremely hazardous to health but areas may be entered with extreme care. Full protective clothing, including self contained breathing apparatus, coat, pants, gloves, boots and bands around legs, arms and waist should be provided. No skin surface should be exposed.

2. Materials hazardous to health but areas may be entered freely with full face mask self contained breathing apparatus which provides eye protection.

1. Materials only slightly hazardous to health. It may be desirable to wear self contained breathing apparatus.

0. Materials which on exposure under fire conditions would offer no hazard beyond that of ordinary combustible materials.

APPENDIX B

GLOSSARY OF PRINCIPLE VARIABLE NAMES

The following is a list and description of variable names used in the Bubble and Dew point programs.

AA	RKS equation of state parameter defined by eqn.5.5
A(I)	Constant in Antoine vapour pressure equation
A(I,J)	Matrix used in Newton-Raphson method
ACOMB(I,J)	Intermolecular parameter in RKS equation of state a_{ij}
AK(I,J)	Interaction parameter k_{ij}
ALPHA(I,J)	Correction factor in RKS equation α_{mi}
AMIX	Mixing rule intermolecular parameter $\sum_i \sum_j x_i x_j a_i^{0.5} a_j^{0.5}$
ATC(I)	Pure parameter a_i at the critical temperature
BB	RKS equation of state parameter defined by eqn.5.5
B(I)	Constant in Antoine vapour pressure equation
BMIX	Mixture co-volume $\sum_i \sum_j x_i x_j b_{ij}$
C(I)	Constant in Antoine vapour pressure equation
CPA(I),CPB(I) CPC(I),CPD(I)	Heat capacities constants
CONVER	Conversion factor (kmol → kg)
DELTH	Enthalpy departure function $H^{id} - H$
DELP	Increment to P in Secant method
DELTS	Entropy departure function $S^{id} - S$
EA, EB	Error in mole fractions (Bisection method)
ENTAL	Enthalpy of mixture
ENTROP	Entropy of mixture
FA, FB	Ordinates in Bisection method
FL(I)	Liquid phase fugacity of component i, f_I^L
FV(I)	Vapour phase fugacity of component i, f_I^V

HIDEAL	Enthalpy ofideal gas, H^{id}
KEY	Control variable (1 bubble calculation, 2 dew calculation)
NCOMP	Number of components
OMEGAA	Coefficient in the RKS equation of state Ω_A
OMEGAB	Coefficient in the RKS equation of state Ω_B
OMEGA(I)	Pitzer's acentric factor, ω
P	Pressure
PCRIT(I)	Critical pressure of component i, P_{ci}
PHIL(I)	Liquid phase fugacity coefficient of component i, ϕ_i^L
PHIV(I)	Vapour phase fugacity coefficient of component i, ϕ_i^V
PMIX	Mixture critical pressure
PPREV	Pressure of previous iteration
PSAT(I)	Saturated vapour pressure of component i
RE	Array containing polynomial coefficients of RKS equation expressed in compressibility factors
SIDEAL	Entropy of ideal gas, S^{id}
SLOPE	FInite difference derivative in Secant method
SUMP	New pressure calculation
SUMT	New temperature calculation
SUMXY	Error in calculation of mole fractions ($1 - \sum_i x$ or $\sum_i y$)
T	Temperature
TCRIT(I)	Critical temperature of component i, T_{ci}
TMIX	Mixture critical temperature
TPREV	Temperature of previous iteration
VCRIT(I)	Critical volume of component i, V_{ci}
VL	Liquid molar volume
VV	Vapour molar volume

X(I)	Liquid mole fraction of component i
XORY(I)	Dummy array containing mole fractions
Y(I)	Vapour mole fraction of component i
Z	Compressibility factor, Z

SUBROUTINES

INPUT	Reads in data
INIT	Provides master program with initial values of mole fractions (Raoult's law)
PHI	Calculates the fugacity coefficients
ABMIX	Calculates the parameters a and b of the RKS equation of state
SPIN	Calculates the roots of the spinodal curve
RKSEQN	Calculates the roots of the RKS equation of state
NEWRAF	Evaluates matrix A(I,J) for Newton-Raphson method
ENTHALPY	Calculates the enthalpy of mixture
ENTROPY	Calculates the entropy of mixture.

FLOW CHART FOR BUBBLE AND DEW TEMPERATURE CALCULATIONS

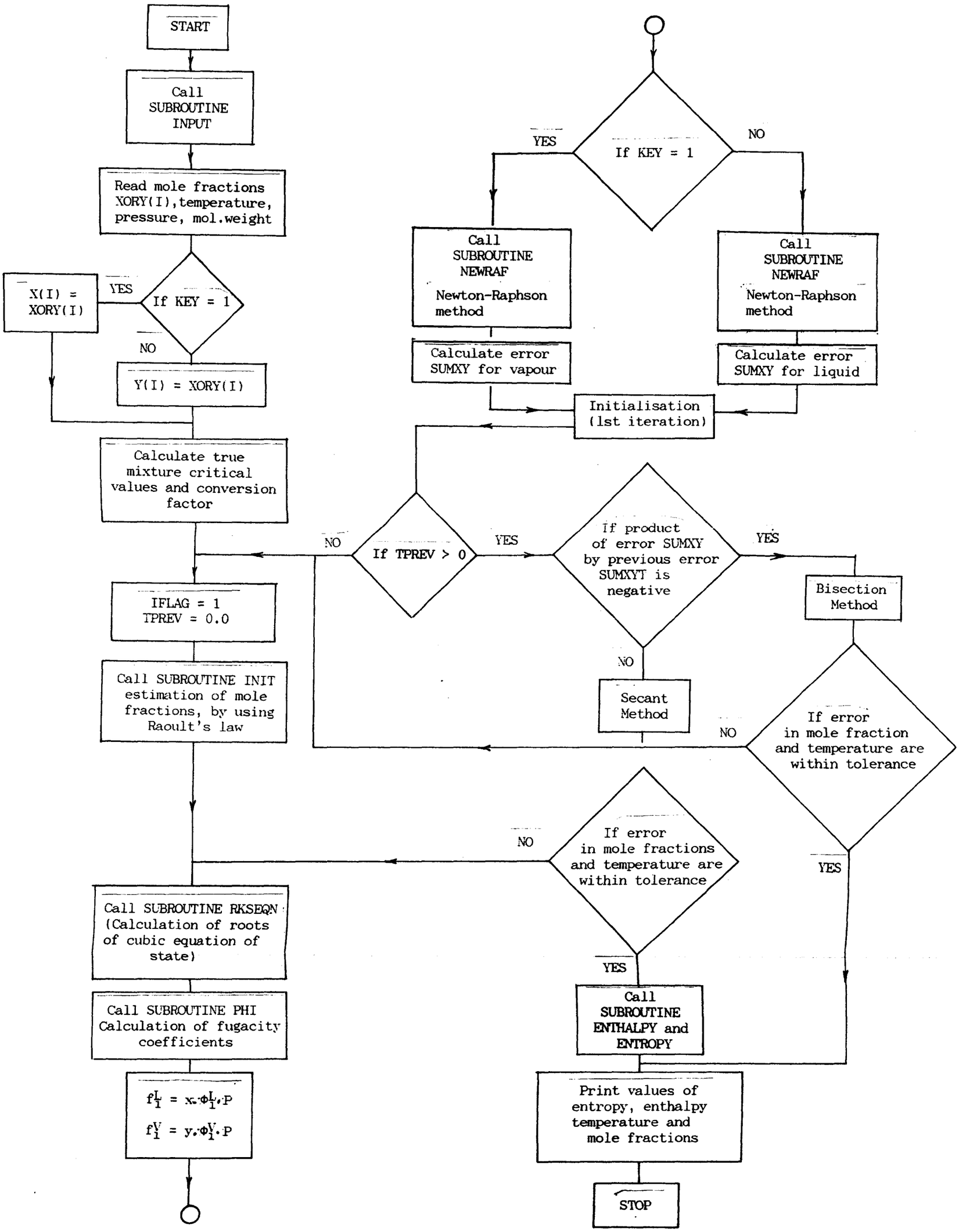

```
C       BUDET
C       THIS PROGRAM CALCULATES BUBBLE AND DEW TEMPERATURES AS WELL AS
C       CORRESPONDING ENTROPIES AND ENTHALPIES. THE REDLICH-KWONG-SOAVE
C       CUBIC EQUATION OF STATE IS USED TO EVALUATE VAPOUR-LIQUID
C       EQUILIBRIUM AND ESTIMATE THERMODYNAMIC PROPERTIES
C
        IMPLICIT DOUBLE PRECISION (A-H,O-Z)
        COMMON/VAL/R,T,P,X(3),Y(3),WMOL(3),KEY,NCOMP
        COMMON/PURPRO/OMEGA(3),TCRIT(3),PCRIT(3),AK(3,3),ALPHA(3)
        COMMON/NEWTON/ACOMB(3,3),FUG(3)
        COMMON TMIX
        DIMENSION FL(3),FV(3),PHIL(3),PHIV(3),VCRIT(3),FACTOR(3),TARR(80)
        DIMENSION A(3,3),B(3),C(3),WKSPCE(3),AA(3,3),BB(3),XORY(3)
        OPEN(UNIT=7,FILE='penneo',STATUS='OLD',FORM='FORMATTED')
        REWIND(7)
        CALL INPUT
        WRITE(6,5)
    5   FORMAT(5X," ENTER KEY:  DEW TEMPERATURE=2 BUBBLE TEMPERATURE=1 ")
        READ(5,*) KEY
        WRITE(6,15)
   15   FORMAT(5X,' ENTER RANGE OF PRESSURES: finalP,initialP,Pstep in Kpa
     &')
        READ(5,*) PF,PI,PSTEP
        WRITE(6,17)
   17   FORMAT(5X,' ENTER MOLE FRACTIONS: make sure mole fractions add up
     & to 1.0')
        READ(5,*) (XORY(I),I=1,NCOMP)
        CHEK=0.0
        DO 2 I=1,NCOMP
        CHEK=CHEK+XORY(I)
    2   CONTINUE
        IF( DABS(CHEK-1.0) .GT. 1E-8) THEN
        PRINT*,' MOLE FRACTIONS DO NOT ADD UP TO 1.0'
        STOP
        ELSE
        END IF
        DO 1 I=1,NCOMP
        IF(KEY .EQ. 2) Y(I)=XORY(I)
        IF(KEY .EQ. 1) X(I)=XORY(I)
1       CONTINUE
        P=PI
        IF(KEY .EQ. 1) THEN
        WRITE(6,300)
  300   FORMAT(//,5X,'LIQUID MOLE FRACTIONS',5X,'VAPOUR MOLE FRACTIONS',
     & 5X,'PRESSURE',5X,'BUBBLE TEMPERATURE',5X,'ENTHALPY',5X,'ENTROPY'
     &)
        WRITE(6,350)
  350   FORMAT(/,57X,'(in kpa)',7X,'(in degrees K)',6X,'(in KJ/KG)',2
     &X,'(in KJ/KG K)')
        ELSE
        WRITE(6,400)
  400   FORMAT(//,5X,'LIQUID MOLE FRACTIONS',5X,'VAPOUR MOLE FRACTIONS',
     &5X,'PRESSURE',5X,'DEW TEMPERATURE',5X,'ENTHALPY',5X,'ENTROPY')
        WRITE(6,450)
  450   FORMAT(/,57X,'(in Kpa)',5X,'(in degrees K)',6X,'(in KJ/KG)',3
     &X,'(in KJ/KG K)')
```

```
      END IF
      NCASE=INT((PF-PI)/PSTEP+1)
C
C     CALCULATION OF PSEUDO MIXTURE CRITICAL TEMPERATURE
C
      VOLUME=0.0
      DO 220 I=1,NCOMP
      VCRIT(I)=0.33*R*TCRIT(I)/PCRIT(I)
      VOLUME=VOLUME+XORY(I)*VCRIT(I)
  220 CONTINUE
      DO 225 I=1,NCOMP
      FACTOR(I)=XORY(I)*VCRIT(I)/VOLUME
  225 CONTINUE
      TMIX=0.0
      DO 230 I=1,NCOMP
      TMIX=TMIX+FACTOR(I)*TCRIT(I)
  230 CONTINUE
C
C     ESTIMATION OF PSEUDO MIXTURE CRITICAL PRESSURE
C
      ACENTRIC=0.0
      PMEAN=0.0
      TMEAN=0.0
      DO 260 I=1,NCOMP
      PMEAN=PMEAN+XORY(I)*PCRIT(I)
      TMEAN=TMEAN+XORY(I)*TCRIT(I)
      ACENTRIC=ACENTRIC+XORY(I)*OMEGA(I)
  260 CONTINUE
      PMIX=PMEAN*(1.0+(5.808+4.93*ACENTRIC)*(TMIX/TMEAN-1.0))
      DO 1000 ICASE=1,NCASE
      IFLAG=1
      TPREV=0.0
      IF(ICASE .GT. 3) THEN
      T=TARR(ICASE-3)+3*(TARR(ICASE-1)-TARR(ICASE-2))
      ELSE
      CALL INIT
      END IF
   25 IF(KEY .EQ. 1) THEN
      CALL RKSEQN(SXZ,BXZ,KK,X)
      ELSE
      CALL RKSEQN(SXZ,BXZ,KK,Y)
      END IF
      CALL PHI(SXZ,X,PHIL)
      CALL PHI(BXZ,Y,PHIV)
C
C     CALCULATION OF FUGACITIES
C
      SUMXY=0.0
      DO 30 I=1,NCOMP
      IF(KEY .EQ. 2) FV(I)=Y(I)*PHIV(I)*P
      IF(KEY .EQ. 1) FL(I)=X(I)*PHIL(I)*P
   30 CONTINUE
      SUMP=0.0
      IF(KEY .EQ. 2) GO TO 55
C
C     UPDATING VAPOUR MOLE FRACTION VALUES
```

$$P_{cT} = P^* \left[1.0 + (5.808 + 4.93\omega)\left(\frac{T_{cT}}{T^*} - 1\right)\right]$$

where

$$P^* = \sum_j y_j P_{cTj}$$

$$T^* = \sum_j y_j T_{cTj}$$

$$\omega = \sum_j y_j \omega_j$$

where P_{cTj} = critical pressure of component j

ω_j = accentric factor of component j.

```
C       (NEWTON-RAPHSON METHOD)
C
  45    ICONV=0
        CALL PHI(BXZ,Y,PHIV)
        CALL NEWRAF(A,Y,BXZ)
        DO 35 I=1,NCOMP
        DO 35 J=1,NCOMP
        IF(J .EQ. I) A(I,J)=A(I,J)+1.0/Y(I)
   35   CONTINUE
        DO 37 I=1,NCOMP
        B(I)=LOG(FL(I)/P)-LOG(Y(I))-FUG(I)
   37   CONTINUE
        IFAIL=0
        CALL F04AEF(A,3,B,3,NCOMP,1,C,3,WKSPCE,AA,3,BB,3,IFAIL)
  160   ISC=0
        DO 165 I=1,NCOMP
        IF(Y(I)+C(I) .LT. 0.0 .OR. Y(I)+C(I) .GT. 1.0) ISC=1
        IF(DABS(C(I)) .GT. 0.1) ISC=1
  165   CONTINUE
        IF(ISC .EQ. 0) GO TO 175
        DO 170 I=1,NCOMP
        C(I)=C(I)/4.0
  170   CONTINUE
        GO TO 160
  175   DO 40 I=1,NCOMP
        IF(DABS(C(I)) .GT. 1D-6) ICONV=1
        Y(I)=Y(I)+C(I)
   40   CONTINUE
        IF(ICONV .EQ. 1) GO TO 45
C
C       ACCUMULATING ERROR SUMXY IN BUBBLE CALCULATION
C
        DO 50 I=1,NCOMP
        SUMP=SUMP+FL(I)/PHIV(I)
        SUMXY=SUMXY+Y(I)
   50   CONTINUE
        GO TO 150
C
C       UPDATING LIQUID MOLE FRACTION VALUES
C       (NEWTON-RAPHSON METHOD)
C
   55   ICONV=0
        CALL PHI(SXZ,X,PHIL)
        CALL NEWRAF(A,X,SXZ)
        DO 60 I=1,NCOMP
        DO 60 J=1,NCOMP
        IF(I .EQ. J) A(I,J)=A(I,J)+1.0/X(I)
   60   CONTINUE
        DO 65 I=1,NCOMP
        B(I)=LOG(FV(I)/P)-LOG(X(I))-FUG(I)
   65   CONTINUE
        IFAIL=0
        CALL F04AEF(A,3,B,3,NCOMP,1,C,3,WKSPCE,AA,3,BB,3,IFAIL)
  180   ISC=0
        DO 185 I=1,NCOMP
        IF(X(I)+C(I) .LT. 0.0 .OR. X(I)+C(I) .GT. 1.0) ISC=1
```

```
      IF(DABS(C(I)) .GT. 0.1) ISC=1
  185 CONTINUE
      IF(ISC .EQ. 0) GO TO 195
      DO 190 I=1,NCOMP
      C(I)=C(I)/2.0
  190 CONTINUE
      GO TO 180
  195 DO 70 I=1,NCOMP
      IF(DABS(C(I)) .GT. 1D-6) ICONV=1
      X(I)=X(I)+C(I)
   70 CONTINUE
      IF(ICONV .EQ. 1) GO TO 55
C
C     ACCUMULATING ERROR SUMXY IN DEW CALCULATION
C
      DO 75 I=1,NCOMP
      SUMP=SUMP+FV(I)/PHIL(I)
      SUMXY=SUMXY+X(I)
   75 CONTINUE
C
C     INITIALIZATION OF SECANT METHOD
C
  150 SUMXY=SUMXY-1.0
      IF(IFLAG .EQ. 2) GO TO 80
      IF(TPREV .GT. 0.0) GO TO 85
      SUMXYP=SUMXY
      TPREV=T
      IF(SUMXY .GT. 0.0) T=T*1.05
      IF(T .GT. TMIX) T=TPREV*0.9
      IF(SUMXY .LT. 0.0) T=T*0.98
      GO TO 25
   85 IF(SUMXY*SUMXYP .GE. ODO) GO TO 90
C
C    INITIALIZATION OF BISECTION METHOD
C
      FA=T
      FB=TPREV
      EA=SUMXY
      EB=SUMXYP
      IFLAG=2
      GO TO 95
   80 IF(DABS(SUMXY) .LT. 1E-6 .AND. DABS((T-FA)/T) .LT. 1E-6) GO TO 110
      IF(SUMXY*EA  .LT. ODO) GO TO 100
C
C    IMPLEMENTATION OF BISECTION METHOD
C
      FA=T
      EA=SUMXY
      GO TO 95
  100 FB=T
      EB=SUMXY
   95 T=(FA+FB)/2.0
      GO TO 25
C
C    IMPLEMENTATION OF SECANT METHOD
C
```

```
   90  IF(DABS(SUMXY) .LT. 1E-6 .AND. DABS((T-TPREV)/T) .LT. 1E-6) GO TO
      & 110
       IF(DABS(SUMXY) .LE. DABS(SUMXYP)) GO TO 91
       S=SUMXY
       SUMXY=SUMXYP
       SUMXYP=S
       S=T
       T=TPREV
       TPREV=S
   91  SLOPE=(T-TPREV)/(SUMXY-SUMXYP)
       SUMXYP=SUMXY
       TPREV=T
       DELT=SLOPE*SUMXY
       IF((DABS(DELT)-0.1*T) .LE. 0.0) GO TO 105
       DELT=DSIGN(0.1*T,DELT)
  105  T=T-DELT
       GO TO 25
  110  IF(KEY .EQ. 2) GO TO 115
C
C     PRINT*OUT VALUES OF TEMPERATURE,PRESSURE AND MOLE FRACTIONS
C
       CALL ENTHALPY(SXZ,ENTAL)
       CALL ENTROPY(SXZ,ENTROP)
       WRITE(6,120) X(1),Y(1)
       WRITE(6,125) P,T,ENTAL,ENTROP
       WRITE(6,130) X(NCOMP),Y(NCOMP)
  120  FORMAT(/,8X,E14.6,12X,E14.6)
  125  FORMAT(55X,E12.6,6X,E12.6,7X,E11.5,3X,E11.5)
  130  FORMAT(8X,E14.6,12X,E14.6)
       GO TO 155
  115  CALL ENTHALPY(BXZ,ENTAL)
       CALL ENTROPY(BXZ,ENTROP)
       WRITE(6,135) X(1),Y(1)
       WRITE(6,140) P,T,ENTAL,ENTROP
       WRITE(6,145) X(NCOMP),Y(NCOMP)
  135  FORMAT(/,8X,E14.6,12X,E14.6)
  140  FORMAT(55X,E12.6,6X,E12.6,7X,E11.5,3X,E11.5)
  145  FORMAT(8X,E14.6,12X,E14.6)
  155  P=P+PSTEP
       TARR(ICASE)=T
 1000  CONTINUE
       WRITE(6,235) TMIX
  235  FORMAT(/,5X,' PSEUDO MIXTURE CRITICAL TEMPERATURE=',
      &E12.5,1X,'KELVIN')
       WRITE(6,270) PMIX
  270  FORMAT(/,5X,' PSEUDO MIXTURE CRITICAL PRESSURE= ',E12.5,1X,'KPAS')
       STOP
       END
C
C  THIS SUBROUTINE PROVIDES ALL NECESSARY DATA REQUIRED BY THE MAIN
C  PROGRAM AND ITS SUBROUTINES
C
       SUBROUTINE INPUT
       IMPLICIT DOUBLE PRECISION (A-H,O-Z)
       COMMON/VAL/R,T,P,X(3),Y(3),WMOL(3),KEY,NCOMP
       COMMON/PURPRO/OMEGA(3),TCRIT(3),PCRIT(3),AK(3,3),ALPHA(3)
```

```
      COMMON/VAPRES/A(3),B(3),C(3)
      COMMON/RESIDUO/ATC(3),CPA(3),CPB(3),CPC(3),CPD(3)
      WRITE(6,5)
    5 FORMAT(5X," ENTER NUMBER OF COMPONENTS ")
      READ(5,*) NCOMP
      WRITE(6,20)
   20 FORMAT(5X," ENTER INITIAL VALUE OF TEMPERATURE in degrees Kelvin
     &")
      READ(5,*) T
      DO 30 I=1,NCOMP
      READ(7,*) TCRIT(I),PCRIT(I),OMEGA(I),A(I),B(I),C(I),WMOL(I)
   30 CONTINUE
      DO 50 I=1,NCOMP
      READ(7,*) CPA(I),CPB(I),CPC(I),CPD(I)
   50 CONTINUE
      WRITE(6,15)
   15 FORMAT(5X,' ENTER INTERACTION PARAMETER: type 0.0 if it is not know
     &n ')
      DO 60 I=1,NCOMP-1
      AK(I,I)=0.0
      DO 70 J=I+1,NCOMP
      READ(5,*) AK(I,J)
      AK(J,I)=AK(I,J)
   70 CONTINUE
   60 CONTINUE
      R=8.3143
      RETURN
      END
C
C  THIS SUBROUTINE PROVIDES INITIALS ESTIMATES OF THE UNKNOWN MOLE
C  FRACTIONS FOR THE ITERATIVE METHODS USED IN THE MAIN PROGRAM.
C  THESE ARE CALCULATED BY RAOULT'S LAW.
C
      SUBROUTINE INIT
      IMPLICIT DOUBLE PRECISION (A-H,O-Z)
      COMMON/VAL/R,T,P,X(3),Y(3),WMOL(3),KEY,NCOMP
      COMMON/VAPRES/A(3),B(3),C(3)
      COMMON TMIX
      DIMENSION PSAT(3)
      TT=T-273.15
   20 DO 10 I=1,NCOMP
      PSAT(I)=EXP(A(I)-(B(I)/(TT+C(I))))
      IF(KEY .EQ. 2) X(I)=Y(I)*P/PSAT(I)/100
      IF(KEY .EQ. 1) Y(I)=X(I)*PSAT(I)*100/P
   10 CONTINUE
      IF(KEY .EQ. 1) GO TO 40
      ADD=0.0
      DO 30 I=1,NCOMP
      ADD=ADD+X(I)
   30 CONTINUE
      IF(ADD .GE. 1.0) THEN
      TT=TT+5.0
      GO TO 20
      END IF
      T=TT+268.15
   60 IF(T .GT. TMIX) THEN
```

$y_i P = x_i P_i^s$

where P_i^s is the saturated vapour pressure

```
      T=T-5.0
      GO TO 60
      END IF
      RETURN
   40 AD=0.0
      DO 50 I=1,NCOMP
      AD=AD+Y(I)
   50 CONTINUE
      IF(AD .GT. 1.0) THEN
      TT=TT-5.0
      GO TO 20
      END IF
      T=TT+268.15
      RETURN
      END
C
C THIS SUBROUTINE CALCULATES THE FUGACITY COEFFICIENTS
C
      SUBROUTINE PHI(Z,W,PH)
      IMPLICIT DOUBLE PRECISION (A-H,O-Z)
      COMMON/VAL/R,T,P,X(3),Y(3),WMOL(3),KEY,NCOMP
      COMMON/PURPRO/OMEGA(3),TCRIT(3),PCRIT(3),AK(3,3),ALPHA(3)
      COMMON/SOAVE/DMIX,AA,BB,SLOPEM(3)
      COMMON/NEWTON/ACOMB(3,3),FUG(3)
      DIMENSION PH(3),W(3)
      CALL ABMIX(AMIX,BMIX,ACOMB,W)
      IF(BB .GT. Z) THEN
      PRINT*,' YOUR INITIAL VALUE OF TEMPERATURE WAS UNSUCCESSFUL. TRY AG
     &AIN. '
      STOP
      ELSE
      END IF
      DO 20 I=1,NCOMP
      AMIXJ=0.0
      DO 10 J=1,NCOMP
      AMIXJ=AMIXJ+W(J)*ACOMB(I,J)
   10 CONTINUE
      FUG(I)=((0.08664*R*TCRIT(I)/PCRIT(I))/BMIX)*(Z-1.0)
     &-LOG(Z-BB)-(AA/BB)*(2.0*AMIXJ/AMIX-(0.08664*R*TCRIT(I)/
     &PCRIT(I))/BMIX)*LOG(1.0+BB/Z)
      PH(I)=EXP(FUG(I))
   20 CONTINUE
      RETURN
      END
C
C     THIS SUBROUTINE CALCULATES PARAMETERS a AND b OF THE SOAVE'S
C     EQUATION OF STATE
C
      SUBROUTINE ABMIX(AMIX,BMIX,ACOMB,W)
      IMPLICIT DOUBLE PRECISION (A-H,O-Z)
      COMMON/VAL/R,T,P,X(3),Y(3),WMOL(3),KEY,NCOMP
      COMMON/PURPRO/OMEGA(3),TCRIT(3),PCRIT(3),AK(3,3),ALPHA(3)
      COMMON/RESIDUO/ATC(3),CPA(3),CPB(3),CPC(3),CPD(3)
      COMMON/SOAVE/DMIX,AA,BB,SLOPEM(3)
      DIMENSION ACOMB(3,3),W(3),A(3),B(3)
C
```

$$\ln \Phi_i = \frac{b_i}{b}(Z-1) - \ln(Z-B) - \frac{A}{B}\left[2\sum_j \frac{w_j a_{ij}}{a} - \frac{b_i}{b}\right].\ln\left(1+\frac{B}{Z}\right)$$

$A = \frac{aP}{R^2T^2}$ and $B = \frac{bP}{RT}$ with w_j = either liquid or vapour mole fractions

```
C       FUNCTION STATEMENTS
C
        OMEGAA=0.42748
        OMEGAB=0.08664
        DO 10 I=1,NCOMP
        SLOPEM(I)=0.48508+1.55171*OMEGA(I)-0.15613*(OMEGA(I)**2)
        ALPHA(I)=(1.0+SLOPEM(I)*(1.0-SQRT(T/TCRIT(I))))**2
        ATC(I)=(OMEGAA*((R*TCRIT(I))**2))/PCRIT(I)
        A(I)=ALPHA(I)*ATC(I)
        B(I)=(OMEGAB*R*TCRIT(I))/PCRIT(I)
   10   CONTINUE
C
C       COMBINING RULES
C
        DO 20 I=1,NCOMP
        DO 20 J=1,NCOMP
        ACOMB(I,J)=(1.0-AK(I,J))*SQRT(A(I)*A(J))
   20   CONTINUE
C
C       MIXING RULES
C
        AMIX=0.0
        BMIX=0.0
        DO 30 I=1,NCOMP
        BMIX=BMIX+W(I)*B(I)
        DO 30 J=1,NCOMP
        AMIX=AMIX+W(I)*W(J)*ACOMB(I,J)
   30   CONTINUE
        AA=AMIX*P/(R*T)**2
        BB=BMIX*P/R/T
        RETURN
        END
C
C       THIS SUBROUTINE CALCULATES THE ROOTS OF THE SPINODAL CURVE
C       WHICH REPLACE COMPLEX ROOTS FROM CUBIC EQUATION OF STATE
C
        SUBROUTINE SPIN(VV,VL,W)
        IMPLICIT DOUBLE PRECISION (A-H,O-Z)
        COMMON/VAL/R,T,P,X(3),Y(3),WMOL(3),KEY,NCOMP
        COMMON/PURPRO/OMEGA(3),TCRIT(3),PCRIT(3),AK(3,3),ALPHA(3)
        COMMON/RESIDUO/ATC(3),CPA(3),CPB(3),CPC(3),CPD(3)
        COMMON/SOAVE/DMIX,AA,BB,SLOPEM(3)
        COMMON/NEWTON/ACOMB(3,3),FUG(3)
        DIMENSION XZ(4),YZ(4),RE(5)
        IF(KEY .EQ. 1) THEN
        CALL ABMIX(AMIX,BMIX,ACOMB,X)
        ELSE
        CALL ABMIX(AMIX,BMIX,ACOMB,Y)
        END IF
C
C       ROOTS OF THE SPINODAL CURVE
C
        RE(1)=1.0
        RE(2)=2.0*(BMIX-(AMIX/(R*T)))
        RE(3)=(BMIX**2)+(3.0*AMIX*BMIX)/(R*T)
        RE(4)=0.0
```

$$m_i = 0.48508 + 1.55171\omega_i - 0.15613\,\omega_i^2$$

$$\alpha_{mi}^{0.5} = 1 + m_i\,(1 - T_{ri}^{0.5})$$

$$\Omega_a = \frac{1}{[9\,(2^{1/3} - 1)]}$$

$$\Omega_b = \frac{(2^{1/3} - 1)}{3}$$

```
      RE(5)=-(AMIX*(BMIX**3))/(R*T)
      N=5
      P1=0.1E0
      TOL=X02AAF(P1)
      IFAIL=1
      CALL C02AEF(RE,N,XZ,YZ,TOL,IFAIL)
      IF(IFAIL .NE. 0) GO TO 5
C
C     SORTS ROOTS OUT
C
      KK=0
      BXZ=0.0
      SXZ=0.0
      DO 10 I=1,4
      IF(DABS(YZ(I)) .GT. TOL) THEN
      PRINT*,'A PHASE CANNOT BE FOUND OR YOUR INITIAL VALUE OF TEMPERATU
     &RE WAS UNSUCCESSFUL. TRY AGAIN.'
      STOP
      ELSE
      IF(XZ(I) .LE. 0.0) GO TO 10
      IF(XZ(I) .LE. BMIX) GO TO 10
      IF(KK .EQ. 0) SXZ=XZ(I)
      IF(XZ(I) .GT. BXZ) BXZ=XZ(I)
      IF(XZ(I) .LE. SXZ) SXZ=XZ(I)
      KK=KK+1
      END IF
 10   CONTINUE
      VL=SXZ
      VV=BXZ
      RETURN
  5   WRITE(6,15) IFAIL
 15   FORMAT(' IFAIL ERROR NUMBER SPINODAL: ',I2)
      RETURN
      END
C
C THIS SUBROUTINE CALCULATES THE VAPOR MOLAR VOLUME AND THE LIQUID
C MOLAR VOLUME FROM THE REDLICH-KWONG-SOAVE EQUATION OF STATE
C
      SUBROUTINE RKSEQN(SXZ,BXZ,KK,W)
      IMPLICIT DOUBLE PRECISION (A-H,O-Z)
      COMMON/VAL/R,T,P,X(3),Y(3),WMOL(3),KEY,NCOMP
      COMMON/PURPRO/OMEGA(3),TCRIT(3),PCRIT(3),AK(3,3),ALPHA(3)
      COMMON/SOAVE/DMIX,AA,BB,SLOPEM(3)
      COMMON/NEWTON/ACOMB(3,3),FUG(3)
      DIMENSION XZ(3),YZ(3),RE(4)
C
C     ROOTS OF THE CUBIC EQUATION
C
      IF(KEY .EQ. 1) THEN
      CALL ABMIX(AMIX,BMIX,ACOMB,X)
      ELSE
      CALL ABMIX(AMIX,BMIX,ACOMB,Y)
      END IF
      RE(1)=1.0
      RE(2)=-1.0
      RE(3)=AA-BB-(BB**2)
```

$$V^4 + 2\left[b - \left[\frac{a}{RT}\right]\right] V^3 + \left[b^2 + \left[\frac{3ab}{RT}\right]\right] V^2 - \frac{ab^3}{RT} = 0$$

```
      RE(4)=-(AA*BB)
      N=4
      P1=0.1E0
      TOL=X02AAF(P1)          Z^3 - Z^2 + (A - B - B^2)Z - AB = 0
      IFAIL=1
      CALL C02AEF(RE,N,XZ,YZ,TOL,IFAIL)
      IF(IFAIL .NE. 0) GO TO 5
C
C     SORTS ROOTS OUT
C
      KK=0
      BXZ=0.0
      SXZ=0.0
      DO 10 I=1,3
      IF(DABS(YZ(I)) .GT. TOL) GO TO 10
      IF(KK .EQ. 0) SXZ=XZ(I)
      IF(XZ(I) .GT. BXZ) BXZ=XZ(I)
      IF(XZ(I) .LT. SXZ) SXZ=XZ(I)
      KI=I
      KK=KK+1
 10   CONTINUE
      IF(KK .GT. 1) RETURN
      V=XZ(KI)*R*T/P
      IF(KEY .EQ. 1) THEN
      CALL SPIN(VV,VL,X)
      ELSE
      CALL SPIN(VV,VL,Y)
      END IF
      PRT=P/(R*T)
      IF(V .GT. VV) GO TO 20
      IF(V .LT. VL) GO TO 30
      WRITE(6,40) V,VV,VL
 40   FORMAT( ' ERROR ',' V=',E12.6,' VV=',E12.6,'VL=',E12.6)
 20   BXZ=PRT*V
      SXZ=PRT*VL
      RETURN
 30   SXZ=PRT*V
      BXZ=PRT*VV
      RETURN
  5   WRITE(6,50) IFAIL
 50   FORMAT(' IFAIL ERROR NUMBER: ',I2)
      RETURN
      END
C
C     THIS SUBROUTINE EVALUATES MATRIX A(I,J) FOR NEWTON-RAPHSON METHOD
C
      SUBROUTINE NEWRAF(A,W,Z)
      IMPLICIT DOUBLE PRECISION (A-H,O-Z)
      COMMON/VAL/R,T,P,X(3),Y(3),WMOL(3),KEY,NCOMP
      COMMON/PURPRO/OMEGA(3),TCRIT(3),PCRIT(3),AK(3,3),ALPHA(3)
      COMMON/SOAVE/DMIX,AA,BB,SLOPEM(3)
      COMMON/NEWTON/ACOMB(3,3),FUG(3)
      DIMENSION B1(3),A(3,3),W(3),AMIXJ(3)
      CALL ABMIX(AMIX,BMIX,ACOMB,W)
      DO 5 I=1,NCOMP
      B1(I)=0.08664*R*TCRIT(I)/PCRIT(I)
```

```
    5  CONTINUE
       DO 10 I=1,NCOMP
       AMIXJ(I)=0.0
       DO 10 K=1,NCOMP
       AMIXJ(I)=AMIXJ(I)+ACOMB(I,K)*W(K)
   10  CONTINUE
       DO 20 I=1,NCOMP
       DO 20 J=1,NCOMP
       A1=B1(J)*(P/R/T/(Z-BB)-B1(I)*(Z-1.0)/BMIX**2)
       A2=(AA/BB)*(B1(I)/BMIX-2.0*AMIXJ(I)/AMIX)*P*B1(J)/R/T/(Z+BB)
       A3=2.0*LOG(1.0+BB/Z)*((B1(I)*AMIXJ(J)+B1(J)*AMIXJ(I))/BMIX
      &-AMIX*B1(I)*B1(J)/BMIX/BMIX-ACOMB(I,J))/BMIX/R/T
       A(I,J)=A1+A2+A3
   20  CONTINUE
       RETURN
       END
C
C      THIS SUBROUTINE CALCULATES THE ENTHALPY OF MIXTURES
C
       SUBROUTINE ENTHALPY(Z,ENTAL)
       IMPLICIT DOUBLE PRECISION (A-H,O-Z)
       COMMON/VAL/R,T,P,X(3),Y(3),WMOL(3),KEY,NCOMP
       COMMON/PURPRO/OMEGA(3),TCRIT(3),PCRIT(3),AK(3,3),ALPHA(3)
       COMMON/RESIDUO/ATC(3),CPA(3),CPB(3),CPC(3),CPD(3)
       COMMON/SOAVE/DMIX,AA,BB,SLOPEM(3)
       COMMON/NEWTON/ACOMB(3,3),FUG(3)
       DIMENSION A(3),FACTOR(3,3),XORY1(3)
       TNOT=273.15
       DO 10 I=1,NCOMP
       IF(KEY .EQ. 1) XORY1(I)=X(I)
       IF(KEY .EQ. 2) XORY1(I)=Y(I)
   10  CONTINUE
       IF(KEY .EQ. 1) THEN
       CALL ABMIX(AMIX,BMIX,ACOMB,Y)
       ELSE
       CALL ABMIX(AMIX,BMIX,ACOMB,X)
       END IF
C
C      MOLECULAR WEIGHT FACTOR
C
       CONVER=0.0
       DO 15 I=1,NCOMP
       CONVER=CONVER+XORY1(I)*WMOL(I)
   15  CONTINUE
C
C      RESIDUAL ENTHALPY
C
       DO 20 I=1,NCOMP
       A(I)=ALPHA(I)*ATC(I)
       DO 20 J=1,NCOMP
       FACTOR(I,J)=SLOPEM(J)*(1.0-AK(I,J))*DSQRT(A(I)*ATC(J)*T/TCRIT(J))
   20  CONTINUE
       DMIX=0.0
       DO 30 I=1,NCOMP
       DO 30 J=1,NCOMP
       DMIX=DMIX+XORY1(I)*XORY1(J)*FACTOR(I,J)
```

```
   30  CONTINUE
       DELTH=R*T*((1.0-Z)+(AA/BB)*(1.0+DMIX/AMIX)*LOG(1.0+BB/Z))
       DELTH=DELTH/CONVER
C
C      IDEAL ENTHALPY
C
       HIDEAL=0.0
       DO 40 I=1,NCOMP
       HIDEAL=HIDEAL+XORY1(I)*(CPA(I)*(T-TNOT)+0.5*CPB(I)*(T**2-
      &TNOT**2)+0.33333*CPC(I)*(T**3-TNOT**3)+
      &0.25*CPD(I)*(T**4-TNOT**4))
   40  CONTINUE
       HIDEAL=HIDEAL/CONVER
       HCORREC=469.88
       ENTAL=HIDEAL-DELTH+HCORREC
       RETURN
       END
C
C      THIS SUBROUTINE CALCULATES THE ENTROPY OF MIXTURES
C
       SUBROUTINE ENTROPY(Z,ENTROP)
       IMPLICIT DOUBLE PRECISION (A-H,O-Z)
       COMMON/VAL/R,T,P,X(3),Y(3),WMOL(3),KEY,NCOMP
       COMMON/PURPRO/OMEGA(3),TCRIT(3),PCRIT(3),AK(3,3),ALPHA(3)
       COMMON/RESIDUO/ATC(3),CPA(3),CPB(3),CPC(3),CPD(3)
       COMMON/SOAVE/DMIX,AA,BB,SLOPEM(3)
       COMMON/NEWTON/ACOMB(3,3),FUG(3)
       DIMENSION XORY1(3)
       TNOT=273.15
       PNOT=33.47543
       DO 10 I=1,NCOMP
       IF(KEY .EQ. 1) XORY1(I)=X(I)
       IF(KEY .EQ. 2) XORY1(I)=Y(I)
   10  CONTINUE
C
C      MOLECULAR WEIGHT FACTOR
C
       CONVER=0.0
       DO 5 I=1,NCOMP
       CONVER=CONVER+XORY1(I)*WMOL(I)
    5  CONTINUE
       IF(KEY .EQ. 1) THEN
       CALL ABMIX(AMIX,BMIX,ACOMB,Y)
       ELSE
       CALL ABMIX(AMIX,BMIX,ACOMB,X)
       END IF
C
C      RESIDUAL ENTROPY
C
       DELTS=-R*LOG(Z-BB)+R*(AA*DMIX/BB/AMIX)*LOG(1.0+BB/Z)
C
C      IDEAL ENTROPY
C
       SIDEAL=0.0
       DO 20 I=1,NCOMP
       SIDEAL=SIDEAL+XORY1(I)*(CPA(I)*LOG(T/TNOT)+CPB(I)*(T-TNOT)+
```

```
     &0.5*CPC(I)*(T**2-TNOT**2)+0.333333*CPD(I)*
     &(T**3-TNOT**3)-R*LOG(XORY1(I)*P/PNOT))
  20 CONTINUE
     SIDEAL=SIDEAL/CONVER
     DELTS=DELTS/CONVER
C
C    ENTROPY OF MIXING
C
     SMIX=0.0
     DO 30 I=1,NCOMP
     SMIX=SMIX+R*XORY1(I)*LOG(XORY1(I))
  30 CONTINUE
     SMIX=SMIX/CONVER
     SCORREC=2.2517
     ENTROP=SIDEAL-DELTS+SCORREC-SMIX
     CONTINUE
     RETURN
     END
```

FLOW CHART FOR BUBBLE AND DEW PRESSURE CALCULATION

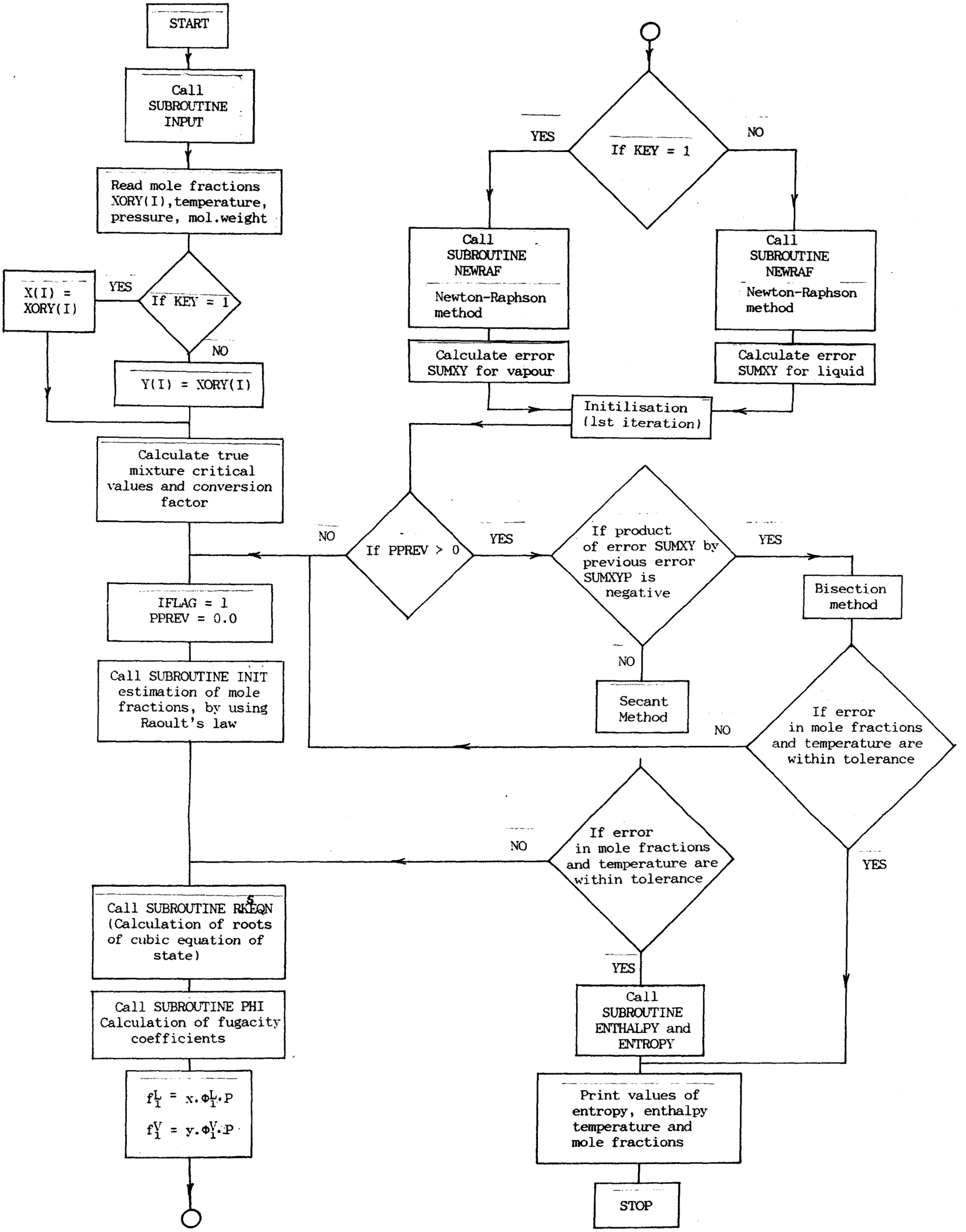

```
C     BUDEP
C     THIS PROGRAM CALCULATES BUBBLE AND DEW PRESSURES AS WELL AS
C     CORRESPONDING ENTROPIES AND ENTHALPIES. THE REDLICH-KWONG-
C     SOAVE CUBIC EQUATION OF STATE IS USED TO EVALUATE VAPOUR-
C     LIQUID EQUILIBRIUM AND THERMODYNAMIC PROPERTIES.
C
      IMPLICIT DOUBLE PRECISION (A-H,O-Z)
      COMMON/VAL/R,T,P,X(3),Y(3),WMOL(3),KEY,NCOMP
      COMMON/PURPRO/OMEGA(3),TCRIT(3),PCRIT(3),AK(3,3),ALPHA(3)
      COMMON/NEWTON/ACOMB(3,3),FUG(3)
      DIMENSION A(3,3),B(3),C(3),WKSPCE(3),AA(3,3),BB(3),XORY(3)
      DIMENSION FV(3),FL(3),PHIL(3),PHIV(3),VCRIT(3),FATOR(3)
      OPEN(UNIT=7,FILE='penneo',STATUS='OLD',FORM='FORMATTED')
      REWIND(7)
      CALL INPUT
      WRITE(6,5)
    5 FORMAT(5X,' ENTER KEY: BUBBLE PRESSURE=1; DEW PRESSURE=2')
      READ(5,*) KEY
      WRITE(6,16)
   16 FORMAT(5X,' ENTER TEMPERATURE in degrees kelvin')
      READ(5,*) T
      WRITE(6,15)
   15 FORMAT(5X,' ENTER MOLE FRACTIONS:make sure mole fractions add up
     &to 1.0')
      READ(5,*) (XORY(I),I=1,NCOMP)
      CHEK=0.0
      DO 2 I=1,NCOMP
      CHEK=CHEK+XORY(I)
    2 CONTINUE
      IF( DABS(CHEK-1.0) .GT. 1E-8 ) THEN
      PRINT*,'  MOLE FRACTIONS DO NOT ADD UP TO 1.0'
      STOP
      ELSE
      END IF
      DO 20 I=1,NCOMP
      IF(KEY .EQ. 2) Y(I)=XORY(I)
      IF(KEY .EQ. 1) X(I)=XORY(I)
   20 CONTINUE
C
C      CALCULATION OF PSEUDO MIXTURE CRITICAL TEMPERATURE
C
      VOLUME=0.0
      DO 220 I=1,NCOMP
      VCRIT(I)=0.33*R*TCRIT(I)/PCRIT(I)
      VOLUME=VOLUME+XORY(I)*VCRIT(I)
  220 CONTINUE
      DO 225 I=1,NCOMP
      FATOR(I)=XORY(I)*VCRIT(I)/VOLUME
  225 CONTINUE
      TMIX=0.0
      DO 230 I=1,NCOMP
      TMIX=TMIX+FATOR(I)*TCRIT(I)
  230 CONTINUE
C
C     ESTIMATION OF PSEUDO MIXTURE CRITICAL PRESSURE
C
```

```
      ACENTRIC=0.0
      PMEAN=0.0
      TMEAN=0.0
      DO 260 I=1,NCOMP
      PMEAN=PMEAN+XORY(I)*PCRIT(I)
      TMEAN=TMEAN+XORY(I)*TCRIT(I)
      ACENTRIC=ACENTRIC+XORY(I)*OMEGA(I)
  260 CONTINUE
      PMIX=PMEAN*(1.0+(5.808+4.93*ACENTRIC)*(TMIX/TMEAN-1.0))
      IFLAG=1
      PPREV=0.0
      IF(P .GT. PMIX) P=PMIX*0.8
      CALL INIT
   25 IF(KEY .EQ. 1) THEN
      CALL RKSEQN(SXZ,BXZ,KK,X)
      ELSE
      CALL RKSEQN(SXZ,BXZ,KK,Y)
      END IF
      CALL PHI(SXZ,X,PHIL)
      CALL PHI(BXZ,Y,PHIV)
C
C     CALCULATION OF FUGACITIES
C
      DO 30 I=1,NCOMP
      IF(KEY .EQ. 2)  FV(I)=Y(I)*PHIV(I)*P
      IF(KEY .EQ. 1)  FL(I)=X(I)*PHIL(I)*P
   30 CONTINUE
      SUMXY=0.0
      SUMP=0.0
      IF (KEY .EQ. 2) GO TO 55
C
C    UPDATING VAPOUR MOLE FRACTIONS
C     (NEWTON-RAPHSON METHOD)
   45 ICONV=0
      CALL PHI(BXZ,Y,PHIV)
      CALL NEWRAF(A,Y,BXZ)
      DO 35 I=1,NCOMP
      DO 35 J=1,NCOMP
      IF(I .EQ. J) A(I,J)=A(I,J)+1.0/Y(I)
   35 CONTINUE
      CALL PHI(BXZ,Y,PHIV)
      DO 37 I=1,NCOMP
      B(I)=LOG(FL(I)/P)-LOG(Y(I))-FUG(I)
   37 CONTINUE
      IFAIL=0
      CALL F04AEF(A,3,B,3,NCOMP,1,C,3,WKSPCE,AA,3,BB,3,IFAIL)
  160 ISC=0
      DO 165 I=1,NCOMP
      IF(Y(I)+C(I) .LT. 0.0 .OR. Y(I)+C(I) .GT. 1.0) ISC=1
  165 CONTINUE
      IF(ISC .EQ. 0) GO TO 175
      DO 170 I=1,NCOMP
      C(I)=C(I)/4.0
  170 CONTINUE
      GO TO 160
  175 DO 40 I=1,NCOMP
```

```
      IF(DABS(C(I)) .GT. 1D-6) ICONV=1
      Y(I)=Y(I)+C(I)
   40 CONTINUE
      IF(ICONV .EQ. 1) GO TO 45
C
C     ACCUMULATING ERROR SUMXY IN BUBBLE CALCULATION
C
      DO 50 I=1,NCOMP
      SUMP=SUMP+FL(I)/PHIV(I)
      SUMXY=SUMXY+Y(I)
   50 CONTINUE
      GO TO 150
C
C     UPDATING LIQUID MOLE FRACTION VALUES
C      (NEWTON-RAPHSON METHOD)
C
   55 ICONV=0
      CALL PHI(SXZ,X,PHIL)
      CALL NEWRAF(A,X,SXZ)
      DO 60 I=1,NCOMP
      DO 60 J=1,NCOMP
      IF(I .EQ. J) A(I,J)=A(I,J)+1.0/X(I)
   60 CONTINUE
      CALL PHI(SXZ,X,PHIL)
      DO 65 I=1,NCOMP
      B(I)=LOG(FV(I)/P)-LOG(X(I))-FUG(I)
   65 CONTINUE
      IFAIL=0
      CALL F04AEF(A,3,B,3,NCOMP,1,C,3,WKSPCE,AA,3,BB,3,IFAIL)
  180 ISC=0
      DO 185 I=1,NCOMP
      IF(X(I)+C(I) .LT. 0.0 .OR. X(I)+C(I) .GT. 1.0) ISC=1
  185 CONTINUE
      IF(ISC .EQ. 0) GO TO 195
      DO 190 I=1,NCOMP
      C(I)=C(I)/4.0
  190 CONTINUE
      GO TO 180
  195 DO 70 I=1,NCOMP
      IF(DABS(C(I)) .GT. 1D-6) ICONV=1
      X(I)=X(I)+C(I)
   70 CONTINUE
      IF(ICONV .EQ. 1) GO TO 55
C
C     ACCUMULATING ERROR SUMXY IN DEW CALCULATION
C
      DO 75 I=1,NCOMP
      SUMP=SUMP+FV(I)/PHIL(I)
      SUMXY=SUMXY+X(I)
   75 CONTINUE
C
C    INITIALIZATION OF SECANT METHOD
C
  150 SUMXY=SUMXY-1.0
      IF(IFLAG .EQ. 2) GO TO 80
      IF(PPREV .GT. 0.0) GO TO 85
```

```
      SUMXYP=SUMXY
      PPREV=P
      P=SUMP*0.9
      IF(SUMXY .LT. 0.0) P=P*1.5
      GO TO 25
   85 IF(SUMXY*SUMXYP .GE. 0.D0) GO TO 90
C
C       INITIALIZATION OF BISECTION METHOD
C
      FA=P
      FB=PPREV
      EA=SUMXY
      EB=SUMXYP
      IFLAG=2
      GO TO 95
   80 IF(DABS(SUMXY) .LT. 1D-6 .AND. DABS((P-FA)/P) .LT. 1D-6) GO TO 110
      IF(SUMXY*EA .LT. 0.D0) GO TO 100
C
C       IMPLEMENTATION OF BISECTION METHOD
C
      FA=P
      EA=SUMXY
      GO TO 95
  100 FB=P
      EB=SUMXY
   95 P=(FA+FB)/2.0
      GO TO 25
C
C       IMPLEMENTATION OF SECANT METHOD
C
   90 IF(DABS(SUMXY) .LT. 1E-6 .AND. DABS((P-PREV)/P) .LT. 1E-6) GO TO
     & 110
      IF(DABS(SUMXY) .LE. DABS(SUMXYP)) GO TO 91
      S=SUMXY
      SUMXY=SUMXYP
      SUMXYP=S
      S=P
      P=PPREV
      PPREV=S
   91 SLOPE=(P-PPREV)/(SUMXY-SUMXYP)
      SUMXYP=SUMXY
      PPREV=P
      DELP=SLOPE*SUMXY
      IF((DABS(DELP)-0.1*P) .LE. 0.0) GO TO 105
      DELP=DSIGN(0.1*P,DELP)
  105 P=P-DELP
      IF(DABS(SUMXY) .LT. 1D-6 .AND. DABS((P-PPREV)/P) .LT. 1D-6)
     &GO TO 110
      GO TO 25
  110 IF(KEY .EQ. 2) GO TO 115
C
C       PRINT*OUT VALUES OF PRESSURE,TEMPERATURE AND MOLE FRACTIONS
C
      WRITE(6,120) P,T
  120 FORMAT(//5X,'BUBBLE PRESSURE=',E12.5,' Kpa',3X,'TEMPERATURE=',
     &E12.4,1X,'Kelvin')
```

```
      WRITE(6,125)
  125 FORMAT(5X,/,'LIQUID MOLE FRACTIONS',10X,'VAPOUR MOLE FRACTIONS')
      WRITE(6,130) (X(I),Y(I),I=1,NCOMP)
  130 FORMAT(/,2X,E14.6,18X,E14.6)
      CALL ENTHALPY(SXZ,ENTAL)
      CALL ENTROPY(SXZ,ENTROP)
      GO TO 155
  115 WRITE(6,135) P,T
  135 FORMAT(//,5X,' DEW PRESSURE=',E12.5,' Kpa',3X,'TEMPERATURE=',E12.4
     &,1X,'Kelvin')
      WRITE(6,140)
  140 FORMAT(5X,/,'LIQUID MOLE FRACTIONS',15X,'VAPOUR MOLE FRACTIONS')
      WRITE(6,145) (X(I),Y(I),I=1,NCOMP)
  145 FORMAT(/,2X,E14.6,18X,E14.6)
      CALL ENTHALPY(BXZ,ENTAL)
      CALL ENTROPY(BXZ,ENTROP)
  155 WRITE(6,235) TMIX
  235 FORMAT(/,5X,' PSEUDO MIXTURE CRITICAL TEMPERATURE='
     &,E12.5,1X,'Kelvin')
      WRITE(6,270) PMIX
  270 FORMAT(/,5X,' PSEUDO MIXTURE CRITICAL PRESSURE=',E12.5,1X,'Kpa')
      STOP
      END
C
C  THIS SUBROUTINE PROVIDES ALL NECESSARY DATA REQUIRED BY THE MAIN
C  PROGRAM AND ITS SUBROUTINES
C
      SUBROUTINE INPUT
      IMPLICIT DOUBLE PRECISION (A-H,O-Z)
      COMMON/VAL/R,T,P,X(3),Y(3),WMOL(3),KEY,NCOMP
      COMMON/PURPRO/OMEGA(3),TCRIT(3),PCRIT(3),AK(3,3),ALPHA(3)
      COMMON/VAPRES/A(3),B(3),C(3)
      COMMON/RESIDUO/ATC(3),CPA(3),CPB(3),CPC(3),CPD(3)
      WRITE(6,5)
    5 FORMAT(5X," ENTER NUMBER OF COMPONENTS ")
      READ(5,*) NCOMP
      WRITE(6,10)
   10 FORMAT(5X,' ENTER INITIAL VALUE OF PRESSURE in kpa')
      READ(5,*) P
      DO 15 I=1,NCOMP
      READ(7,*) TCRIT(I),PCRIT(I),OMEGA(I),A(I),B(I),C(I),WMOL(I)
   15 CONTINUE
      DO 20 I=1,NCOMP
      READ(7,*) CPA(I),CPB(I),CPC(I),CPD(I)
   20 CONTINUE
      WRITE(6,25)
   25 FORMAT(5X,' ENTER INTERACTION PARAMETER: type 0.0 if it is not know
     &n ')
      DO 30 I=1,NCOMP-1
      AK(I,I)=0.0
      DO 40 J=I+1,NCOMP
      READ(5,*) AK(I,J)
      AK(J,I)=AK(I,J)
   40 CONTINUE
   30 CONTINUE
      R=8.3143
```

```
      RETURN
      END
C
C  THIS SUBROUTINE PROVIDES INITIALS ESTIMATES OF THE UNKNOWN MOLES
C  FRACTIONS FOR THE  ITERATIVE  METHODS  USED IN THE PROGRAM.
C  THESE ARE CALCULATED BY RAOULT'S LAW.
C
      SUBROUTINE INIT
      IMPLICIT DOUBLE PRECISION (A-H,O-Z)
      COMMON/VAL/R,T,P,X(3),Y(3),WMOL(3),KEY,NCOMP
      COMMON/VAPRES/A(3),B(3),C(3)
      DIMENSION PSAT(3)
      TT=T-273.15
      IF(KEY .EQ. 2) GO TO 30
    5 DO 10 I=1,NCOMP
      PSAT(I)=EXP(A(I)-(B(I)/(TT+C(I))))
      Y(I)=X(I)*PSAT(I)*100/P
   10 CONTINUE                                  y_i P = x_i P_i^s
      ADD=0.0
      DO 20 I=1,NCOMP        where P_i^s is the saturated vapour pressure
      ADD=ADD+Y(I)
   20 CONTINUE
      IF( ADD .GT.  1.0) THEN
      P=P+10
      GO TO 5
      END IF
      IF( ADD .LT.  0.05) THEN
      P=P-10
      GO TO 5
      END IF
      RETURN
   30 DO 40 I=1,NCOMP
      PSAT(I)=EXP(A(I)-(B(I)/(TT+C(I))))
      X(I)=Y(I)*P/100/PSAT(I)
   40 CONTINUE
      ADD=0.0
      DO 50 I=1,NCOMP
      ADD=ADD+X(I)
   50 CONTINUE
      IF( ADD .GT.  1.0) THEN
      P=P-10
      GO TO 30
      END IF
      IF( ADD .LT.  0.01) THEN
      P=P+10
      GO TO 30
      END IF
      RETURN
      END
C
C THIS SUBROUTINE CALCULATES THE FUGACITY COEFFICIENTS
C
      SUBROUTINE PHI(Z,W,PH)
      IMPLICIT DOUBLE PRECISION (A-H,O-Z)
      COMMON/VAL/R,T,P,X(3),Y(3),WMOL(3),KEY,NCOMP
      COMMON/PURPRO/OMEGA(3),TCRIT(3),PCRIT(3),AK(3,3),ALPHA(3)
```

$A = \frac{aP}{R^2T^2}$ and $B = \frac{bP}{RT}$ with w_j = either liquid or vapour mole fractions

```
      COMMON/NEWTON/ACOMB(3,3),FUG(3)
      COMMON/SOAVE/DMIX,AA,BB,SLOPEM(3)
      DIMENSION PH(3),W(3)
      CALL ABMIX(AMIX,BMIX,ACOMB,W)
      DO 20 I=1,NCOMP
      AMIXJ=0.0
      DO 10 J=1,NCOMP
      AMIXJ=AMIXJ+W(J)*ACOMB(I,J)
   10 CONTINUE
      FUG(I)=((0.08664*R*TCRIT(I)/PCRIT(I))/BMIX)*(Z-1.0)
     &-LOG(Z-BB)-(AA/BB)*(2.0*AMIXJ/AMIX-(0.08664*R*TCRIT(I)/
     &PCRIT(I))/BMIX)*LOG(1.0+BB/Z)
      PH(I)=EXP(FUG(I))
   20 CONTINUE
      RETURN
      END
```

$$\ln \Phi_i = \frac{b_i}{b}(Z-1) - \ln(Z-B) - \frac{A}{B}\left[2\sum_j \frac{w_j a_{ij}}{a} - \frac{b_i}{b}\right].\ln\left(1+\frac{B}{Z}\right)$$

```
C
C     THIS SUBROUTINE CALCULATES PARAMETERS a AND b OF THE SOAVE'S
C     EQUATION OF STATE AS WELL AS THE SPINODAL POINTS OF INTERCEP-
C     TION WITH THE CUBIC EQUATION
C
      SUBROUTINE ABMIX(AMIX,BMIX,ACOMB,W)
      IMPLICIT DOUBLE PRECISION (A-H,O-Z)
      COMMON/VAL/R,T,P,X(3),Y(3),WMOL(3),KEY,NCOMP
      COMMON/PURPRO/OMEGA(3),TCRIT(3),PCRIT(3),AK(3,3),ALPHA(3)
      COMMON/RESIDUO/ATC(3),CPA(3),CPB(3),CPC(3),CPD(3)
      COMMON/SOAVE/DMIX,AA,BB,SLOPEM(3)
      DIMENSION ACOMB(3,3),W(3),A(3),B(3)
C
C     FUNCTION STATEMENTS
C
      OMEGAA=0.42747
      OMEGAB=0.08664
      DO 10 I=1,NCOMP
      SLOPEM(I)=0.48508+1.55171*OMEGA(I)-0.15613*(OMEGA(I)**2)
      ALPHA(I)=(1.0+SLOPEM(I)*(1.0-DSQRT(T/TCRIT(I))))**2
      ATC(I)=(OMEGAA*((R*TCRIT(I))**2))/PCRIT(I)
      A(I)=ALPHA(I)*ATC(I)
      B(I)=(OMEGAB*R*TCRIT(I))/PCRIT(I)
   10 CONTINUE
C
C     COMBINING RULES
C
      DO 20 I=1,NCOMP
      DO 20 J=1,NCOMP
      ACOMB(I,J)=(1.0-AK(I,J))*DSQRT(A(I)*A(J))
   20 CONTINUE
C
C     MIXING RULES
C
      AMIX=0.0
      BMIX=0.0
      DO 30 I=1,NCOMP
      BMIX=BMIX+W(I)*B(I)
      DO 30 J=1,NCOMP
      AMIX=AMIX+W(I)*W(J)*ACOMB(I,J)
```

$$m_i = 0.48508 + 1.55171\omega_i - 0.15613\,\omega_i^2$$

$$\alpha_{mi}^{0.5} = 1 + m_i\,(1 - T_{ri}^{0.5})$$

$$\Omega_a = \frac{1}{[9\,(2^{1/3}-1)]}$$

$$\Omega_b = \frac{(2^{1/3}-1)}{3}$$

```
   30  CONTINUE
C
C      THE FOLLOWING ARE THE PARAMETERS  a AND b OF THE SOAVE'S EQUATION
C
       AA=AMIX*P/(R*T)**2
       BB=BMIX*P/R/T
       RETURN
       END
C
C      THIS SUBROUTINE CALCULATES THE ROOTS OF THE SPINODAL CURVE
C      WHICH REPLACE COMPLEX ROOTS FROM CUBIC EQUATION OF STATE
C
       SUBROUTINE SPIN(VV,VL,W)
       IMPLICIT DOUBLE PRECISION (A-H,O-Z)
       COMMON/VAL/R,T,P,X(3),Y(3),WMOL(3),KEY,NCOMP
       COMMON/PURPRO/OMEGA(3),TCRIT(3),PCRIT(3),AK(3,3),ALPHA(3)
       COMMON/RESIDUO/ATC(3),CPA(3),CPB(3),CPC(3),CPD(3)
       COMMON/SOAVE/DMIX,AA,BB,SLOPEM(3)
       COMMON/NEWTON/ACOMB(3,3),FUG(3)
       DIMENSION XZ(4),YZ(4),RE(5)
       IF(KEY .EQ. 1) THEN
       CALL ABMIX(AMIX,BMIX,ACOMB,X)
       ELSE
       CALL ABMIX(AMIX,BMIX,ACOMB,Y)
       END IF
C
C      ROOTS OF THE SPINODAL CURVE
C
       RE(1)=1.0
       RE(2)=2.0*(BMIX-(AMIX/(R*T)))
       RE(3)=(BMIX**2)+(3.0*AMIX*BMIX)/(R*T)
       RE(4)=0.0
       RE(5)=-(AMIX*(BMIX**3))/(R*T)
       N=5
       P1=0.1E0
       TOL=X02AAF(P1)
       IFAIL=1
       CALL C02AEF(RE,N,XZ,YZ,TOL,IFAIL)
       IF(IFAIL .NE. 0) GO TO 5
C
C      SORTS ROOTS OUT
C                                  V^4 + 2 [b - (a/RT)] V^3 + [b^2 + (3ab/RT)] V^2 - ab^3/RT = 0
       KK=0
       BXZ=0.0
       SXZ=0.0
       DO 10 I=1,4
       IF(DABS(YZ(I)) .GT. TOL) THEN
       PRINT*,' A PHASE CANNOT BE FOUND OR YOUR INITIAL VALUE OF PRESSURE
      & WAS UNSUCCESSFUL. TRY AGAIN. '
       STOP
       ELSE
       IF(XZ(I) .LE. 0.0) GO TO 10
       IF(XZ(I) .LE. BMIX) GO TO 10
       IF(KK .EQ. 0) SXZ=XZ(I)
       IF(XZ(I) .GT. BXZ) BXZ=XZ(I)
       IF(XZ(I) .LE. SXZ) SXZ=XZ(I)
```

```
      KK=KK+1
      END IF
   10 CONTINUE
      VL=SXZ
      VV=BXZ
      RETURN
    5 WRITE(6,88) IFAIL
   88 FORMAT(' IFAIL ERROR NUMBER SPINODAL: ',I2)
      RETURN
      END
C
C     THIS SUBROUTINE CALCULATES THE VAPOR MOLAR VOLUME AND THE LIQUID
C     MOLAR VOLUME FROM THE REDLICH-KWONG-SOAVE EQUATION OF STATE
C
      SUBROUTINE RKSEQN(SXZ,BXZ,KK,W)
      IMPLICIT DOUBLE PRECISION (A-H,O-Z)
      COMMON/VAL/R,T,P,X(3),Y(3),WMOL(3),KEY,NCOMP
      COMMON/PURPRO/OMEGA(3),TCRIT(3),PCRIT(3),AK(3,3),ALPHA(3)
      COMMON/SOAVE/DMIX,AA,BB,SLOPEM(3)
      COMMON/NEWTON/ACOMB(3,3),FUG(3)
      DIMENSION XZ(3),YZ(3),RE(4)
C
C     ROOTS OF THE CUBIC EQUATION
C
      IF(KEY .EQ. 1) THEN
      CALL ABMIX(AMIX,BMIX,ACOMB,X)
      ELSE
      CALL ABMIX(AMIX,BMIX,ACOMB,Y)
      END IF
      RE(1)=1.0
      RE(2)=-1.0
      RE(3)=AA-BB-(BB**2)
      RE(4)=-(AA*BB)
      N=4
      P1=0.1E0
      TOL=X02AAF(P1)
      IFAIL=1
      CALL C02AEF(RE,N,XZ,YZ,TOL,IFAIL)
      IF(IFAIL .NE. 0) GO TO 5
C
C     SORTS ROOTS OUT
C
      KK=0
      BXZ=0.0
      SXZ=0.0
      DO 10 I=1,3
      IF(DABS(YZ(I)) .GT. TOL) GO TO 10
      IF(KK .EQ. 0) SXZ=XZ(I)
      IF(XZ(I) .GT. BXZ) BXZ=XZ(I)
      IF(XZ(I) .LT. SXZ) SXZ=XZ(I)
      KI=I
      KK=KK+1
   10 CONTINUE
      IF(KK .GT. 1) RETURN
      V=XZ(KI)*R*T/P
      IF(KEY .EQ. 1) THEN
```

$$Z^3 - Z^2 + (A - B - B^2)Z - AB = 0$$

```
      CALL SPIN(VV,VL,X)
      ELSE
      CALL SPIN(VV,VL,Y)
      END IF
      PRT=P/(R*T)
      IF(V .GT. VV) GO TO 20
      IF(V .LT. VL) GO TO 30
      WRITE(6,92) V,VV,VL
   92 FORMAT( ' ERROR ',' V=',E12.6,' VV=',E12.6,'VL=',E12.6)
   20 BXZ=PRT*V
      SXZ=PRT*VL
      RETURN
   30 SXZ=PRT*V
      BXZ=PRT*VV
      RETURN
    5 WRITE(6,900) IFAIL
  900 FORMAT(' IFAIL ERROR NUMBER: ',I2)
      RETURN
      END
C
C     THIS SUBROUTINE EVALUATES MATRIX A(I,J) FOR NEWTON-RAPHSON METHOD
C
      SUBROUTINE NEWRAF(A,W,Z)
      IMPLICIT DOUBLE PRECISION (A-H,O-Z)
      COMMON/VAL/R,T,P,X(3),Y(3),WMOL(3),KEY,NCOMP
      COMMON/PURPRO/OMEGA(3),TCRIT(3),PCRIT(3),AK(3,3),ALPHA(3)
      COMMON/SOAVE/DMIX,AA,BB,SLOPEM(3)
      COMMON/NEWTON/ACOMB(3,3),FUG(3)
      DIMENSION B1(3),A(3,3),W(3),AMIXJ(3)
      CALL ABMIX(AMIX,BMIX,ACOMB,W)
      DO 5 I=1,NCOMP
      B1(I)=0.08664*R*TCRIT(I)/PCRIT(I)
    5 CONTINUE
      DO 10 I=1,NCOMP
      AMIXJ(I)=0.0
      DO 10 K=1,NCOMP
      AMIXJ(I)=AMIXJ(I)+ACOMB(I,K)*W(K)
   10 CONTINUE
      DO 20 I=1,NCOMP
      DO 20 J=1,NCOMP
      A1=B1(J)*(P/R/T/(Z-BB)-B1(I)*(Z-1.0)/BMIX**2)
      A2=(AA/BB)*(B1(I)/BMIX-2.0*AMIXJ(I)/AMIX)*P*B1(J)/R/T/(Z+BB)
      A3=2.0*LOG(1.0+BB/Z)*((B1(I)*AMIXJ(J)+B1(J)*AMIXJ(I))/BMIX
     &-AMIX*B1(I)*B1(J)/BMIX/BMIX-ACOMB(I,J))/BMIX/R/T
      A(I,J)=A1+A2+A3
   20 CONTINUE
      RETURN
      END
C
C     THIS SUBROUTINE CALCULATES THE ENTHALPY OF MIXTURES
C
      SUBROUTINE ENTHALPY(Z,ENTAL)
      IMPLICIT DOUBLE PRECISION (A-H,O-Z)
      COMMON/VAL/R,T,P,X(3),Y(3),WMOL(3),KEY,NCOMP
      COMMON/PURPRO/OMEGA(3),TCRIT(3),PCRIT(3),AK(3,3),ALPHA(3)
      COMMON/RESIDUO/ATC(3),CPA(3),CPB(3),CPC(3),CPD(3)
```

```
      COMMON/SOAVE/DMIX,AA,BB,SLOPEM(3)
      COMMON/NEWTON/ACOMB(3,3),FUG(3)
      DIMENSION A(3),FACTOR(3,3),XORY1(3)
      TNOT=273.15
      DO 10 I=1,NCOMP
      IF(KEY .EQ. 1) XORY1(I)=X(I)
      IF(KEY .EQ. 2) XORY1(I)=Y(I)
   10 CONTINUE
      IF(KEY .EQ. 1) THEN
      CALL ABMIX(AMIX,BMIX,ACOMB,Y)
      ELSE
      CALL ABMIX(AMIX,BMIX,ACOMB,X)
      END IF
C
C     MOLECULAR WEIGHT FACTOR
C
      CONVER=0.0
      DO 5 I=1,NCOMP
      CONVER=CONVER+XORY1(I)*WMOL(I)
    5 CONTINUE
      DO 20 I=1,NCOMP
      A(I)=ALPHA(I)*ATC(I)
      DO 20 J=1,NCOMP
      FACTOR(I,J)=SLOPEM(J)*(1.0-AK(I,J))*DSQRT(A(I)*ATC(J)*T/TCRIT(J))
   20 CONTINUE
      DMIX=0.0
      DO 30 I=1,NCOMP
      DO 30 J=1,NCOMP
      DMIX=DMIX+XORY1(I)*XORY1(J)*FACTOR(I,J)
   30 CONTINUE
C
C     RESIDUAL ENTHALPY
C
      DELTH=R*T*((1.0-Z)+(AA/BB)*(1.0+DMIX/AMIX)*LOG(1.0+BB/Z))
      DELTH=DELTH/CONVER
C
C     IDEAL ENTHALPY
C
      HIDEAL=0.0
      DO 40 I=1,NCOMP
      HIDEAL=HIDEAL+XORY1(I)*(CPA(I)*(T-TNOT)+0.5*CPB(I)*(T**2-TNOT**
     &2)+0.33333*CPC(I)*(T**3-TNOT**3)+0.25*CPD(I)*(T**4-TNOT**4))
   40 CONTINUE
      HIDEAL=HIDEAL/CONVER
C
C     FINAL VALUE OF ENTHALPY
C
      ENTAL=HIDEAL-DELTH
      WRITE(6,60) ENTAL
   60 FORMAT(/,5X,' ENTHALPY=',E11.5,1X,'KJ/KG')
      RETURN
      END
C
C     THIS SUBROUTINE CALCULATES THE ENTROPY OF MIXTURES
C
      SUBROUTINE ENTROPY(Z,ENTROP)
```

```
      IMPLICIT DOUBLE PRECISION (A-H,O-Z)
      COMMON/VAL/R,T,P,X(3),Y(3),WMOL(3),KEY,NCOMP
      COMMON/PURPRO/OMEGA(3),TCRIT(3),PCRIT(3),AK(3,3),ALPHA(3)
      COMMON/RESIDUO/ATC(3),CPA(3),CPB(3),CPC(3),CPD(3)
      COMMON/SOAVE/DMIX,AA,BB,SLOPEM(3)
      COMMON/NEWTON/ACOMB(3,3),FUG(3)
      DIMENSION XORY1(3)
      TNOT=T
      PNOT=58.825706
      DO 10 I=1,NCOMP
      IF(KEY .EQ. 1) XORY1(I)=X(I)
      IF(KEY .EQ. 2) XORY1(I)=Y(I)
   10 CONTINUE
C
C     MOLECULAR WEIGHT FACTOR
C
      CONVER=0.0
      DO 5 I=1,NCOMP
      CONVER=CONVER+XORY1(I)*WMOL(I)
    5 CONTINUE
      IF(KEY .EQ. 1) THEN
      CALL ABMIX(AMIX,BMIX,ACOMB,Y)
      ELSE
      CALL ABMIX(AMIX,BMIX,ACOMB,X)
      END IF
C
C     RESIDUAL ENTROPY
C
      DELTS=-R*LOG(Z-BB)+R*(AA*DMIX/BB/AMIX)*LOG(1.0+BB/Z)
C
C     IDEAL ENTROPY
C
      SIDEAL=0.0
      DO 20 I=1,NCOMP
      SIDEAL=SIDEAL+XORY1(I)*(CPA(I)*LOG(T/TNOT)+CPB(I)*(T-TNOT)+
     &0.5*CPC(I)*(T**2-TNOT**2)+0.333333*CPD(I)*(T**3-TNOT**3)
     &-R*LOG(XORY1(I)*P/PNOT))
   20 CONTINUE
      SIDEAL=SIDEAL/CONVER
      DELTS=DELTS/CONVER
C
C     ENTROPY OF MIXING
C
      SMIX=0.0
      DO 30 I=1,NCOMP
      SMIX=SMIX+R*XORY1(I)*LOG(XORY1(I))
   30 CONTINUE
      SMIX=SMIX/CONVER
C
C     FINAL VALUE OF THE ENTROPY
C
      ENTROP=SIDEAL-DELTS-SMIX
      WRITE(6,40) ENTROP
   40 FORMAT(/,5X,' ENTROPY=',E11.5,1X,'KJ/KG K')
      CONTINUE
      RETURN
```

```
      OPEN (8,FILE='wfluid',STATUS='OLD',FORM='FORMATTED')
      OPEN (9,FILE='penneo12',STATUS='OLD',FORM='FORMATTED')
      OPEN (10,FILE='ts-size',STATUS='OLD',FORM='FORMATTED')
      REWIND(8)
      REWIND(9)
      REWIND(10)
      CALL PLOTDAT
      CALL AXISET
      CALL TITLE
      STOP
      END
C
C     TO SET UP THE PLOTTER AXES AND WINDOW AREA ACCORDING
C     TO USER SPECIFIED MIN.  AND MAX.  RANGE AND DIAGRAM SIZE.
C
      SUBROUTINE AXISET
      COMMON/LIMITS/SMAX,SMIN,TMAX,TMIN
      COMMON/TPSAT/TS(70),SS(70),M,ET(2),ES(2)
      COMMON SIZ1,SIZE,NS,NT
      SIZE = 1.0/SIZ1
      CALL HP7550
      CALL DEVPAP(380.,270.,1)
      CALL WINDO2(0.,380.,0.,270.)
      CALL PICCLE
      CALL SCALE(SIZE)
      CALL CHASIZ(3.,3.)
      CALL AXIPOS(1,100.,100.,600.,1)
      CALL AXIPOS(1,100.,100.,450.,2)
      CALL AXISCA(3,NS,SMIN,SMAX,1)
      CALL AXISCA(3,NT,TMIN,TMAX,2)
      CALL CHASWI(1)
      CALL AXIDRA(-1,1,1)
      CALL AXIDRA(0,-1,2)
      CALL GRID(3,0,0)
      CALL MOVTO2(350.,80.)
      CALL CHAHOL(26HSPECIFIC ENTROPY KJ/KG.K*.)
      CALL MOVTO2(80.,350.)
      CALL ROTAT2(90.)
      CALL CHAHOL(19HTEMPERATURE DEG.C*.)
      CALL ROTAT2(-90.0)
      CALL CHASIZ(3.,3.)
      CALL MOVTO2(75.,75.)
      CALL LINTO2(75.,575.)
      CALL LINTO2(725.,575.)
      CALL LINTO2(725.,75.)
      CALL LINTO2(75.,75.)
      RETURN
      END
C
C
C
      SUBROUTINE PLOTDAT
C
C      TO READ IN THE USER SUPPLIED DATA FOR THE DIAGRAM REQUIREMENTS
C
      COMMON/LIMITS/SMAX,SMIN,TMAX,TMIN
```

```
      COMMON/TPSAT/TS(70),SS(70),M,ET(2),ES(2)
      COMMON/HEADER/ITITLE1(11),ITITLE2(11)
      COMMON SIZ1,SIZE,NS,NT
      READ(10,*)SMAX,SMIN,TMAX,TMIN,SIZ1
      WRITE(6,1)
    1 FORMAT(' TYPE IN SCALE ENTROPY-TEMPERATURE ')
      READ(5,*) NS,NT
      WRITE(6,2)
    2 FORMAT(' TYPE IN NUMBER OF POINTS ')
      READ(5,*) M
      DO 3 I=1,11
      READ(8,4) ITITLE1(I)
    4 FORMAT(A4)
    3 CONTINUE
      DO 6 I=1,11
      READ(8,4) ITITLE2(I)
    6 CONTINUE
      DO 7 I=1,M
      READ(9,*) TS(I),SS(I)
    7 CONTINUE
      WRITE(6,10)
   10 FORMAT(' TYPE IN COORDINATES (T1,S1) AND (T2,S2) ')
      DO 11 I=1,2
      READ(5,*) ET(I),ES(I)
   11 CONTINUE
      WRITE(6,12)
   12 FORMAT(15H *PLOTDAT DONE )
      RETURN
      END
C
C
      SUBROUTINE TITLE
      COMMON/LIMITS/SMAX,SMIN,TMAX,TMIN
      COMMON/TPSAT/TS(70),SS(70),M,ET(2),ES(2)
      COMMON/HEADER/ITITLE1(11),ITITLE2(11)
      COMMON SIZ1,SIZE,NS,NT
      CALL PENSEL(7,0.5,2)
      CALL MOVTO2(194.,340.)
      CALL CHAHOL(9HISOBARS*.)
      CALL MOVTO2(194.,490.)
      CALL CHASIZ(5.,5.)
      CALL PENSEL(2,0.5,2)
      CALL CHAHOL(21HTHE CITY UNIVERSITY*.)
      CALL MOVTO2(176.,460.)
      CALL CHAHOL(29HTEMPERATURE-ENTROPY DIAGRAM*.)
      CALL MOVTO2(136.,400.)
      CALL CHAARR(ITITLE1,11,4)
      CALL MOVTO2(194.,420.)
      CALL CHAHOL(19HBINARY MIXTURE OF*.)
      CALL MOVTO2(136.,380.)
      CALL CHAARR(ITITLE2,11,4)
      CALL CHASIZ(3.,3.)
      CALL MOVTO2(185.,475.)
      CALL CHAHOL(38HDEPARTMENT OF MECHANICAL ENGINEERING*.)
      CALL MOVTO2(234.,440.)
      CALL CHAHOL(5HFOR*.)
```

```
      CALL MOVTO2(194.,320.)
      CALL CHASIZ(3.,3.)
      CALL PENSEL(2,0.5,2)
      CALL CHAHOL(19HEXPANSION PROCESS*.)
      CALL MOVTO2(130.,514.)
      CALL LINTO2(360.,514.)
      CALL LINTO2(360.,370.)
      CALL LINTO2(130.,370.)
      CALL LINTO2(130.,514.)
      CALL PENSEL(1,0.5,2)
      CALL MOVTO2(196.,300.)
      CALL CHAHOL(17HSATURATION LINE*.)
      CALL GRALIN(SS(4),TS(4))
      CALL GRACUR(SS,TS,M)
      CALL PENSEL(7,0.5,2)
      R1=(M-1)/2.0
      N1=(M-1)/2
      IF( ABS(R1-N1) .GT. 0.0) N1=N1+1
      DO 10 I=2,N1
      NM=M+1-I
      CALL GRAMOV(SS(I),TS(I))
      CALL GRALIN(SS(NM),TS(NM))
10    CONTINUE
      CALL PENSEL(2,0.5,2)
      CALL GRAMOV(ES(1),ET(1))
      CALL GRALIN(ES(2),ET(2))
      WRITE(6,11)
11    FORMAT('**PLOTTING COMPLETE**')
      CALL DEVEND
      RETURN
      END
```

APPENDIX C NUMERICAL METHODS

1) The Secant Method

The Secant Method can be considered to be a simplification of the Newton-Raphson method which solves iteratively for a root via:

$$x_{n+1} = x_n - f(x_n)/f'(x_n)$$

in the Secant method, the derivative is approximated by:

$$f'(x_n) = \frac{f(xn) - f(xn-1)}{x_n - x_{n-1}}$$

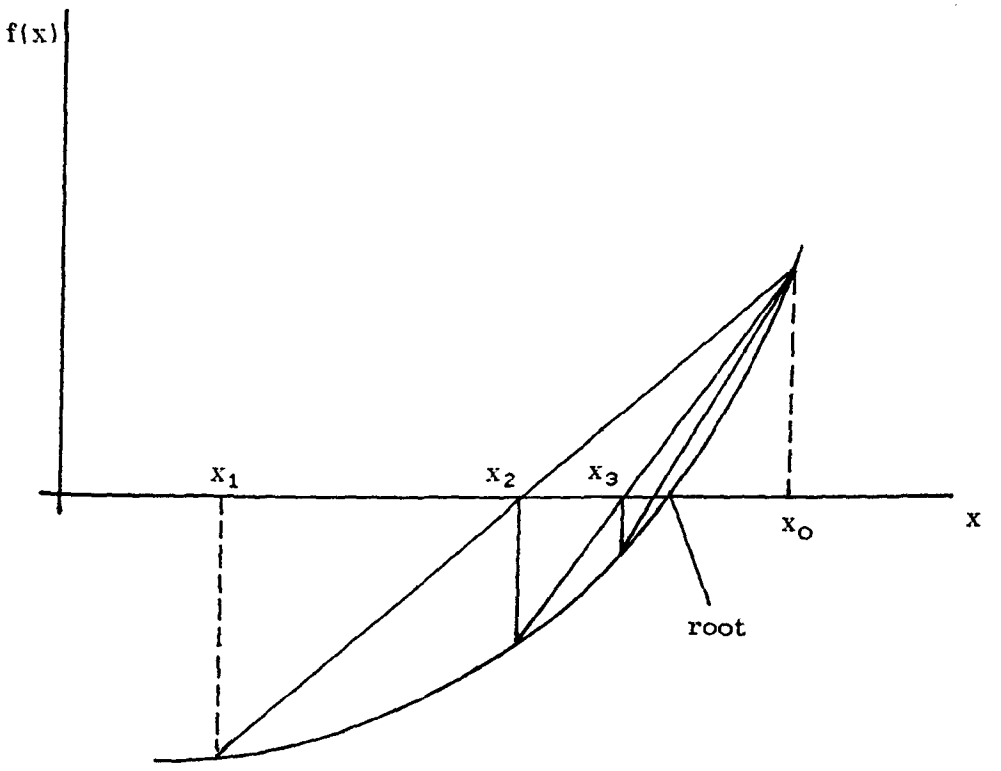

When applying, say, to the bubble pressure calculation we have:

Find P such that $\sum_i y_i$ (SUMXY) = 1?

Let $E(P) = \sum_i y_i(P) - 1$ therefore find P such that E(P) = 0

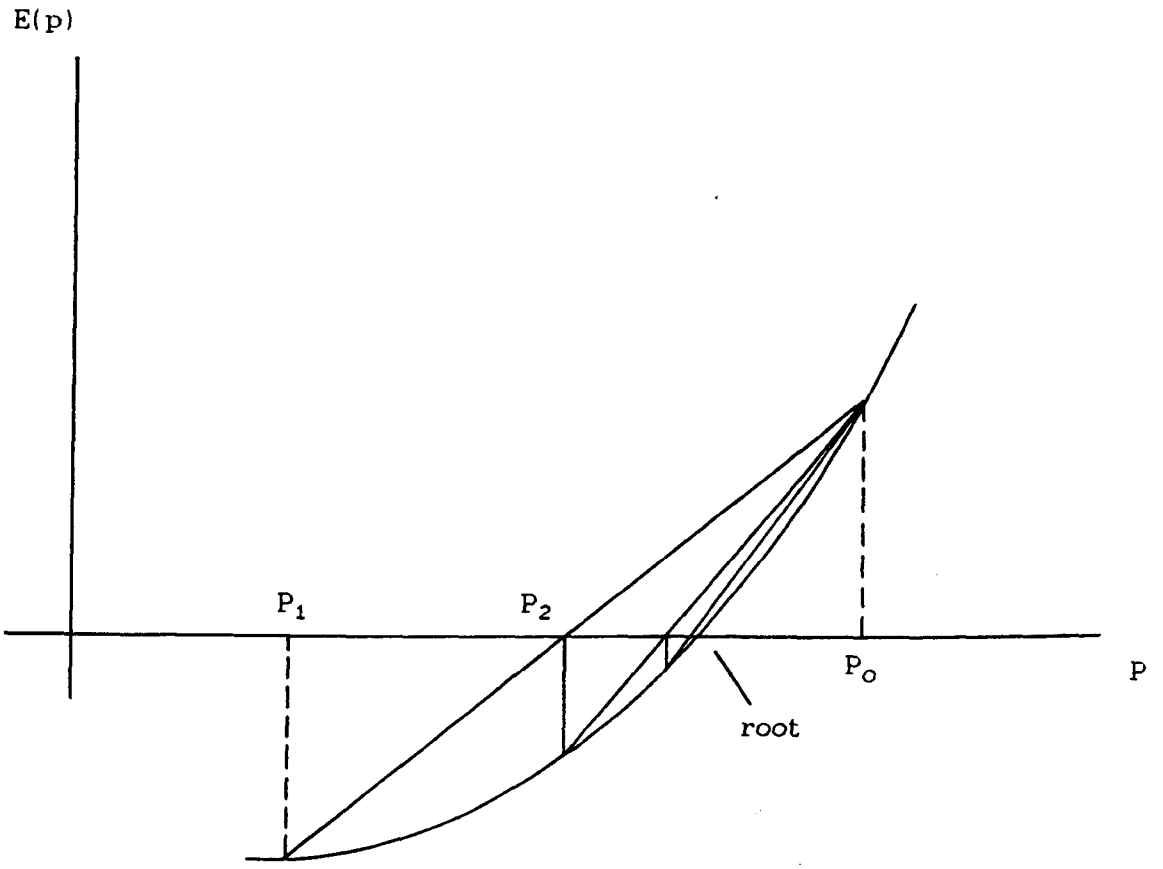

Start with P_o and P_1

Straight line going from $(P_o, E(P_o))$ to $(P_1, E(P_1))$

$$\frac{E - E_1}{P - P_1} = \frac{E_1 - E_o}{P_1 - P_o}$$

Find P such E = 0

$$P = P_1 - \frac{E_1(P_1 - P_o)}{E_1 - E_o}$$

Replace (P_1, E_1) by (P_2, E_2).

APPENDIX D VAN DER WAAL'S SPINODAL CURVE

The Van der Waal's spinodal curve is defined as the locus of maxima and minima of all subcritical isotherms of a given cubic equation of state. This is realized for the Redlich-Kwong-Soave EOS as follows:

$$P = \frac{RT}{V - b} - \frac{a(T)}{V(V + b)}$$

setting the first derivative equal to zero (maximum and minimum condition) we have:

$$\left[\frac{\partial P}{\partial V}\right]_T = 0$$

$$- \frac{RT}{(V - b)^2} + \frac{a(2V + b)}{(V^2 + Vb)^2} = 0$$

which after some algebraic manipulations yields:

$$V^4 + 2\left[b - \left[\frac{a}{RT}\right]\right] V^3 + \left[b^2 + \left[\frac{3ab}{RT}\right]\right] V^2 - \frac{ab^3}{RT} = 0$$

The Van der Waal's spinodal curve is therefore a polynomial of fourth degree in volume.

2) The Bisection Method

The method of Bisection is based on the use of sign changes to detect a root. This procedure produces an interval with half of the length of the original one in which a root must lie. We repeat the procedure until we arrive at an interval of sufficiently small length which contains a root. By sufficiently small we mean that the roots have been located to such an accuracy that we are prepared to assume that either there is only one root in the interval or, if there is more than one root, then the roots are so close that we are willing to consider them as a repeated root.

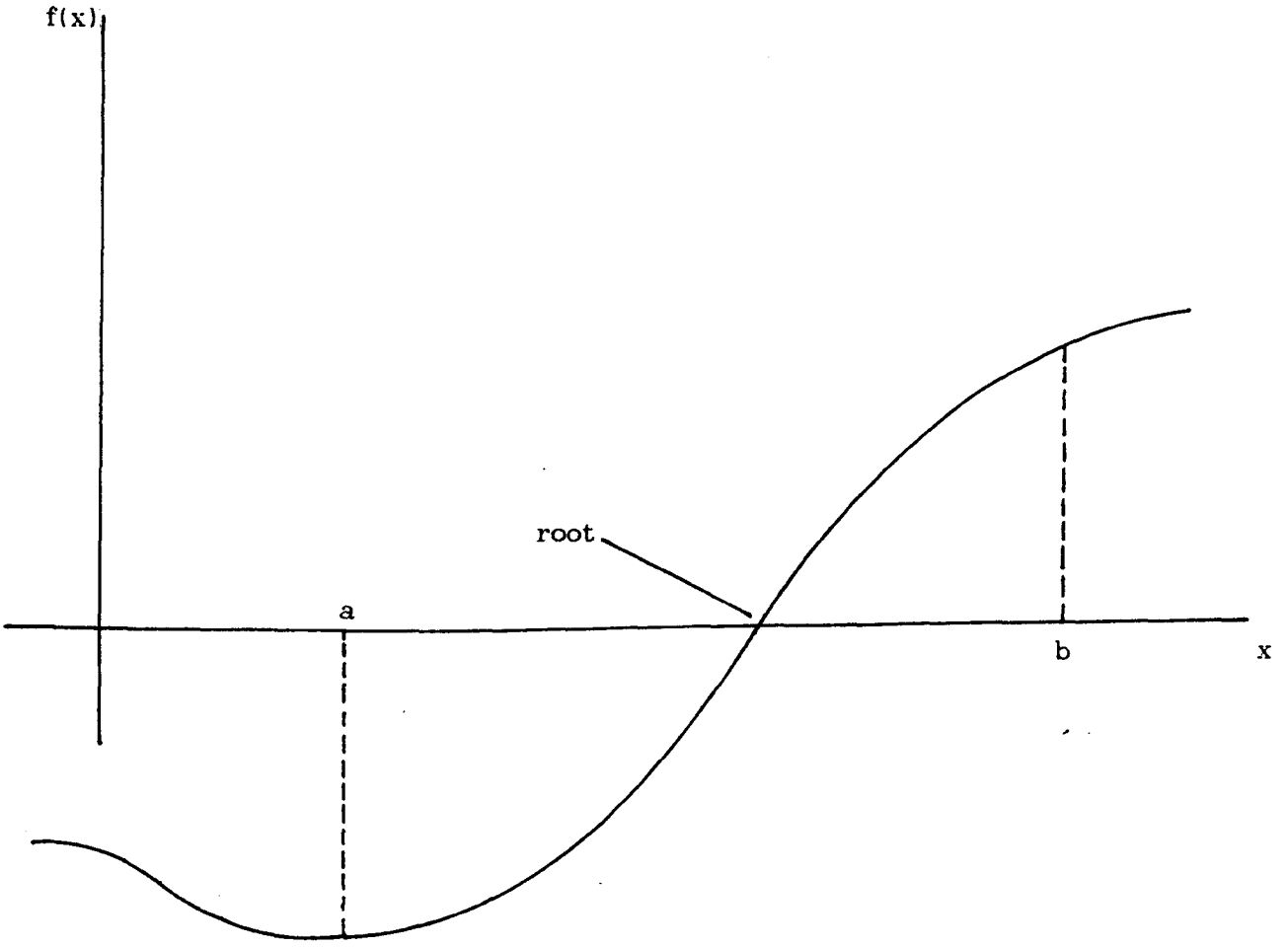

ADDENDUM TO CHAPTER 7

Coordinates for plotting the expansion process(red line in binary mixture T-S diagrams) are given below along with its corresponding enthalpy values.

Sample

85% of n-pentane
15% of 2,2-dimethylpropane

condensing temperature 35°C

turbine efficiency 80%

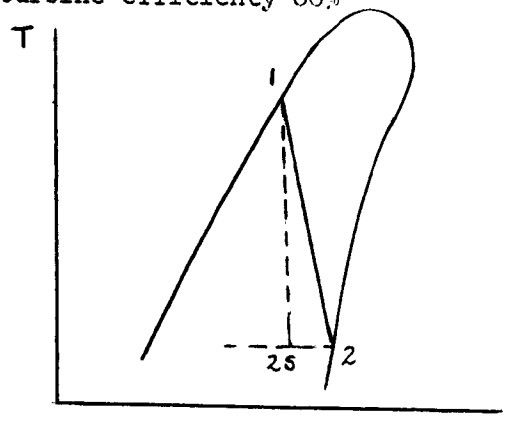

$(T_1, S_1) = (175.2°C, 2.389\ kJ/°K)$ $H_1 = 600\ kJ/kg°K$

$(T_2, S_2) = (35°C, 2.43\ kJ/°K)$ $H_2 = 528.1\ kJ/kg°K$